BRUCE PEEL SPECIAL COLLECTIONS LIBRARY
University of Alberta

REQUEST FOR DUPLICATION

I wish a photocopy of the thesis by_____

entitled_____

The copy is for the sole purpose of private scholarly or scientific study and research. I will not reproduce, sell or distribute the copy I request, and I will not copy any substantial part of it in my own work without the permission of the copyright owner. I understand that the Library performs the service of copying at my request, and I assume all copyright responsibility for the item requested.

Name_____

Address_____

List pages copied_____

Date_____   Signature_____

Name_____

Address_____

List pages copied_____

Date_____   Signature_____

Name_____

Address_____

List pages copied_____

Date_____   Signature_____

Name_____

Address_____

List pages copied_____

Date_____   Signature_____

Name_____

Address_____

List pages copied_____

Date_____   Signature_____

University of Alberta

Library Release Form

NAME OF AUTHOR: Pauline Orr

TITLE OF THESIS: Geochemistry and Petrology of the Yamba Lake Kimberlites, Central Slave Province, Northwest Territories

DEGREE: Master of Science

YEAR THIS DEGREE WAS GRANTED: 1998

University of Alberta

Geochemistry and Petrology of the Yamba Lake Kimberlites, Central Slave Province, Northwest Territories

by

Pauline Orr

©

A thesis submitted to the Faculty of Graduate Studies and Research in partial fulfillment of the requirements for the degree of Master of Science

Department of Earth and Atmospheric Sciences

Edmonton, Alberta

Spring 1998

University of Alberta

Geochemistry and Petrology of the Yamba Late Kimberlites, Central Slave Province, Northwest Territories

by

A thesis submitted to the Faculty of Graduate Studies and Research in partial fulfillment of the requirements for the degree of Master of Science

Department of Earth and Atmospheric Sciences

Edmonton, Alberta

Spring 2006

University of Alberta

Faculty of Graduate Studies and Research

The undersigned certify that they have read, and recommend to the Faculty of Graduate Studies and Research for acceptance, a thesis entitled **Geochemistry and Petrology of the Yamba Lake Kimberlites, Central Slave Province, Northwest Territories** submitted by Pauline Orr in partial fulfillment of the requirements for the degree of Master of Science.

This work is dedicated to my parents

Abstract

The sub-economic Torrie, Sputnik and Eddie pipes, located near Yamba Lake, central Slave province, NWT, are diatreme-facies macrocrystic, heterolithic, volcaniclastic kimberlite breccias. Major-element chemistry of pyroxene and garnet xenocrysts and megacrysts in the Torrie and Sputnik kimberlites is consistent with their derivation from disaggregated garnet lherzolite and high temperature deformed lherzolite, with minor contributions from eclogite, spinel lherzolite, garnet harzburgite and websterite. The presence of primary phlogopite and more evolved spinels, and the lack of mantle xenocrysts, xenoliths and megacrystic ilmenite distinguish the Eddie kimberlite pipe from the Torrie and Sputnik pipes.

Large variations in $\delta^{18}O$ of garnet and clinopyroxene xenocrysts (+3.98 to +6.36‰) coupled with isotopic reversals between these minerals are consistent with metasomatic enrichment of depleted mantle by slab-derived fluids. Partial melting of subducted ancient oceanic crust and the subsequent migration of these melts and fluids into overlying, depleted peridotite resulted in relatively 'fertile' peridotite and disequilibrium intermineral isotope distributions. Furthermore, a large variation in $\delta^{18}O$ (+3.55-5.44‰) of magnesian ilmenite, inferred to have crystallized from kimberlitic melts, also reflects heterogeneity in their source region that resulted from partial melting of refertilized peridotite.

The Torrie and Sputnik kimberlite pipes have diamond indicator minerals consistent with their low diamond grades; however, transient-heating events may have also played a role in their reduced diamond contents. High temperatures and metasomatism just prior to eruption of the kimberlites may have caused the resorption of diamonds.

Acknowledgement

Table of Contents

List of Tables

List of Figures

Chapter 1

Introduction

In 1991, the first potentially economic diamond-bearing kimberlite pipes were found in the Lac de Gras region, NWT, by a small company called Dia Met Minerals. This started the largest staking rush in Canadian history, resulting in the entire Slave province being staked. To date, there have been approximately 100 pipes found, of which 35 contain diamonds (Schiller,1994). Most of the diamond-bearing pipes are sub-economic but several of them have been reported to be economic. The search for diamonds in Canada is only at the exploration level but in the Fall of 1998, the Northwest Territories will be host to Canada's first diamond mine.

Although diamonds provide valuable evidence about past processes in the mantle, much of the research on them is inspired by the fact that diamonds are a valuable commodity. Unfortunately, diamond exploration in Canada has always been poorly documented and shrouded by proprietary concerns. As a result, most published research is on well-known barren or sub-economic kimberlite occurrences such as on Somerset Island, NWT and in Saskatchewan (Mitchell, 1978a,1979; Scott Smith, 1995,1996; Kjarsgaard, 1996c). Very little research has been published on the more recent discoveries in the Slave province because of the limited access to the samples.

Mantle-derived xenoliths, xenocrysts and megacrysts, transported to the Earth's surface by kimberlite, give insight not only into the geochemical variations in the mantle, but also into the types of environments in which diamonds are formed and preserved. Xenocrysts are added to the kimberlite magma by disaggregation of xenoliths during transportation to the surface. Kimberlite indicator minerals (such as spinel, olivine and ilmenite) that are resistant to weathering are found in esker and till samples and are a valuable exploration tool used in the NWT to find the kimberlites themselves. This use of indicator mineral "trails" is especially important because the kimberlites weather easily and do not usually crop out but rather form local depressions, often filled by lakes. Diamond exploration companies typically look for a subset of kimberlite indicator minerals called 'diamond indicators' such as sub-calcic Cr pyrope garnets, Cr-pyrope garnet, high Na-Ti pyrope almandine garnet, high Cr-Mg chromite and Cr diopside. These minerals are

typically associated with diamonds, so their presence indicates the potential presence of diamonds.

Tanqueray Resources discovered five sub-economic kimberlite pipes in 1994 near Yamba Lake, NWT, just 30 km north of where Dia Met Minerals made the economic Lac de Gras kimberlite discovery. The Torrie pipe has a very poor reported grade of 2.59 carats/100t (Tanqueray Resources, annual report, 1994). Relatively fresh and altered drill core samples from the Torrie, Eddie and Sputnik kimberlite pipes were obtained in January, 1995, for a detailed geochemical, petrographic and petrologic study. At the time, the company restricted sampling of xenoliths to those that were apparent on visual inspection of the core. Subsequent workers were allowed to disaggregate much of the core, which allowed them to obtain xenoliths that were not visible in the surface of the core at the time of our selection.

The objectives of this thesis are fourfold: first, to describe the petrographic and geochemical characteristics of the three kimberlite pipes and compare them with the well-documented kimberlites from other cratons; second, to examine the mantle samples represented by the xenocryst and megacryst suite; third, to constrain the geotherm of the upper mantle at the time of the kimberlite eruption in this area of the Slave province by using geothermometry and baromentry on coexisting minerals in polyphase xenoliths; and fourth, to determine why these kimberlite pipes contain so few diamonds.

Major-elements were analyzed in kimberlite phenocrysts, xenocrysts, megacrysts, two mantle xenoliths and a crustal xenolith. The xenocrysts and mantle xenoliths are derived from peridotite, pyroxenite and eclogite source regions in the mantle. $\delta^{18}O$ values were determined in garnet and clinopyroxene xenocrysts, Mg ilmenite and coexisting garnet and clinopyroxene in the mantle xenoliths.

Chapter 2

Geologic Setting

The Torrie, Sputnik and Eddie kimberlite pipes are located near Yamba Lake on property staked by Tanqueray Resources in the south-central part of the Slave province, a Late Archean craton that covers 213 000 km^2 in the northwestern Canadian Shield (Fig. 2.1). Recent interpretations of the geology of the Slave province have been presented by Padgham and Fyson (1992), Hoffman (1989) and Fyson and Helmstaedt (1988). The Slave province consists of a 2.7 to 2.5 Ga sedimentary-dominated granite-greenstone terrain (Henderson, 1981) bounded by the Thelon orogen (2.0 to 1.9 Ga) to the east and the Wopmay orogen (1.9 to 1.8 Ga) to the west (Hoffman, 1989). It has inliers of older gneiss (4.0-2.8 Ga) and younger sedimentary rocks. Radiogenic isotopic values (Sm/Nd and U/Pb) are consistent with the presence of an ancient crustal component in the western part of the province and a relatively primitive, juvenile crust to the east (Davis and Hegner, 1992). Dominantly tholeiitic mafic-felsic volcanic packages are common in the west and intermediate-felsic calc-alkaline series are more abundant in the east. The complex record of rock deformation is interpreted to reflect early subhorizontal regional shortening (thrusting), later polyphase folding, diapiric plutonism and late faulting. Low-pressure, high-temperature metamorphism (Thompson et al, 1996), characteristic of much of the Slave province, is a result of local heating by plutonism or uplift resulting from crustal thickening.

The geology of the province can be subdivided into five groups: 1) sialic basement rocks; 2) Older Shelf Assemblage; 3) Yellowknife Supergroup rocks (Volcanic-Turbidite Series); 4) post-Volcanic-Turbidite Series conglomerates and sandstones and 5) pre-, syn- to post-deformation granitoid intrusions.

Exposures of very ancient sialic basement are restricted to the western margin where the world's oldest rock, the Acasta gneiss, which is dated at 3.96 Ga (Bowring et al., 1989), crops out. The gneissic and migmatite granitic basement rocks in other parts of the Slave province, range in age from 2.84 to 3.96 Ga, consistent with suggestions that the basement is made up of a mixture of Early to Late Archean rocks (Davis, 1991).
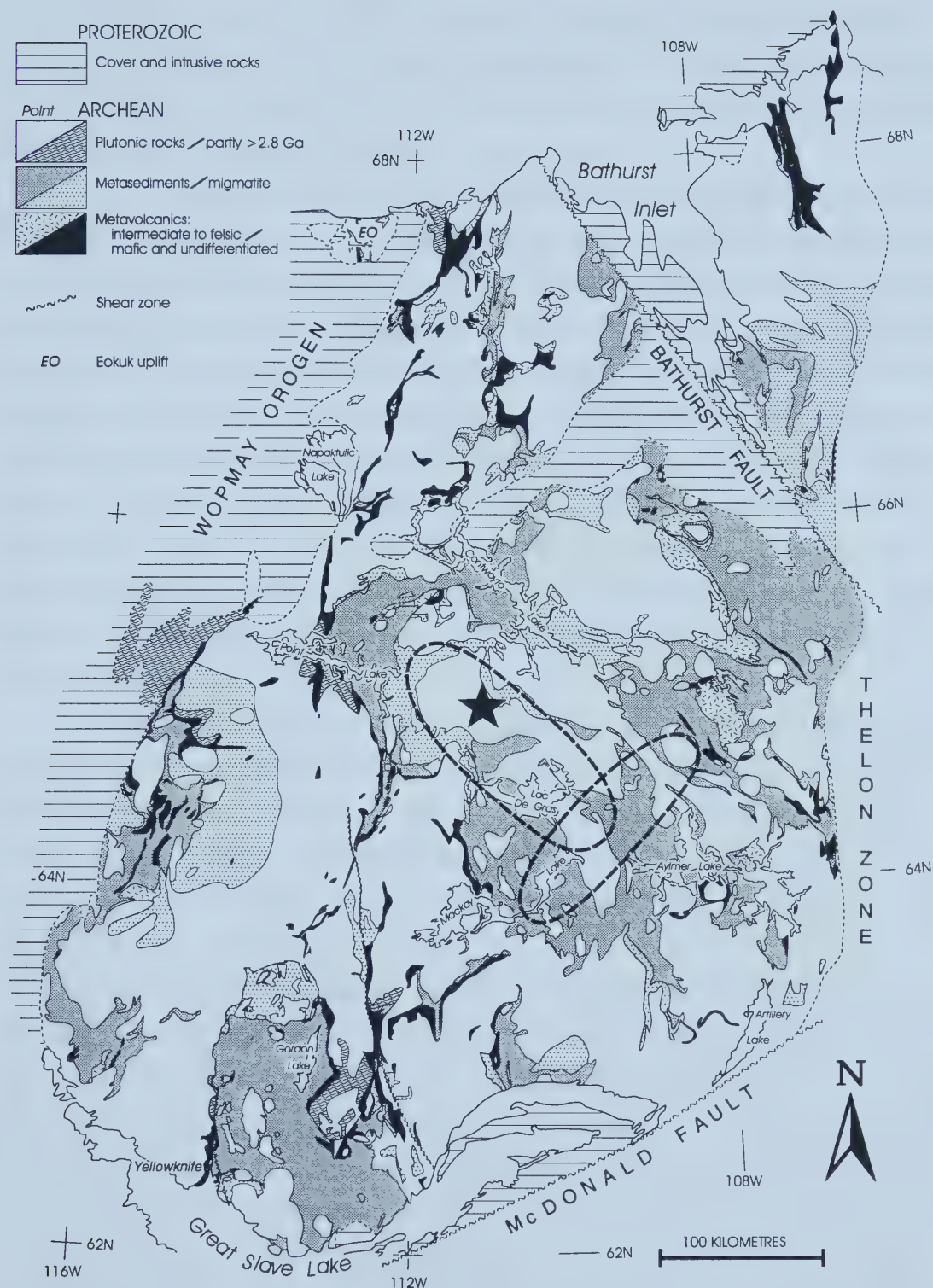
Figure 2.1 General geology of the Slave province (modified from Fyson, 1993) and location of known kimberlite pipes (Pell, 1995). The dashed ellipses represent the approximate area of the northwest (diamond-bearing) and northeast (barren) trending kimberlite pipes. The star indicates the location of the Torrie, Eddie and Sputnik kimberlite pipes.

A shelf-type quartz arenite unit, deposited on sialic basement, is overlain by felsic volcanic rocks and chert-magnetite banded-iron formation that are commonly intruded by ultramafic dykes and sills. These units predate the supracrustal sequences of the Yellowknife Supergroup (Padgham et al., 1992).

The supracrustal rocks of the Yellowknife Supergroup (Henderson, 1970) consist of thick, folded complexes of volcanic rocks overlain by tightly folded meta-turbidite (greywacke, sandstone and shale) sequences that accumulated between 2.71 and 2.65 Ga (Mortensen at al,1988). There are two types of volcanic belts within the Yellowknife supergroup: Yellowknife-type and Hackett River-type. The supracrustal rocks of the Yellowknife-type consist of thick sequences of dominantly tholeiitic basalt flows overlain by alkalic felsic volcanic rocks and the Hackett River-type are intermediate to felsic calc-alkaline pyroclastic rocks (Padgham, 1985). The supracrustal rocks cover approximately 33% of the province; with a ratio of approximately 1:3 volcanic:sedimentary rocks. In contrast to other greenstone belts (i.e. Superior province), turbiditic sediments are significantly more abundant than volcanic rocks in the Slave province.

Approximately 65% of the Slave province is underlain by pre-, syn- and post-deformational intrusive rocks ranging in composition from gabbro to syenogranite with ages of emplacement between 3.6 and 2.6 Ga (Padgham and Fyson, 1992). Post Volcanic-Turbidite Series sandstones and polymictic conglomerate units, containing boulders of post-Yellowknife Supergroup granites, comprise the youngest Archean supracrustal rocks (Padgham et al., 1992).

Numerous conflicting tectonic models have been proposed to account for the evolution of the Slave province: ensialic rifting (Henderson,1981), closure of a back-arc basin (Fyson and Helmstaedt, 1988), and crustal accretion (Kusky, 1989). Major tectonic events that occurred between 3.1-2.8 Ga are rifting, intrusion of mafic dykes, followed by explosive felsic volcanism. Continued crustal thinning and more extensive rifting permitted Volcanic-Turbidite Series volcanism (Yellowknife Supergroup). Kimberlite magmatism in the Slave province occurred during the Ordovician, Cretaceous (Kjarsgaard, 1996a) and Eocene (Davis and Kjarsgaard, 1996). Multiple emplacement ages indicate that the Slave province is a Type III kimberlite province similar to South Africa and Yakutia (Kjarsgaard and Heaman, 1995). Type III kimberlite provinces have kimberlite fields with more than two different emplacement ages in the same region (Mitchell, 1986). Type I and Type II kimberlite provinces have kimberlite fields with one and two emplacement ages,

respectively. This study focuses on the petrology of three pipes: Torrie, Sputnik and Eddie, found by Tanqueray Resources.

Location of pipes

The Torrie (499000E/7211000N), Sputnik (499550E/7211150N) and Eddie (499100E/7205550N) kimberlite pipes are part of a cluster of diamond-bearing pipes in a northwest-trending zone in the Lac de Gras region (Fig. 2.1). A second group of pipes, which are predominantly barren, trends east-northeasterly and overlaps the southern end of the Lac de Gras cluster (Pell, 1997). The Torrie and Sputnik pipes are found very close together on NTS 76E/3 while the Eddie pipe is located approximately 10 km south on NTS 76D/14.

Chapter 3

Petrography

What is a kimberlite?

The following definition of a kimberlite is from Mitchell (1986,1995).

"Kimberlites are a group of volatile-rich (dominantly CO_2) potassic ultrabasic rocks commonly exhibiting a distinctive inequigranular texture resulting from the presence of macrocrysts (and in some instances megacrysts), set in a fine-grained matrix. The mega/macrocryst assemblage consists of anhedral crystals of olivine, magnesian ilmenite, Cr-poor titanian pyrope, diopside (commonly sub-calcic), phlogopite, enstatite, and Ti-poor chromite. Olivine macrocrysts are a characteristic constituent in all but fractionated kimberlites. The matrix contains a second generation of primary euhedral-to-subhedral olivine which occurs together with one or more of the following primary minerals: monticellite, phlogopite, perovskite, spinel, (magnesian ulvöspinel-Mg-chromite-ulvöspinel-magnetite solid solutions), apatite, and serpentine. Many kimberlites contain late-stage poikilitic micas belonging to the barian phlogopite-kinoshitalite series. Nickeliferous sulfides and rutile are common accessory minerals. The replacement of earlier-formed olivine, phlogopite, monticellite, and apatite by deuteric serpentine and calcite is common. Evolved members of the group may be poor in, or devoid of, macrocrysts and/or composed essentially of second-generation olivine, calcite, serpentine, and magnetite, together with minor phlogopite, apatite, and perovskite."

Figure 3.1 is a generalized model of the classic kimberlite magmatic system. It shows the relationship between the crater (lavas, pyroclastic and resedimented volcaniclastic rocks), diatreme (predominantly volcaniclastic kimberlite breccias) and hypabyssal facies rocks (blows, dykes and sills).

In-situ pyroclastic (crater facies kimberlite) rocks are rare because erosion rapidly destroys the craters; however, they are known to occur in Tanzania and Botswana (Mannard, 1962, Hawthorne, 1975 and Dawson, 1994). In these occurrences, the pyroclastics occur as tuffs and usually have sedimentary structures such as stratification,
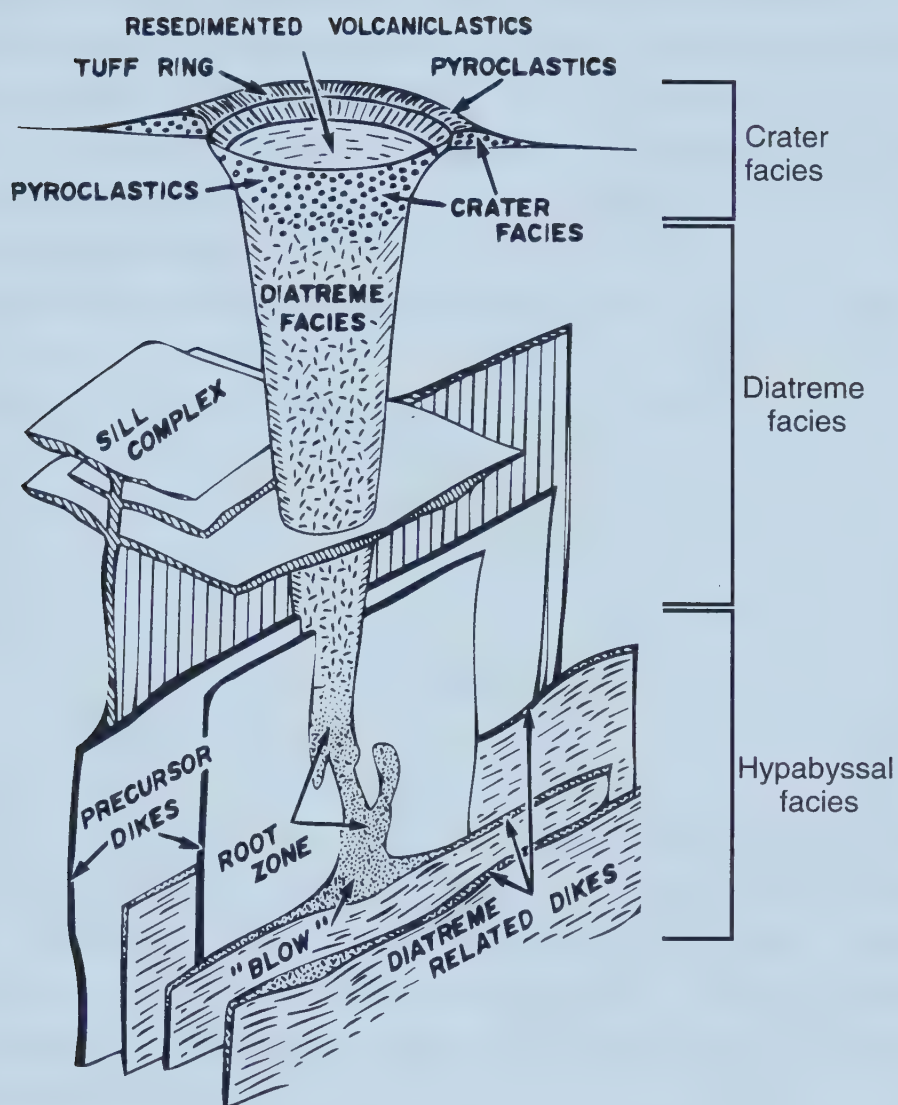
Figure 3.1 Generalized model of a kimberlite magmatic system showing the relationship between crater, diatreme and hypabyssal facies (modified from Mitchell, 1986).

layering, complex folding related to slumping or grading. Glassy or aphyric kimberlitic lavas are extremely rare and have been identified from only one tuff cone in Tanzania (Sampson, 1953 referenced in Mitchell, 1986). Resedimented volcaniclastic rocks produced by fluvial reworking and redeposition of kimberlitic tuffs in crater lakes above diatremes have been reported from many locations in Africa and from one location in Kansas, USA.   Moreover, pyroclastic kimberlite and associated resedimented volcaniclastic kimberlite that form tephra cones have been recently recognized in central Saskatchewan (Kjarsgaard, 1996c).

Diatreme-facies kimberlites are characterized by small rounded lower crustal and mantle-derived xenoliths, autolithic clasts that are fragments of earlier generations of hypabyssal kimberlite, pelletal lapilli, bituminous shale and/or carbonized wood fragments (Mitchell, 1986).   The presence of carbonized wood and angular to rounded unmetamorphosed country rock fragments indicates a low temperature emplacement.

Particularly characteristic of diatremes are pelletal lapilli, which are discrete spherical-to-elliptical lapilli (2-64mm) sized clasts of fine grained primary igneous material (Mitchell, 1995).   They commonly contain phlogopite or olivine macrocrysts, crystal fragments or country rock clasts at the center surrounded by a mantle of very fine grained microphenocrystal/primary groundmass material (perovskite, calcite, spinel and serpentine) characterisic of the parental magma. Prismatic minerals such as phlogopite may be oriented around the core forming poorly-to-well developed concentric structures (Mitchell, 1986).   Pelletal lapilli, derived from CO_2-rich magmas, are thought to represent magma droplets that have formed by explosive fragmentation of magma as a result of either rapid expulsion of dissolved volatiles (Clement 1973, Dawson, 1980) or interaction with groundwater (Mitchell 1986).

Rocks of the hypabyssal facies form the root zone of diatremes and occur as dikes and sills (Mitchell, 1986).   Globular segregations, characteristic of hypabyssal facies, are spherical masses of fine grained hypabyssal material found in coarser-grained, uniformly textured hypabyssal kimberlite.   They may be distinguished from pelletal lapilli by their coarser grained texture and lack of a macrocrystal nucleus. Mitchell (1986) proposes that they are formed by surface tension effects in boiling magmas in near-surface hypabyssal environments.

The groundmass in kimberlites may be described as either uniform- or segregation-textured depending on the distribution of groundmass minerals. Segregation-textured kimberlites have amoeboid-to-spherical discrete regions of coarse grained

primary phlogopite-kinoshitalite, apatite, calcite, and serpentine (Mitchell 1995). Serpentine and calcite segregations, typically lacking perovskite and spinel, are also common. The segregations result from the separation of late crystallizing phases of the groundmass into discrete masses (Mitchell, 1995). A general consensus as to the origin of the segregations has not been reached, however, Mitchell (1986) regards them as low-temperature residual fluids generated by surface tension effects between the water-rich segregation and more viscous crystal-rich silicate oxide groundmass. Other hypotheses for their origin include gas condensates in vesicles, filled breached vesicles, and immiscible liquids (Dawson and Hawthorne, 1973, Donaldson and Reid, 1982, and Clement, 1982).

Autoliths, found in all facies, are angular-to-subrounded lapilli- to ash-sized clasts formed by fragmentation of earlier solidified kimberlite material (Mitchell, 1995). Subrounded autoliths in diatremes may be difficult to distinguish from pelletal lapilli with weak concentric structures, however, autoliths commonly contain fractured crystals at their margins distinguishing them from pelletal lapilli. Furthermore, autoliths in hypabyssal facies kimberlites are typically coarser grained and less altered than diatreme facies autoliths.

The discrete nodule suite found in kimberlite consists of large 1-20 cm single crystals (megacrysts) of Mg ilmenite, Cr-poor titanian pyrope, calcic to sub-calcic diopside, enstatite, phlogopite and zircon (Mitchell, 1986). Fragments of the megacrysts are termed macrocrysts. Opinions differ as to a xenocryst or cognate origin of the discrete nodule suite. Boyd and Nixon (1975) believe the xenocrysts crystallize from a 'crystal mush magma' that was sampled by the kimberlite during ascent. Gurney et al (1979) and Harte and Gurney (1981) interpret the megacrysts as products of isobaric crystallization from a protokimberlite magma and Mitchell (1977, 1979) invokes a cognate high pressure origin for the megacrysts. The 'crystal mush' and protokimberlite magmas may be genetically related to the kimberlite magma. A better understanding of the phase equilibria in kimberlitic systems is required to constrain the origin of these megacrysts.

Subhedral-to-euhedral phenocrysts and microphenocrysts of olivine, phlogopite and chromite are the primary liquidus phases in kimberlite. Groundmass minerals include olivine, phlogopite, Ti-bearing spinels and trace perovskite, zircon, barite, monticellite, apatite, calcite and serpentine.

Description of the Torrie, Sputnik and Eddie kimberlites

The kimberlites from the Torrie, Sputnik and Eddie pipes are hybrid rocks with crystals originating from disaggregated upper mantle and crustal xenoliths, discrete nodule suites, and primary phenocryst phases. Well preserved upper mantle xenoliths, found only within the Torrie pipe, include coarse-grained garnet websterite and eclogite. Crustal xenoliths (i.e. granulite) are found throughout the three pipes although their preservation is variable. Chrome diopside and chrome pyrope xenocrysts from disaggregated lherzolite xenoliths, megacrysts and macrocrysts from the discrete nodule suite are found in both Torrie and Sputnik although macrocrysts are best preserved and most abundant in the Torrie pipe. The Eddie pipe contains predominantly serpentinized olivine macrocrysts, spinel phenocrysts, and groundmass phlogopite and oxides.

The textural genetic classification of Clement and Skinner (1979) and Clement (1982), as modified by Mitchell (1986), is used to classify the Torrie and Sputnik pipes as diatreme facies macrocrystic garnet and diopside, heterolithic, volcaniclastic kimberlite breccias (> 15% volume of clasts > 4mm) and the Eddie pipe as macrocrystic olivine, heterolithic, volcaniclastic kimberlite breccias. The kimberlites have an overall well-mixed homogeneous appearance even though there are abundant heterogeneous fragments.

Torrie, the best preserved of the three pipes, is a dark gray-black kimberlite (Fig.3.2 and 3.3). It contains 10-25% megacrysts (rounded crystals > 1cm) and 20-25% macrocrysts (rounded-anhedral crystals 5-10mm) of garnet (Fig. 3.2a), olivine (Fig. 3.2b), Cr diopside (Fig. 3.2c & d), two well preserved mantle xenoliths (a sub-rounded garnet websterite; Fig. 3.2e and an angular eclogite; Fig. 3.2f), carbonized wood fragments (Fig. 3.2f), second generation euhedral olivine phenocrysts (Fig. 3.4a), several autoliths (Fig. 3.3a & 3.4b) and several small (up to 3.5 cm) angular to rounded crustal country rock xenoliths (Fig. 3.3e) set in a fine grained microcrystalline matrix of predominantly serpentine, secondary calcite and clay minerals. At a drill core depth of approximately 549 feet, the Torrie pipe grades downward from a macrocrystic volcaniclastic kimberlite breccia to a megacrystic volcaniclastic kimberlite breccia that may represent a transition from diatreme to hypabyssal facies (compare Fig. 3.2 to Fig. 3.3b, c & d). There are abundant strongly altered mantle xenoliths (Fig. 3.3e), angular crustal xenoliths (Fig. 3.3e & 3.4c) and fragments of quartz, feldspar (Fig. 3.4d) and biotite, strongly serpentinized olivine macrocrysts (Fig. 3.5a & b), olivine and orthopyroxene neoblasts (Fig. 3.5c & d), possible magmatic segregation textures (Fig. 3.6a) and the groundmass decreases from approximately 50% to 10% by volume. Serpentinization is represented by the fine-

grained, microcrystalline groundmass, fine-grained alteration of olivine as well as radiating crystals on macrocrystic olivine rims (Fig. 3.5b).

The moderately altered Sputnik kimberlite pipe is a dark greenish-gray kimberlite that contains 15% macrocrysts (olivine, diopside, garnet and chromite), several megacrystic garnet and Cr diopside xenocrysts (Fig. 3.6b & c) and second generation, euhedral olivine and minor phlogopite set in a dark brown-black segregation-textured groundmass of serpentine, clay minerals and oxides (Fig. 3.7). Pelletal lapilli (Fig. 3.6d, 3.7a & b) have fragmented serpentinized olivine macrocrysts at their cores surrounded by euhedral phenocrystic olivine, oxides and groundmass serpentine. Several autoliths (Fig. 3.7c & d), strongly serpentinized mantle xenoliths, a crustally-derived (feldspar + pyroxene) xenolith (Fig. 3.6c) and wood fragments are also present in Sputnik. The presence of wood fragments and pelletal lapilli confirms that the sampled sections of the Sputnik pipe represent the diatreme facies.

The Eddie pipe is 80% altered to serpentine and clay minerals (Fig. 3.8a), which makes classification difficult; however, it does contain groundmass high Ti-spinels that are characteristic of kimberlites. It contains 20-25% macrocrystic olivine, most of which are serpentine pseudomorphs after subhedral to rounded olivine, and relatively well-preserved crustal xenoliths set in a dark gray-black groundmass of chromite, spinel, ilmenite, trace phlogopite and secondary carbonates and clay minerals (Fig. 3.8b). The groundmass has localized segregation textures. The oxides are also found as inclusions in olivine. It is not clear whether the Eddie pipe represents diatreme or hypabyssal facies, however, the presence of an unmetamorphosed pyroxenite xenolith, abundant autoliths (Fig. 3.8c & d) and wood fragments are consistent with a diatreme origin.

Figure 3.2 The Torrie pipe is a macrocrystal volcaniclastic kimberlite breccia with a) garnet megacrysts b) olivine macrocrysts c) clinopyroxene macrocrysts d) clinopyroxene megacrysts e) peridotite (websterite) xenolith and f) eclogite xenolith (E) and wood fragments (W). Photos a-f represent increasing depth (193 ft-509 ft).
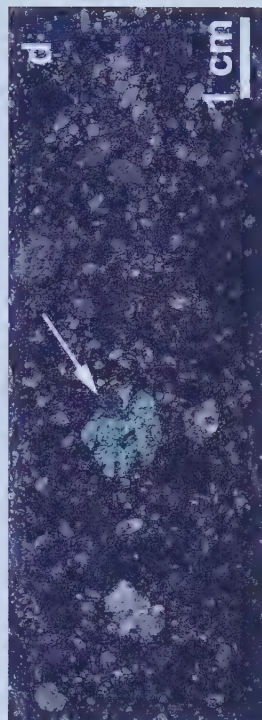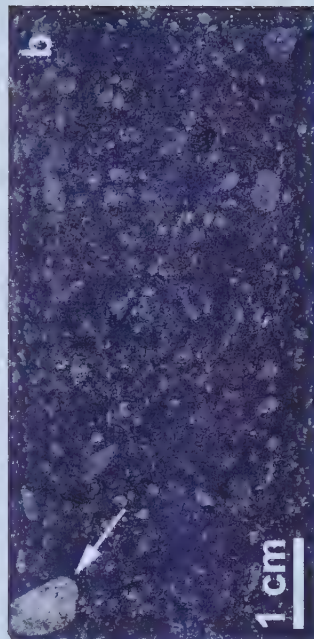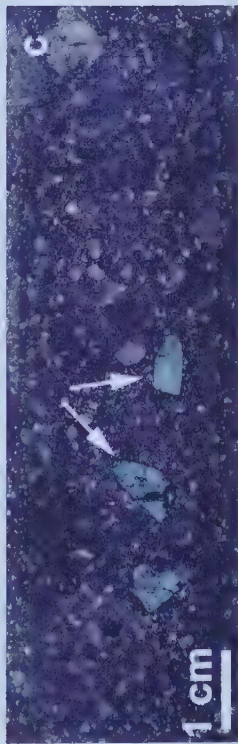
Figure 3.3 Photos a-e represent increasing depth (547 ft- 577 ft) in Torrie pipe.
a) autolith b) macrocrystal hypabyssal kimberlite breccia
c) hypabyssal-facies kimberlite with arrow indicating large crustal
xenolith d) hypabyssal facies kimberlite with abundant garnet (red)
and chrome diopside (bright green) and olivine (pale green)
e) altered mantle (M) and crustal (C) xenoliths. (FOV=2.4X1.7mm)

a   b   c   d   e

1 cm

C   M   M
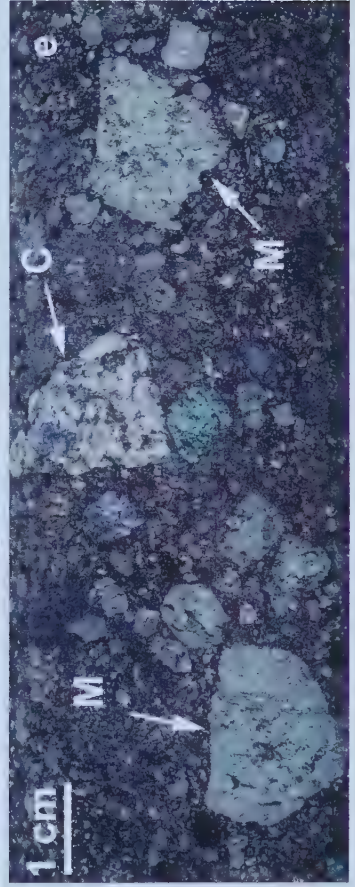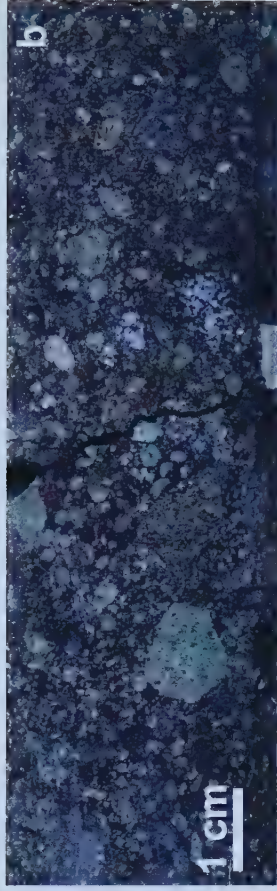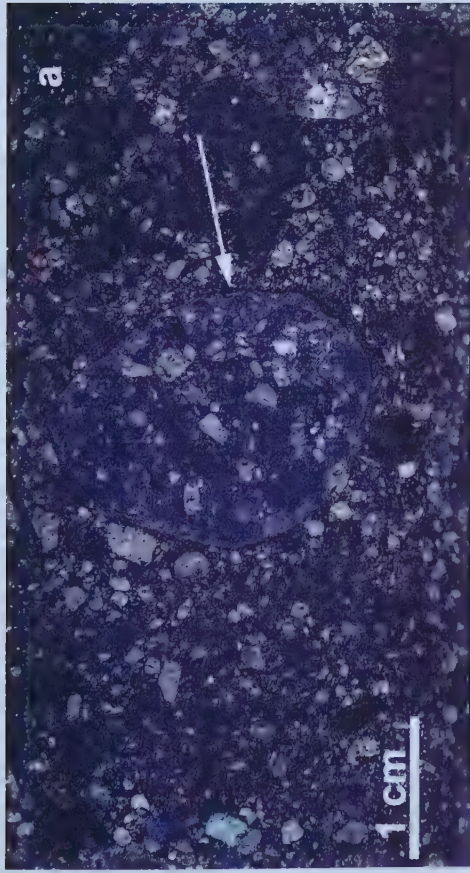
Figure 3.4   Torrie pipe a) first generation macrocryst (M) and second generation
            euhedral (E) olivine in the Torrie pipe b) autolith c) crustal xenolith
            with symplectic garnet (worm-like texture indicated by arrow)
            d) feldspar xenocryst (metamorphic basement) at core of autolith
            (FOV=2.4X1.7mm).
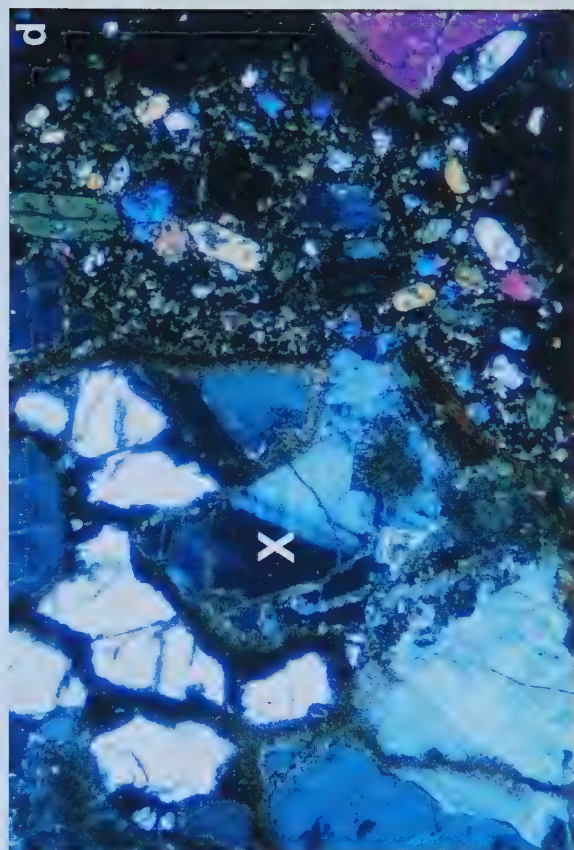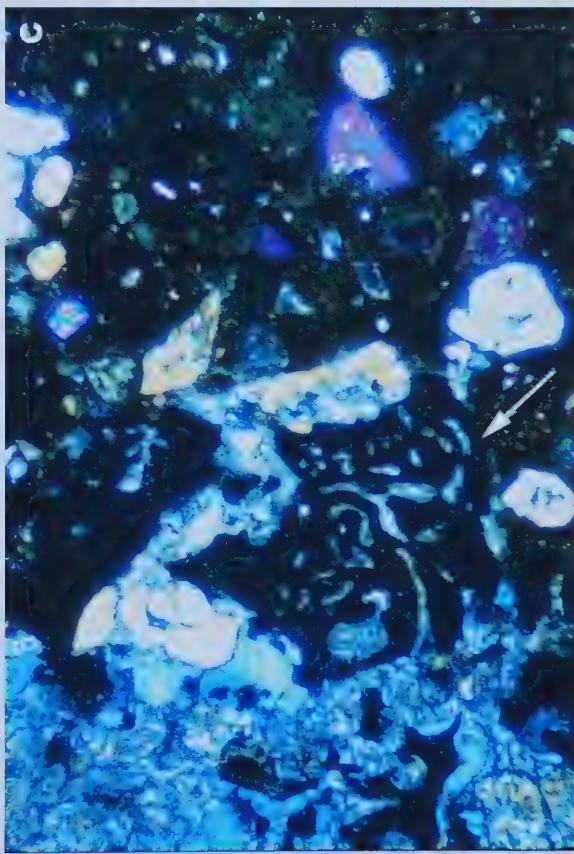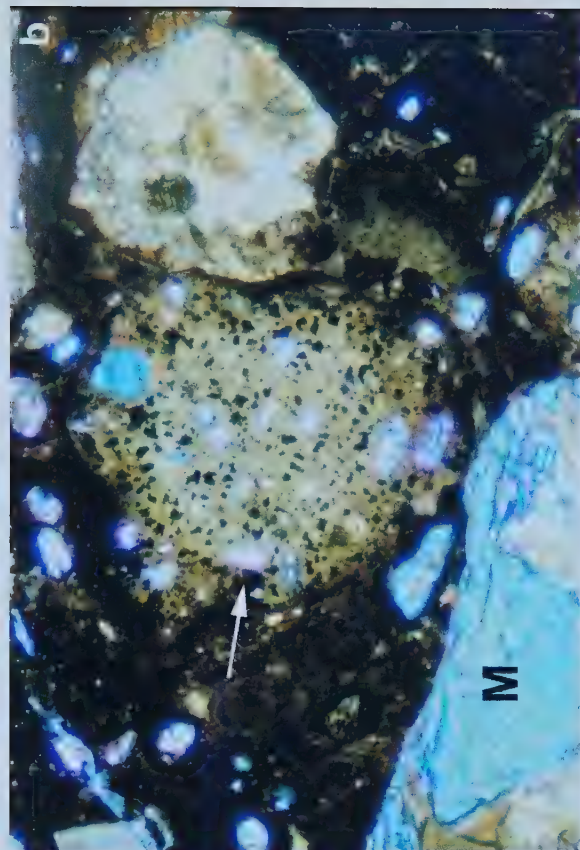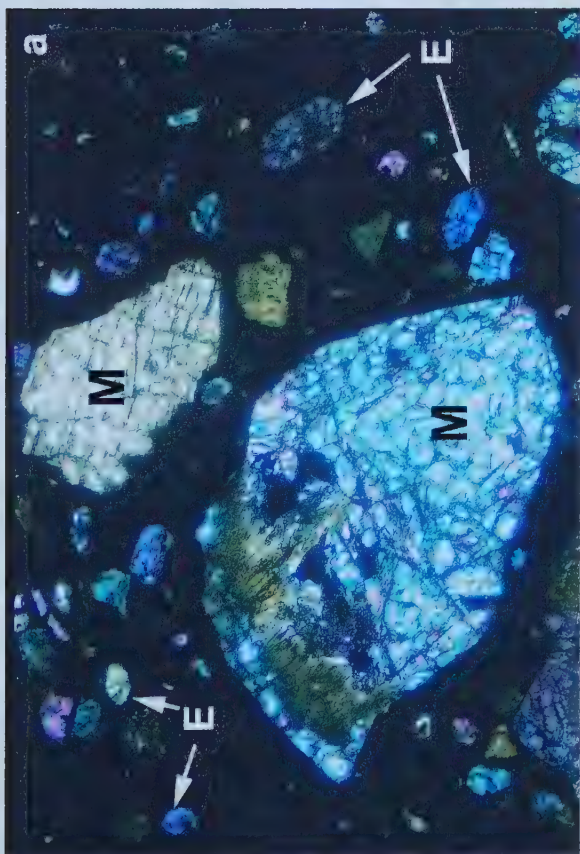
Figure 3.5 Torrie pipe a) strongly serpentinized olivine macrocrysts
b) serpentinized olivine (M) with radiating serpentine crystals
c) olivine and orthopyroxene neoblasts and d) olivine neoblasts
(FOV=2.4X1.7mm).
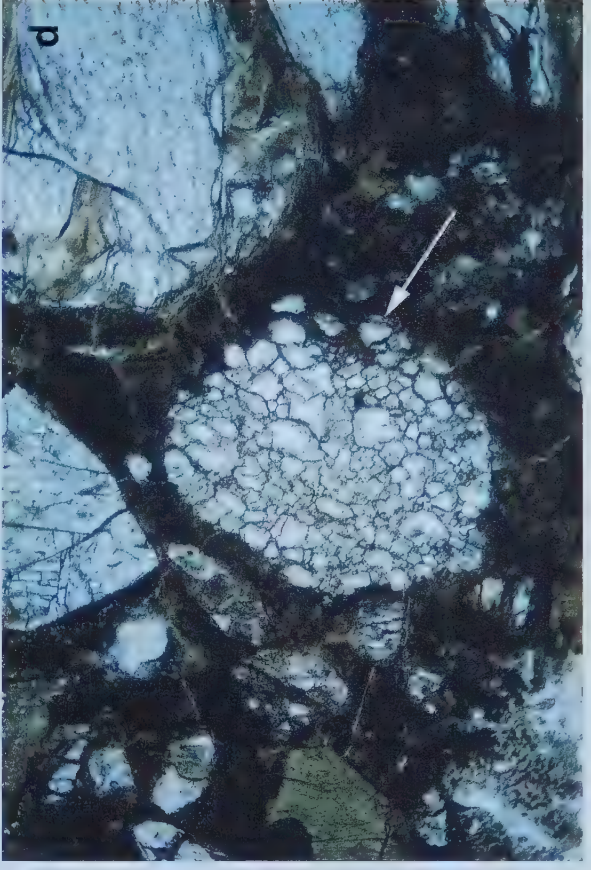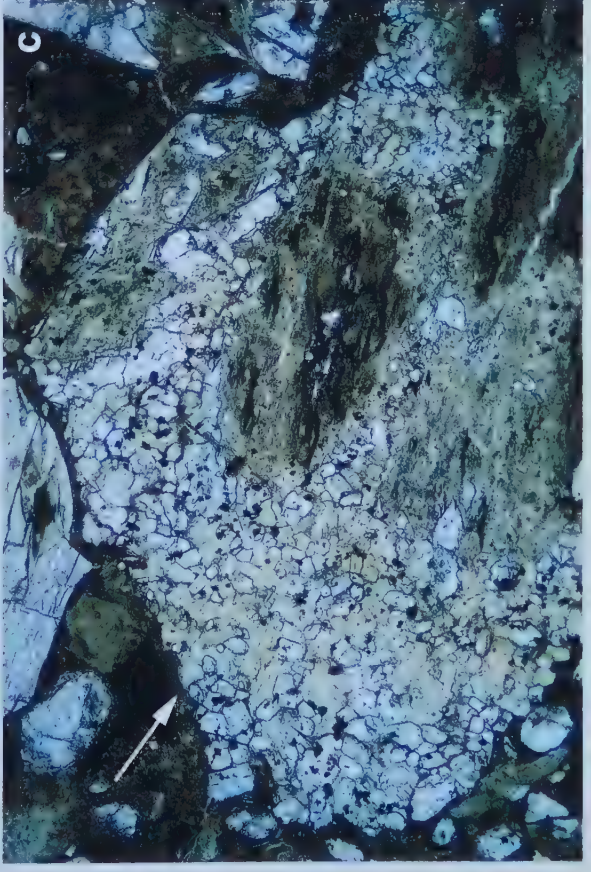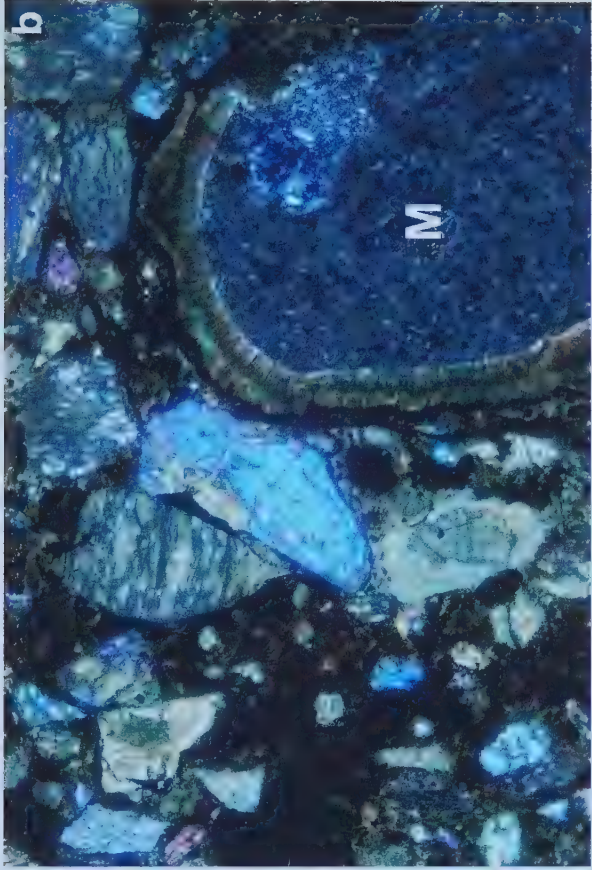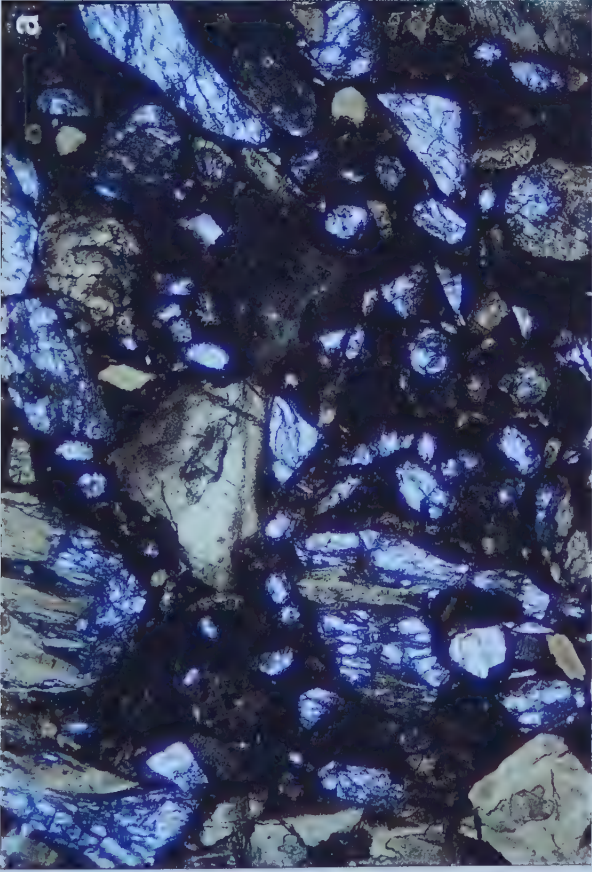
Figure 3.6   a) Irregularly shaped magmatic segregations in the Torrie pipe
             (depth=577 ft). Note the very small volume of groundmass
             b) Sputnik kimberlite pipe c) Cr-diopside megacryst (M) and crustal
             xenolith in Sputnik d) pelletal lapilli with clinopyroxene core
             (FOV=2.4X1.7mm).

1 cm
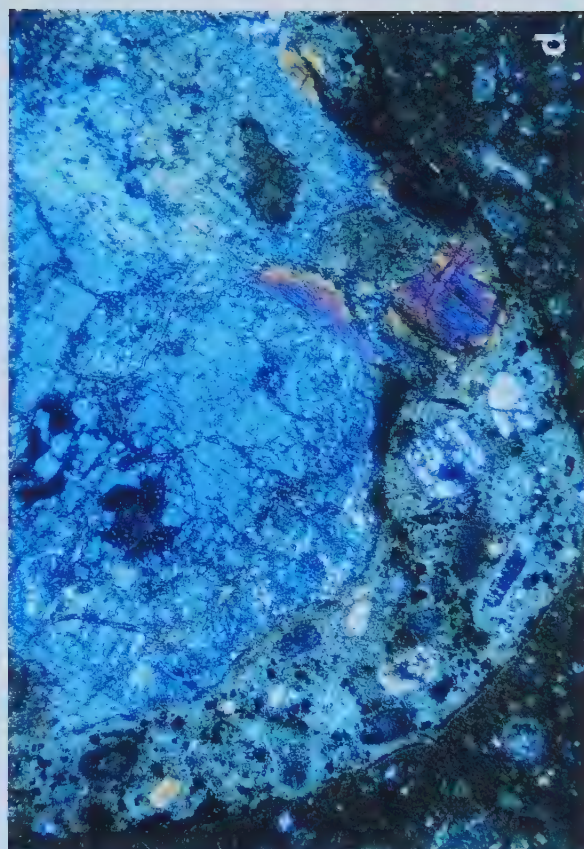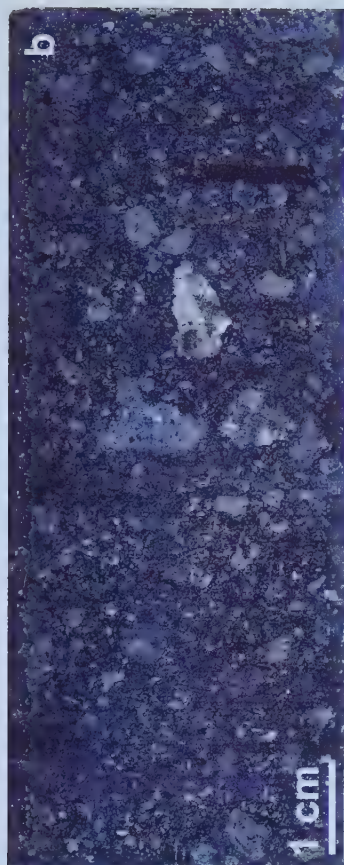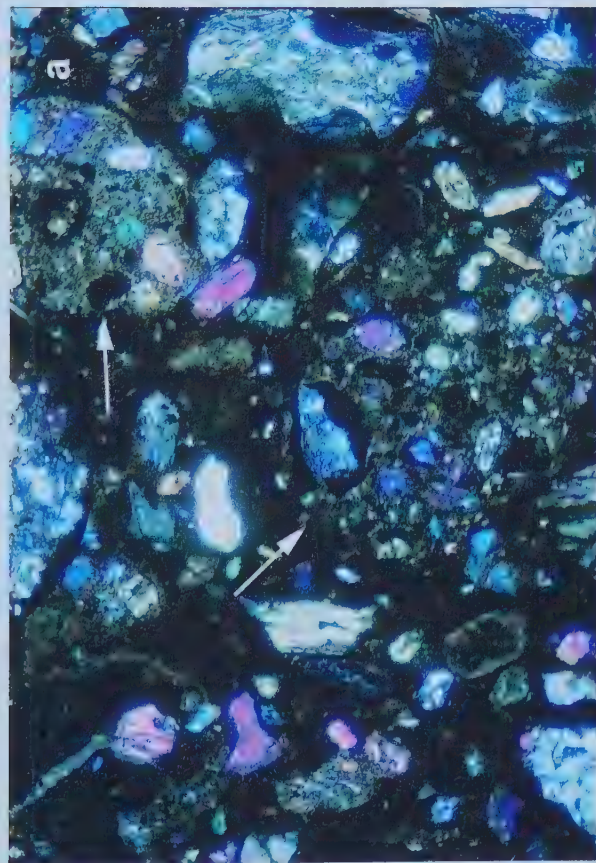
Figure 3.7   Sputnik pipe a) pelletal lapilli with olivine core b) pelletal lapilli
            c) autolith d) autolith (FOV=2.4X1.7mm).
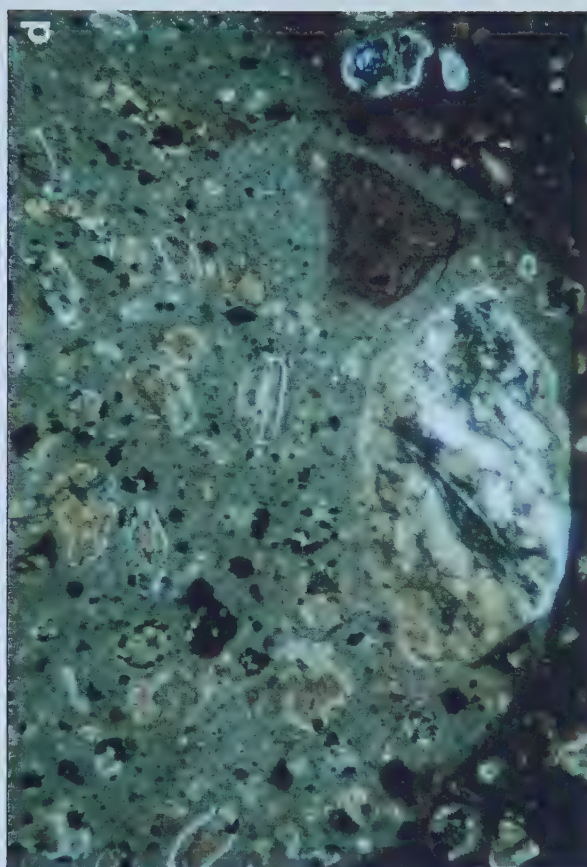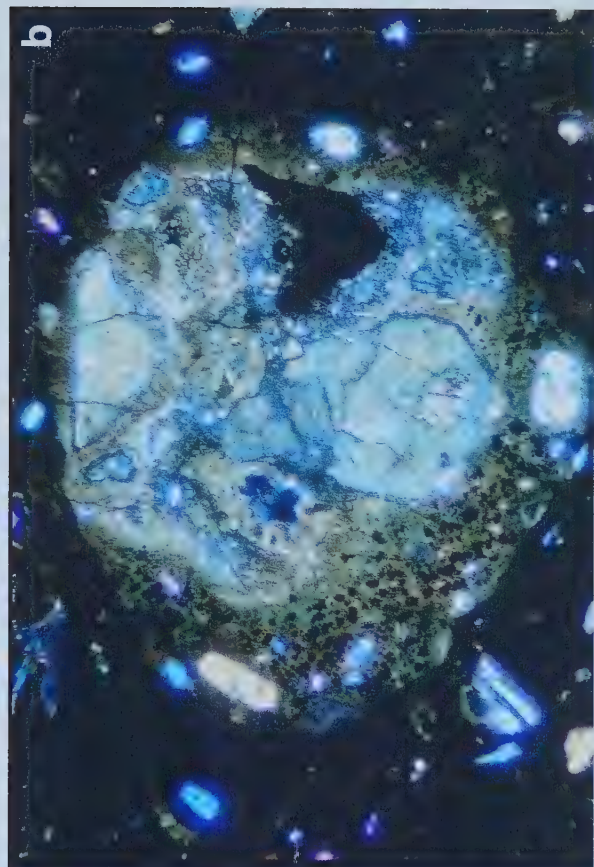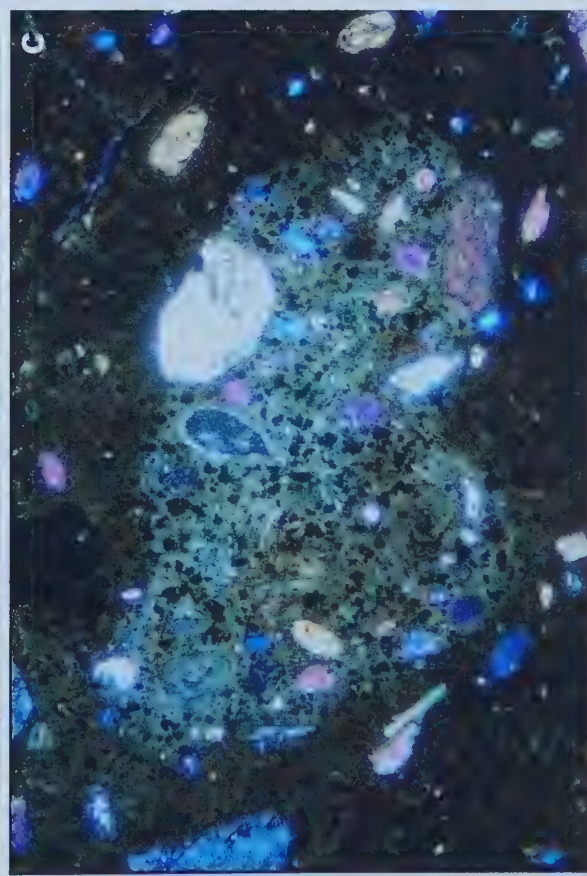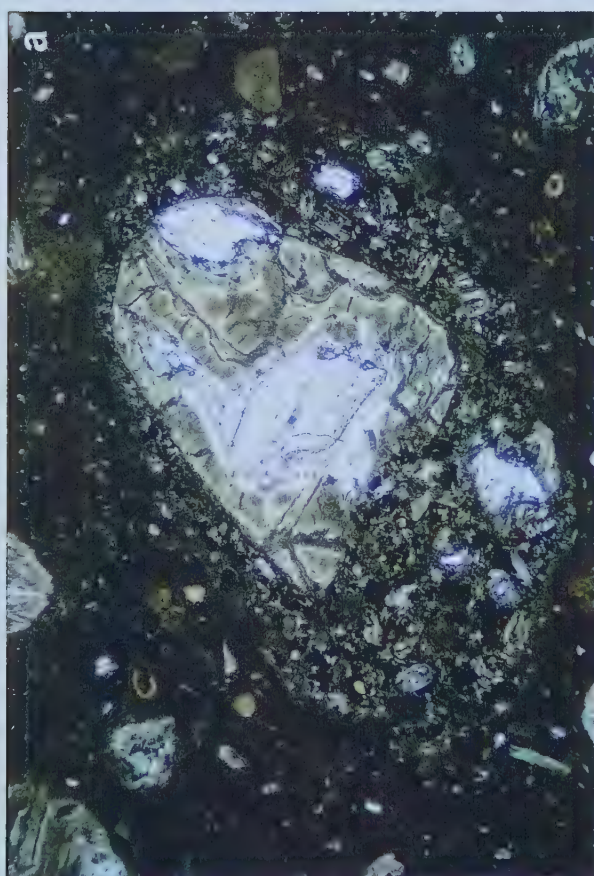
Figure 3.8 Strongly altered Eddie kimberlite pipe a) altered mantle xenolith
b) segregation-textured autolith in a groundmass of chromite, spinel,
ilmenite, phlogopite and secondary carbonates and clay minerals
c) autolith d) autolith (FOV=2.4X1.7mm).

1 cm
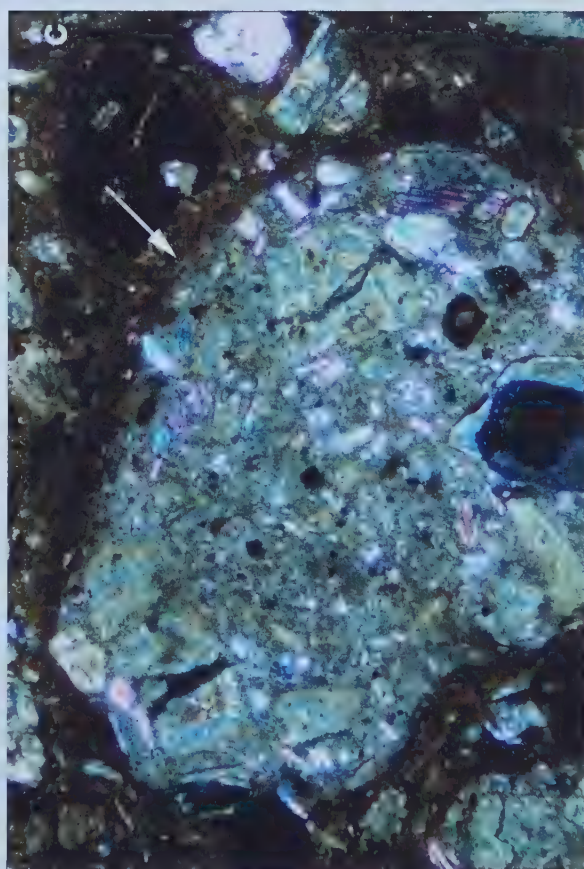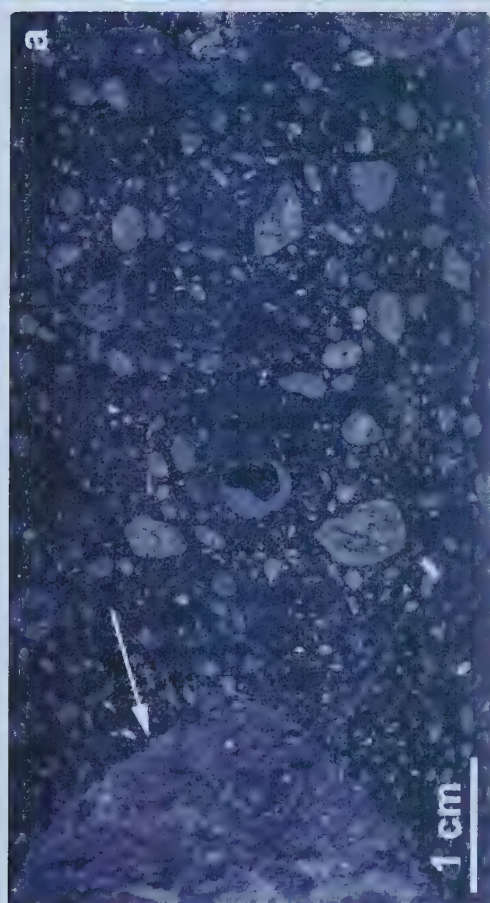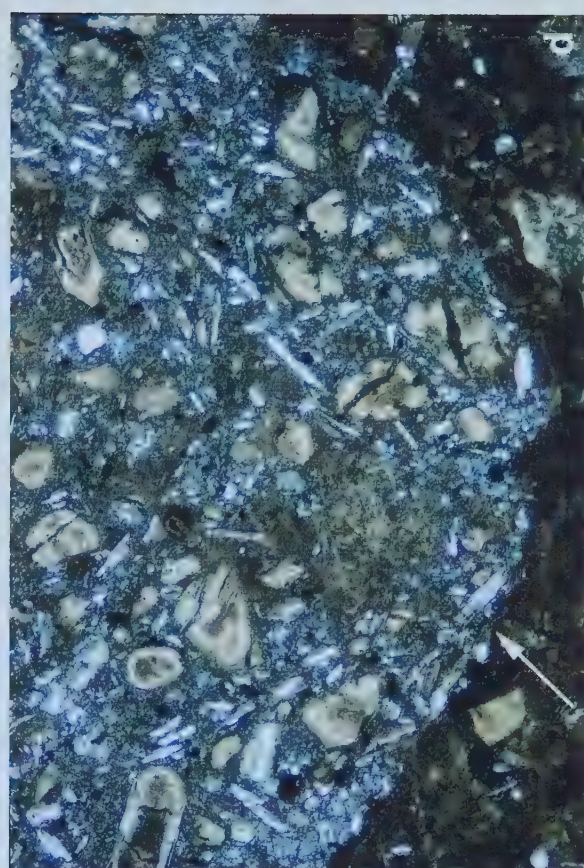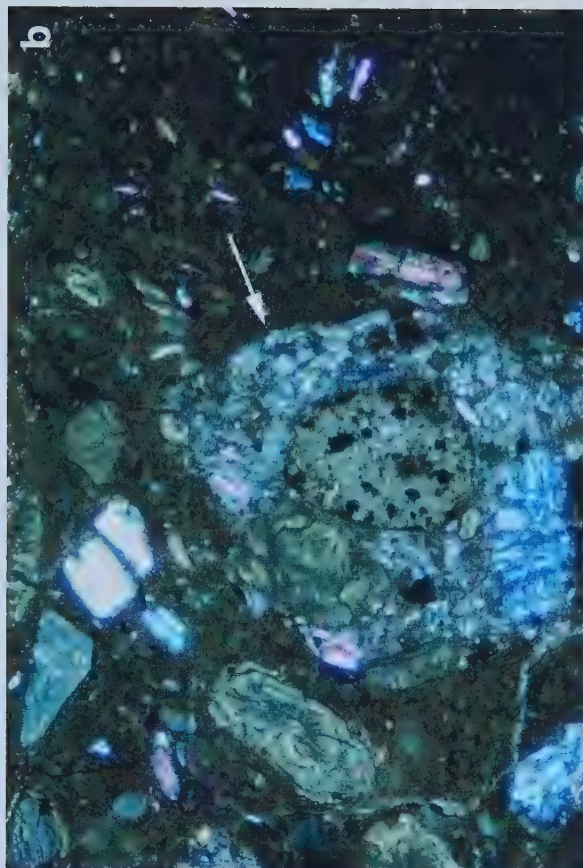
Chapter 4

Major-element mineral chemistry

Analytical methods

Major element compositions of minerals were analyzed at the University of Alberta on a JEOL JXA-8900R electron microprobe using four wavelength-dispersive spectrometers. All analyses, except micas, were obtained with a 15 kV beam accelerating potential, 15 nA beam current measured on a Faraday cup, a 3 μm beam diameter and a 20 second count time on peaks. Micas were analyzed with the same accelerating potential and beam current with a 0 and 1μm beam diameter because of their small size.

Representative major-element analyses of olivine, pyroxene, garnet, mica, spinel and ilmenite are shown in Tables 4.1-4.7. Standards are listed in Appendix A. Major-element compositions of 180 olivine, 117 garnet, 182 clinopyroxene, 29 orthopyroxene, 40 mica, 107 spinel and 131 ilmenite from heavy mineral concentrates and thin sections are shown in Appendix B: Table 1-7. Olivine, garnet, orthopyroxene, clinopyroxene (excluding 3 megacrysts in Sputnik and Eddie) and mica analyses are based on one point per grain. Spinel and ilmenite analyses, however, represent both discrete crystals and center-rim pairs (see Appendix). Not all analyses may represent the true core of the crystals because the plane of the thin section may not intersect the core of the grain, and some of the grains are broken. This causes some problems when trying to interpret the mineral data as analyses on individual fragmented grains may actually represent within grain variations from a single grain.

Olivine

Olivine, the most common mineral of the Torrie, Sputnik and Eddie kimberlite pipes, has three types of occurrence (Mitchell, 1986) giving the kimberlite a characteristic inequigranular texture: euhedral-to-subhedral microphenocrysts (<0.3 mm) and phenocrysts (0.3-3 mm), rounded and fragmented macrocrysts (3-10mm; interpreted as disaggregated xenoliths) and rare megacrysts (>1cm; interpreted as part of the discrete nodule suite). Olivines exhibit various degrees of alteration ranging from minor serpentinization or chloritization to complete alteration and pseudomorphism by

serpentine and carbonate minerals. Olivine in the Eddie pipe is nearly completely altered and was not analyzed.

Petrographically, it is difficult to distinguish between olivines that are resorbed phenocrysts and those derived from disaggregation of ultramafic xenoliths (macrocrysts). The macrocrysts are rounded or fragmental and commonly show signs of reactions with the groundmass at their margins. Several rounded macrocryst olivines are embayed and corroded as a result of absorption. In the Torrie pipe, rare crystals are strained, display undulose extinction or have mosaic-textured recrystallized olivines (neoblasts; Fig. 3.5d). These are plausibly derived from deformed peridotite xenoliths.

Representative olivine compositions of discrete crystals for Torrie and Sputnik are given in Table 4.1a & b. The histograms in Figure 4.1 show a relatively wide compositional distribution in the kimberlite olivine populations (Fo_{86-95}), however, Sputnik ($Fo_{89.1-93.4}$) has a more restricted range in Fo contents than Torrie ($Fo_{86-94.4}$). The majority of olivines in both pipes have core compositions between Fo_{91-93}. Olivine compositions from the garnet websterite xenolith (Fo_{90-91}) are also shown for comparison (Fig. 4.1c).

Combined petrographic and geochemical studies indicate that the phenocryst, xenocryst and megacryst populations overlap; however, there are several groupings that may represent several olivine populations. Three distinct groups in Sputnik and Torrie can be distinguished from each other based on Fo contents (Table 4.1a and Figures 4.2 and 4.3). The gap between the groups most likely results from a lack of olivine analyses.

Table 4.1a. Olivine groups in Torrie and Sputnik based on Fo contents.

| Group | Fo [$Mg/(Mg+Fe^{2+}_T)$] | | Origin |
	Torrie	Sputnik	
1	86-89.2	<90.0	Late crystallizing groundmass phase
2	89.5-93.3	90.5-93.5	Phenocrysts and peridotite xenocrysts
3	>94	none	Rare high pressure macrocrysts and early crystallizing phenocrysts

The olivine groups are characterized by different geochemical features that reflect the different crystallization environments. Chemical variation plots of NiO, Cr_2O_3, MnO, TiO_2

Table 4.1b. Representative olivine microprobe analyses (Cations on basis of 4 oxygen).

	Torrie-193	Torrie-570	Torrie 509	Torrie-508	Torrie-508	Torrie-193	Torrie-508	Torrie-193	Sputnik-513	Sputnik-513	Sputnik-365	Sputnik-513	Sputnik-513
SiO_2	39.82	40.08	40.19	40.99	40.78	41.11	41.02	41.39	40.52	40.60	40.94	41.05	41.48
TiO_2	0.05	0.03	0.00	0.06	0.00	0.00	0.25	0.02	0.06	0.00	0.00	0.02	0.00
Al_2O_3	0.00	0.01	0.01	0.00	0.00	0.01	0.15	0.00	0.01	0.03	0.03	0.02	0.00
Cr_2O_3	0.00	0.03	0.03	0.09	0.06	0.04	0.02	0.00	0.01	0.04	0.07	0.05	0.00
FeO_T	13.55	11.31	11.00	8.80	7.56	7.31	5.87	5.70	10.65	8.65	8.34	8.15	6.63
MnO	0.16	0.13	0.12	0.11	0.12	0.08	0.18	0.06	0.17	0.13	0.13	0.10	0.09
MgO	46.70	47.41	48.32	50.24	51.70	51.86	51.78	53.49	49.14	50.34	50.03	50.82	52.61
CaO	0.00	0.02	0.03	0.10	0.04	0.01	0.25	0.00	0.04	0.03	0.07	0.03	0.00
NiO	0.31	0.10	0.22	0.29	0.37	0.36	0.02	0.33	0.15	0.21	0.31	0.29	0.22
Na_2O	0.02	0.02	0.04	0.03	0.02	0.01	0.02	0.02	0.02	0.00	0.03	0.02	0.01
Total	100.60	99.14	99.94	100.72	100.66	100.78	99.56	101.01	100.77	100.02	99.95	100.54	101.05
Si	0.989	0.998	0.992	0.994	0.986	0.990	0.993	0.988	0.990	0.991	0.998	0.994	0.992
Ti	0.001	0.001	0.000	0.001	0.000	0.000	0.005	0.000	0.001	0.000	0.000	0.000	0.000
Al	0.000	0.000	0.000	0.000	0.000	0.000	0.004	0.000	0.000	0.001	0.001	0.001	0.000
Cr	0.000	0.001	0.001	0.002	0.001	0.001	0.001	0.000	0.000	0.001	0.001	0.001	0.000
Fe^{2+}	0.150	0.236	0.225	0.179	0.153	0.182	0.119	0.142	0.218	0.177	0.170	0.165	0.133
Mn	0.003	0.003	0.002	0.002	0.002	0.002	0.004	0.001	0.003	0.003	0.003	0.002	0.002
Mg	1.729	1.760	1.779	1.817	1.863	1.862	1.868	1.903	1.790	1.832	1.819	1.835	1.876
Ca	0.000	0.001	0.001	0.003	0.001	0.000	0.007	0.000	0.001	0.001	0.002	0.001	0.000
Ni	0.006	0.002	0.004	0.006	0.007	0.007	0.000	0.006	0.003	0.004	0.006	0.006	0.004
Na	0.001	0.001	0.002	0.001	0.001	0.000	0.001	0.001	0.001	0.000	0.001	0.001	0.000
Total	2.880	3.002	3.006	3.004	3.014	3.044	3.001	3.041	3.009	3.008	3.001	3.005	3.008
Forsterite	86.01	88.20	88.68	91.05	92.42	92.68	94.02	94.37	89.16	91.21	91.45	91.75	93.39
Fayalite	13.99	11.80	11.32	8.95	7.58	7.32	5.98	5.63	10.84	8.79	8.55	8.25	6.61
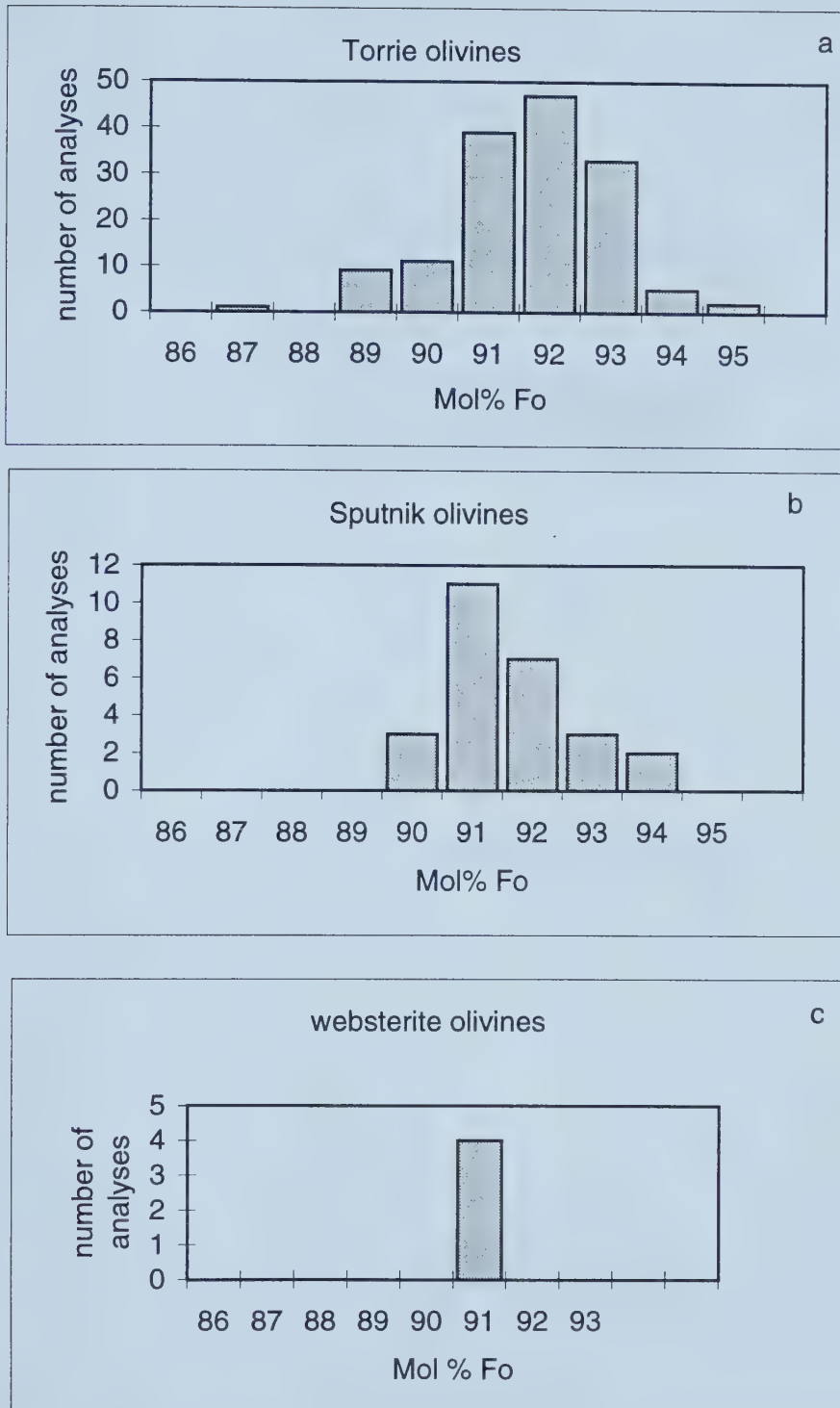
Figure 4.1 Histograms of mol% Fo [Mg/(Mg+Fe)] contents in phenocryst, xenocryst and megacryst olivines from a) Torrie b) Sputnik and c) garnet websterite xenolith.
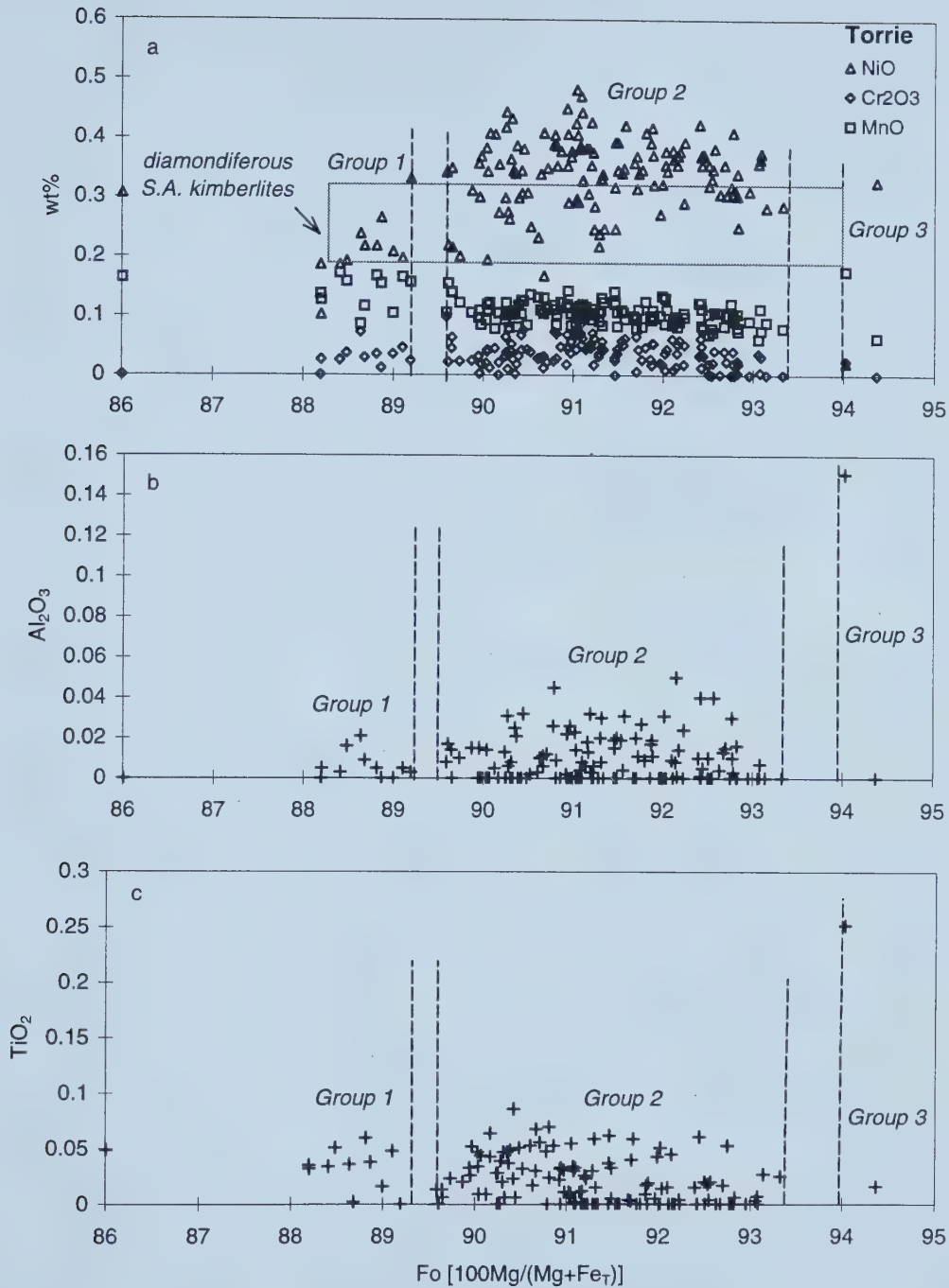
Figure 4.2. Chemical variation plots of Fo versus Cr_2O_3, MnO, NiO, Al_2O_3 and TiO_2 for Torrie olivine. Rectangle indicates the NiO vs. Fo contents for phenocrystic olivine in diamondiferous kimberlites from South Africa (Moore, 1988). Group 1 is a late crystallizing groundmass phase. Group 2 are phenocrysts and peridotite xenocrysts. Group 3 contains rare high temperature megacrysts and early crystallizing phenocrystic olivine.
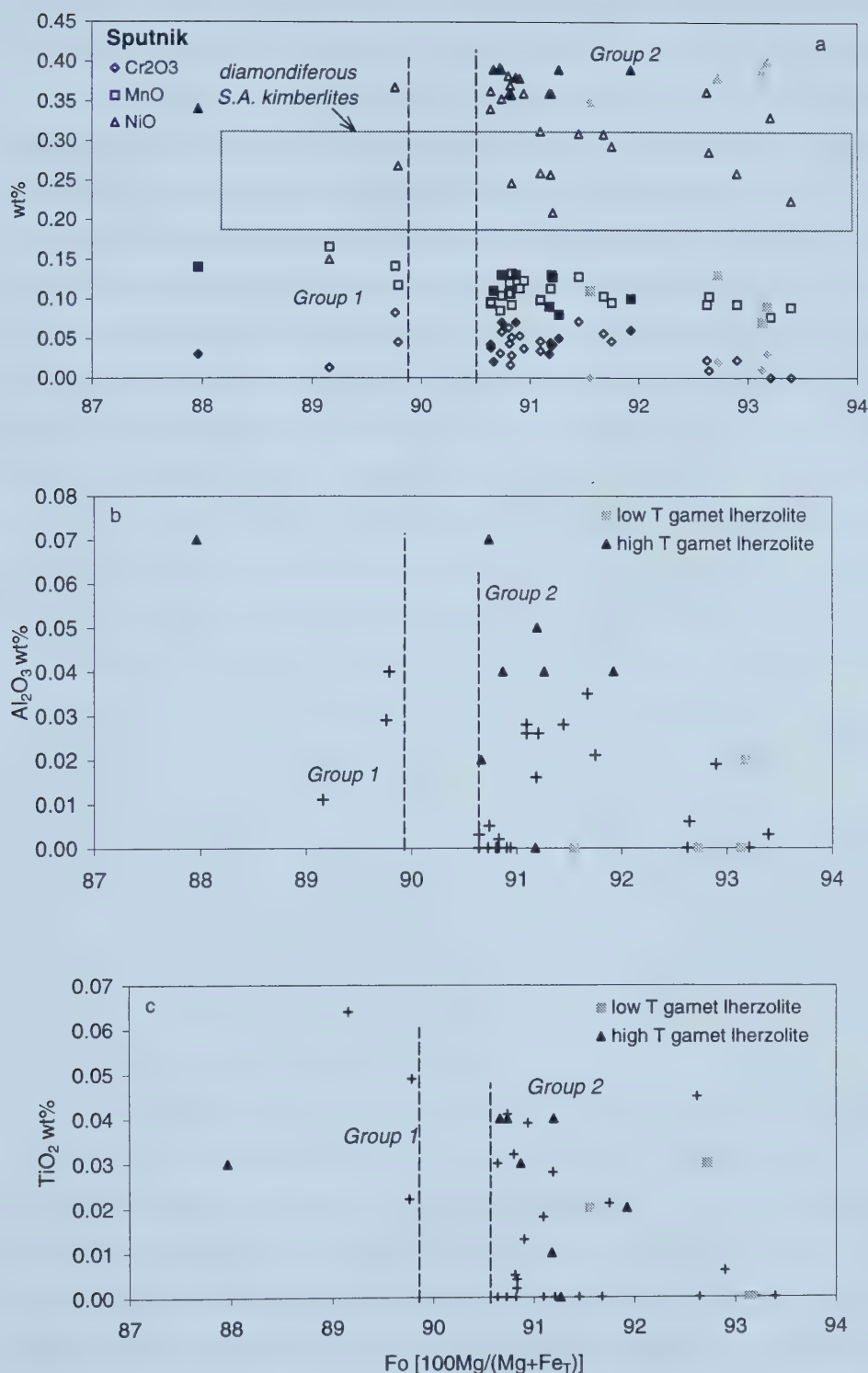
Figure 4.3. Chemical variation plots of Fo versus Cr_2O_3, MnO, NiO, Al_2O_3 and TiO_2 for Sputnik olivine compared to olivine in garnet lherzolites from South African kimberlites. Samples are from Luth et al (1990). Filled symbols are garnet lherzolite (gray=low temperature; black=high temperature). Group 1 is a late crystallizing groundmass phase. Group 2 are phenocrysts and peridotite xenocrysts. Rectangle indicates the NiO vs. Fo contents for phenocrystic olivine in diamondiferous kimberlites from South Africa (Moore, 1988).

and Al_2O_3, versus Fo contents for Torrie and Sputnik are shown in Figures 4.2 and 4.3. There are no apparent inter-element trends within the groups in Sputnik and Torrie.

The olivines from Group 2 (Fo ~89.5-92) in Torrie and Sputnik represent first (phenocrysts) and second (microphenocrystic groundmass) generation olivine and xenocrysts derived from disaggregated high and low temperature garnet lherzolites. Phenocrystic olivine from diamondiferous South African kimberlites (Moore, 1988) have a large range in Fo (88.3-94) and relatively low NiO contents (~0.2-0.3 wt%) and are shown for comparison in Figure 4.3. Mitchell (1978a, 1986) also suggests that olivine less magnesian than Fo_{91} probably crystallized from the kimberlite magma. Olivine from high- and low-temperature garnet lherzolite xenoliths (Luth et al, 1990) from South African kimberlites are also shown for comparison in Figure 4.2a and 4.3a. The olivines from the garnet lherzolite xenoliths have higher NiO (>0.34 wt%) than the phenocryst and groundmass olivine. The more iron-rich, Group 1 olivines in Torrie and Sputnik are interpreted to represent a late crystallizing groundmass phase.

The more refractory olivine compositions (Fo>93, low NiO, Cr_2O_3) in Sputnik and Torrie plausibly represent first generation macrocrysts and megacrysts of either phenocrystic or xenocrystic origin that crystallized within the upper mantle. Diamondiferous kimberlites from South Africa have more refractory phenocrystic olivines (Fo_{94}; Figure 4.2a and 4.3a) whereas the most refractory olivines in barren kimberlites from South Africa and Kentucky, USA are close to or below Fo_{92} (Moore, 1988). The Torrie kimberlite was also capable of crystallizing high magnesian olivine similar to diamondiferous South African kimberlites as a small, euhedral phenocrystic olivine from Torrie also has a high Fo content (Fo_{93}).

An unusually high magnesian olivine (Fo_{94}) with corresponding very high Al_2O_3 (0.15%), MnO (0.18%), CaO (0.25%) and TiO_2 (0.25%), very low NiO (0.02%) and low Cr_2O_3 (0.02%) was analyzed from the Torrie pipe (Fig. 4.2). Agee and Walker (1990) have shown experimentally that Al_2O_3 increases with pressure and temperature while MnO and Cr_2O_3 decrease with increasing temperature in olivine from komatiite and peridotite at pressures of 2.5-6 GPa and temperatures of 1650-1960 °C. NiO also shows a similar negative correlation with temperature, however, there is larger scatter in their data. According to Agee and Walker (1990), olivine can accept up to 0.2% Al_2O_3 but only at pressures greater than 6 Gpa. The very high Al_2O_3, low NiO and Cr_2O_3 are consistent with high-pressure crystallization (Agee and Walker, 1990). It follows that the

unusual Torrie macrocrystic olivine has a higher pressure origin than other olivines found within the pipe.

The large range in compositions of the phenocryst and groundmass minerals implies that either a) olivine is a ubiquitous mineral and crystallized out of an evolving magma b) the groundmass olivine resulted from mixing of different batches of magma (Mitchell, 1986) or c) not all analyses may represent the true core (most Mg-rich) of the grain because the plane of the thin section did not intersect the core of the grain.   The olivine phenocrysts and groundmass from the Torrie and Sputnik kimberlites have typical kimberlite compositions when compared to other analyses in the literature (Mitchell, 1986, 1995; Kostrovitskiy and Fiveyskaya, 1983; and Moore, 1988).

In summary, the olivine in Torrie and Sputnik has several origins. Group 1 is interpreted to be a late crystallizing groundmass phase. Group 2 olivines are first and second generation phenocrysts and xenocrysts from disaggregated peridotite xenoliths. Group 3 is interpreted as rare high temperature megacrysts and early crystallizing phenocrysts.   The large scatter in the data can be attributed to the different origins for the olivines and the uncertainty in analyzing true core compositions.

Garnet

Garnet has been found to be the most important discriminant in assessing the diamond potential of a kimberlite (Fipke et al., 1995). In the peridotitic (chrome rich) diamond paragenesis, there are three recognized potentially diamondiferous sources: garnet harzburgite, chromite harzburgite and garnet lherzolite (in order of decreasing importance with respect to diamonds; Gurney 1984). Therefore, it is important to distinguish between garnets from a lherzolite source (usually barren) and a harzburgite source (potentially diamondiferous).   As a general rule, the greater the abundance of macrocrysts (garnet, pyroxene, chromite etc.) from disaggregated, potentially diamondiferous mantle rocks in a kimberlite pipe, the higher the grade may be.

Of the pipes studied here, only the Torrie and Sputnik pipes contain garnet. In these pipes, garnet occurs as large rounded macrocrysts (0.5-1 cm) and megacrysts (1-2 cm). The macrocrysts range in color from pale orange, reddish orange, pink to deep orange whereas the megacrysts are usually a deep red to purple color. Macrocrysts are commonly fragmented and fractured.   Several rounded macrocryst garnets have rare kelyphitic mantles. Fragments > 5 mm most likely reflect a megacryst origin.

There are a number of schemes that use cluster analysis or multiple component discriminant analyses of compositions used to classify garnets according to their source rocks (Dawson and Stevens, 1975; Danchin and Wyatt, 1979; Jago and Mitchell, 1989). Dawson and Stevens (1975), the most widely used classification scheme, classified macrocryst garnets from kimberlite into 12 groups (Table 4.2a).

Table 4.2a. Macrocrystic garnet classification (Dawson and Stephens, 1975).

Group	Name	Source
1	Ti-pyrope	Sheared lherzolite, megacrysts
2	High Ti-pyrope	Megacrysts
3*	Ca-pyrope almandine	Diamondiferous eclogite
4	Ti-Ca-Mg-almandine	Eclogite (diamond inclusions)
5	Mg-almandine	Eclogite (metamorphic basement)
6	Pyrope-grossular almandine	Peraluminous (kyanite) eclogite, diamondiferous eclogite
7	Ferro-magnesian uvarovite-grossular	Megacrysts
8	Grospydite	Kyanite eclogite
9*	Cr-pyrope	Garnet lherzolite, websterite
10*	Low Ca-pyrope	Harzburgite, dunite (diamond inclusions)
11	Ti-pyrope, Ti-Cr-pyrope, uvarovite pyrope	Megacrysts
12	Knorringitic uvarovite-pyrope	Megacrysts

* important in diamond exploration

Garnets from Torrie and Sputnik fall into six groups in the statistical classification of Dawson and Stephens (1975) i.e. groups 1,3,5,9,10,11.   Representative analyses of Torrie and Sputnik garnets from each group are shown in Table 4.2b. Chrome-pyrope xenocrysts (group 9 or G9), which are interpreted to be derived from disaggregated garnet lherzolite, typify the majority of garnet xenocrysts from the pipes (Fig. 4.4a). Lower

Table 4.2b. Representative garnet microprobe analyses. Groups are defined by Dawson and Stephens (1975) (Cations on basis of 12 oxygen).

Group	Torrie-193 1	Torrie-509 1	Torrie-457 1 (megacryst)	Torrie-509 3	Torrie-547 3	Torrie-570 5	Torrie-508 9	Torrie-547 9	Torrie-508 9	Torrie-547 10
SiO_2	40.46	41.77	40.86	39.95	39.49	38.26	40.59	41.43	41.42	41.87
Al_2O_3	19.90	20.48	19.90	22.48	22.68	20.83	18.43	19.43	21.10	20.78
Cr_2O_3	3.64	3.14	3.08	0.17	0.08	0.06	6.53	5.83	2.63	4.88
TiO_2	0.55	0.52	0.78	0.09	0.04	0.08	0.14	0.01	0.38	0.01
FeO_T	9.89	7.61	10.06	14.95	23.33	28.83	7.41	6.56	7.63	7.34
MnO	0.40	0.34	0.40	0.28	0.67	0.81	0.37	0.31	0.24	0.39
MgO	16.33	20.70	17.94	13.04	8.94	4.97	19.73	19.52	20.86	21.95
CaO	8.30	5.21	6.60	8.62	6.36	6.91	5.10	6.90	5.01	2.35
NiO	0.00	0.00	0.01	0.00	0.06	0.04	0.00	0.00	0.00	0.02
Na_2O	0.06	0.07	0.06	0.06	0.00	0.00	0.00	0.00	0.00	0.00
Total	99.52	99.82	99.68	99.64	101.66	100.80	98.29	99.99	99.27	99.58
Si	2.976	2.995	2.983	2.970	2.971	2.997	2.987	2.988	2.979	2.991
Al	1.725	1.730	1.713	1.969	2.011	1.923	1.598	1.652	1.788	1.749
Cr	0.211	0.178	0.178	0.010	0.005	0.004	0.380	0.332	0.150	0.276
Ti	0.030	0.028	0.043	0.005	0.002	0.005	0.008	0.000	0.020	0.001
Fe^{2+}	0.608	0.456	0.614	0.929	1.468	1.889	0.456	0.396	0.459	0.438
Mn	0.025	0.020	0.025	0.018	0.043	0.054	0.023	0.019	0.014	0.024
Mg	1.790	2.212	1.953	1.445	1.003	0.581	2.164	2.099	2.237	2.337
Ca	0.654	0.400	0.516	0.686	0.513	0.580	0.402	0.533	0.386	0.180
Ni	0.000	0.000	0.000	0.000	0.004	0.003	0.000	0.000	0.000	0.001
Na	0.009	0.009	0.008	0.008	0.000	0.000	0.001	0.000	0.000	0.000
Total	8.030	8.028	8.033	8.040	8.019	8.035	8.017	8.020	8.032	7.996
Fe^{2+}_T	0.606	0.454	0.612	0.925	1.464	1.881	0.455	0.395	0.457	0.438
Fe^{2+}	0.518	0.371	0.513	0.805	1.407	1.777	0.404	0.336	0.360	0.450
Fe^{3+}	0.088	0.084	0.098	0.119	0.057	0.104	0.051	0.059	0.097	0.000
FeO	8.45	6.21	8.44	13.02	22.42	27.24	6.57	5.58	6.01	7.54
Fe_2O_3	1.60	1.56	1.80	2.15	1.01	1.77	0.92	1.09	1.80	0.00
Mg#*	0.75	0.83	0.76	0.61	0.41	0.24	0.83	0.84	0.83	0.84
Ca#**	0.27	0.15	0.21	0.32	0.34	0.50	0.16	0.20	0.15	0.07

Table 4.2b. (continued)

Group	Torrie-193	Torrie-193	Torrie-509	Torrie-509	Sputnik-513	Sputnik-365	Sputnik-513	Sputnik-365	Sputnik-365
	11	11	11	11	1	5	9	11	11
SiO_2	40.35	40.51	41.24	39.98	41.41	37.63	41.40	39.78	40.40
Al_2O_3	15.56	17.12	18.73	17.73	20.82	22.08	20.27	14.48	18.30
Cr_2O_3	9.52	8.49	5.77	4.81	2.53	0.07	3.99	11.37	5.11
TiO_2	0.55	0.28	0.44	0.85	0.51	0.08	0.30	0.15	0.77
FeO_T	7.28	6.35	6.61	9.00	8.80	34.43	7.93	7.57	9.08
MnO	0.37	0.36	0.29	0.37	0.32	1.13	0.33	0.39	0.47
MgO	19.48	20.05	20.84	17.35	19.58	5.80	19.86	18.13	16.74
CaO	6.67	5.94	5.61	8.61	5.20	0.98	5.25	7.63	8.54
NiO	0.00	0.00	0.00	0.00	0.02	0.04	0.00	0.03	0.02
Na_2O	0.02	0.03	0.08	0.10	0.04	0.06	0.08	0.05	0.07
Total	99.80	99.14	99.62	98.81	99.22	102.31	99.39	99.58	99.49
Si	2.972	2.970	2.981	2.974	2.996	2.930	2.992	2.969	2.983
Al	1.350	1.479	1.595	1.554	1.776	2.027	1.727	1.273	1.593
Cr	0.554	0.492	0.330	0.283	0.145	0.005	0.228	0.671	0.298
Ti	0.030	0.015	0.024	0.048	0.028	0.005	0.016	0.009	0.043
Fe^{2+}	0.448	0.389	0.399	0.560	0.533	2.243	0.479	0.472	0.560
Mn	0.023	0.023	0.018	0.023	0.020	0.075	0.020	0.025	0.029
Mg	2.139	2.191	2.245	1.924	2.112	0.673	2.139	2.017	1.842
Ca	0.527	0.467	0.435	0.686	0.403	0.082	0.407	0.610	0.676
Ni	0.000	0.000	0.000	0.000	0.001	0.003	0.000	0.002	0.001
Na	0.003	0.004	0.012	0.015	0.006	0.009	0.011	0.007	0.009
Total	8.047	8.031	8.038	8.067	8.019	8.052	8.019	8.054	8.034
Fe^{2+}_T	0.446	0.388	0.397	0.555	0.531	2.228	0.478	0.469	0.558
Fe^{2+}	0.307	0.294	0.282	0.355	0.475	2.027	0.420	0.308	0.456
Fe^{3+}	0.139	0.093	0.115	0.200	0.057	0.156	0.058	0.161	0.102
FeO	5.01	4.82	4.70	5.76	7.86	32.02	6.97	4.97	7.42
Fe_2O_3	2.52	1.70	2.12	3.60	1.04	2.68	1.06	2.89	1.84
Mg#*	0.83	0.85	0.85	0.78	0.80	0.23	0.82	0.81	0.77
Ca#**	0.20	0.18	0.16	0.26	0.16	0.11	0.16	0.23	0.27

Mg#*=Mg/(Mg+Fe^{2+}), Ca#**=Ca/(Ca+Mg)

a   Garnet classification

b
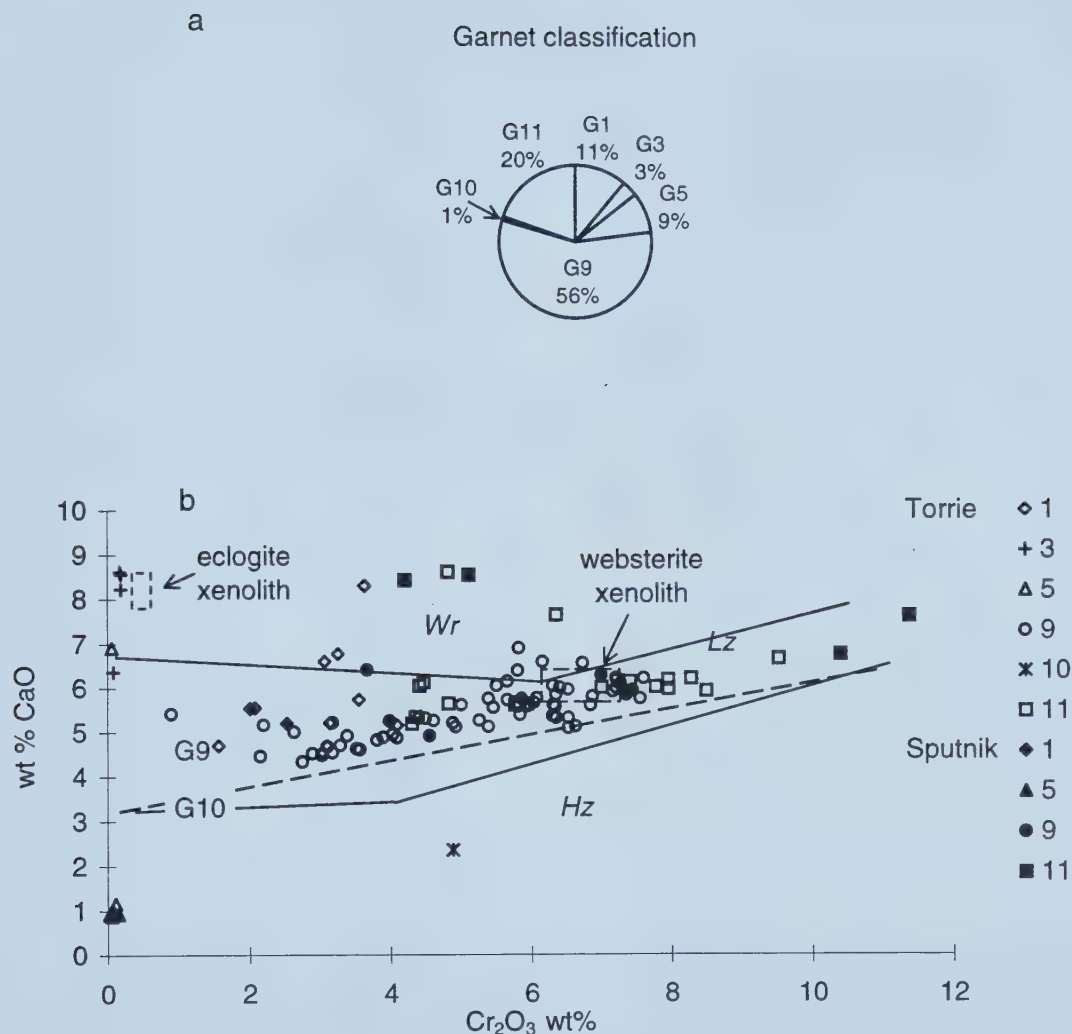
Figure 4.4 a) Pie diagram showing relative abundance of garnet xenocrysts from heavy mineral concentrate. Groups are classified according to Dawson and Stephens (1975). G1: Ti-pyrope; G3: Ca-pyrope-almandine; G5: almandine;G9: Cr-pyrope; G10: low Ca-pyrope; G11: Ti-pyrope and Ti-Cr-pyrope b) Chemical variation plots of Cr_2O_3 vs CaO Wr=wehrlite, Lz=lherzolite and Hz=harzburgite (Sobolev, 1977). Dashed line distinguishes diamond-bearing (G10) from barren (G9) garnet populations.
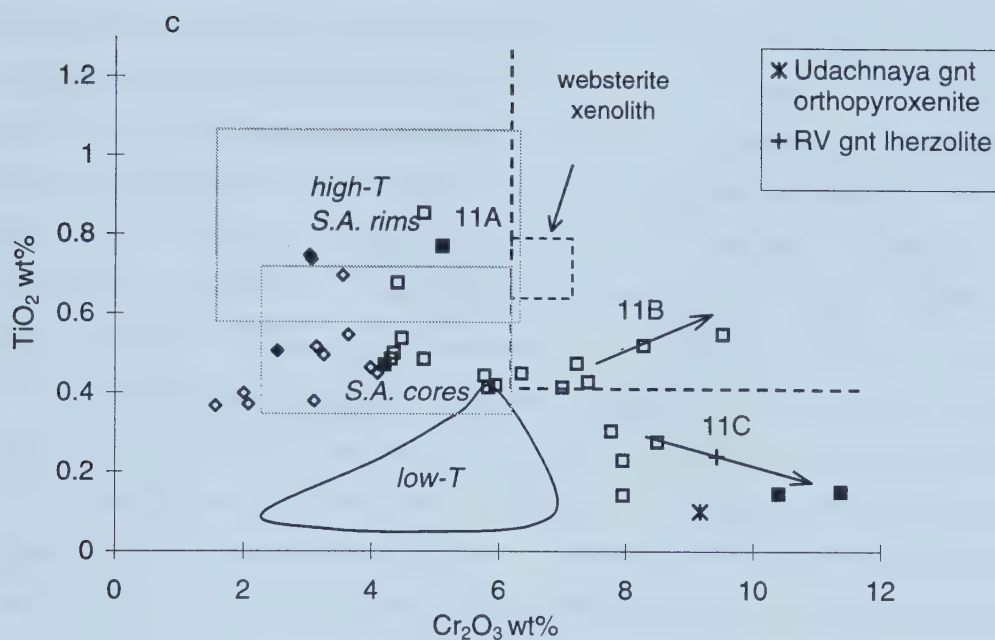
Fig 4.4c) Cr_2O_3 vs TiO_2 for G1 and G11garnets. High-T (temperature) (Luth et al, 1990) and low-T fields (Luth et al, 1990, Viljoen et al, 1992) are from South African garnet lherzolites. Gray rectangles are core and rim compositions of garnets from high-T garnet lherzolites from South Africa (Smith and Boyd, 1986). Xenoliths from Udachnaya and Roberts Victor (RV) are shown for comparison (Solovjeva, 1997).

abundances of Ti-pyrope (groups 1 and 11; sheared lherzolite or megacryst), Ca-pyrope almandine (group 3: diamondiferous eclogite), almandine (group 5; metamorphic basement) and low Ca-pyrope (group 10 or G10; harzburgite or dunite) are also present.

Group 9 is composed of titanium poor (0-0.4 wt%), chrome-pyrope garnets, containing moderate Cr_2O_3 (0.9-7.6 wt%) and low to moderate CaO (4.3-6.3 wt%). There is a positive correlation between CaO and Cr_2O_3 indicating solid solution toward uvarovite ($Ca_3Cr_2Si_3O_{12}$) (Fig. 4.4b). G9 garnets are considered by Dawson and Stephens (1975) to represent peridotite-derived xenoliths. Using the garnet classification based on CaO versus Cr_2O_3 variations (Sobolev et al., 1977), the majority of garnets belong to a lherzolitic (G9) rather than a harzburgitic (G10) source (Fig. 4.4b). Furthermore, Gurney (1984) demonstrated that a line drawn across a CaO/Cr_2O_3 plot can distinguish between nearly all diamondiferous (G10) and non-diamondiferous (G9) kimberlite localities (Fig 4.4b). This distinction is based on the premise that diamonds occur preferentially in harzburgites rather than lherzolites. This model has been tested with success in both Siberia and South Africa. The significance of this plot is that garnets from known diamond-bearing kimberlites plot in the low calcium field below the line. Only one garnet from the Torrie pipe falls into the sub-calcic G10 field typical of harzburgites. It has low CaO (2.4 wt%), moderately high Cr_2O_3 (4.9 wt%) and very low TiO_2 (0.01 wt%) compared to garnets in groups 9 and 11. The other Torrie garnets that plot in this field at the low Cr end are classified as G5 (metamorphic basement) based on their very high FeO, MnO and very low MgO and CaO, and are not G10 garnets (Table 4.2; sample Sputnik-365). The lack of G10 garnet macrocrysts in the Torrie and Sputnik pipes indicates that these kimberlite magmas sampled very little of a potentially diamondiferous harzburgite portion of the mantle.

Garnets falling into Dawson and Stephens (1975) group 11 form three distinct clusters in terms of their Cr_2O_3, TiO_2 and Na_2O contents. As a result of these groupings, I have divided them into subgroups, 11A, 11B and 11C (Fig. 4.4c). Group 11A is characterised by high TiO_2 (0.39-0.85 wt%), high Na_2O (0.03-0.111 wt%), relatively low Cr_2O_3 (4.2-5.8 wt%) and a steep positive correlation between Cr_2O_3 and TiO_2. The high Ti-pyrope garnets are most likely derived from disaggregated high-T garnet lherzolites, similar to xenoliths found in South African kimberlite pipes (Luth et al., 1990, Smith and Boyd (1986). Smith and Boyd (1986) observed that subtly zoned garnets from sheared peridotite xenoliths, with calculated equilibrium temperatures >1220°C, typically have rims relatively enriched in Ti (0.52-1.2 wt% TiO_2), Na and Fe and depleted in Cr (1.7-6.1 wt%

Cr_2O_3) compared to their cores (Fig. 4.4c). Several garnets from the sheared peridotites with high equilibration temperatures (1280-1460°C) have homogeneous TiO_2 (0.44-0.74 wt%) and Cr_2O_3 (2.6 wt%) contents. Analyses of discrete garnet grains from groups 11A in Torrie and Sputnik have similar Ti and Na enrichment and lower Cr contents to the core and rim compositions of garnets from high-T sheared lherzolite xenoliths from several South African kimberlites.

Group 11B garnets have high Cr_2O_3 (5.8-9.5 wt%), low Na_2O (<0.05 wt%) as well as low TiO_2 (0.42-0.55 wt%) abundances that display a shallow positive correlation with Cr_2O_3. The high Ti-chrome pyropes (Cr_2O_3 >6 wt% and TiO_2 >0.4 wt%; Fig. 4.4c) reflect high temperature, Cr-rich megacrysts and are interpreted to be part of the high temperature discrete nodule (megacryst) suite (Mitchell, 1986, 1995). The high Cr_2O_3 and TiO_2 contents in brown-red garnets from a websterite xenolith are consistent with a high temperature paragenesis as well and are shown for comparison in figure 4.4c.

Garnets in group 11C (uvarovite pyrope) have higher Cr_2O_3 (7.8-11.4 wt%) and much lower TiO_2 contents (<0.3 wt%) than groups 11A and 11B (Fig. 4.4c). Their origin is uncertain as they are similar (high CaO, Cr_2O_3 and low TiO_2) to garnets in a metasomatized garnet orthopyroxenite from Udachnaya (Solovjeva et al., 1997) and a low temperature garnet lherzolite from the Roberts Victor kimberlite, South Africa (Viljoen et al, 1992).

Several group 1 garnet xenocrysts have similar chemical variations to group 11A (Fig. 4.4c), which were interpreted to be derived from high-T sheared lherzolites. Group 1 garnets are characterized by high TiO_2 (0.43-0.737 wt%), relatively low Cr_2O_3 (3-4.1 wt%), a positive correlation between TiO_2 and Cr_2O_3 and a weak correlation between CaO and Cr_2O_3. A 1 cm garnet megacryst, however, (Torrie-457;Table 4.2), unlikely to be derived from fragmented xenoliths because of its size, also has similar chemistry to the group 1 garnets, which indicates that group 1 garnets may also be derived from a high-temperature discrete nodule (megacryst) paragenesis. According to Dawson and Stevens (1975), group 1 garnets are derived from either fragmented, high-temperature sheared lherzolites or megacrysts. Several garnets classified as G1 and G11, but with much lower Mg/(Mg+Fe) ratios (74-79) than the rest of the G1 and G11 garnets, plot in the wehrlite (clinopyroxene + olivine) field (Fig. 4.4b).

Garnets from groups 3 and 10 are the most important indicators of the diamond potential. Unfortunately, garnets from these groups make up only 4% of the total garnets analyzed. Moreover, garnets from Groups 3 and 10 were only found in the Torrie pipe.

Group 3 garnets are eclogite-derived according to the scheme of Dawson and Stephens (1975), however, Na_2O levels for this group are <0.07 wt%, which is low for garnets from diamondiferous eclogites (Gurney and Zweistra, 1995). In general, there are two distinct varieties of eclogite that are entrained in kimberlite: Group I, which has measurable enrichments in Na (>0.07 wt% Na_2O) and Group II, which lacks Na (<0.07 wt%) and K (<0.08 wt%) enrichments in garnet and clinopyroxene, respectively (McCandless and Gurney, 1989). Diamonds are found only in association with Group I eclogites (Fipke et al., 1995). G3 garnets from the Torrie pipe have major-element chemistry similar to Group II eclogites. They have high FeO (14.6-23.3 wt%) and CaO (6.4-8.6 wt%) and low MgO (8.9-13.1 wt%), TiO_2 (0.04-0.1), Cr_2O_3 (0.08-0.19 wt%) and Na_2O (0-0.06 wt%). This group of garnets may also be representative of megacrysts as opposed to having a diamondiferous eclogite signature (Gurney and Zweistra, 1995). Garnets from the eclogite xenolith entrained in the Torrie pipe, however, also have <0.07 wt% Na_2O, with one exception.

Group 5, almandine pyrope garnets, are characteristic of crustal granulites with very high FeO (24-34.6 wt%) and very low TiO_2 (<0.1 wt%), Cr_2O_3 (<0.15 wt%) and CaO (<1.2 wt%). One garnet in this group is more similar to an eclogitic (group 3) garnet, however, as it has higher CaO (6.9 wt%) and lower FeO (28.8 wt%) than crustal-derived group 5 garnets.

Homogeneity in the garnets was not confirmed by multiple analyses of each grain, but there are large inter-grain variations observed within groups. For example, Cr-pyrope garnets (G9) from Torrie with similar Mg# (83-84) have relatively large inter-grain Al_2O_3 (17.4-22.0 wt%), TiO_2 (0-0.4 wt%), Cr_2O_3 (2.8-7.6 wt%), CaO (4.3-6.6 wt%) and Na_2O (0-0.08 wt%) variations. Similar inter-grain variations are seen in garnets from the same group in Sputnik. If it is assumed that garnets in each population are derived from the same source then these inter-grain variations are most likely a result of fractional crystallization.

Clinopyroxene

Representative clinopyroxene analyses for the Torrie and Sputnik kimberlite pipes are given in Table 4.3. The majority of clinopyroxenes in these pipes are bright green chrome diopsides and augites with high magnesian $[100Mg/(Mg+Fe)]$ (90.3-94.8), $100Ca/(Ca+Mg)$ ratios in the range 40-51 and Wo>42% (Wo=Ca/Ca+Mg+Fe). They have low to moderate Cr_2O_3 (0.3-2.5 wt%), moderate to high TiO_2 (0.04-0.31 wt%), low Al_2O_3 (0.5-2.5 wt%) and low Na_2O (0.4-1.7 wt%) (Fig. 4.5). There is a minor proportion of Fe-augite with low $100Mg/(Mg+Fe)$ (57-65), moderate $100Ca/(Ca+Mg)$ (57-60) and very low Cr_2O_3 (<0.07 wt%), comparable to clinopyroxene in granulite xenoliths from the pipes. Three megacryst clinopyroxenes from Sputnik and Eddie have $100Ca/(Ca+Mg)$ =44-45, ~1 wt% Cr_2O_3 and ~1.36 wt% Na_2O (Appendix B: Table 3b and c). The large inter-grain variations in the clinopyroxenes reflect either derivation from different source regions or may be characteristic of one source region.

The clinopyroxene xenocrysts have major-element compositions similar to South African kimberlites (e.g. Boyd and Nixon, 1975; Rudnick et al., 1994). In Figure 4.5, clinopyroxenes from Torrie, Sputnik and Eddie are compared to clinopyroxenes from coarse (low-T) and deformed (high-T) garnet lherzolite xenoliths (Luth et al, 1990, Viljoen et al, 1994). The clinopyroxenes have similar Al_2O_3, $Ca/(Ca+Mg)$ and TiO_2 contents to low-T garnet lherzolites, however, many of the xenocrysts have lower Cr_2O_3 than clinopyroxenes in the low-T lherzolites. The lower Cr abundances for the xenocrysts compared to the low-T lherzolites may be the result of a higher pressure origin (Brey et al., 1990). Experiments on natural lherzolitic compositions indicate that Cr decreases with increasing pressure at constant temperature (Brey et al., 1990).

The $Ca/(Ca+Mg)$ for the clinopyroxenes are shown in Figure 4.5 and 4.6. This ratio, which reflects the miscibility gap between ortho- and clinopyroxene, is temperature sensitive (in the presence of orthopyroxene) and has been used as a geothermometer for peridotite xenoliths and pyroxene megacrysts from kimberlite (Davis and Boyd, 1966; Wells, 1977, and many others). The Ca content in clinopyroxenes decreases with increasing temperature while the Ca in orthopyroxene increases with increasing temperature of formation (Boyd, 1970). Because the majority of garnet xenocrysts are derived from garnet lherzolites, it may be assumed that orthopyroxene, clinopyroxene, garnet and olivine are in equilibrium. The $Ca/(Ca+Mg)$ ratios in the clinopyroxene range

Table 4.3. Representative clinopyroxene microprobe analyses (Cations on basis of 6 oxygen).

	Torrie-570	Torrie-570	Torrie-193	Torrie-508	Torrie-570	Sputnik-513	Sputnik-513	Sputnik-365	Sputnik-365
SiO_2	51.24	55.01	54.43	54.20	55.26	55.05	54.97	54.81	54.95
TiO_2	0.31	0.14	0.26	0.21	0.27	0.04	0.23	0.19	0.11
Al_2O_3	3.27	1.12	1.60	2.24	1.70	2.20	1.58	1.59	0.53
Cr_2O_3	0.06	0.52	0.86	1.54	2.46	0.30	0.65	1.05	2.02
FeOt	12.44	2.70	2.92	3.10	2.14	4.23	2.80	2.81	1.91
MnO	0.26	0.10	0.05	0.09	0.10	0.06	0.08	0.08	0.04
MgO	10.21	16.83	16.73	16.56	16.81	15.54	17.16	17.34	16.81
CaO	21.11	21.77	21.30	19.92	18.54	20.55	20.73	19.91	21.47
NiO	0.00	0.02	0.04	0.02	0.03	0.07	0.02	0.03	0.04
Na_2O	0.97	0.91	1.18	1.68	1.68	1.36	1.13	1.11	1.26
K_2O	0.01	0.05	0.04	0.07	0.06	0.02	0.06	0.06	0.04
Total	99.89	99.16	99.40	99.61	99.06	99.43	99.40	98.98	99.17
Si	1.943	2.007	1.985	1.973	2.005	2.007	1.997	1.997	2.006
Ti	0.009	0.004	0.007	0.006	0.007	0.001	0.006	0.005	0.003
Al	0.146	0.048	0.069	0.096	0.073	0.095	0.068	0.068	0.023
Cr	0.002	0.015	0.025	0.044	0.071	0.009	0.019	0.030	0.058
Fe^{2+}	0.395	0.082	0.089	0.094	0.065	0.129	0.085	0.086	0.058
Mn	0.008	0.003	0.002	0.003	0.003	0.002	0.002	0.003	0.001
Mg	0.577	0.915	0.909	0.898	0.910	0.845	0.929	0.942	0.915
Ca	0.858	0.851	0.832	0.777	0.721	0.803	0.807	0.777	0.840
Ni	0.000	0.000	0.001	0.001	0.001	0.002	0.001	0.001	0.001
Na	0.071	0.064	0.084	0.118	0.119	0.096	0.080	0.078	0.089
K	0.001	0.002	0.002	0.003	0.003	0.001	0.003	0.003	0.002
Total	4.010	3.992	4.004	4.013	3.977	3.989	3.995	3.990	3.996
Mg#	0.59	0.92	0.91	0.91	0.93	0.87	0.92	0.92	0.94
Ca/(Ca+Mg)	0.60	0.48	0.48	0.46	0.44	0.49	0.46	0.45	0.48
Ca%	46.89	46.05	45.46	43.89	42.51	45.20	44.30	43.06	46.32
Mg%	31.55	49.50	49.68	50.78	53.65	47.55	51.03	52.19	50.47
Fe%	21.56	4.45	4.86	5.33	3.83	7.26	4.67	4.75	3.22
Name	Fe-augite	diopside	diopside	augite	augite	diopside	augite	augite	diopside
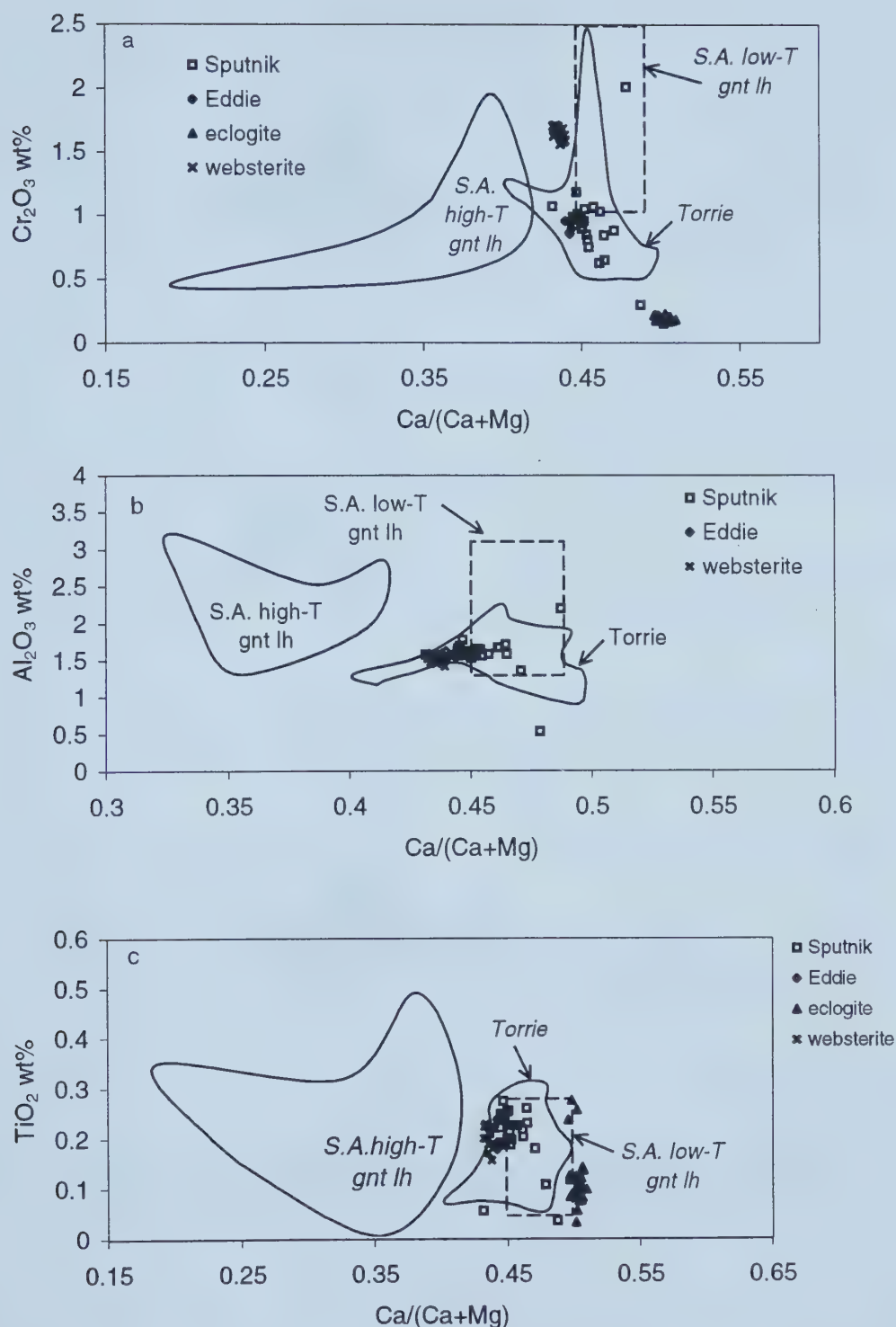
Figure 4.5. Chemical variation diagrams for clinopyroxene xenocrysts and clinopyroxene from xenoliths a) Ca/(Ca+Mg) vs Cr_2O_3 (Note that lower Ca/(Ca+Mg) reflects a higher temperature of formation b) Ca/(Ca+Mg) vs Al_2O_3 c) Ca/(Ca+Mg) vs TiO_2. Fields for high-T (Luth et al, 1990) and low-T (Luth et al, 1990, Viljoen et al, 1992) are from clinopyroxenes in garnet lherzolites (gnt lh) from South African kimberlites.
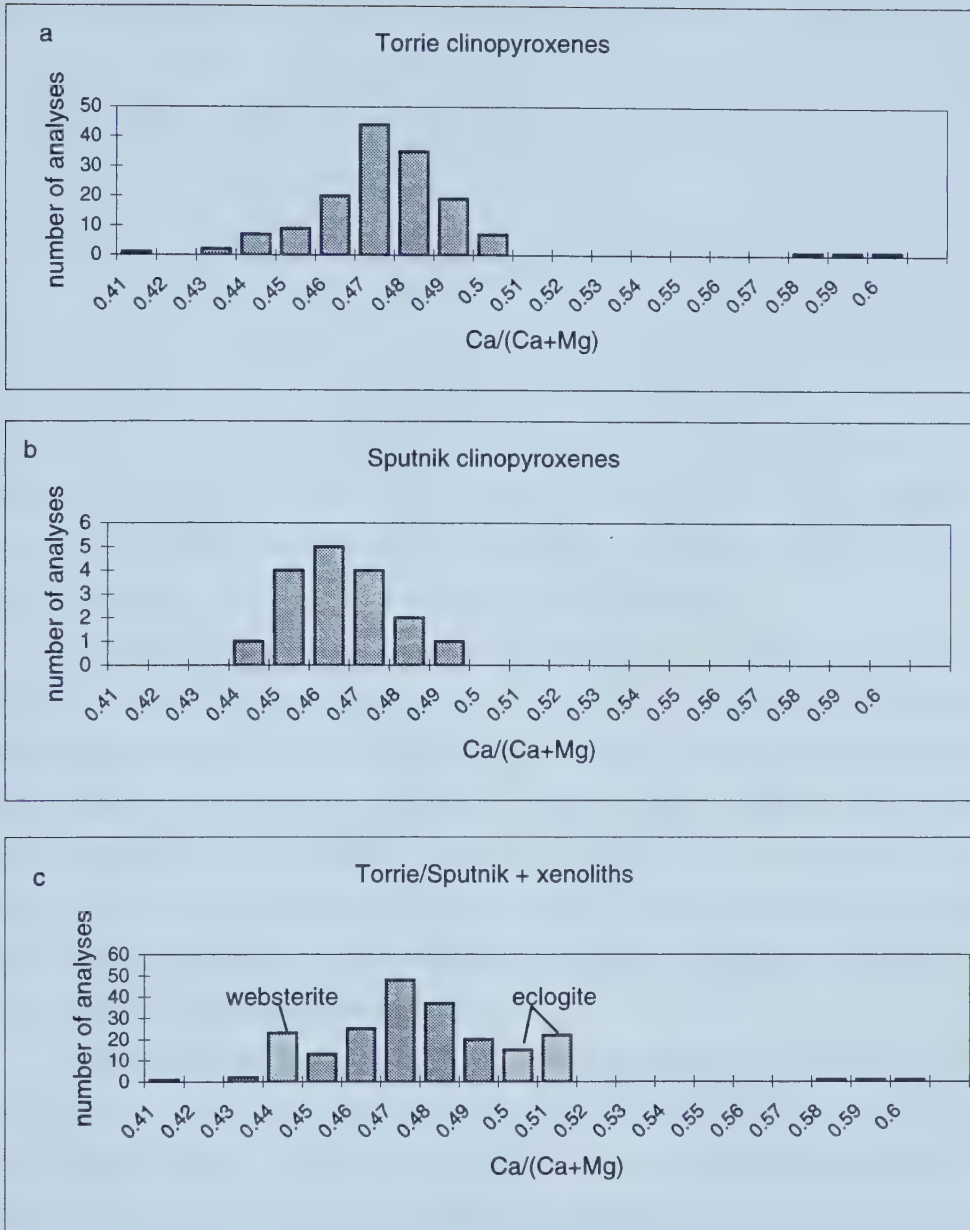
Figure 4.6. Histograms of Ca/(Ca+Mg) contents in clinopyroxene from a)Torrie xenocrysts b) Sputnik xenocrysts and c) clinopyroxene from xenoliths and Torrie/Sputnik xenocrysts.

from 0.40-0.60 for Torrie and 0.43-0.49 for Sputnik (Fig. 4.6), which require a large range of equilibration temperatures (1300-1060°C for Torrie and 1260-1090°C for Sputnik at 50kb using the two-pyroxene thermometer of Brey and Köhler, 1990) for the xenoliths from which the clinopyroxenes were derived. The temperature calculations were made using the clinopyroxenes with the highest (low-T) and lowest (high-T) Ca/(Ca+Mg) ratio and the corresponding orthopyroxenes with the lowest (low-T) and highest (high-T) Ca/(Ca+Mg) ratio in each pipe in order to get the maximum and minimum temperatures. Clinopyroxene from Torrie and Sputnik have unimodal distributions at 0.47 and 0.46 (~1027-1127 °C) respectively (Fig. 4.5a and b). The large range in equilibration temperatures at relatively constant Al_2O_3 contents (Gasparik, 1984), however, most likely represents a sampling event over a large range in pressure along a geotherm (i.e. from 160-190 km depth on a continental geotherm of 47 mW/m^2).

The garnet websterite xenolith, entrained by the Torrie kimberlite pipe, is also shown for comparison in Figures 4.5 and 4.6. The compositions of the clinopyroxenes from the websterite xenolith differ from that of the majority of clinopyroxene xenocrysts. They display higher Cr_2O_3 (1.5-1.7 wt%), higher Na_2O (1.5-1.8 wt%), lower 100Ca/(Ca+Mg) (44) and similar Al_2O_3 (1.4 -1.6 wt%) and TiO_2 (0.16-0.22 wt%) to the xenocrysts (Fig. 4.6). The lower Ca/(Ca+Mg) ratios for websterite clinopyroxenes and similar xenocrysts imply a higher temperature origin for these clinopyroxenes compared to the majority of pyroxene xenocrysts.

Clinopyroxenes from the eclogite xenolith have higher 100Ca/(Ca+Mg) (51) and a large range in Na_2O content (1.5-4.2 wt%) compared to the xenocryst population. The large range in Na_2O content (1.5-4.1 wt%) is also similar to late stage metasomatic clinopyroxenes in an eclogite xenolith from Udachnaya (Snyder et al., 1997). One macrocryst from Sputnik also displays increasing Na content from core to rim (1.28-1.35 wt%). Several xenocryst pyroxenes from the mineral separates have compositions similar to the xenoliths, consistent with a garnet websteritic and eclogitic parageneses.

Orthopyroxene

Representative orthopyroxene analyses are presented in Table 4.4. Enstatites in the Torrie and Sputnik kimberlites have Mg# (Mg/(Mg+Fe)) ranging from 91.8-94.3 and can be divided into two groups: one with low Al_2O_3 (0.51-0.7 wt%) and high TiO_2 (0.03-0.12 wt%) and one with high Al_2O_3 (1.2-3.3 wt%) and low TiO_2 (<0.01 wt%; Fig. 4.7).

Table 4.4. Representative orthopyroxene microprobe analyses (Cations on basis of 6 oxygen).

	Torrie-508	Torrie-508	Torrie-547	Torrie-570	Torrie-508	Sputnik-513	Sputnik-513	Sputnik-513	Sputnik-513	Sputnik-513
SiO_2	58.14	57.33	55.00	57.15	55.96	56.32	57.14	57.36	57.14	56.88
TiO_2	0.02	0.11	0.06	0.00	0.00	0.12	0.03	0.00	0.00	0.01
Al_2O_3	0.51	0.56	1.78	2.06	3.28	0.65	0.66	1.20	1.73	2.19
Cr_2O_3	0.22	0.33	0.00	0.37	0.63	0.25	0.25	0.49	0.54	0.40
FeO_T	4.11	5.60	16.36	4.52	4.40	5.76	5.21	4.44	4.37	4.50
MnO	0.13	0.11	0.14	0.11	0.09	0.14	0.14	0.12	0.10	0.12
MgO	36.44	35.85	26.80	34.55	35.31	33.60	34.18	35.45	35.69	34.71
CaO	0.22	0.60	0.23	0.30	0.59	0.77	0.90	0.70	0.20	0.37
NiO	0.02	0.10	0.02	0.02	0.07	0.07	0.05	0.01	0.01	0.02
Na_2O	0.04	0.12	0.00	0.06	0.06	0.10	0.08	0.10	0.00	0.00
K_2O	nd	nd	0.02	nd	nd	nd	nd	nd	nd	nd
Total	99.84	100.71	100.42	99.14	100.40	97.77	98.63	99.87	99.78	99.18
Si	1.986	1.963	1.973	1.969	1.912	1.985	1.990	1.967	1.958	1.960
Ti	0.001	0.003	0.002	0.000	0.000	0.003	0.001	0.000	0.000	0.000
Al	0.021	0.022	0.075	0.083	0.132	0.027	0.027	0.048	0.070	0.089
Cr	0.006	0.009	0.000	0.010	0.017	0.007	0.007	0.013	0.015	0.011
Fe^{2+}	0.117	0.160	0.491	0.130	0.126	0.170	0.152	0.127	0.125	0.130
Mn	0.004	0.003	0.004	0.003	0.003	0.004	0.004	0.004	0.003	0.003
Mg	1.856	1.830	1.433	1.775	1.799	1.765	1.774	1.813	1.823	1.783
Ca	0.008	0.022	0.009	0.011	0.022	0.029	0.034	0.026	0.007	0.014
Ni	0.001	0.003	0.001	0.000	0.002	0.002	0.001	0.000	0.000	0.001
Na	0.003	0.008	0.000	0.004	0.004	0.007	0.006	0.006	0.000	0.000
K	0.000	0.000	0.001	0.000	0.000	0.000	0.000	0.000	0.000	0.000
Total	4.001	4.023	3.989	3.986	4.016	3.999	3.995	4.005	4.000	3.990
Mg#	0.94	0.92	0.74	0.93	0.93	0.91	0.92	0.93	0.94	0.93
Ca/(Ca+Mg)	0.00	0.01	0.01	0.01	0.01	0.02	0.02	0.01	0.00	0.01
Ca%	0.40	1.10	0.46	0.58	1.12	1.49	1.72	1.32	0.38	0.70
Mg%	93.67	90.94	74.15	92.63	92.42	89.87	90.54	92.21	93.22	92.57
Fe%	5.93	7.96	25.39	6.79	6.46	8.64	7.74	6.48	6.41	6.73

Figure 4.7. Chemical variations of orthopyroxenes a) Al_2O_3 vs Cr_2O_3 b) Al_2O_3 vs TiO_2 c) Ca/(Ca+Mg) *100 vs Na_2O. Sodium contents >0.07 wt% reflect higher pressure (lherzolite paragenesis). Sodium contents <0.07 wt% reflect lower pressure (harzburgite-dunite paragenesis). Field for South African garnet harzburgites is from Nixon et al, (1987). Fields for high-T are from Luth et al., (1990) and low-T garnet lherzolite are from Luth et al., (1990), Canil and O'Neill (1996) and Nixon et al., (1987; sample 2823). Southeast Australian (SEA) spinel lherzolite (Canil and O'Neill, 1996).

The low Al_2O_3 group with low Cr_2O_3 (0.2-0.48 wt%) and moderately high TiO_2 in Figure 4.7 is similar to orthopyroxene in low-temperature garnet lherzolites from South Africa (Luth et al., 1990; Canil and O'Neill, 1996; Nixon et al., 1987). The high Al_2O_3 group, however, is more similar to orthopyroxene derived from spinel lherzolite (>2.5 wt% Al_2O_3) and garnet harzburgite (0.6-2.2 wt% Al_2O_3) and are characterized by high Cr_2O_3 (0.35-0.65 wt%) and very low TiO_2 (<0.02 wt%; Fig. 4.7). One of the enstatite xenocrysts has high Al_2O_3 (1.8 wt%), moderately high TiO_2 (0.06 wt%) and undetectable Cr_2O_3 contents, which are very similar to the composition of orthopyroxene from the granulite xenolith.

The CaO, Al_2O_3, Cr_2O_3 and Na_2O contents reflect the conditions of formation of the orthopyroxenes. Boyd (1970) experimentally established that Al_2O_3 contents in enstatite, in equilibrium with pyropic garnet, decrease with increasing pressure under isothermal conditions. Therefore, low Al_2O_3 and Cr_2O_3 contents of xenocrysts in Figure 4.7a probably reflect higher pressures of formation for the xenoliths from which the orthopyroxenes are derived. Sobolev (1977) established that sodium content in pyroxenes increases with increasing pressure and used sodium content in enstatites associated with diamonds as a tool for identifying the paragenesis of enstatite xenocrysts. He suggested that enstatite with low Na_2O contents (<0.07 wt%) formed without clinopyroxene present, perhaps in a harzburgite-dunite paragenesis, whereas high Na_2O (>0.07 wt%) enstatites most likely originated in lherzolites. In the Torrie and Sputnik kimberlites, orthopyroxenes from the low Al-group have higher Na_2O contents (0.07-0.17 wt%) than the high Al-group (<0.08 wt%) indicating that the low Al-group orthopyroxenes may originate from greater depths in the mantle.

In summary, the low Al_2O_3, high Na_2O and TiO_2 group enstatites in the Torrie and Sputnik pipes are most likely derived from low-T garnet lherzolite similar to garnet lherzolites from South Africa. The high Al_2O_3, Cr_2O_3, low Na_2O and low TiO_2 group enstatites are derived from spinel lherzolite and garnet harzburgite similar to orthopyroxenes in spinel peridotites from southeast Australia and garnet harzburgites from South Africa.

Phlogopite

Phlogopite occurs as phenocrysts in kimberlite and xenocrysts from metasomatized peridotite in the Torrie, Sputnik and Eddie kimberlite pipes. Primary groundmass phlogopite is relatively abundant in Eddie and absent in Torrie and

Sputnik. Its composition is sensitive to changes in magma chemistry and is useful to monitor magma evolution. Representative compositions of phlogopite are given in Table 4.5.

Macrocrystic mica compositions in kimberlites are very similar to macrocrystic/microphenocrystic micas in orangeites and plot within the field for 'Orangeite primitive micas" in Figure 4.8a and b. Mica compositions in kimberlites, however, follow two evolutionary trends that plot away from the primitive mica field: the Al-enrichment trend and the tetraferriphlogopite trend (Fig. 4.8b). The majority of phlogopite in the Eddie pipe has high Al_2O_3 (14-18 wt%), moderate TiO_2 (1.3-2.7 wt%), FeO_T (4.5-6.2 wt%) and low Cr_2O_3 (<1.1 wt%) equivalent to primary groundmass micas in kimberlite (Fig. 4.8). They have similar compositions to groundmass micas in the Antochka and Bounoudou kimberlites from Guinea and the Udachnaya and Yubileinaya kimberlites from Siberia (Mitchell, 1995).

Several phlogopites with lower Al_2O_3 (~12 wt%) than the groundmass micas fall within the field for more primitive micas. Micas from peridotite xenoliths in Udachnaya (Solovjeva et al, 1997) and the Ham pipe (Somerset Island, NWT; Mitchell, 1986), however, also fall within this field. High iron (7.7 wt%) phlogopite (which display kinked textures) with otherwise similar composition to groundmass micas are similar to micas in mantle xenoliths from Udachnaya that are interpreted to have a metasomatic origin (Fig. 4.8b) (Solovjeva et al., 1997). The very high Cr_2O_3 (2.2 wt%), TiO_2 (2.8 wt%; Fig. 4.8c) and low Al_2O_3 (12.9 wt%) and FeO (4.2 wt%) phlogopites from Torrie are similar to secondary phlogopites in metasomatized peridotite and pyroxenite xenoliths from Udachnaya (Solovjeva et al., 1997) and lherzolite xenoliths from South Africa (sample 73-66; Delaney et al., 1980). The Eddie pipe also contains very small (<30um) micas that are part of a less common evolutionary trend toward tetraferriphlogopite (Fig. 4.8b). They are interpreted to be very late-crystallizing groundmass phases similar to Al-poor micas that developed as either discrete thin mantles on cores of Al-rich groundmass mica or very small groundmass phases in the Aries pipe, western Australia (Edwards et al., 1992). The appearance of the tetraferriphlogopite trend in kimberlite is very unusual and signifies an abrupt change in

Table 4.5. Representative phlogopite microprobe analyses (Cations on basis of 22 oxygen).

	490-4 Eddie	555a-2core Eddie	555a-2rim Eddie	555a-3core Eddie	555a-3rim Eddie	555a-8core Eddie	555a-8rim Eddie	555a-13 Eddie	508-13a Torrie	508-15 Torrie	307-18a Sputnik
SiO_2	41.04	35.26	35.84	36.18	36.81	38.04	37.56	40.51	40.08	41.77	40.64
TiO_2	0.67	2.58	2.34	1.74	1.76	1.38	1.48	1.52	1.79	2.79	0.87
Al_2O_3	6.99	16.44	15.96	14.90	16.56	14.55	14.89	12.20	14.95	12.22	11.82
FeO_T	10.22	6.26	6.35	4.81	4.61	5.76	5.76	3.81	7.72	4.18	4.69
MnO	0.05	0.06	0.06	0.05	0.06	0.05	0.05	0.03	0.02	0.03	0.03
MgO	24.89	21.21	21.53	22.74	24.03	22.64	22.30	23.84	20.68	20.95	24.15
CaO	0.15	0.25	0.14	0.14	0.17	0.07	0.08	0.35	0.20	0.41	0.10
Na_2O	0.03	0.19	0.17	0.09	0.11	0.12	0.13	0.07	0.23	0.26	0.06
K_2O	9.10	9.09	9.63	10.29	9.56	10.45	10.31	10.30	10.49	10.13	10.10
BaO	0.07	1.68	1.47	1.59	2.81	0.68	0.67	0.32	0.12	0.16	0.06
Cr_2O_3	0.41	0.14	0.12	0.00	0.00	0.54	1.01	0.63	0.52	2.18	0.31
NiO	0.08	0.02	0.05	0.02	0.02	0.06	0.03	0.10	0.10	0.14	0.15
F	0.53	0.15	0.15	0.14	0.24	0.15	0.14	0.26	1.33	0.16	0.26
Cl	0.00	0.05	0.02	0.01	0.04	0.00	0.00	0.02	0.10	0.07	0.07
Total	93.99	93.30	93.77	92.63	96.68	94.42	94.36	93.83	97.73	95.38	93.19
Si	6.113	5.261	5.324	5.425	5.301	5.568	5.506	5.880	5.709	5.967	5.939
Ti	0.075	0.289	0.262	0.196	0.191	0.152	0.164	0.165	0.191	0.300	0.096
Al	1.228	2.891	2.795	2.633	2.811	2.510	2.574	2.087	2.510	2.057	2.035
Fe^{2+}	1.273	0.782	0.788	0.603	0.555	0.705	0.706	0.462	0.919	0.499	0.573
Mn	0.006	0.007	0.008	0.006	0.008	0.006	0.006	0.004	0.002	0.004	0.004
Mg	5.526	4.717	4.768	5.083	5.157	4.941	4.874	5.158	4.391	4.461	5.261
Ca	0.023	0.040	0.023	0.022	0.027	0.010	0.012	0.054	0.030	0.063	0.016
Na	0.007	0.054	0.048	0.027	0.032	0.033	0.038	0.021	0.064	0.071	0.018
K	1.729	1.730	1.824	1.969	1.756	1.952	1.928	1.907	1.907	1.846	1.883
Ba	0.004	0.098	0.086	0.094	0.158	0.039	0.039	0.018	0.007	0.009	0.003
Cr	0.049	0.017	0.015	0.000	0.000	0.063	0.117	0.072	0.059	0.246	0.036
Ni	0.010	0.002	0.005	0.002	0.002	0.007	0.004	0.011	0.011	0.016	0.018
F	0.249	0.068	0.072	0.065	0.110	0.067	0.064	0.117	0.601	0.072	0.122
Cl	0.001	0.013	0.005	0.002	0.009	0.000	0.001	0.004	0.024	0.017	0.018
Total	16.292	15.970	16.023	16.127	16.116	16.053	16.033	15.961	16.426	15.629	16.019
Mg#	0.813	0.858	0.858	0.894	0.903	0.875	0.874	0.918	0.827	0.899	0.902
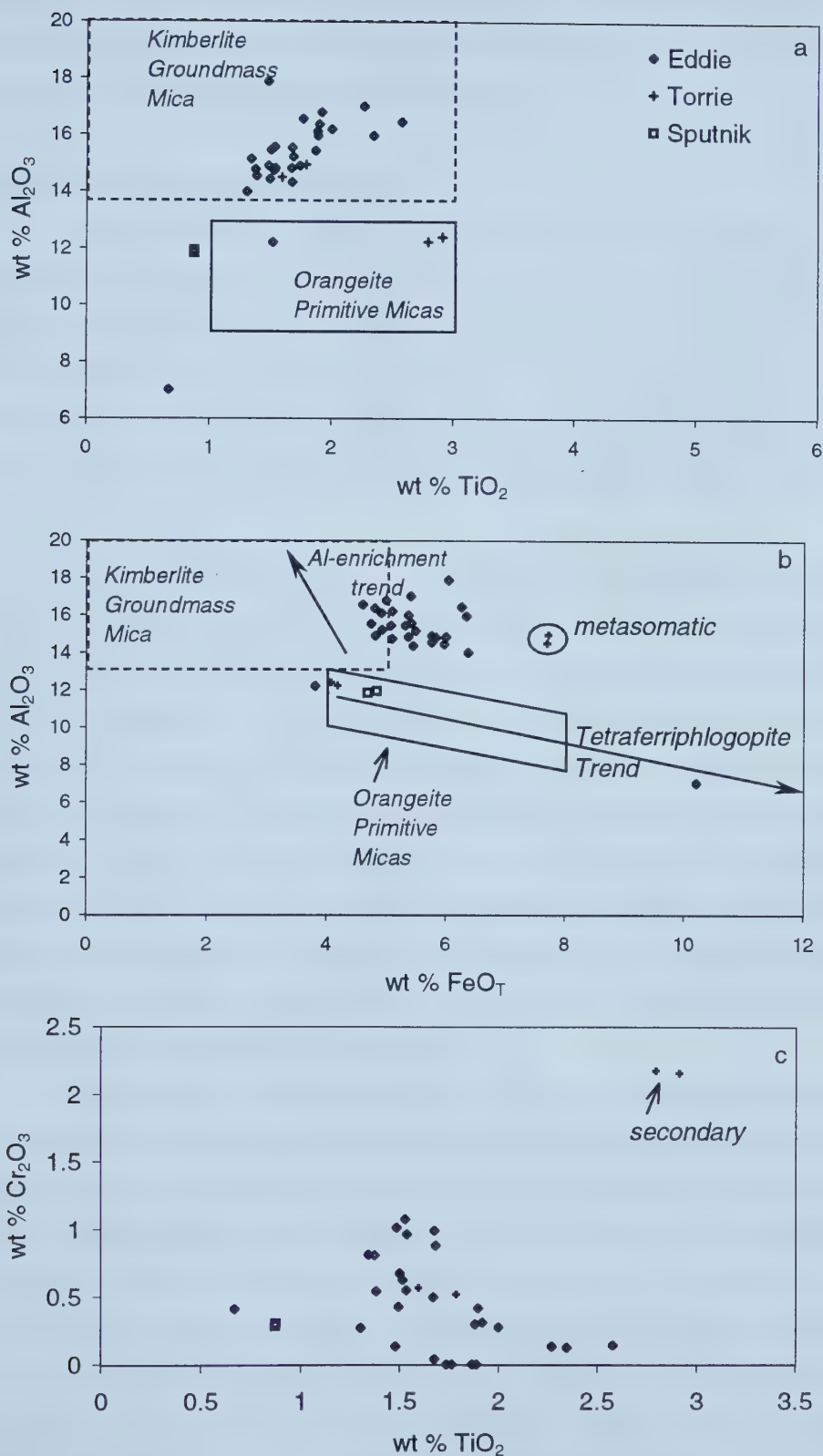
Figure 4.8. Variation diagrams for phlogopite a) TiO_2 vs Al_2O_3
b) FeO_T vs Al_2O_3 c) TiO_2 vs Cr_2O_3. Compositional fields of kimberlite
groundmass micas and orangeite primitive micas are from Mitchell (1995).

the redox conditions during the final stages of crystallization (Mitchell, 1995). Mitchell (1995) suggests that tetraferriphlogopite formation may be associated with groundwater addition to the magma and/or rapid CO_2 loss.

Oxide mineralogy and chemistry

Oxide minerals, which are abundant in the groundmass of kimberlites, are intrinsically sensitive to changes in the magma chemistry, temperature and oxygen fugacity (fO_2) (Hunter et al., 1984) and record mid- to late-stages of the melt evolution of the kimberlite melt. The oxide minerals in the Torrie, Sputnik and Eddie kimberlites consist of ilmenite, Al-rich phenocryst and groundmass spinels, magnesiochromites derived from mantle xenoliths, and rare groundmass perovskite.

Spinel

Representative analyses of different types of kimberlitic spinel present in the Torrie, Sputnik and Eddie kimberlites are given in Table 4.6a. Using the nomenclature of Mitchell (1986), the five types of spinel are 1) aluminous-magnesian-chromite (AMC) and titanian magnesian chromite (TMC) 2) titaniferous-magnesian-aluminous-chromite (TIMAC) 3) magnesian ulvöspinel-ulvöspinel-magnetite (MUM) 4) groundmass titanian-ferrian pleonaste (TFP) and 5) Al-rich spinels as inclusions in garnet and hercynitic-spinels mantling TIMAC, TMC and MUM. The AMC, TMC and TIMAC belong to the $FeCr_2O_4$-$MgCr_2O_4$-$FeAl_2O_4$-$MgAl_2O_4$ (chromite-magnesiochromite-hercynite-spinel) solid solution series. The MUM and TFP belong to the Mg_2TiO_4-Fe_2TiO_4-$FeAl_2O_4$-$MgAl_2O_4$ (magnesian ulvöspinel-ulvöspinel-hercynite-spinel) solid solution series and trend toward $MgFe_2O_4$ (magnesioferrite) and Fe_3O_4 (magnetite).

Mitchell (1986, 1995) has shown that four distinct spinel trends are present in kimberlite: (1) macrocrystal or aluminous magnesian chromite (AMC) trend (2) magnesian ulvöspinel trend (magmatic trend 1) (3) titanomagnetite trend (magmatic trend 2) and (4) Al-rich groundmass spinels. The fourth group of spinels is rare in kimberlite and forms the pleonaste reaction trend. Figure 4.9a illustrates the 3 major trends plotted in a 6-component reduced spinel prism. Figures 4.9b and c represent the front face and base, respectively, of the reduced spinel prism. Spinels with significant quantities of the magnesian ulvöspinel endmember (magmatic trend 1) are the hallmark of kimberlites (Mitchell, 1986) and have proven to be a useful exploration tool.

Table. 4.6a. Representative spinel microprobe analyses (Cations on basis of 4 oxygen).

name	AMC	AMC	TIMAC	TIMAC	Ti-Fe pleonastes	
	Torrie	Torrie	Torrie	Torrie	Torrie	Torrie
SiO_2	0.031	0.033	0.092	0.256	0.094	0.125
TiO_2	0.160	0.212	2.597	2.531	16.982	20.692
Al_2O_3	4.061	4.536	8.264	9.508	7.574	11.753
Cr_2O_3	66.632	59.561	51.321	49.252	5.101	2.558
FeO_T	21.112	20.670	20.714	21.231	46.931	36.445
MnO	0.415	0.392	0.353	0.290	0.569	0.554
MgO	9.828	10.964	13.372	13.497	17.560	22.092
NiO	0.000	0.142	0.114	0.184	0.170	0.203
ZnO	0.058	0.263	0.012	0.132	0.468	0.230
Nb_2O_5	0.000	0.004	0.000	0.027	0.086	0.086
Total	102.62	97.46	97.59	97.70	98.56	96.94
Si	0.001	0.001	0.003	0.008	0.003	0.004
Ti	0.004	0.006	0.065	0.063	0.415	0.487
Al	0.159	0.185	0.325	0.371	0.290	0.434
Cr	1.750	1.626	1.352	1.288	0.131	0.063
Fe^{2+}	0.505	0.420	0.390	0.390	0.538	0.437
Fe^{3+}	0.081	0.176	0.187	0.197	0.738	0.517
Mn	0.012	0.011	0.010	0.008	0.016	0.015
Mg	0.487	0.564	0.664	0.666	0.851	1.031
Ni	0.000	0.004	0.003	0.005	0.004	0.005
Zn	0.001	0.007	0.000	0.003	0.011	0.005
Nb	0.000	0.000	0.000	0.000	0.001	0.001
Total	3.000	3.000	3.000	3.000	3.000	3.000
Cr/(Cr+Al)	0.917	0.898	0.806	0.777	0.311	0.127
Ti/(Ti+Cr+Al)	0.002	0.003	0.037	0.037	0.496	0.495

AMC (aluminous magnesian chromite); TIMAC (titanium magnesium aluminous chromite);MUM (magnesian ulvospinel-ulvospinel-magnetite)

Table 4.6a. (continued)

name	AMC Eddie	AMC Eddie	MUM Eddie	MUM Eddie	MUM Eddie	UM Eddie	UM Eddie	TIMAC* Sputnik	SPINEL** Sputnik	MUM Sputnik	MUM Sputnik
SiO_2	0.178	0.000	0.045	0.022	0.031	0.020	0.035	0.122	0.000	0.055	0.055
TiO_2	1.612	0.059	9.301	9.657	10.712	16.906	13.169	1.631	0.144	15.205	14.938
Al_2O_3	7.102	12.919	16.789	14.168	10.588	0.868	5.397	9.499	46.629	9.917	13.003
Cr_2O_3	57.221	56.036	0.000	0.000	0.469	0.570	0.175	51.718	12.588	0.000	0.009
FeO_T	17.715	18.029	53.453	55.283	58.034	67.190	63.935	19.686	14.711	55.595	50.563
MnO	0.373	0.353	0.529	0.499	0.500	0.646	0.563	0.302	0.137	0.478	0.457
MgO	14.455	12.109	16.296	14.744	13.875	9.275	11.466	13.574	18.983	14.307	15.426
NiO	0.143	0.033	0.000	0.000	0.068	0.216	0.140	0.134	0.000	0.124	0.102
ZnO	0.029	0.000	0.039	0.000	0.000	0.000	0.000	0.088	0.000	0.097	0.029
Nb_2O_5	0.000	0.043	0.000	0.000	0.005	0.063	0.024	0.058	0.000	0.000	0.094
Total	99.47	99.89	100.49	98.43	98.46	99.70	99.16	97.55	93.91	99.29	97.81
Si	0.006	0.000	0.001	0.001	0.001	0.001	0.001	0.004	0.000	0.002	0.002
Ti	0.040	0.001	0.218	0.235	0.267	0.449	0.339	0.041	0.003	0.375	0.365
Al	0.273	0.491	0.616	0.541	0.413	0.036	0.218	0.371	1.559	0.383	0.497
Cr	1.478	1.428	0.000	0.000	0.012	0.016	0.005	1.354	0.282	0.000	0.000
Fe^{2+}	0.327	0.410	0.448	0.510	0.567	0.938	0.735	0.362	0.197	0.659	0.607
Fe^{3+}	0.158	0.076	0.945	0.987	1.039	1.046	1.096	0.183	0.152	0.864	0.765
Mn	0.010	0.010	0.014	0.014	0.014	0.019	0.016	0.008	0.003	0.013	0.013
Mg	0.704	0.582	0.757	0.712	0.685	0.488	0.585	0.670	0.803	0.699	0.746
Ni	0.004	0.001	0.000	0.000	0.002	0.006	0.004	0.004	0.000	0.003	0.003
Zn	0.001	0.000	0.001	0.000	0.000	0.000	0.000	0.002	0.000	0.002	0.001
Nb	0.000	0.001	0.000	0.000	0.000	0.001	0.000	0.001	0.000	0.000	0.001
Total	3.000	3.000	3.000	3.000	3.000	3.000	3.000	3.000	3.000	3.000	3.000
Cr/(Cr+Al)	0.844	0.744	0.000	0.000	0.029	0.306	0.021	0.785	0.153	0.000	0.000
Ti/(Ti+Cr+Al)	0.022	0.001	0.261	0.303	0.385	0.896	0.604	0.023	0.002	0.495	0.423

* inclusion in olivine macrocryst, ** inclusion in garnet xenocryst (lherzolite, G9)
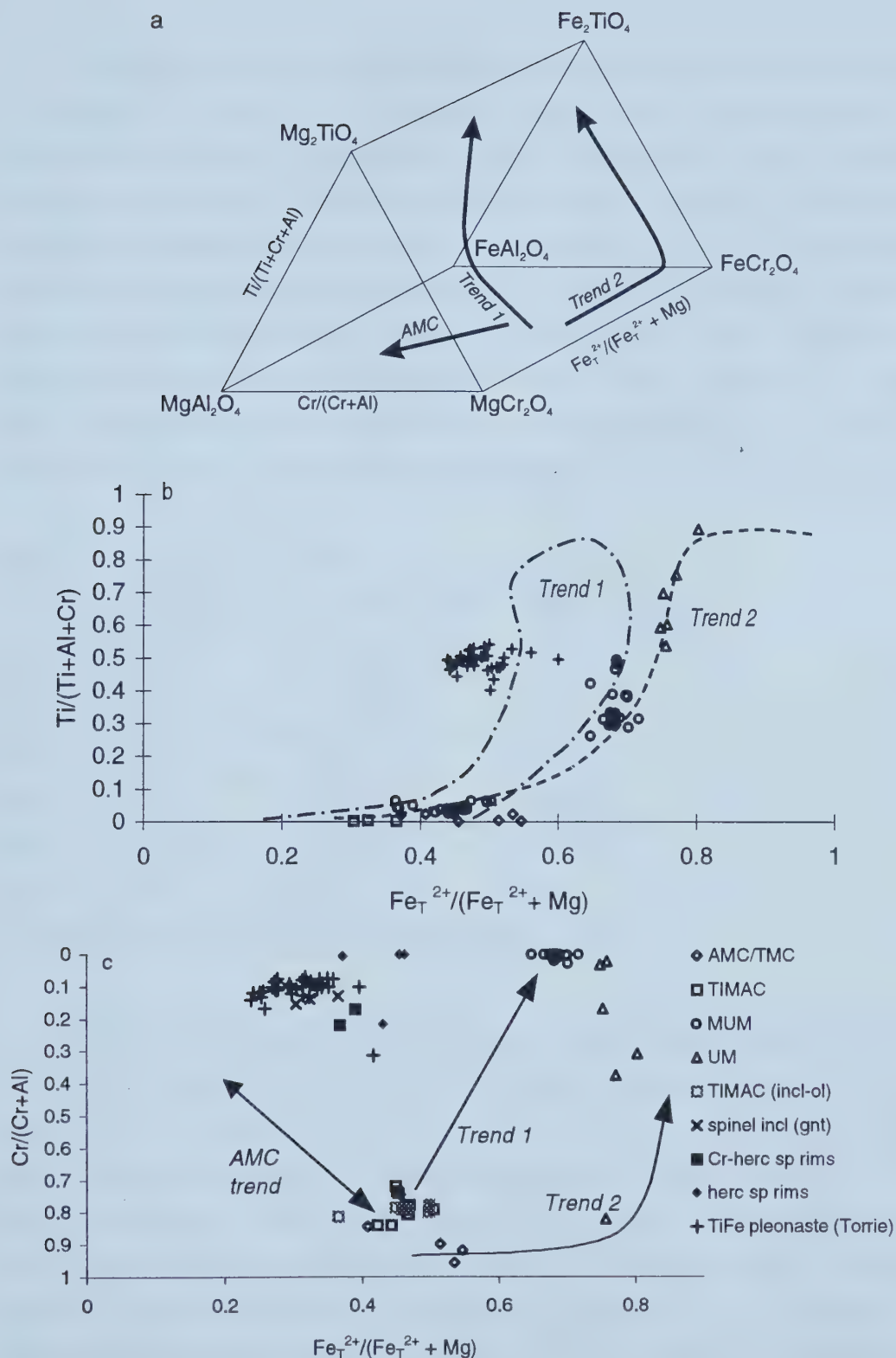
Figure 4.9. A) Compositional trends of spinels from kimberlites plotted in the reduced spinel prism (Mitchell, 1986, 1995). b) $Fe_T^{2+}/(Fe_T^{2+} + Mg)$ vs $Ti/(Ti+Al+Cr)$ in spinels from Torrie, Sputnik and Eddie. This plot represents the $MgCr_2O_4$-$FeCr_2O_4$-$MgTiO_4$-Fe_2TiO_4 projection (front face) of the spinel prism. Symbols as in Fig. 4.9c. c) This plot represents the base of the spinel prism. See text for description of legend symbols.

Chrome-rich spinel xenocrysts (chromite), like garnet, are used as an indication of the amount of diamonds in diatremes derived from disaggregated, potentially diamondiferous chromite harzburgite. Three compositional types of chromite are recognized as important for the exploration of diamonds (Table 4.6b). They are chromites of diamond inclusion (DI) and intergrowth compositions (high Cr and Mg), high Cr-Ti chromite (phenocrysts from kimberlite) and low Cr, high Al and/or high Fe chromites (from igneous rocks of relatively shallow derivation) (Fipke et al., 1995). Because the chrome content in chromites is pressure dependent (Danchin, 1991, referenced in Fipke et al., 1995), chromites associated with diamonds have high chrome content (>58 wt% Cr_2O_3), moderate to high MgO (9-18 wt%) and very low TiO_2 (<0.6 wt%)(Fipke et al., 1995).

Table 4.6b. Typical compositional ranges of chromites

	DI chromites	Cr-Ti chromites	Al/Fe chromites
Cr_2O_3	57.8-69.0	36.3-63.66	17.2-60.8
MgO	8.7-18.7	6.4-16.8	0-21.0
TiO_2	<0.6	0.8-8.7	<5.3
Al_2O_3	1.9-14.0	0.57-16.8	3.8-50.0
FeO*	9.3-20.0	13.7-30.2	8.7-50.0
MnO	<1.0	<1.6	<1.9

(DI (diamond inclusions); data is from Fipke et al., 1995)

Rare AMC occur as 0.7-1 mm rounded, compositionally homogeneous crystals in the Torrie and Eddie pipes. AMC from Torrie are characterized by lower TiO_2 (<0.2 wt%), Al_2O_3 (4.1-4.5 wt%) and MgO (9.8-11.0 wt%) than AMC from the Eddie pipe (Table 4.6a). Chromite from diamondiferous harzburgite has high Cr, high Mg and low Ti similar to chromite inclusions in diamonds and diamond intergrowths (Table 4.6b; Fig. 4.10). As only one of the magnesio-chromites from Torrie has Cr_2O_3 and MgO values typical of diamond inclusions/intergrowths, the potential contribution of xenocrysts, including diamond, from harzburgites is very low (Fig. 4.10). The AMC/TMC with Cr/Cr+Al=0.72-0.92 and $Fe_T^{2+}/(Fe_T^{2+}+Mg)$=0.41-0.55 (Fig. 4.9) are probably derived from
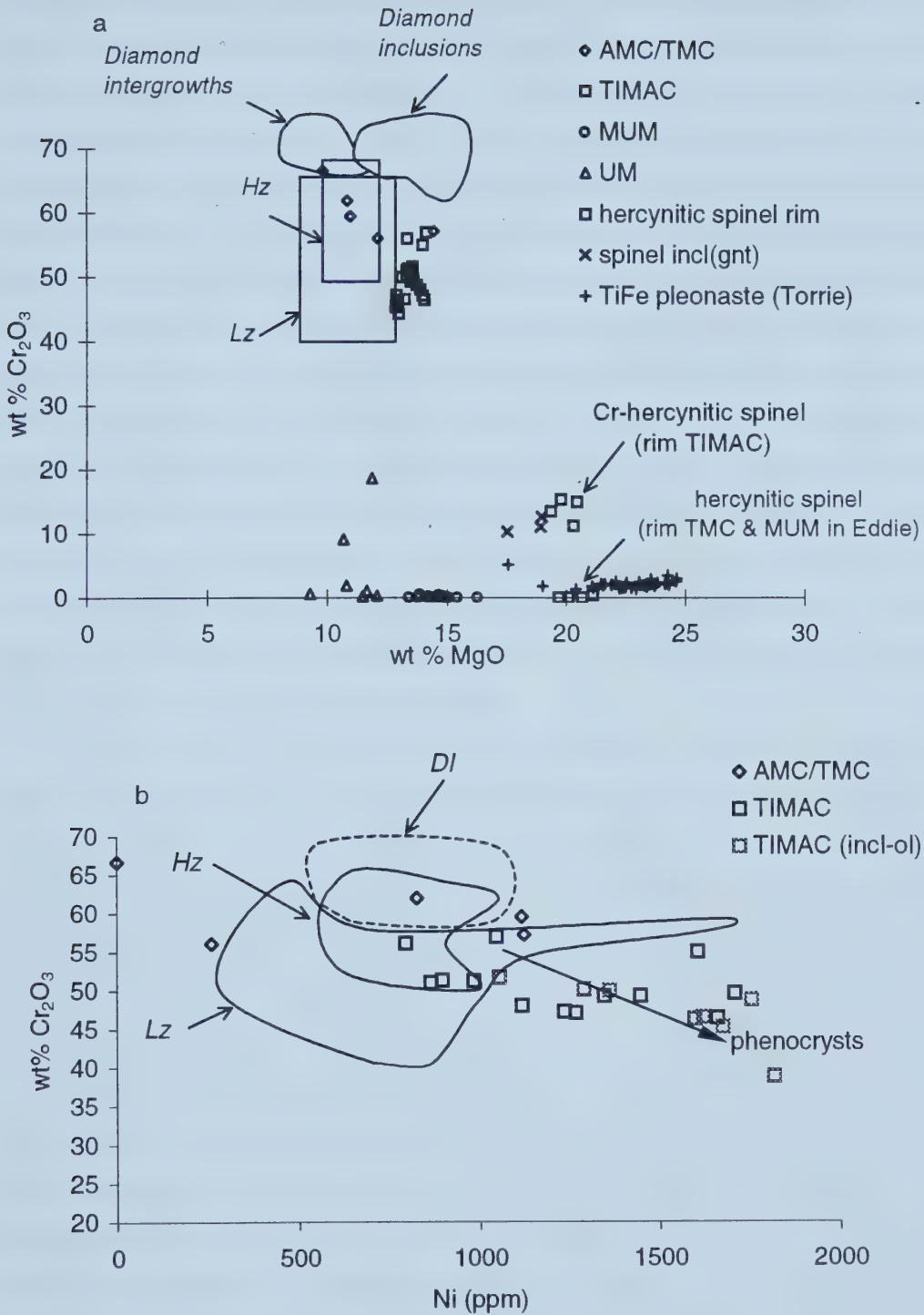
Figure 4.10. Compositions of spinels from Torrie, Sputnik and Eddie plotted as a) MgO vs Cr_2O_3 b) Ni (ppm) vs Cr_2O_3. Fields for diamond intergrowths and inclusions (DI) are from Fipke (1995). Harzburgite and lherzolite xenolith fields are from Griffin et al., (1994).

disaggregated garnet lherzolite xenoliths similar to South Africa (Griffin et al., 1994) with a minor contribution from disaggregated harzburgites, consistent with the populations of garnets and pyroxenes found (Fig.4.10). Mitchell and Clarke (1976), however, have interpreted AMC macrocrysts with < 1 wt% TiO_2 and very high Al_2O_3 (11-14 wt%) as high-pressure phenocryst phases that crystallized in the mantle before fluidized intrusion of the kimberlite. Chromites in the Eddie and Torrie pipes do not exhibit textural features that would permit an unambiguous conclusion as to their origin, however, one AMC from the Eddie pipe is compositionally very similar (low TiO_2 and high Al_2O_3) to spinels interpreted as high-pressure phenocrysts in the Elwin Bay kimberlite (Mitchell, 1978). Furthermore, the high Al_2O_3 AMC from Eddie also has very low Ni content compared to the xenolith and phenocryst fields (Fig. 4.10b). The other AMC in Torrie and Eddie have low Al_2O_3 and high Ni, and are most likely xenocrysts. The TMC spinel (62 wt% Cr_2O_3) is considered a cognate phase because low Cr-hercynitic spinel rims were observed on both the TMC and MUM from Eddie (Table 4.6c). Because MUM spinels are considered a cognate phase in more evolved kimberlite, the TMC must also be a cognate phase in the Eddie kimberlite.

The evolution of magmatic trend 1 from titanian magnesian aluminous chromite (TIMAC) and titanian magnesian chromite (TMC) toward magnesian ulvöspinel-ulvöspinel-magnetite (MUM) series is characterized by increasing Ti, Fe^{3+}/Fe^{2+} and total Fe and decreasing Cr at nearly constant $Fe_T^{2+}/(Fe_T^{2+} + Mg^{2+})$ ratios (Fig. 4.8c; Mitchell, 1995). TMC and MUM spinels in Eddie are rimmed by Cr-poor hercynitic spinels (Table 4.6c). Subhedral to euhedral TIMAC (0.5-1mm) from Torrie and Eddie have 2.4-4.2 wt% TiO_2, 6-12.3 wt% Al_2O_3, 44.3-51.3 wt% Cr_2O_3 and 12.9-14.1 wt% MgO and are mantled by chrome-rich hercynitic-spinels (33-40 wt% Al_2O_3, 19-21 wt% MgO and 11-15 wt% Cr_2O_3 (Table 4.6c) similar to pleonaste reaction mantles in South African kimberlites (Pasteris, 1983; Boctor and Boyd, 1980) and the Elliot County kimberlite (Agee at al., 1982). The presence of such Al-rich pleonaste reaction mantles on TIMAC with compositions similar to their groundmass TFP indicates a phenocryst origin for the TIMAC in South African kimberlites. Mitchell (1986) has interpreted compositionally similar spinels as a groundmass phase that crystallized entirely after fluidization and emplacement. Furthermore, TIMAC inclusions in olivines from the Torrie pipe demonstrate that olivine and TIMAC crystallized either contemporaneously or TIMAC

Table 4.6c. Microprobe analyses of zoned spinels (cations on basis of 4 oxygen).

	TIMAC core Torrie	Cr-hercynitic spinel rim	TIMAC core Eddie	Cr-hercynitic spinel rim	TMC core Eddie	hercynitic spinel middle	hercynitic spinel rim	MUM core Eddie	hercynitic spinel rim
SiO_2	0.08	0.26	0.12	0.18	0.04	0.00	0.01	0.02	0.00
TiO_2	2.41	3.23	2.10	2.49	1.53	1.38	2.87	9.10	2.82
Al_2O_3	9.00	36.19	7.28	32.84	1.93	46.03	39.80	13.27	41.28
Cr_2O_3	51.25	14.99	56.98	13.45	61.95	0.39	0.00	0.00	0.00
FeO_T	20.68	21.18	18.41	26.06	22.16	22.21	30.10	56.24	29.75
MnO	0.36	0.21	0.36	0.18	0.40	0.12	0.17	0.56	0.22
MgO	13.46	20.45	14.14	19.37	10.84	21.10	19.68	14.74	20.07
NiO	0.13	0.09	0.13	0.00	0.11	0.00	0.00	0.00	0.00
ZnO	0.12	0.00	0.00	0.00	0.09	0.00	0.00	0.00	0.00
Nb_2O_5	0.00	0.00	0.03	0.02	0.06	0.00	0.02	0.00	0.00
Total	98.23	98.01	100.15	96.55	99.72	93.06	95.03	98.18	96.49
Si	0.003	0.007	0.004	0.005	0.001	0.000	0.000	0.001	0.000
Ti	0.061	0.069	0.051	0.055	0.040	0.029	0.062	0.223	0.060
Al	0.359	1.211	0.279	1.136	0.079	1.539	1.357	0.510	1.380
Cr	1.370	0.337	1.465	0.312	1.711	0.009	0.000	0.000	0.000
Fe^{2+}	0.384	0.204	0.357	0.209	0.473	0.134	0.210	0.492	0.206
Fe^{3+}	0.187	0.299	0.144	0.431	0.161	0.393	0.517	1.042	0.500
Mn	0.010	0.005	0.010	0.005	0.012	0.003	0.004	0.016	0.005
Mg	0.678	0.866	0.686	0.847	0.564	0.893	0.849	0.717	0.849
Ni	0.003	0.002	0.003	0.000	0.003	0.000	0.000	0.000	0.000
Zn	0.003	0.000	0.000	0.000	0.002	0.000	0.000	0.000	0.000
Nb	0.000	0.000	0.000	0.000	0.001	0.000	0.000	0.000	0.000
Total	3.000	3.000	3.000	3.000	3.000	3.000	3.000	3.000	3.000
Fe^{2+}_T	0.469	0.376	0.426	0.444	0.539	0.383	0.478	0.771	0.470
FeO	13.90	8.57	13.12	8.51	16.52	5.64	8.70	18.03	8.69
Fe_2O_3	7.53	14.01	5.88	19.50	6.26	18.40	23.78	42.46	23.40
Ti/(Ti+Cr+Al)	0.03	0.04	0.03	0.04	0.02	0.02	0.04	0.30	0.00
Cr/(Cr+Al)	0.79	0.22	0.84	0.22	0.96	0.01	0.00	0.00	0.04
Mg#	0.54	0.63	0.16	0.78	0.47	0.63	0.54	0.30	1.00

preceded olivine in the crystallization sequence. MUM series spinels are present only in Sputnik and Eddie. Their presence in these pipes and not in Torrie is consistent with a more highly evolved magma than for Torrie.

The Cr-rich (mantle TIMAC in Torrie and Eddie) and Cr-poor (mantle TMC/MUM in Eddie) hercynitic spinels (pleonaste reaction mantles), however, do not resemble the titanian ferrian pleonaste (TFP) crystals in Torrie that are interpreted to be a groundmass phase. TFP spinels occur as discrete anhedral-to-euhedral crystals within globular segregations in Torrie. They are characterized by higher TiO_2 (12.3-22.5 wt%), FeO_T (33.8-46.9 wt%), and lower Al_2O_3 (7.6-14.1 wt%) compared to Cr-rich and Cr-poor hercynitic spinel rims on TIMAC-trend 1 spinels (Fig. 4.8a and c). The majority of Al-rich groundmass spinels in the literature have been described as mantling chromites or magnesian ulvöspinel-ulvöspinel-magnetite members in phlogopite-rich kimberlites (Pasteris, 1980,1983). When phlogopite ceased to crystallize upon kimberlite ascent, available Al_2O_3 was partitioned into pleonaste. Boctor and Boyd (1980) describe pleonastes in the Liqholong kimberlite as both reaction rims on megacrystal ilmenites as well as discrete groundmass crystals near reaction mantles on ilmenite nodules. Discrete pleonaste crystals (0.5-1mm) in Torrie are compositionally very similar to the groundmass spinels found in the Liqholong kimberlite and are interpreted to have crystallized, instead of phlogopite, as a late-stage groundmass phase.

Spinels from magmatic trend 1 are characteristic of kimberlite and are not present in orangeites whereas spinels from magmatic trend 2 are very rare in kimberlite (Mitchell, 1995). Spinels from magmatic trend 2 have been recognized in kimberlites that have crystallized abundant phlogopite prior to crystallization of the majority of groundmass spinels i.e. the Elwin Bay (Mitchell, 1978), Tunraq (Mitchell, 1979), Marushkaya, Zagodochnaya (Rozova et al., 1982), De Beers Peripheral (Pasteris, 1980) and Koidu (Tompkins and Haggerty, 1985) kimberlites. Trend 2 contains spinels with compositions from AMC through titanian magnesian chromite (TMC) to ulvöspinel-magnetite (UM) series. Ulvöspinel-magnetite, similar to trend 2 spinels, is present as a groundmass phase in the Eddie kimberlite pipe (Table 4.6a and Fig. 4.9). These spinels are usually formed in more evolved segregation-textured kimberlites (Mitchell, 1986) which is consistent with their presence in Eddie as it has segregation-textured groundmass and contains abundant groundmass phlogopite. They have lower Al_2O_3 (0.9-5.5 wt%), higher Ti/(Ti+Al+Cr) and higher $Fe^{2+}/(Fe_T^{2+}+Mg^{2+})$ ratios than the MUM spinels from magmatic trend 1 (Fig. 4.9). It

is likely that the UM spinels from trend 2 crystallized either contemporaneously with phlogopite or after phlogopite ceased to form as available Al_2O_3 was partitioned into phlogopite.

In summary, the Torrie pipe contains spinels from the AMC trend, early crystallizing TIMAC (Cr-rich hercynite rims) from magmatic trend 1 and TFP as a late crystallizing groundmass phase. The more evolved MUM spinels are absent from the Torrie pipe. The Eddie kimberlite pipe contains spinels from the AMC trend, TIMAC (Cr-rich hercynite rim), TMC (Cr-poor hercynite rim) and MUM (Cr-poor hercynite rim) spinels from magmatic trend 1 and UM spinels from magmatic trend 2. Sputnik contains TIMAC as inclusions in olivine and more evolved MUM spinels from trend 1. The AMC trend is absent in this pipe.

Ilmenite

Magnesian ilmenite is the third important kimberlite indicator mineral (after pyrope-garnet and chromite). Not only can it indicate the presence of a kimberlite, but it is also thought to contain information about the oxidation state of the kimberlite and hence, the degree of diamond preservation (Fipke et al., 1989). Mg-ilmenites with high Fe^{3+}/Fe^{2+} values may indicate oxidizing conditions in the kimberlite magma. The logic here is that the more oxidized the transporting kimberlite, the more rapidly diamond would react with, and dissolve in, the kimberlite. Although ilmenite is thought to be the product of fractional crystallization in the upper mantle, the relationship between the parent magma of the ilmenite and the kimberlite is unclear as they may be the same or related (protokimberlitic magma) (Smith et al., 1995). Schultze et al. (1995) believe that Cr-poor ilmenite have geochemical trends consistent with an origin by fractional crystallization in the mantle and therefore, originate from a protokimberlitic magma.

Black shiny single crystals of high Cr-Mg ilmenite are abundant in the Torrie and Sputnik kimberlite pipes and are absent in the Eddie pipe. Major-element compositions are given in Table 4.7. Cr-rich magnesian ilmenite in the Torrie and Sputnik kimberlite pipes occur as rare coarse megacrysts (>1cm) and abundant macrocrysts (3-10mm). The high MgO and Cr_2O_3 contents for ilmenites from the Torrie pipe range from 10.2-14.5 wt% MgO and 1.8-4.4 wt% Cr_2O_3 (Fig. 4.11a). The MgO and Cr_2O_3 ranges in

Table. 4.7. Representative ilmenite microprobe analyses (Cations on basis of 3 oxygen).

	Torrie	Torrie	Torrie	Torrie	Sputnik	Sputnik	Sputnik	Sputnik
SiO_2	0.04	0.00	0.01	0.01	0.03	0.05	0.03	0.02
TiO_2	48.84	50.24	51.68	45.07	46.75	49.70	47.42	48.75
Al_2O_3	0.07	0.33	0.55	0.62	0.31	0.56	0.61	0.63
Cr_2O_3	0.19	1.86	3.09	4.35	1.89	2.86	3.55	4.39
FeO_T	48.64	34.89	29.93	32.92	35.61	32.47	30.93	30.72
FeO^*	42.05	25.01	22.89	18.87	23.18	22.81	21.00	23.00
$Fe_2O_3^*$	7.33	10.98	7.82	15.61	13.82	10.73	11.03	8.59
MnO	0.52	0.30	0.21	0.24	0.33	0.27	0.24	0.25
MgO	0.78	11.48	13.29	12.53	10.87	12.27	12.24	11.80
NiO	0.06	0.13	0.16	0.13	0.06	0.09	0.13	0.11
ZnO	0.21	0.00	0.00	0.00	0.01	0.37	0.02	0.04
Nb_2O_5	0.06	0.35	0.26	0.30	0.29	0.26	0.16	0.31
Total	99.46	100.00	99.84	97.05	99.98	99.52	96.43	97.90
Si	0.001	0.000	0.000	0.000	0.001	0.001	0.001	0.001
Ti	0.946	0.904	0.912	0.841	0.880	0.893	0.882	0.890
Al	0.002	0.009	0.015	0.018	0.009	0.016	0.018	0.018
Cr	0.004	0.035	0.057	0.085	0.037	0.054	0.069	0.084
Fe^{2+}_T	1.048	0.698	0.587	0.683	0.746	0.649	0.640	0.623
Mn	0.011	0.006	0.004	0.005	0.007	0.005	0.005	0.005
Mg	0.030	0.409	0.465	0.464	0.406	0.437	0.451	0.427
Ni	0.001	0.002	0.003	0.003	0.001	0.002	0.003	0.002
Zn	0.004	0.000	0.000	0.000	0.000	0.006	0.000	0.001
Nb	0.001	0.004	0.003	0.003	0.003	0.003	0.002	0.003
Total	2.049	2.068	2.047	2.102	2.091	2.066	2.071	2.054
Mg#	2.769	36.976	44.184	40.433	35.997	40.262	41.367	40.639
Fe^{2+}	0.906	0.500	0.449	0.392	0.485	0.456	0.434	0.467
Fe^{3+}	0.142	0.198	0.138	0.291	0.260	0.193	0.205	0.157
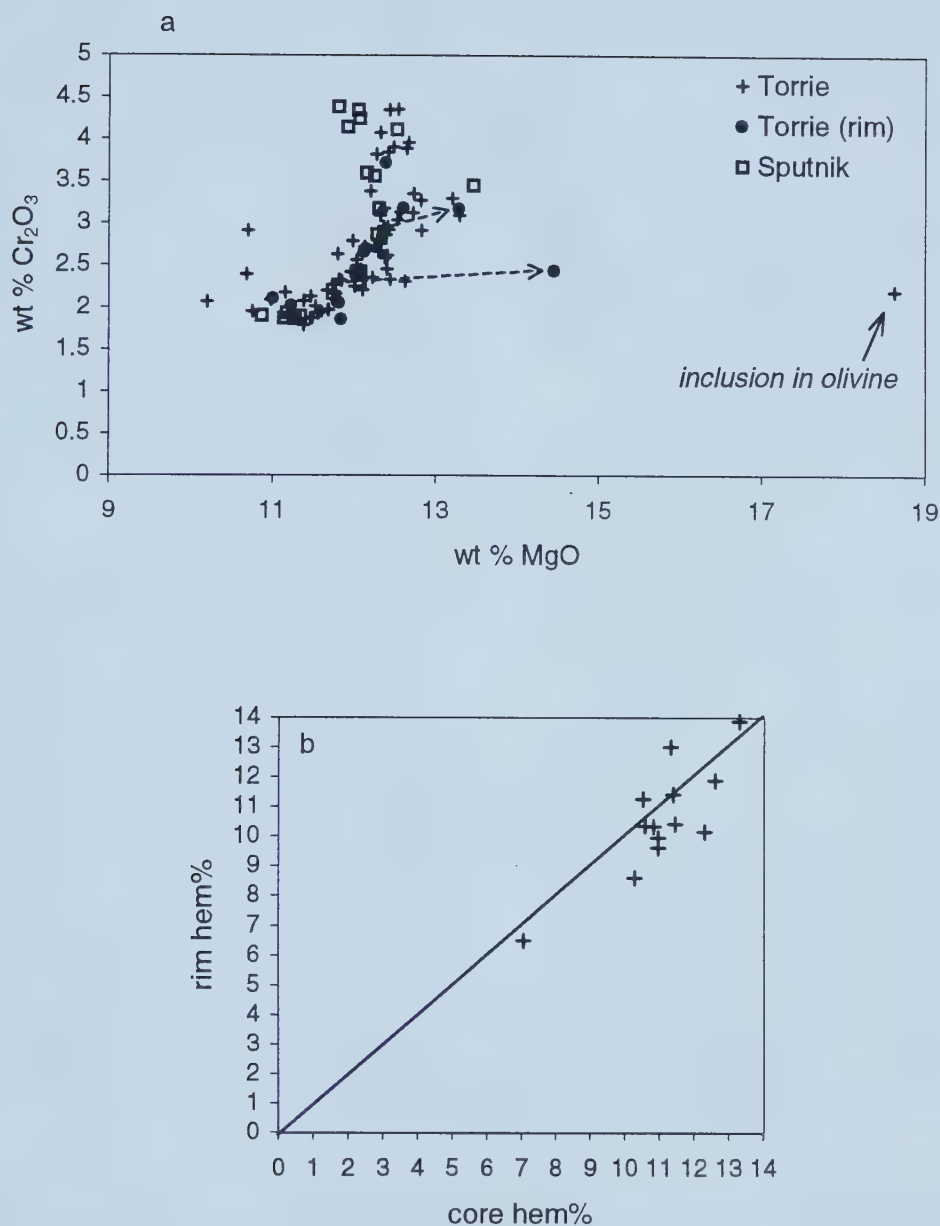
Figure 4.11. Compositional variations of ilmenite a) MgO vs Cr_2O_3 b) mole % hematite $(0.05Fe^{3+}/(0.5Fe^{3+}+Fe^{2+}+Mg))$ in cores and rims (Torrie) c) MgO vs Nb_2O_5 d) Cr_2O_3 vs Nb_2O_5. Dotted arrow points to rim compositions.
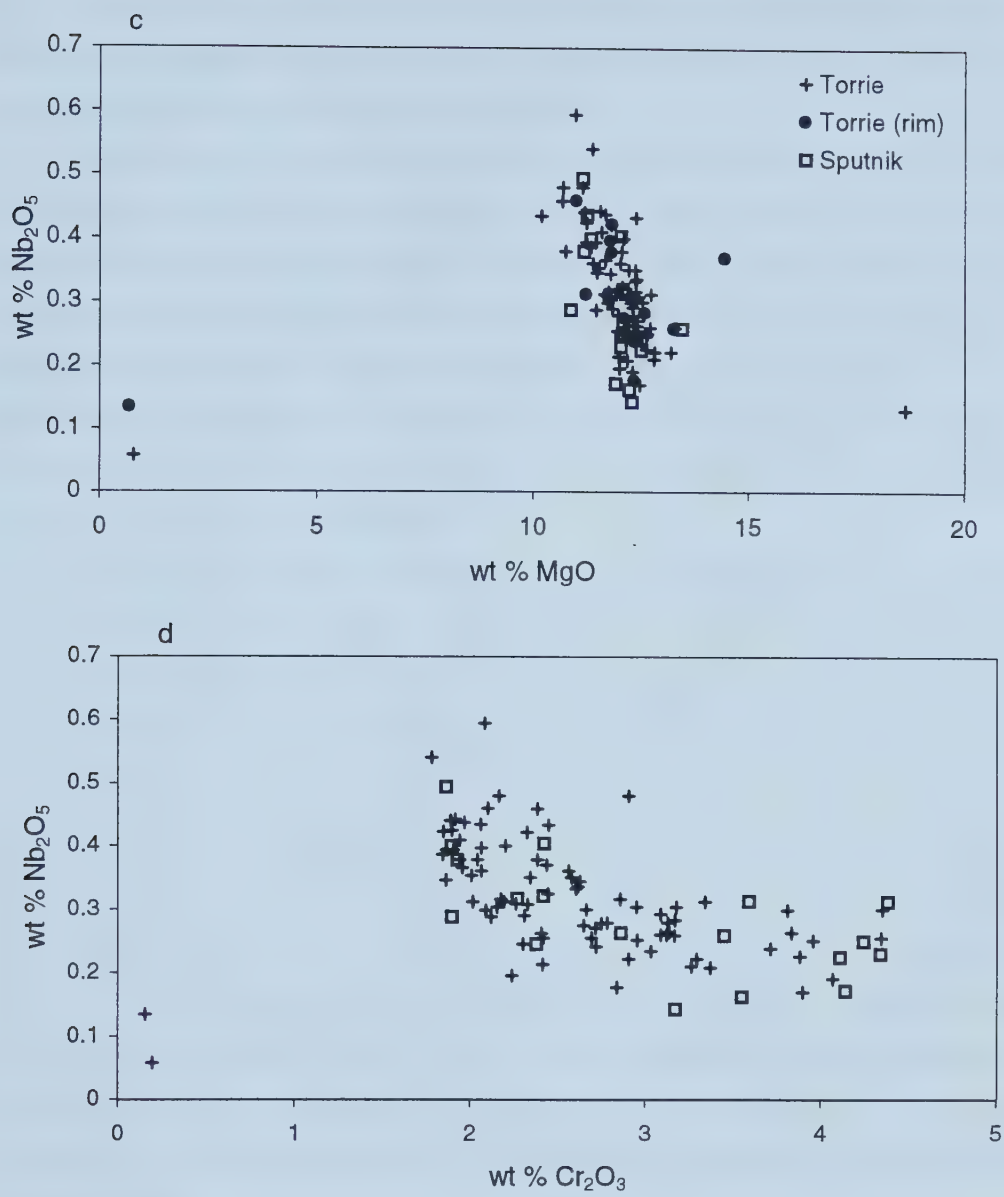
Figure 4.11.(continued)

Sputnik are slightly smaller, but are within the ranges stated for Torrie. A positive correlation between MgO and Cr_2O_3 for Mg ilmenites (Fig. 4.11a) in the pipes is consistent with a fractional crystallization origin.

The mole % hematite component ($0.5Fe^{3+}/(Mg+Fe^{2+}+0.5Fe^{3+})$), calculated as in Shultze et al. (1995), is a useful monitor of the oxidation state of the kimberlite and hence, its potential for diamond resorption (Fipke et al., 1994). Shultze (1995) suggests that this model is not universally applicable and that there is no conclusive evidence to support the hypothesis that oxidized ilmenite correlates with increased potential for the resorption of diamonds in a kimberlite. This model is used, nonetheless, by exploration companies worldwide, because they have found it to be a valuable tool if used in conjunction with garnet and chromite compositions.

Ferric iron contents in ilmenite from Torrie and Sputnik are calculated based on charge balance and 2 cations (Droop, 1987). The core hematite values are low-to-moderate for Torrie (6.5-15 mole %) and Sputnik (8-13 mole %) relative to ilmenites from 26 North American kimberlites (including 3 Canadian localities) studied by Shultze et al. (1995) (Fig. 4.11b). The high MgO, high Cr_2O_3 and range in hematite component are comparable to ilmenites from the Williams (Missouri Breaks, Montana), Bucke-1 (Kirkland Lake, Ontario) and Sloan-2 (State Line District, Colorado-Wyoming) kimberlites. The hematite components in ilmenite from Torrie and Sputnik, however, have a slightly larger range in hematite content compared to ilmenite from the Buck-1 and Sloan-2 kimberlites (Fig. 4.11). The low-to-moderate hematite values for Torrie and Sputnik ilmenite are consistent with a more reduced protokimberlitic magma in which the ilmenites crystallized compared to the majority of ilmenites from the pipes studied by Schultz (1995).

The majority of ilmenites appear homogeneous as MgO, Cr_2O_3 and Fe_2O_3 contents of the rims are very similar to the cores, but analyses of the true rims was not always possible because many grains were broken fragments. Several ilmenites had higher MgO contents in their rims and a lower hematite component (Fig. 4.11), which indicates that some of the ilmenites tried to equilibrate with a more reduced, Mg-rich kimberlitic magma. Schultze et al. (1995) suggests that late-stage Mg enrichment of ilmenite rims may have resulted from reaction with a kimberlite that was enriched in Mg by the decomposition of megacrystalline magnesite.

Niobium contents in the ilmenites range from 0.14-0.6 wt% Nb_2O_5 and correlate negatively with MgO, consistent with Nb behaving as an incompatible element in ilmenite

(Fig. 4.11c). Nb_2O_5 in ilmenites from Torrie and Sputnik remains constant (up to 0.3 wt%) or increases slightly (up to 0.6 wt%) as Cr_2O_3 decreases from 2.7 wt% to 1.5 wt% (Fig. 4.11d). Ilmenite also occurs as rare inclusions in olivine. These ilmenites are characterized by extremely high MgO (~18.5 wt%) and moderate Cr_2O_3 (2.2 wt%) contents, similar to ilmenite inclusions within olivine phenocrysts in the Wesselton Mine (Shee,1984). This observation suggests that the very high Mg-ilmenites are possibly cognate. The majority of ilmenite in Torrie and Sputnik, however, are considered to have crystallized from a protokimberlitic magma within the upper mantle as they have geochemical trends consistent with a fractional crystallization origin.

Chapter 5

Xenoliths

Petrography and Mineral Chemistry

Two small well-preserved mantle xenoliths and one crustal xenolith were found in the Torrie kimberlite. They represent three groups: garnet websterite, bimineralic eclogite and granulite. Electron microprobe studies have been carried out on these rocks to determine compositions in order to infer P-T conditions of equilibration using geothermobarometry. Representative analyses of mineral assemblages of each of the xenoliths are given in Table 5.1. Each analysis represents an average core compositon. The largest intra-grain variations are enclosed in brackets.

The websterite xenolith (~2 cm in diameter) is medium-grained and has an equigranular texture. Mineralogically, it is comprised of 50% orthopyroxene, 30% Na-Cr augite, 18% Ti-pyrope and 2% olivine (visual estimate). The orthopyroxene displays moderate inter-grain (core-to-core) variations in Cr_2O_3 (0.18-0.38 wt%), TiO_2 (0.06-0.2 wt%), and Al_2O_3 (0.4-0.5 wt%). Both Ca/Ca+Mg (0.010-0.013) and 100Mg/(Mg+Fe) (91.6-91.8) in the orthopyroxenes are very restricted. The Na-Cr-augite has very high Cr_2O_3 (1.6-1.7 wt%), high Na_2O (1.6-1.8 wt%) and low Ca/(Ca+Mg) (0.43-0.44) compared to the majority of clinopyroxene xenocrysts. The websterite garnets are classified as Group 11 (Dawson and Stephens, 1975), Ti pyrope, and are characterized by high TiO_2 (0.58-0.73 wt%), Cr_2O_3 (6.1-7 wt%) and Na_2O (0.05-0.12 wt%) and moderate CaO (5.8-6.4 wt%) contents compared to the garnet xenocrysts. Intra-grain variations in the pyroxenes and garnet are very small (Table 5.1) confirming compositional homogeneity within grains.

The small (1.8 cm in diameter) coarse-grained, equigranular eclogite is composed of 60% clinopyroxene and 40% garnet. Minor amounts of Nb-bearing rutile needles are present as inclusions in the garnet and clinopyroxene. The omphacitic clinopyroxene is pale green, transparent, anhedral and displays significant inter-grain and intra-grain variations. The grains of clinopyroxene vary considerably in their Al_2O_3 (4.8-8 wt%), Na_2O (1.7-4.1 wt%), Ca/Ca+Mg ratios (0.45-0.51), Cr_2O_3 (0.15-0.22 wt%) and

Table 5.1. Average (core) major-element mineral compositions for xenoliths and xeno/megacrysts used in geothermobarometry calculations.

	Garnet Websterite			Eclogite		Gamet Granulite			Xenocryst		Megacryst	
	gamet	cpx	opx	gamet	cpx	cpx	opx	gamet	gamet	cpx (incl)	gamet	cpx
SiO_2	40.8	55.41	57.42(57.5-58.1)	40.15(39.8-40.1)	55.4(52.6-53.4)	51.74	50.57	38.63	40.4	54.65	40.86	53.59
Al_2O_3	17.72	1.52	0.45	22.75(22.2-22.9)	7.14(4.8-5.9)	3.21	1.56	21.58	18.3	1.65	19.9	1.58
Cr_2O_3	6.55(6.95-6.59)*	1.65	0.24	0.13	0.19	0.01	0	0.01	5.11	0.85	3.08	0.96
TiO_2	0.66	0.2	0.12	0.04	0.11	0.26	0.23	0.03	0.77	0.2	0.78	0.19
FeO_T	8.79	2.82	5.68(5.5-5.8)	15.06(14.7-15.2)	2.25(2.9-3.5)	11.16	27.61	27.3	9.08	3.07	10.06	2.78
MnO	0.38	0.08	0.11	0.29	0.02	0.15	0.32	1.05	0.47	0.08	0.4	0.06
MgO	18.37	18.05	33.72(34-34.7)	12.54(11.9-12.9)	13.15(12.5-13.3)	11.87	19.1	4.71	16.74	17.44	17.94	18.49
CaO	6.07(6.36-6.14)	19.42	0.53	8.18(8.1-8.8)	18.49(20.4-21.6)	21.64	0.6	7.68	8.54	20.09	6.6	20.88
NiO	0.01	0.05	0.1	0.01	0.08	0.01	0.06	0	0.02	0.02	0.01	0.07
Na_2O	0.08	1.67	0.12	0.04	3.54(1.6-1.9)	0.86	0.04	0.005	0.07	1.18	0.06	1.28
K_2O	n.a.	0.09	n.a.	n.a.	0.02	0.02	0.01	n.a.	n.a.	0.06	n.a.	0.07
Total	99.43	100.96	98.49	99.19	100.39	100.93	100.10	101.00	99.50	99.29	99.69	99.95
Si	3.00	1.98	2.00	2.99	1.97	1.93	1.94	3.00	2.98	1.99	2.98	1.95
Al	1.534	0.064	0.018	1.997	0.299	0.141	0.071	1.977	1.593	0.071	1.713	0.068
Cr	0.381	0.047	0.007	0.008	0.005	0	0	0	0.298	0.024	0.178	0.028
Ti	0.036	0.006	0.003	0.002	0.003	0.007	0.007	0.002	0.043	0.005	0.043	0.005
Fe_T	0.539	0.084	0.163	0.938	0.067	0.348	0.883	1.774	0.56	0.093	0.614	0.085
Fe^{2+}	0.497	0.036	0.163	0.920	0.067	0.288	0.808	1.744	0.458	0.093	0.515	0.000
Fe^{3+}	0.042	0.048	0.000	0.018	0.000	0.060	0.075	0.030	0.102	0.000	0.099	0.085
Mn	0.024	0.003	0.003	0.018	0.001	0.005	0.01	0.069	0.029	0.003	0.025	0.002
Mg	2.012	0.963	1.754	1.393	0.698	0.66	1.089	0.545	1.842	0.946	1.953	1.002
Ca	0.478	0.745	0.02	0.653	0.705	0.865	0.024	0.64	0.676	0.783	0.516	0.813
Ni	0.001	0.001	0.003	0	0.002	0	0.002	0	0.001	0	0	0.002
Na	0.011	0.116	0.008	0.005	0.244	0.062	0.003	0.001	0.009	0.083	0.008	0.09
K	n.a.	0.004	n.a.	n.a.	0.001	0.001	0.001	n.a.	n.a.	0.003	n.a.	0.003
Total	8.01	4.02	3.98	8.01	4.00	4.02	4.03	8.01	8.03	4.00	8.03	4.05

n.a. (not analysed); *largest within-grain variation is enclosed in brackets

MgO (12.5-15.4 wt%) concentrations. Significant intra-grain variations were observed as well for Al_2O_3, FeO, MgO and CaO (Table 5.1). The reddish-orange garnets are anhedral, Ca-pyrope almandines. They are classified as group 3, Ca-pyrope almandine (from diamondiferous eclogite; Dawson and Stephens, 1975) and have variable FeO (14.7-15.4 wt%), CaO (7.7-8.8 wt%), MgO (11.9-12.9 wt%) and Na_2O (0.01-0.08 wt%) inter-grain concentrations. Slight intra-grain variations are observed for Al_2O_3, FeO, MgO and CaO (Table 5.1). Rare kelyphitic rims on garnet are composed of phlogopite and microcrystalline material.

There are 2 models for the origin of eclogite: (1) high-pressure igneous cumulates (products of fractional crystallization in the mantle; Smyth et al., 1989 and references therein) and (2) metamorphic products of subducted oceanic crust (Taylor and Neal, 1989 and references therein). The major-element mineral chemistry of eclogites is consistent with an origin by fractional crystallization from an evolving magma, however, the isotope and REE data are inconsistent with such a petrogenesis (Neal et al., 1989). Three groups of mantle-derived eclogites (Groups A, B and C) have been identified based on petrography, clinopyroxene-garnet mineral chemistry, REE contents of whole rocks and minerals, stable and radiogenic isotopes (Taylor and Neal, 1989; Neal et al., 1989). Group A eclogites are interpreted as high pressure (mantle) cumulates whereas Groups B and C are interpreted as metamorphosed products of oceanic crust. Group B represents the basaltic section and Group C, the cumulate (plagioclase-rich) section of oceanic crust. The three groups of eclogites and their characteristic mineral chemistry are shown in Table 5.2.

The eclogite xenolith from Torrie exhibits chemical affinities with both crustal and mantle rocks. The garnet chemistry is similar to Group B, however, the clinopyroxene has major-element chemistry similar to both Groups A and B (Table 5.2). The garnet (high Fe, low Cr) and clinopyroxene (high Fe, moderate Na, low Cr) compositions are very similar to Group B eclogites found in the Udachnaya and Mir kimberlites in Russia and the Bellsbank kimberlite in South Africa. Group B eclogites from these locations are believed to be metamorphosed ancient subducted oceanic crust (Neal et al., 1990; Snyder et al, 1995).

Table 5.2. Chemical characteristics of eclogite groups identified by Taylor and Neal (1989). The Torrie eclogite is presented for comparison.

	Group A		Group B		Group C		Torrie eclogite	
	garnet	cpx	garnet	cpx	garnet	cpx	garnet	cpx
wt% MgO	Mg-rich (up to 21%)	14-18%		9-14%		5-9%	11.9-13%	12.5-15.4%
wt% FeO	8.7-11%	1.5-2%	Fe-rich (up to 17%)	3.6-4 %	7-10%	<1.2%	14.8-15.4%	2-3.5%
wt% CaO		16%		12-13%	Ca-rich (up to 18.8%)	12-13%	7.9-8.8%	17.7-21.6%
wt% Na$_2$O		<3%		3-6.5%		6.5-9%		1.6-4.1%
wt% Cr$_2$O$_3$	2-4%	0.6-2.3%	<0.15%	<0.1%	<0.15%	<0.1%	0.09-0.18%	0.15-0.23%
δ^{18}O$_{SMOW}$	+5.3 to +5.6‰	+5.0 to +5.8‰	+3.0 to +3.9‰	+2.8 to +4.1‰	+3.1 to +4.9‰	+3.9 to +4.3‰	+5.61‰	+5.34‰

The granulite xenolith has a mafic mineral assemblage of garnet + clinopyroxene + orthopyroxene + plagioclase. Reaction microstructures such as symplectites, coronas and exsolution lamellae are abundant, and may provide insight into the retrograde P-T path taken by the xenolith on cooling from peak metamorphic conditions. For example, worm-like symplectites of alkali feldspar (orthoclase) after garnet may have occurred as a result of interaction with the kimberlite magma. The instability of phlogopite at high temperatures results in the following reaction:

3 spinel + 9 βquartz + 2 phlogopite = 2 k-feldspar + 3 pyrope-garnet + 2 H_2O.

Coronas of garnet around an orthopyroxene core resulted from reaction between the orthoproxene and adjacent plagioclase, consistent with the xenolith undergoing retrograde metamorphism (cooling) prior to entrainment in the kimberlite, for example,

garnet + quartz = orthopyroxene + plagioclase.

Very fine-grained exsolution in ilmenite (probably magnetite) is observed, as is exsolution of clinopyroxene in orthopyroxene and orthopyroxene in clinopyroxene. There is evidence of secondary alteration, such as abundant microcrystalline material along fractures in garnets and along cleavage planes in clinopyroxenes, as well as calcite veining cross-cutting the xenolith. The xenolith probably represents in situ lower crustal material because mafic granulites are generally considered to be the dominant component of the lower Phanerozoic crust (Percival, 1994). Because this granulite was probably derived from the lower crust, it was considered peripheral to this study and was not studied in further detail.

Geothermobarometry

There are many geothermometers and geobarometers available to calculate temperatures and pressures for appropriate mineral assemblages of xenoliths. The appropriate geothermometer/geobarometer, however, should be calibrated to a bulk composition similar to the xenoliths. Further problems arise as different methods may give divergent results as a result of different assumptions about the thermodynamic behavior of the xenolith phases. Taking these considerations into account, the following geothermometers and geobarometers were adopted for the appropriate mineral assemblages. Temperatures are calculated from a) the compositions of coexisting pyroxenes (Brey and Köhler, 1990) b) Fe-Mg exchange between garnet and clinopyroxene

(Krogh, 1988; Ellis and Green, 1979) and pressures are calculated from the Al content of orthopyroxene in equilibrium with coexisting garnet (Brey and Köhler, 1990). The absence of orthopyroxene in the eclogite xenolith and clinopyroxene/garnet xenocrysts, however, does not allow the direct determination of an equilibrium pressure as there are no barometers available. The depth (pressure) was estimated by finding the point of intersection between an assumed geotherm and the calculated temperature. All P-T calculations used average (core) mineral compositions because several of the minerals in the mantle xenoliths show compositional zoning in the rims, which was inferred to reflect changes during transport in the kimberlite. The rapid transport of the xenoliths to the surface, however, should minimize re-equilibration during cooling.

The garnet-clinopyroxene geothermometers require estimates of Fe^{3+}, however, Fe^{3+} calculation procedures (i.e. Droop, 1987) are highly sensitive to analytical errors in SiO_2 and Al_2O_3, especially in low Fe-pyroxenes (Canil and O'Neill, 1996; Carswell and Harley, 1990). Consequently, the calculation of Fe^{3+} by stoichiometry tends to overestimate Fe^{3+} in low-Fe pyroxenes, which results in the calculation of a maximum K_D value and in turn, yields a minimum equilibration temperature for the xenolith assemblage (Table 5.3). Moreover, Mössbauer spectroscopy on mineral separates has shown that, in mantle assemblages, $Fe^{3+}/\Sigma Fe$ in clinopyroxene are greater than those in coexisting orthopyroxene and garnet (Canil and O'Neill, 1996; Luth and Canil, 1993 and Luth et al., 1990). Therefore, in this study, all temperatures are calculated assuming all Fe as FeO, so these temperatures should be considered as maximum temperatures. If Fe^{3+} contents are calculated based on stoichiometry (Droop, 1987), the temperatures for the websterite xenolith were near identical (10 °C lower) for the Brey and Köhler (1990) thermometer and approximately 250 °C lower for the Ellis and Green (1979) thermometer. This reflects the fact that thermometers based on Fe^{2+}-Mg exchange (i.e. Ellis and Green, 1979 and Krogh, 1988) are more sensitive to the presence of Fe^{3+} in garnet and clinopyroxene than is the 2-pyroxene thermometer of Brey and Köhler (1990).

The Fe-Mg exchange thermometer between garnet and clinopyroxene (Ellis and Green, 1979) yields temperatures of approximately 1129 °C (66 kbars) and 1000 °C (50 kbars) for the garnet websterite and garnet/clinopyroxene megacryst, respectively. A higher estimate of equilibrium temperature and pressure for the garnet websterite

Table 5.3. Calculated temperature and pressure estimates for xenoliths, megacrysts and xenocrysts.

Sample	Type	Krogh (1988)		Ellis and Green (1979)		Brey and Kohler (1990)	
		T (C) $Fe=Fe^{2+}$	P (kbar) exp	T (C) $Fe=Fe^{2+}$	P (kbar) exp	T (C) $Fe=Fe^{2+}$	P (kbar)
Torrie	garnet	1100	66	1129	66	*1193	66
	websterite	1035	50	1071	50		
Torrie	eclogite	731	30	*774	30		
		761	40	802	40		
		791	50	831	50		
Sputnik	garnet-cpx	884	30	931	30		
	megacryst	921	40	965	40		
		957	50	*998	50		
		994	60	1032	60		
Sputnik	garnet-cpx(incl)	1193	30	1166	30		
	xenocryst	1236	40	1205	40		
		1280	50	1243	50		
		1323	60	*1281	60		
Torrie	garnet	642	6.4	691	6.4	787	6.4
	granulite	653	10	701	10		

*values plotted in Figure 5.1

$$T_{BKN}=\dfrac{23664+(24.9+126.3X_{Fe}^{cpx})P}{13.38+(\ln K_D^*)+11.59X_{Fe}^{opx}}; \quad X_{Fe}^{opx}=Fe/(Fe+Mg); \quad K_D^*=(1-Ca^*)^{cpx}/(1-Ca^*)^{opx}$$

$$Ca^*=Ca^{M2}/(1-Na^{M2})$$

$$T_{Krogh}=\dfrac{[-6173(X_{Ca}^{Grt})^2+6731X_{Ca}^{Grt}+1879+10P(kbar)]}{(\ln K_D+1.393)}; \quad X_{Ca}^{Grt}=Ca/(Ca+Mg+Fe); \quad K_D=\dfrac{(X_{Fe}/X_{Mg})^{Grt}}{(X_{Fe}/X_{Mg})^{Cpx}}$$

$$T_{E\&G}=\dfrac{3104X_{Ca}^{Grt}+3030+10.86P(kbar)}{\ln K_D+1.9034}; \quad K_D=\dfrac{(Fe/Mg)^{grt}}{(Fe/Mg)^{cpx}}$$

xenolith of 1193°C and 66 kb was obtained using the thermometer and barometer combination of Brey and Köhler (1990). These estimated temperatures plot close to a geotherm of 47-48 mW/m^2 reported by Kopylova et al. (1998) for the Jericho kimberlite, NWT (Figure 5.1). An equilibrium temperature of 830°C, at an assumed pressure of 50 kb, is estimated for the eclogite, which is within the range stated for eclogite samples from the Jericho pipe that have average temperatures at 50 kb of 690-1170°C calculated using the Finnerty and Boyd (1987) thermometer (Kopylova et al., 1998). The eclogite sample from Torrie projects onto the assumed geotherm at ~110 km. Eclogites from the Jericho pipe lie between 90 and 195 km, whereas most porphyroclastic peridotite are derived from below 190 km (1100-1300°C). If a geotherm of 48 mW/m^2 is assumed, then the low equilibrium temperature of the eclogite indicates that it equilibrated outside the diamond stability field (lower pressure) whereas the garnet/cpx megacryst and websterite xenolith equilibrated within the diamond stability field. A Ti-pyrope garnet xenocryst with a clinopyroxene inclusion records a temperature of approximately 1245°C at 50 kb. This temperature is higher than would be present along the proposed geotherm, and may be a result of a transient heating event. Temperature estimates using the Krogh (1988) geothermometer were consistently 40 °C lower than those calculated using the Ellis and Green (1979) thermometer (Table 5.3) except for the high temperature Ti-garnet xenocryst which yielded temperatures 30-40 °C higher than the Ellis and Green (1979) thermometer.

In summary, the majority of xenocryst and xenolith assemblages from Torrie and Sputnik, with the exception of a high-T xenocryst, fall along a cratonic geotherm of 47-48 mW/m^2, similar to the geotherm reported for the Jericho kimberlite (Kopylova et al., 1998). Temperatures recorded by a garnet with a clinopyroxene inclusion are consistent with either a much higher local temperature or derivation from greater depths.
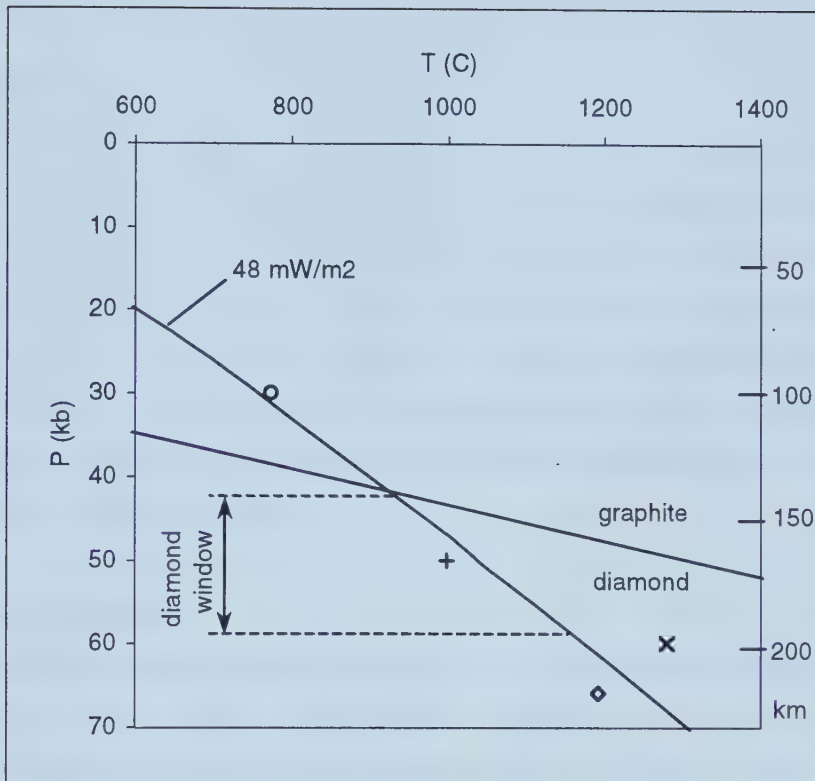
Figure 5.1. Pressure-temperature estimates of primary mineral assemblages from garnet websterite (diamond), eclogite (circle) from Torrie, megacryst(+) and xenocryst (x) from Sputnik; diamond-graphite transition after Kennedy and Kennedy (1976); geothermal gradient after Kopylova et al. (1998).

Chapter 6

O-isotopes

In the past decade, insight into the variations of oxygen isotopes in the mantle samples and processes that caused them has been gained primarily from analyses of basalts and coexisting minerals in mantle-derived xenoliths (Harmon and Hoefs, 1995 and references therein). Studies of oxygen isotopes of mineral separates from kimberlite have the potential to make important contributions to studies of the petrogenesis of kimberlite, the preservation of diamonds and heterogeneity in the mantle. Garnet and clinopyroxene xenocrysts, ilmenite megacrysts and two mantle xenoliths from the Torrie pipe were analyzed for oxygen isotopes.

Analytical methods

Oxygen isotope analyses are reported in the standard delta (δ) notation, in units of per mil variation relative to the SMOW (standard mean ocean water) international standard. Whole-rock kimberlite samples were separated into various size fractions, then ultrasonically washed in distilled water several times and dried at 60°C. Individual mineral separates were then handpicked from the size fractions on the basis of glassiness, minimum degree of alteration and lack of inclusions. Finally, the separates were washed in 2.5 M HCl for 1 hour, rinsed 3x in distilled water, 3x in methanol and dried under a heat lamp. Separates were then powdered in an agate mortar that was cleaned before each sample by grinding silica and rinsing with methanol. Each $\delta^{18}O$ value represents an average, as each sample required 6-10 grains for a reasonable yield. Because of the composite nature of the sample the actual $\delta^{18}O$ variations of the grains are larger than the measured ranges.

Garnet and clinopyroxene samples were pretreated for about 3 hours in BrF_5 at 300°C. Oxygen was extracted from the mineral concentrates in the Stable Isotope Laboratory of Karlis Muehlenbachs at the University of Alberta following the technique of Clayton and Mayeda (1963). Oxygen isotope analyses were measured from CO_2 on a Finnigan Mat 252 mass spectrometer. Two analyses of NBS-28 (quartz standard) each gave $\delta^{18}O=+9.60\pm0.15‰$ (1 S.D.), which are in good agreement with the accepted value of +9.66‰. Duplicate analyses on two xenocryst samples indicate that $\delta^{18}O$ values agree

to ±0.3‰ and duplicate analyses of a garnet sample from the eclogite agree to ±0.02‰ indicating homogeneity in the xenolith.

Variations in $\delta^{18}O$ in the mantle-derived minerals and rocks may be attributed to mantle and crustal processes. Oxygen isotope variations in the mantle are caused by processes such as high and low temperature fractionation among mineral phases and between minerals, melts or other fluids and prior melting events (Harmon and Hoefs, 1995). For example, fractionation between clinopyroxene and garnet is <0.1‰ at 1200°C (Gregory and Taylor, 1986), +0.17‰ at 950°C (Kieffer, 1982) and +0.25 at 730°C (Chiba et al., 1989; Rosenbaum et al., 1994). Because the equilibrium fractionation for the mineral pair is very small over a wide range of temperatures, the cpx-garnet isotopic fractionation serves as a sensitive test of disequilibrium. Furthermore, crystal-melt $\delta^{18}O$ fractionations are <2‰ for the major rock-forming minerals (<1‰ for garnet and clinopyroxene; Taylor and Sheppard, 1986). Overall, intrinsic mantle processes can only account for relatively small variations in $\delta^{18}O$.

Xenoliths

The eclogite and websterite minerals have oxygen isotopic values of +5.3 to +5.7‰±0.15‰, which lie within the typical mantle range of +5 to +6‰. The mineral fractionation between clinopyroxene and garnet ($\Delta^{18}O_{cpx-gnt}$), however, indicates a slight disequilibrium in the websterite and eclogite xenoliths. At high temperatures (~1200°C), similar to that calculated for the websterite xenolith (~1193°C at 66 kbars), equilibrium fractionation between clinopyroxene and garnet should be negligible (Gregory and Taylor, 1986). Therefore, the $\Delta^{18}O_{cpx-gnt}$ =-0.4‰ in the websterite xenolith, not only indicates a slight disequilibrium but also indicates a reversal as garnet is 0.4‰ heavier in $\delta^{18}O$ than clinopyroxene (Table 6.1). The $\Delta^{18}O_{cpx-gnt}$ reversal is interpreted as a disequilibrium process such as metasomatic exchange with oxygen-bearing fluids (Gregory and Taylor, 1986). The oxygen isotopic disequilibrium can be attributed to the different rates of equilibration for each mineral with a metasomatic fluid (Gregory and Taylor, 1986). The typical mantle values and very small variation of $\delta^{18}O$ observed in garnet from the eclogite are consistent with it being more refractory (relatively inert) compared to the clinopyroxene (Farver, 1989; Coghlan, 1990).

As discussed in Chapter 5, the chemistry of the garnet and clinopyroxene indicates that the eclogite has a hybrid origin (i.e. crustal and mantle affinities). Although the $\delta^{18}O$

values are consistent with a mantle derivation, significant intra-grain variations (Al_2O_3, Na_2O and Ca/[Ca+Mg]) in clinopyroxene coupled with a $\Delta^{18}O_{cpx\text{-}gnt}$ reversal are indicative of a metasomatic process. Moreover, the hybrid nature (exhibits both crustal and mantle affinities) of the clinopyroxene and $\Delta^{18}O_{cpx\text{-}gnt}$ reversal are consistent with the fact that pyroxene exchanges oxygen more readily than garnet. One explanation for the origin of the eclogite is that it is crustal (metamorphosed oceanic crust) and tried to re-equilibrate to typical mantle conditions. The origin of the eclogite xenolith from Torrie cannot be resolved without radiogenic isotope studies.

Garnet and clinopyroxene xenocrysts

$\delta^{18}O$ analyses of clinopyroxene, garnet and ilmenite separates are given in Table 6.1 and the variations are illustrated in histogram form in Figure 6.1. As discussed in Chapter 4, the majority of clinopyroxene and garnet xenocrysts are interpreted to be derived from disaggregated garnet lherzolite xenoliths. Clinopyroxene ranges from +3.98 to +5.57±0.15‰ (mean=+4.99‰) and garnet has a narrow range of +5.81 to +6.36±0.15‰ (mean=+6.11‰).

The large range of $\delta^{18}O$ values that deviate from that of the typical mantle (+5.7), indicate that the xenocrysts are in isotopic disequilibrium with "normal" mantle. Inter-mineral disequilibrium $\delta^{18}O$ variations in the garnet and clinopyroxene xenocrysts, however, are difficult to examine, as the minerals are not necessarily coexisting. The disequilibrium between clinopyroxene and garnet xenocrysts may be a result of the kimberlite sampling different regions en route to the surface. The large range in $\delta^{18}O$ compared to typical mantle values (MORB) is significant. Figure 6.2 compares the $\delta^{18}O$ values of the Torrie peridotite xenocrysts to garnet lherzolite (Mattey et al., 1994) and eclogite xenoliths (Neal et al., 1990) from five South African kimberlites (Roberts Victor, Premier, Jagersfontein, Bultfontein and Finsch) and mid-oceanic ridge basalt (MORB). The range in $\delta^{18}O$ values for spinel is from spinel lherzolites in South African kimberlites. Peridotite xenocrysts from the Torrie pipe display a larger range in $\delta^{18}O$ values than typical mantle peridotites from South African kimberlites, which indicates an extent of $\delta^{18}O$ heterogeneity more similar to eclogite xenoliths. The possible sources of the heterogeneity are complex and are discussed further below.

Table 6.1. Oxygen isotope analyses ($\delta^{18}O_{SMOW}$) of garnet, clinopyroxene and ilmenite in the Torrie kimberlite pipe.

Sample	ilmenite	clinopyroxene	garnet
xenocrysts	3.55‰	5.57‰	6.17‰
	4.92‰	3.98‰	5.82‰
	3.83‰	5.41‰	6.36‰
	5.44‰		6.08‰
websterite xenolith		5.26‰	5.70‰
eclogite xenolith		5.34‰	5.61‰
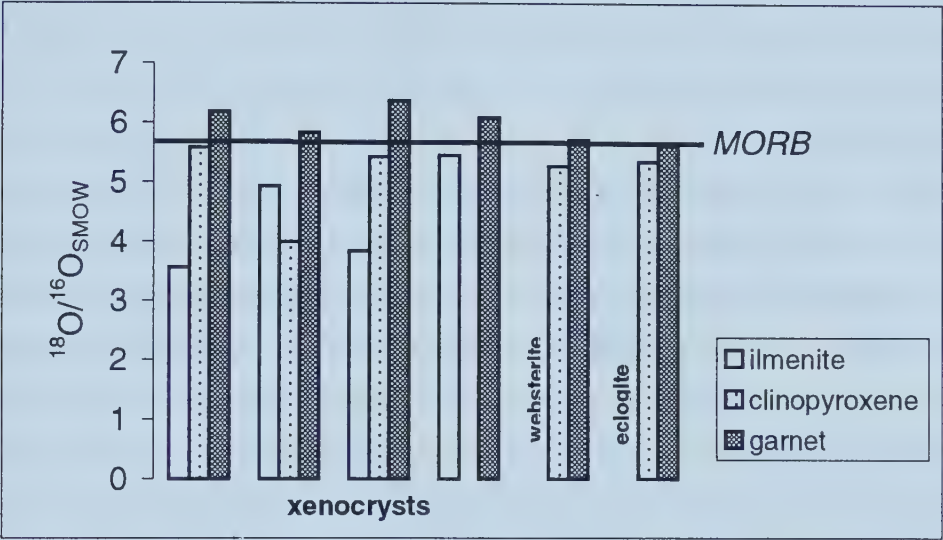
Figure 6.1. Graph illustrating the large oxygen isotope variations of Torrie xenocrysts and minerals from mantle xenoliths compared to a typical mantle value (MORB).
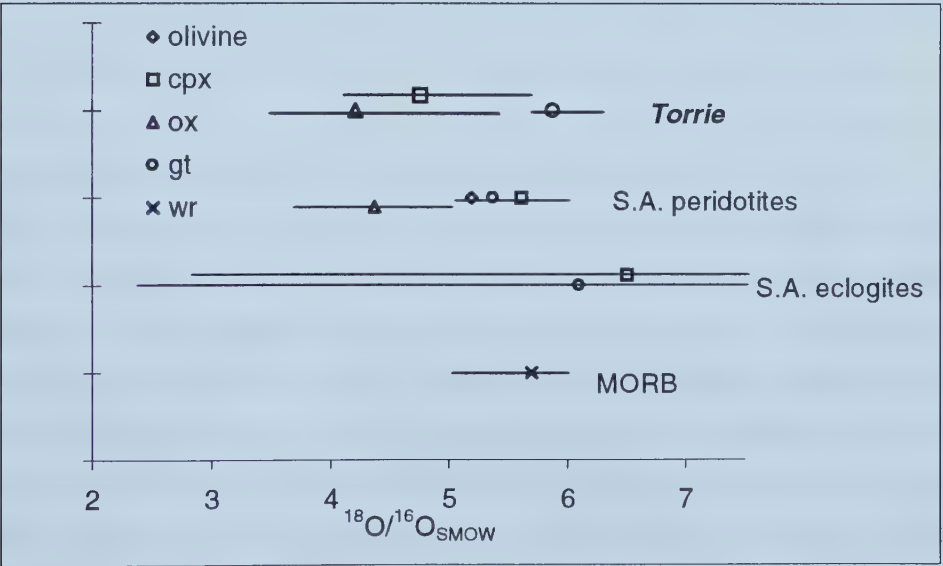
Figure 6.2. $^{18}O/^{16}O$ analyses of the Torrie pipe compared to other mantle-derived rocks; S.A.(South African) eclogites and peridotites, ox (ilmenite in Torrie and spinel in S.A. peridotites), gt(garnet), wr(whole rock). Data from Mattey et al., (1994).

The careful selection of mineral separates coupled with HCl washing and pre-fluorination procedures minimizes the possibility that the observed oxygen variation is a result of post-emplacement, low temperature near-surface alteration of the kimberlite. Post-emplacement modification from metamorphism may also be eliminated because there is no regional metamorphism postdating the emplacement of the kimberlite pipe.

As discussed earlier, intrinsic mantle processes such as isotopic fractionation at high temperatures, can only account for relatively small variations in $\delta^{18}O$ (<1‰). Large $\delta^{18}O$ variations in mantle-derived minerals and rocks, such as those observed in garnet and clinopyroxene xenocrysts from the Torrie pipe, have been attributed to inheritance from crustal processes because of this inability of high-T processes to generate large differences in $\delta^{18}O$ (MacGregor, 1985; Kyser, 1986; Ongley et al., 1987; Jacob et al., 1994; Beard et al., 1996). The observed $\delta^{18}O$ heterogeneity in oceanic crust is the result of low- and high-temperature alteration resulting in enriched and depleted $\delta^{18}O$ signatures, respectively, compared to MORB (+5.7‰) (Muehlenbachs et al, 1986). The uppermost section of an ophiolite sequence (0-1 km) consists of pillow basalts enriched in $\delta^{18}O$ (+7 to +8.5‰) because of low-temperature alteration as a result of interaction with cold seawater. Progressively deeper sections of oceanic crust, consisting of sheeted dike complexes, gabbros and harzburgites, have undergone high temperature alteration, which depletes the crust in $\delta^{18}O$, resulting in values as low as +3.5‰.

The large range in oxygen isotopes (3.55-6.36‰) from deeply derived fragments of mantle origin recorded in the Torrie kimberlite pipe is equalled by eclogite xenoliths from kimberlite pipes. The most reasonable way in which crustal processes may influence mantle-derived samples is by interaction with subducted material. Diamondiferous eclogite nodules from the Roberts Victor kimberlite pipe, South Africa, that display whole-rock $\delta^{18}O$ signatures (+2.2 to +8.3‰), consistent with high- and low-T seawater alteration, establish a link between subduction and the formation of diamonds in eclogites (MacGregor and Manton, 1986). Furthermore, many other eclogites from both Siberian (Mir and Udachnaya) and South African (Bellsbank) kimberlites show convincing major-element and isotopic values consistent with derivation from oceanic crust (Beard et al., 1996; Snyder et al., 1997, 1995: Jacob et al., 1994; Taylor and Neal, 1989; and Ongley et al., 1987). The observed low and high $\delta^{18}O$ signatures from Torrie xenocrysts are similar to eclogites that have undergone high and low temperature alteration, respectively. More eclogite xenoliths from Torrie are necessary, however, to check for consistent mineral-

chemical trends between oxygen isotopic values and microprobe oxide analyses (i.e. $\delta^{18}O$ vs FeO_{cpx} or $\delta^{18}O$ vs CaO_{grt} as in Jacob et al, 1994) that may indicate seawater alteration. For example, the protoliths of the eclogites from Siberian kimberlites experienced Fe enrichment and Ca depletion with increasing ($\delta^{18}O$) seawater alteration (Jacob et al., 1994).

It is proposed that the ultimate source for the $\delta^{18}O$ heterogeneity in the xenocrysts from the Torrie kimberlite pipe is the melting of subducted ancient oceanic crust and the exchange between the partial melts and fluids and the depleted peridotite overlying the subducted slab. The subduction of serpentinized oceanic crust, which underwent initial depletion and enrichment in ^{18}O at surface, most likely occurred during the Archean (related to the formation of the Slave province?) or Proterozoic (related to the Wopmay orogen?). Because the distance between the xenocrysts is unknown, it is difficult to determine the timing of the $\delta^{18}O$ heterogeneity. The metasomatic and/or heating event that caused the inter-mineral $\delta^{18}O$ disequilibrium (isotopic reversals) over a cm-scale in the xenoliths, however, must have occurred within a few years prior to the eruption of the kimberlite if fluids are present. For example, a time of 8 years would probably be required to attain equilibrium over a cm-scale between minerals if fluid is present. If fluid is not present, equilibrium is attained in ~8000 years over a cm-scale (Table 6.2). In other words, the $\Delta^{18}O_{cpx-gnt}$ reversal in the xenoliths indicates that the event that caused the inter-mineral disequilibrium in the xenoliths may have occurred within a few thousand years prior to the eruption of the kimberlite. The bulk oxygen diffusion coefficient (D_{bulk}) that is used is a weighted average of volume diffusion and grain boundary diffusion in the presence of a fluid (~10^{-9} cm^2/s) and in the absence of a fluid (~10^{-12} cm^2/s) (Farquhar et al., 1993).

Table 6.2.   Length scale of oxygen diffusion calculated with and without fluid present.

t (years)	D (cm^2/s)	length (m)
~8	10^{-9} (fluid)	0.01
~8000	10^{-12} (no fluid)	0.01
10^6	10^{-9}	3.5
10^6	10^{-12}	0.1
10^7	10^{-9}	11
10^7	10^{-12}	0.4

Length = $(4D_{bulk}t)^{1/2}$ (Farquhar et al., 1993)

The large variation in $\delta^{18}O$ in the xenocrysts coupled with the isotopic reversal observed in garnet and pyroxene xenocrysts and xenoliths can be attributed to processes related to partial melting of subducted oceanic crust and the subsequent migration of these melts and fluids into overlying depleted peridotite. It is hypothesized that the garnet and clinopyroxene xenocrysts in Torrie have inherited chemical components (predominantly $\delta^{18}O$ heterogeneity) from the slab through the interaction of metasomatic fluids.

In an analogous fashion, Gregory and Taylor (1986) invoke a metasomatic fluid event to account for $\delta^{18}O$ variability in mantle peridotites. They suggest that disequilibrium effects are characteristic of transient, short-lived processes associated with the eruption of the magma that transports the xenoliths as the variability and disequilibrium effects would disappear in a few tens of millions of years or less at mantle temperatures. They interpreted the large variations in $\delta^{18}O$ to be a result of open-system exchange with metasomatic fluids that have been produced from ancient subducted oceanic crust.

Ilmenite megacrysts

The Mg ilmenite megacrysts from Torrie are interpreted as either high-pressure phenocryst phases that formed in the early stages of kimberlite magmatism or crystallization products from a protokimberlitic magma (discussed in Chapter 4). In both interpretations, there is a genetic link between Mg ilmenite and kimberlite. Therefore, the

variations in $\delta^{18}O$ in the ilmenites are interpreted to reflect the kimberlite source region. The ilmenite ranges from +3.55 to +5.44±0.15‰ (mean=+4.44‰).

Oxygen isotope analyses of ilmenite from kimberlite have not been reported in the literature, therefore, $\delta^{18}O$ analyses of ilmenite from Torrie will be compared to spinel (magnetite) analyses as their oxygen fractionation factors are similar (Chiba et al., 1989). The low $\delta^{18}O$ values are similar to $\delta^{18}O$ values in magnetite, which is the lowest $\delta^{18}O$ mineral (Taylor and Sheppard, 1986). The large range in $\delta^{18}O$ is surprising considering the high temperatures (~1200°C) of formation for the ilmenite. If ilmenite is in isotopic equilibrium with a source region, which is assumed to have a bulk composition equal to garnet peridotite (whole rock $\delta^{18}O$=~+5.5‰), the isotopic fractionation (whole rock-ilmenite) should be ~+1.2‰, implying that the ilmenite should have a $\delta^{18}O$=~+4.3‰. Ilmenites from Torrie are both enriched and depleted in ^{18}O (Table 6.1) relative to this value, which indicates heterogeneity in the source region. For the same reasons as outlined above, these values are consistent with involvement with subducted crustal material. One possibility is that the ilmenites crystallized from partial melts derived from garnet peridotite that inherited $\delta^{18}O$ variations from the subducted oceanic crust.

Chapter 7

Discussion

The subeconomic Torrie, Sputnik and Eddie pipes are classified as diatreme-facies macrocrystic, heterolithic kimberlite breccias based on the presence of abundant macrocrysts, autolithic clasts, and carbonized wood fragments. In addition, the presence of pelletal lapilli in Sputnik, mantle and crustal xenoliths in Sputnik and Eddie and an unmetamorphosed crustal xenolith in Eddie are consistent with a diatreme origin for these pipes. The major-element chemistry of phenocrysts and xenocrysts, coupled with oxygen isotope analyses of xenocrysts, megacrysts and xenoliths from the Torrie, Sputnik and Eddie pipes, provide insight into the composition of the upper mantle, the kimberlite source region and magmatism in the central Slave province. Furthermore, the xenocrysts and megacrysts shed light on the very poor diamond grades of these pipes.

The current model for the origin of kimberlite is that the magmas formed by a small degree of partial melting of a carbonated, hydrated garnet peridotite at depths of 150-300 km (Eggler, 1989 and references therein). More recently, it has been proposed that the source region for kimberlites is produced by refertilization of depleted harzburgite by products of partial melting of subducted oceanic crust in the transition zone at depths of 400-650 km (Ringwood, 1990, Ringwood et al., 1992 and references therein). There are three competing theories for the generation of depleted garnet harzburgite. Boyd and Gurney (1982) argue that the refractory harzburgite (or dunite) is the partial melt residue after extraction of komatiitic magmas in the Archean. Kesson and Ringwood (1989) proposed that they are formed by repeated melt extraction at mid-ocean ridges and subsequent subduction and metamorphism. Schultze (1986) suggests that serpentinization of the peridotite protolith (oceanic crust) at low temperature crustal conditions removes Ca from the rock. The subduction and subsequent metamorphism of these serpentinites can account for upper mantle garnet peridotites that are depleted in calcium, such as the clinopyroxene-free garnet harzburgites commonly associated with diamonds (Boyd et al. 1993).

Canil and Wei (1992) designed experiments to test these models. They concluded that the Cr-poor (<4 wt% Cr_2O_3) and Cr-rich (>3 wt% Cr_2O_3) garnets from garnet harzburgites originated as residues of one-stage and multiple-stage ultramafic melt extraction, respectively and low Ca garnets that coexist with spinel as inclusions in

diamonds probably crystallized from Cr-rich harzburgites that originated by multi-stage melt extraction within a Precambrian mid-ocean ridge environment. In other words, the experiments are consistent with suggestions that harzburgitic garnets associated with diamonds originate from residues that underwent multiple melt extraction in either the shallow MORB source region or the deep komatiite source region (Canil and Wei, 1992). Radiogenic (Nd/Sm and Rb/Sr) isotopes of the depleted garnet harzburgites could resolve the problem, as the two source regions should reveal two different signatures. Perhaps the protoliths of garnet harzburgites associated with diamonds formed in both environments.

Origin of xenocrysts and xenoliths from the Torrie and Sputnik pipes

Major-element chemistry and $\delta^{18}O$ analyses of xenolith minerals, xenocrysts and megacrysts from the Torrie and Sputnik pipes not only indicates derivation from different sources, but some features of the chemistry such as $\delta^{18}O$ heterogeneity and disequilibrium are consistent with metasomatism in the source region(s). According to the Dawson and Stephens classification (1975), the majority of xenocryst garnets in Torrie and Sputnik are derived from garnet lherzolite (G9: Cr-pyrope), sheared garnet lherzolite (G11: Ti-pyrope and Cr-Ti pyrope) and megacrysts populations (G1: Ti-pyrope). Similarly, garnets in the websterite and eclogite xenoliths from the Torrie pipe are classified as G11, Ti-pyrope and G3, Ca-pyrope almandine respectively. The majority of clinopyroxene xenocrysts in Torrie and Sputnik are derived from garnet lherzolite.

Garnets and pyroxenes from the websterite xenolith from Torrie indicate slight intra- and inter-grain chemical variations, however, olivines do not display any variations. Moderate intra-grain variations in CaO, Al_2O_3 and Na_2O in clinopyroxene and to a lesser extent, in garnet, from the eclogite xenolith can be attributed to metasomatism. Inter-grain variations in the xenocryst populations are more problematic but can be attributed to three main factors (a) xenocrysts within the same group (i.e. group 9 Cr-pyrope garnets) are from more than one source region and the kimberlite has sampled garnet lherzolite from more than one depth, for example, (b) the xenocrysts are from the same source but crystallized under different conditions and (c) the xenocrysts are a result of large scale heterogeneity caused by metasomatic fluids.

Kesson and Ringwood (1989a and 1989b) suggest that slab-mantle interactions can account for sheared and refertilized garnet peridotite xenoliths as well as the formation of most diamonds. In their model (Figure 7.1), dehydration of serpentinites in subducting oceanic lithosphere fluxes partial melting of overlying eclogite (metamorphosed oceanic crust). The hybridization of the derived melt with overlying depleted peridotite refertilizes the peridotite. Shearing of this refertilized peridotite results from deformation along Waddati-Benioff zones and may be highly localized. The deformation may produce higher temperatures as a result of shear heating (Goetze, 1975), and can be preserved in the xenoliths if they are transported from their source region by contemporaneous kimberlite magmatism.

This model can explain the chemical variations in xenocrysts and megacrysts from Torrie and Sputnik as well as the source for these kimberlites. The garnet and clinopyroxene xenocrysts are derived from refertilized peridotite that inherited oxygen isotope signatures from metasomatic fluids derived from subducted oceanic crust. The disequilibrium observed in the xenoliths most likely reflects a transient heating event that resulted in open-system exchange with metasomatic fluids or melts derived from the slab.

Genesis of kimberlite

High-temperature Ti-pyrope garnet (Cr-rich megacryst suite?), Mg ilmenite megacrysts and a high-T xenolith from Torrie and Sputnik record processes within the mantle that may be related to the genesis of kimberlite and its early stages of evolution. In contrast, oxide minerals and phlogopite in groundmass are sensitive to changes in the magma chemistry, temperature and oxygen fugacity during the mid-to-late-stages of kimberlite melt evolution.

Ringwood et al., (1992) proposed that kimberlite forms by a small degree of partial melting of refertilized peridotite at depths of 400-650 km. The $\delta^{18}O$ heterogeneity observed in ilmenite megacrysts from Torrie and Sputnik is evidence in favor of derivation of the kimberlite from melt-metasomatised (refertilized) peridotites. The refertilized peridotites have inherited $\delta^{18}O$ signatures from subducted oceanic crust by interaction with metasomatic fluids and, the subsequent partial melting of these rocks results in high-P phenocrysts phases (i.e. ilmenite and Ti-pyrope) with similar $\delta^{18}O$

A. Archean/Proterozoic Subduction
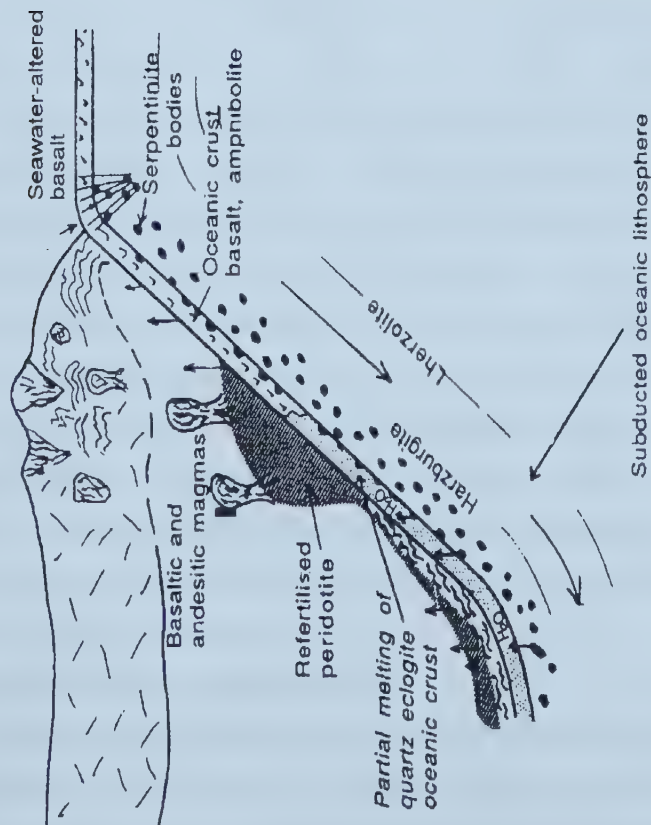
B. Ordovician, Cretaceous and Eocene kimberlite magmatism
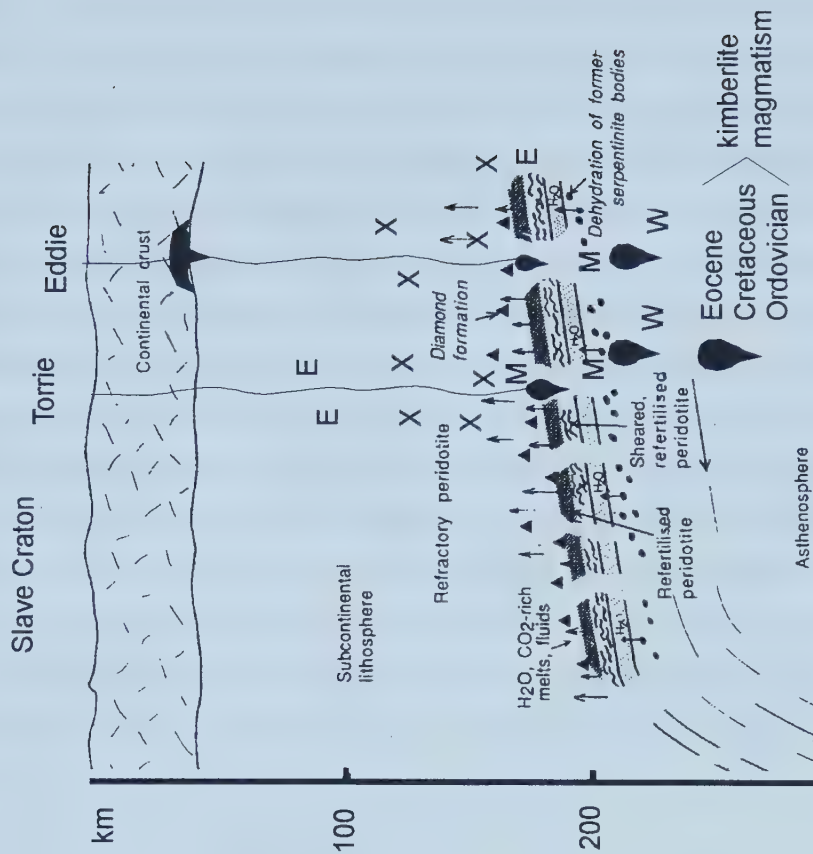
Figure 7.1. Speculative model for the origin of the Torrie, Sputnik and Eddie kimberlites and xenoliths (x), megacrysts (M), eclogite (E) and websterite (W) xenoliths. A. Subduction of oceanic crust beneath the Slave craton during the Archean or Proterozoic. B. Dehydration of serpentinites results in partial melting of eclogitic crust and subsequent refertilization of overlying peridotite (modified from Kesson and Ringwood, 1989).

variations. The disequilibrium observed in mantle xenoliths coupled with a temperature of ~1280°C for a garnet-clinopyroxene xenocryst reflect a higher local geotherm than the interpreted geotherm of 47-48 mW/m^2 that may have been caused by a transient heating event that resulted in open-system exchange with metasomatic fluids or melts and may have triggered kimberlite magmatism. A similar interpretation has been made for high T-megacryst garnets from barren kimberlites in the Shandong and Guizhou Provinces in China (Jianxing et al., 1994). It is hypothesized, however, that the Torrie and Sputnik kimberlites are derived from refertilized peridotite at much shallower depths of ~250-300 km compared to that proposed by Ringwood et al. (1992) based on the lack of mantle minerals derived from high pressure origins (i.e majoritic garnets).

Two factors indicate that kimberlite is deep-seated and forms under reducing conditions in the mantle. First, the presence of a websterite xenolith that crystallized at ~1200°C at a depth of 220 km. Second, low hematite contents (<12% in Sputnik and <14% in Torrie) in Mg ilmenites indicate formation under relatively reduced conditions early in kimberlite formation. Moreover, the relatively reduced nature of the Mg ilmenite population and their large $\delta^{18}O$ variations indicate that metasomatism from slab-mantle interaction is not necessarily oxidizing.

The presence of primary groundmass phlogopite and abundant olivine and groundmass serpentinization, coupled with the lack of mantle-derived xenocrysts and ilmenite megacrysts, makes the Eddie pipe distinctive from the Torrie and Sputnik pipes. Moreover, the unusual formation of tetraferriphlogopite in the Eddie pipe indicates an abrupt change in redox conditions during the final crystallization stage possibly related to the interaction with groundwater and rapid loss of CO_2. The presence of ulvöspinel-magnetite in Eddie indicates that it is a more evolved kimberlite than Torrie and Sputnik. The lack of mantle xenocrysts (i.e. garnet and clinopyroxene) and ilmenite megacrysts may reflect a more shallow origin. It is more likely, however, that it underwent fractionation at shallow levels in the crust and subsequent settling out of xenocrysts (including diamonds), mantle xenoliths and possibly large megacrystic minerals. Ponding of the kimberlite at shallow crustal levels accounts for its more highly evolved mica-rich nature compared to Torrie and Sputnik.

Diamond potential and preservation

Diamond content depends on the diamond-bearing mantle material entrained in the kimberlite, the proportion of eclogitic versus peridotitic mantle sampled and the degree of resorption and mechanical sorting during transport to the surface.

The diamond potential of the Torrie, Sputnik and Eddie kimberlite pipes is very low as a result of two factors. Firstly, the very low grades reflect the limited sampling of the mantle within the diamond window (Fig. 5.1). Secondly, the mantle that the pipes sampled appears to contain more lherzolite and less harzburgite. The Torrie and Sputnik kimberlites have diamond indicator minerals consistent with their low diamond contents, however, transient-heating events may have also reduced the diamond content. Some regions of the mantle have higher temperatures than the typical continental geotherm as a result of either melt-related metasomatism or short-lived heating events. Metasomatism and/or higher temperatures may be unsuitable for diamond preservation as they may cause oxidation and resorption of diamonds.

Chapter 8

Conclusions

The Torrie and Sputnik pipes are diatreme-facies macrocrystic, heterolithic kimberlite breccias. The olivine population consists of megacrysts, xenocrysts, first and second-generation phenocrysts and microphenocrysts. The majority of garnets and clinopyroxenes are derived from disaggregated garnet lherzolite and high temperature deformed lherzolite with a minor contribution from eclogite, harzburgite, websterite and crustal granulites. The low Al_2O_3, high Na_2O and TiO_2 orthopyroxene are derived from low-T garnet lherzolite whereas the high Al_2O_3, Cr_2O_3, low Na_2O and low TiO_2 orthopyroxene are derived from spinel lherzolite and garnet harzburgite. Torrie contains spinels from the AMC trend, early crystallizing TIMAC from magmatic trend 1 and titanian ferrian pleaonaste as a late crystallizing groundmass phase. Sputnik contains TIMAC as inclusions in olivine and more evolved MUM spinels from trend 1. Cr-Mg ilmenite megacrysts with low-to-moderate hematite contents are abundant in Torrie and Sputnik.

The Eddie pipe is a strongly serpentinized, diatreme-facies, macrocrystic kimberlite breccia. The presence of primary phlogopite, more evolved MUM spinels from trend 1 and UM spinels from trend 2, and the lack of mantle-derived xenocrysts and Mg ilmenite, however, makes the Eddie pipe distinctive from Torrie and Sputnik. The Eddie pipe also contains spinels from the AMC trend, TIMAC and TMC from trend 1.

P-T estimates for xenolith and megacryst mineral assemblages from Torrie indicate a continental geotherm of 47-48 mW/m^2 and that the kimberlite sampled the diamond stability field at the time of the kimberlite eruption. The very low diamond grades of Torrie and Sputnik, however, are consistent with the lack of garnet, pyroxene and chromite xenocrysts from garnet and chromite harzburgite. A Ti-garnet xenocryst with a clinopyroxene inclusion gave an elevated temperature of ~1245 °C at 50 kb which is interpreted to reflect a short-lived heating event immediately prior to entrainment in the kimberlite.

The $\delta^{18}O$ heterogeneity, disequilibrium and major-element variations in xenocrysts and mantle xenoliths are the result of partial melting of ancient oceanic crust that was subducted in the Archean or Proterozoic and the subsequent migration of these melts and fluids into overlying depleted peridotite.

The $\delta^{18}O$ heterogeneity in ilmenite megacrysts, which are interpreted as high-P kimberlitic phenocrysts, is consistent with metasomatism in the kimberlite source region. Therefore, it is proposed that the Torrie and Sputnik kimberlites are derived from partial melting of refertilized peridotites (at depths of 250-300 km) that have inherited $\delta^{18}O$ signatures from subducted oceanic crust by metasomatic fluids. The $\delta^{18}O$ disequilibrium in the mantle xenoliths is interpreted to represent a transient-heating event just prior to the eruption of the kimberlite.

References Cited

Agee, C.B., and Walker, D. 1990. Aluminum partitioning between olivine and ultrabasic silicate liquid to 6 Gpa. Contributions to Mineralogy and Petrology, 105: 243-254.

Agee, J.J., Garrison, J.R., and Taylor, L.A. 1982. Petrogenesis of oxide minerals in kimberlite, Elliot County, Kentucky. American Mineralogist, 67: 28-42.

Beard, B.L., Fraracci, K.N., Taylor, L.A., Snyder, G.A., Clayton, R.A., Mayeda, T.K., and Sobalev, N.V. 1996. Petrography and geochemistry of eclogites from the Mir kimberlite, Yakutia, Russia. Contributions to Mineralogy and Petrology, 125: 293-310.

Boctor, N.Z., and Boyd, F.R. 1980. Oxide minerals in the Liqhobong kimberlite, Lesotho. American Mineralogist, 65: 631-638.

Bowring, S.A., Williams, I.S., and Compston, W. 1989. 3.96 Ga gneisses from the Slave Province, Northwest Territories, Canada. Geology, 17: 971-975.

Boyd, Jr., F.R. 1970. Garnet peridotites and the system $CaSiO_3$-$MgSiO_3$-Al_2O_3. Special paper, Mineralogical Society of America, 3: 63-75.

Boyd, F.R. and Gurney, J.J. 1982. Low-calcium garnets: keys to craton structure and diamond crystallization. Carnegie Institute. Washington Yearbook, 81: 261-267.

Boyd, F.R., and Nixon, P.H. 1975. Origins of the ultramafic nodules from some kimberlites of Northern Lesotho and the Monastery Mine, South Africa. Physics and Chemistry of the Earth, 9: 431-454. Not seen, as in Mitchell, 1986.

Brey, G.P. and Köhler, T., and Nickel, K.G. 1990. Geothermometry in four-phase lherzolites I. Experimental results from 10 to 60 kb. Journal of Petrology, 31: 1313-1351.

Brey, G.P. and Köhler, T. 1990. Geothermometry in four-phase lherzolites II. New thermobarometer, and practical assessment of existing thermobarometers. Journal of Petrology, 31: 1353-1378.

Canil, D., and O'Neill, H.St. C. 1996. Distribution of ferric iron in some upper-mantle assemblages. Journal of Petrology, 37: 609-635.

Carswell, D.A. and Harley, S.L.. 1990. Mineral barometry and thermometry. Edited by D.A. Carswell. In Eclogite Facies Rocks. p. 83-110.

Chiba, H., Chacko, T., Clayton, R.N., and Goldsmith, J.R. 1989. Oxygen isotope fractionations involving diopside, forsterite, magnetite, and calcite: Application to geothermometry. Geochimica et Cosmochimica Acta, 53: 2985-2995.

Clayton, R.N. and Mayeda, T.K. 1963. The use of bromine pentafluoride in the extraction of oxygen from oxides and silicates for isotopic analysis. Geochimica et Cosmochimica Acta, 23: 43-52.

Clement, C.R. 1982. A comparative geological study of some major kimberlite pipes in the Northern Cape and Orange Free State. Ph. D. thesis (2 vols.), University of Cape Town, South Africa. Not seen, as in Mitchell, 1986.

Clement, C.R. 1973. Kimberlites from the Kao pipe, Lesotho. Lesotho Kimberlites, 110-121. Not seen, as in Mitchell, 1986.

Clement, C.R., and Skinner, E.M.W. 1979. A textural genetic classification of kimberlite rocks. Kimberlite Symposium II, Cambridge (Extended Abstracts). Not seen, as in Mitchell, 1986.

Coghlan, R.A.N. 1990. Studies in diffusional transport; grain boundary transport of oxygen in feldspars, diffusion of oxygen, strontium and the REEs in garnet, and thermal histories of granitic intrusions in south-central Maine using oxygen isotopes. PhD Thesis, Brown University.

Danchin, R.V., and Wyatt, B. A. 1979. Statistical cluster analysis of garnets from kimberlites and their xenoliths. *In* Kimberlite Symposium II, Cambridge, pp. 22-27. Not seen, as in Gurney and Zweistra, 1995.

Davis, B.T.C., and Boyd, Jr., F.R. 1966. The join Mg_2SiO_6-$CaMgSi_2O_6$ at 30 kilobars pressure and its application to pyroxenes from kimberlites. Journal of Geophysical Research, 71: 3567-3576.

Davis, W.J. 1991. Granitoid geochemistry and Late Archean crustal evolution in the central Slave province. PhD Thesis, Memorial University of Newfoundland.

Davis, W.J., and Hegner, E. 1992. Neodymium isotopic evidence for the tectonic assembly of Late Archean crust in the Slave Province, northwest Canada. Contributions to Mineralogy and Petrology, 111: 493-504.

Davis, W.J., and Kjarsgaard, B.A. 1997. A Rb-Sr isochron age for a kimberlite from the recently discovered Lac de Gras Field, Slave province, Northwest Canada. Journal of Geology, 105: 503-509.

Dawson, J.B. 1980. Kimberlites and their xenoliths. Springer Verlag, New York.

Dawson, J.B. 1994. Quaternary kimberlitic volcanism on the Tanzania Craton. Contributions to Mineralogy and Petrology, 116: 473-485.

Dawson, J.B. and Hawthorne, J.B. 1973. Magmatic sedimentation and carbonatitic differentiation in kimberlite sills at Benfontein, South Africa. Journal of the Geological Soceity of London, 129: 61-85. Not seen, as in Mitchell, 1995.

Dawson, J.B., and Stephens, W.E. 1975. Statistical classification of garnets from kimberlite and associated xenoliths. Journal of Geology, 83: 589-607.

Delaney, J.S., Smith, J.V., Carswell, D.A., and Dawson, J.B. 1980. Chemistry of micas from kimberlites and xenoliths II. Primary- and secondary-textured micas from peridotite xenoliths. Geochimica et Cosmochimica Acta, 44: 857-872.

Donaldson, C.H. and Reid, A.M. 1982. Multiple intrusion of a kimberlite dike. Transactions. Geological Society of South Africa, 85: 1-12. Not seen, as in Mitchell, 1995.

Droop, G.T.R. 1987. A general equation for estimating Fe^{3+} concentrations in ferromagnesian silicates and oxides from microprobe analyses, using stoichiometric criteria. Mineralogical Magazine, 51: 431-5.

Edwards, D., Rock, N.M.S., Taylor, W.R. Griffin, B.J., and Ramsay, R.R. 1992. Mineralogy and petrology of the Aries diamondiferous kimberlite pipe, Central Kimberly Block, Western Australia. Journal of Petrology, 33: 1157-1191.

Eggler, D.H. 1989. Kimberlites: How do they form? *In* Kimberlites and Related Rocks. *Edited by* J. Ross. Geological Soceity of Australia, Special Publication 14, Volume I, Blackwell Scientific, pp. 323-342.

Ellis, D.J. and Green, D.H. 1979. An experimental study of the effect of Ca upon garnet-clinopyroxene Fe-Mg exchange equilibria. Contributions to Mineralogy and Petrology, 71: 13-22.

Farquhar, J., Chacko, T., and Frost, R.B. 1993. Strategies for high-temperature oxygen isotope thermometry: a worked example from the Laramie Anorthosite Complex, Wyoming, USA. 117: 407-422.

Farver, J.R. 1989. Oxygen self-diffusion in diopside with application to cooling rate determinations. Earth and Planetary Science Letters, 92: 386-396.

Fipke, C.E. 1994. Significance of chromite, ilmenite, G5 Mg-almandine garnet, zircon and tourmaline in heavy mineral detection of diamond bearing lamproite. *In* Fifth International Kimberlite Conference, Brazil, 1991. CPRM, Special Publication 2/91, p. 97-100.

Fipke, C.E., Gurney, J.J., Moore, R.O., and Nassichuk, W.W. 1989. The development of advanced technology to distinguish between productive diamondiferous and barren diatremes. Geological Survey of Canada, Open File 2124.

Fipke, C.E., Gurney, J.J., and Moore, R.O. 1995. Diamond exploration techniques emphasizing indicator mineral geochemistry and Canadian examples. Geological Survey of Canada Bulletin 423, 83p.

Finnerty, A.A., and Boyd, J.J. 1987. Thermobarometry for garnet peridotites: basis for the determination of thermal and compositional structure of the upper mantle. *In* Mantle xenoliths. Edited by P.H. Nixon. p. 381-402.

Fyson, W.K. 1996. Corel Draw diagrams of the Geology of the Slave Structural Province. EGS 1996-08, NWT Geology Division DIAND, Yellowknife.

Fyson, W.K., and Helmstaedt, H. 1988. Structural patterns and tectonic evolution of supracrustal domains in the Archean Slave province, Canada. Canadian Journal of Earth Sciences, 25: 301-315.

Gasparik, T. 1984. Two-pyroxene thermobarometry with new experimental data in the system CaO-MgO-Al$_2$O$_3$-SiO2. Contributions to Mineralogy and Petrology, 87: 87-97.

Goetze, C. 1975. Sheared lherzolites: from the point of view of rock mechanics. Geology, 3: 172-173.

Gregory, R.T., and Taylor, H.P. 1986. Non-equilibrium, metasomatic ^{18}O/^{16}O effects in upper mantle mineral assemblages. Contributions to Mineralogy and Petrology, 93: 124-135.

Griffin, W.L., Ryan, C.G., Gurney, J.J., Sobolev, N.V. and Win, T.T. 1994. Chromite macrocrysts in kimberlites and lamproites: geochemistry and origin. *In* Kimberlites, Related Rocks and Mantle Xenoliths. Edited by H.O.A. Meyer and O.H. Leonardos. CPRM Special Publication 1A/91, pp. 366-377.

Gurney, J.J. 1984. A correlation between garnets and diamonds in kimberlites. *In* Kimberlite occurrence and origin: a basis for conceptual models in exploration. Edited by J.E. glover and P. G. Harris. The University of Western Australia Publication, 8: 143-166. Not seen, as in Gurney and Zweistra, 1995.

Gurney, J.J., and Zweistra, P. 1995. The interpretation of the major element compositions of mantle minerals in diamond exploration. Journal of Geochemical Exploration, 53: 293-309.

Gurney, J.J., Jakob, W.R.O., and Dawson, J.B. 1979. Megacrysts from the Monastery Kimberlite pipe, South Africa, Second International Kimberlite Conference 2: 227-243.

Harmon, R.S., and Hoefs, J. 1995. Oxygen isotope heterogeneity of the mantle deduced from global O systematics of basalts from different geotectonic settings. Contributions to mineralogy and Petrology, 120: 95-114.

Harte, B., and Gurney, J.J. 1981. The mode of formation of chromium-poor megacryst suites from kimberlites. Journal of Geology, 89: 749-753.

Henderson, J.B. 1970. Stratigraphy of the Yellowknife Supergroup, Yellowknife Bay-Prosperous Lake area, District of Mackenzie. Geological Survey of Canada, Paper 70-26.

Henderson, J.B. 1981. Archean basin evolution in the Slave province, Canada. *In* Precambrian Plate tectonics. Edited by A. Kroner. Elseviser Amsterdam, pp. 213-235.

Hawthorne, J.B. 1975. Model of a kimberlite pipe. Physics and Chemistry of the Earth, 9: 1-15. Not seen, as in Mitchell, 1986.

Hoffman, P.F. 1989. Precambrian geology and the tectonic history of North America. The Geology of North America - an overview. Geological Society of America, A: 447-512.

Hunter, R.H. Kissling, R.D. and Taylor, L.A. 1984. Mid-to-Late stage kimberlitic melt evolution, phlogopites and oxides from the Fayette county kimberlite, Pennsylvania. American Mineralogist, 69: 30-40.

Jacob, D., Jagoutz, E., Lowry, D., Mattey, D., and Kudrjavtseva, G. 1994. Diamondiferous eclogites from Siberia: Remnants of Archean oceanic crust. Geochimica et Cosmochimica Acta, 58: 5191-5207.

Jago, B. C., and Mitchell, R.H. 1989. A new garnet classification technique: divisive cluster analysis applied to garnet populations from Somerset Island kimberlites. *In* Kimberlites and Related Rocks. Edited by J. Ross. Geological Soceity of Australia, Special Publication 14, Volume I, Blackwell Scientific, pp. 966-989.

Jianxing, Z., Griffin, W.L., Jaques, A.L., Ryan, C.G., and Win, T.T. 1994. *In* Kimberlites, related rocks and mantle zenoliths. Edited by H.O.A.Meyer and O.H. Leonardos. Fifth international kimberlite conference, Special Publication v. 2, pp. 285-301.

Kennedy, C.S., and Kennedy, G.C. 1976. The equilibrium boundary between graphite and diamond. Journal of Geophysical Research, 81: 2467-2470.

Kesson, S.E., and Ringwood, A.E. 1989a. Slab-mantle interactions 1. Sheared garnet peridotite xenoliths-examples of Wadati-Benioff zones? Chemical Geology, 78: 83-96.

Kesson, S.E., and Ringwood, A.E. 1989b. Slab-mantle interactions 2. The formation of diamonds. Chemical Geology, 78: 97-118.

Kieffer, S.W. 1982. Thermodynamics and lattice vibrations of minerals: 5. Applications to phase equilibria, isotopic fractionation, and high-pressure thermodynamic properties. Reviews of Geophysics and Space Physics, 20: 827-849.

Kjarsgaard, B.A. 1996a. Slave province kimberlites, NWT. *In* Searching for diamonds in Canada. Edited by A.N. LeCheminant, D.G. Richardson, R.N.W. DiLabio and K.A. Richardson. Geological Survey of Canada, Open File 3228, pp. 29—38.

Kjarsgaard, B.A. 1996c. Prairie kimberlites. *In* Searching for diamonds in Canada. Edited by A.N. LeCheminant, D.G. Richardson, R.N.W. DiLabio and K.A. Richardson. Geological Survey of Canada, Open File 3228, pp. 67-72.

Kjarsgaard, B.A., and Heaman, L.M. 1995. Distinct emplacement periods of Phanerozoic kimberlites in North America, and implications for the Slave province. *In* Exploration Overview 1995, Northwest Territories. *Compiled by* E.I. Igboji. Department of Indian and Northern Affairs, Yellowknife, NWT, pp. 3-22.

Kopylova, M.G., Russell, J.K., and Cookenboo, H. 1998. Upper-mantle stratigraphy of the Slave craton, Canada: Insights into a new kimberlite province. Geology. In press.

Kostrovitskiy, S.I., and Fiveyskaya, L.V. 1983. Geochemical features of olivines from kimberlites. Translated from Geokhimiya 5: 717-729.

Krogh, E.J. 1988. The garnet-clinopyroxene Fe-Mg geothermometer-a reinterpretation of existing experimental data. contributions to Mineralogy and Petrology, 99: 44-48.

Kusky, T.M. 1989. Accretion of the Archean Slave province. Geology, 17: 63-67.

Kyser, T.K. 1986. Stable isotope variations in the mantle. *In* Stable isotopes in high temperature geological processes. Edited by J.W. Valley, H.P. Jr. Taylor, and J.R. O'Neil. Reviews in Mineralogy v. 16. p. 141-163.

Luth, R.W. and Canil, D. 1993. Ferric iron in mantle-derived pyroxenes and a new oxybarometer for the mantle. Contributions to Mineralogy and Petrology, 113: 236-248.

Luth, R.W., Virgo, D., Boyd, F.R., and Wood, B.J. 1990. Ferric iron in mantle-derived garnets-Implications for thermometry and for the oxidation state of the mantle. Contributions to Mineralogy and Petrology, 104: 56-72.

MacGregor, I.D. 1985. The Roberts Victor eclogites: ancient oceanic crust. Abstract, Geological Society of America, Annual Meeting, 650.

MacGregor, I.D. and Manton, W.I. 1986. Roberts Victor eclogites: ancient oceanic crust. Journal of Geophysical Research, 91: 14063-14079.

Mannard, G.W. 1962. The Singida kimberlite pipes, Tanganyika. Ph. D. thesis, McGill University, Montreal, Quebec. Not seen, as in Mitchell, 1986.

Mattey, D.P., Lowry, D., Macpherson, C.G., and Chazot, G. 1994. Oxygen isotope composition of mantle minerals by laser fluorination analysis: homogeneity in peridotites, heterogeneity in eclogites. Goldschmidt conference Edinburgh, Mineralogical Magazine, 58A: 573-574.

McCandless, T.E., and Gurney, J.J. 1989. Sodium in garnet and potassium in clinopyroxene: criteria for classifying mantle eclogites. *In* Kimberlites and Related Rocks. *Edited by* J. Ross. Geological Soceity of Australia, Special Publication 14, Volume I, Blackwell Scientific, pp. 827-832.

Mitchell, R.H. 1995. Kimberlites, Orangeites, and Related Rocks. Plenum Press, New York and London, 410 p.

Mitchell, R.H. 1986. Kimberlites: Mineralogy, Geochemistry, and Petrology. Plenum Press, New York, 442 p.

Mitchell, R.H. 1979. Mineralogy of the Tunraq kimberlite, Somerset Island, NWT, Canada. Second International Kimberlite Conference, pp. 161-171.

Mitchell, R.H. 1978a. Mineralogy of the Elwin Bay kimberlite, Somerset Island, NWT, Canada. American Mineralogist, 63: 47-57.

Mitchell, R.H. 1977. Geochemistry of magnesian ilmenites from kimberlites from South Africa and Lesotho. Lithos, 10: 29-37.

Mitchell, R.H., and Clarke, D.B. 1976. Oxide and sulphide mineralogy of the Peuyuk kimberlite, Somerset Island, NWT, Canada. Contributions to Mineralogy and Petrology, 56: 157-172.

Moore, A.E. 1988. Olivine: a monitor of magma evolutionary paths in kimberlites and olivine melilites. Contributions to Mineralogy and Petrology, 99: 238-248.

Moore, R.O., Griffin, W.L., Gurney, J.J., Ryan, C.G., Cousens, D.R., Sie, S.H., and Suter, G.F. 1992. Trace element geochemistry of ilmenite megacrysts from the Monastery kimberlite, South Africa. Lithos, 29: 1-18.

Mortensen, J.K., Thorpe, R.I., Padgham, W.A., King, J.E., and Davis, W.J. 1988. U-Pb zircon ages for felsic volcanism in Slave province, NWT. In Radiogenic age and isotopic studies: Report 2. Geological Survey of Canada, Paper 88-2, p. 85-95.

Muehlenbachs, K. 1986. Alteration of the oceanic crust and the ^{18}O history of seawater. In Stable isotopes in high temperature geological processes. Edited by J.W. Valley, H.P. Jr. Taylor, and J.R. O'Neil. Reviews in Mineralogy v. 16. p. 425-444.

Neal, C.R., Taylor, L., Davidson, J.P., Holden, P., Halliday, A.N., Nixon, P.H., Paces, J.B., Clayton, R.N., and Mayeda, T.K. 1990. Eclogites with oceanic crustal and mantle signatures from the Bellsbank kimberlite, South Africa, part 2: Sr, Nd, and O isotope geochemistry. Earth and Planetary Science Letters, 99: 362-379.

Nixon, P.H., van Calsteren, P.W.C., Boyd, F.R., and Hawkesworth, C.J. 1987. Harzburgites with garnets of diamond facies from southern African kimberlites. In Mantle Xenoliths. Edited `by P.H. Nixon. Wiley and Sons, New York, p. 523-533.

Ongley, J.S. Basu, A.R., and Kyser, K.T. 1987. Oxygen isotopes in coexisting garnets, clinopyroxenes and phlogopites of Roberts Victor eclogites: implications for petrogenesis and mantle metasomatism. Earth and Planetary Science Letters, 83: 80-84.

Padgham, W.A. 1985. Observations and speculations on supracrustal successions in the Slave Structural Province. In Evolution of Archean Supracrustal Sequences. Edited by L.D. Ayres, P.C. Thurston, K.D. Card and W. Weber. Geological Association of Canada, Special Paper 28, pp. 133-151.

Padgham, W.A., and Fyson, W.K. 1992. The Slave province: A distinct Archean craton. Canadian Journal of Earth Sciences, 29: 2072-2086.

Pasteris, J.D. 1980b. Opaque oxide phases of the De Beers Pipe kimberlite, Kimberley, South Africa and their petrologic significance, Ph.D. Thesis, Yale University.

Pasteris, J.D. 1983. Spinel zonation in the De Beers kimberlite, South Africa: Possible role of phlogopite. Canadian Mineralogist, 21: 41-58.

Pell, J. 1995. NWT kimberlite database (digital), EGS 1995-02, NWT Geological Mapping Division, DIAND.

Pell, J. 1997. Kimberlites in the Slave craton, Northwest Territories, Canada: A preliminary review. Russian Geology and Geophysics. Sixth International Kimberlite Conference, 38: 5-15.

Percival, J. 1994. Archean high-grade metamorphism. *In* Archean Crustal Evolution. Edited by K.C. Condie. Elsevier, Amsterdam, p. 357-410.

Ringwood, A.E. 1990. Slab-mantle interactions 3. Petrogenesis of intraplate magmas and structure of the upper mantle. Chemical Geology, 82: 187-207.

Ringwood, A.E., Kesson, S.E., Hibberson, W., and Ware, N. 1992. Origin of kimberlites and related magmas. Earth and Planetary Science Letters, 113: 521-538.

Rosenbaum, J.M., Mattey, D.P., and Elphick, S. 1994. Equilibrium garnet-calcite oxygen isotope fractionation. Mineralogical Magazine, 58A: 787-788.

Rozova, Y.V., Frantsesson, E.V., Pleshakov, A.P., Botova, M.M., and, Filipova, L.P. 1982. High-iron chrome spinels in kimberlites of Yakutia. International Geology Review, 24: 1417-1425.

Rudnick, R.L., McDonough, W.F., and Orpin, A. 1994. Northern Tanzanian peridotite xenoliths: a comparison with Kaapvaal peridotites and inferences on metasomatic interactions. *In* Kimberlites and Related Rocks, Fifth International Kimberlite Conference. Edited by H.O.A. Meyer and O.H. Leonardos, 1: 336-353.

Sampson, D.N. 1953. The volcanic hills at Igwisi. Records. Geological Survey of Tanganyika, 3: 48-53. Not seen, as in Mitchell, 1986.

Schulze, D.J. 1986. Calcium anomalies in the mantle and a subducted origin for diamonds. Nature, 316: 483-485.

Schulze, D.J., and Anderson, P.E.N. 1995. Origin and significance of ilmenite megacrysts and macrocrysts from kimberlite. International Geology Review, 37: 780-812.

Scott Smith, B.H. 1995. Geology of the Sturgeon Lake 02 kimberlite block, Saskatchewan. Exploration and Mining Geology, 4: 141-151.

Scott Smith, B.H., Letendre, J.P., and Robinson, H.R. 1996. Geology of the Sturgeon Lake 01 kimberlite block, Saskatchewan. Exploration and Mining Geology, 5: 251-261.

Shee, S.R. 1984. The oxide minerals of the Wesselton Mine kimberlite, Kimberley, South Africa. *In* Kimberlites and Related Rocks, Third International Kimberlite Conference, Edited by J. Kornprobst, 1: 59-73.

Schiller, E.A. 1994. Success at Lac de Gras. Mining North, NWT Chamber of Mines, v.3, no. 1, pp. 21-29.

Smith, D., and Boyd, F.R. 1986. Compositional heterogeneities in minerals of sheared lherzolite inclusions from African kimberlites. *In* Kimberlites and Related Rocks, Fourth International Kimberlite Conference, Volume 2. Edited by J. Ross. Blackwell Scientific, pp. 709-724.

Smith, C.B., Schulze, D.J., Bell, D., and Viljoen, K.S. 1995. Bearing of the subcalcic, Cr-poor megacryst suite on kimberlite petrogenesis and lithosphere structure. Extended Abstracts Sixth International Kimberlite Conference, Novosibirsk, Russia, p. 546-548.

Smyth, J.R., Caporuscio, F.A., and McCormick, T.C. 1989. Mantle eclogites: Evidence of igneous fractionation in the mantle. Earth and Planetary Science Letters, 93: 133-141.

Snyder, G.A., Taylor, L.A., Jerde, E.A., Clayton, R.N., Mayeda, T.K. Deines, P., Rossman, G.R., and Sobolev, N.V. 1995. Archean mantle heterogeneity and the origin of diamondiferous eclogites, Siberia: Evidence from stable isotopes and hydroxyl in garnet. American Mineralogist, 80: 799-809.

Snyder, G.A., Taylor, L.A., Crozaz, G., Halliday, A.N., Beard, B.L., Sobolev, V.N., and Sobolev, N.V. 1997. The origins of Yakutian eclogite xenoliths. Journal of Petrology, 38: 85-113.

Sobalev, N.V. 1977. Deep-seated inclusions in kimberlites and the problem of the composition of the upper mantle. American Geophysical Union, 279p.

Solovjeva, L.V., Egorov, K.N., Markova, M.E., Kharkiv, A.D., Popolitov, K.E., and Barankevich, V.G. 1997. Mantle metasomatism and melting in mantle-derived xenoliths from the Udachnaya kimberlite; their possible relationship with diamond and kimberlite formation. Russian Geology and Geophysics. Sixth International Kimberlite Conference, 38: 182-202.

Tanqueray Resources. 1994. Annual Report.

Taylor, L.A., and Neal, C.R. 1988. Eclogites with oceanic crustal and mantle signatures from the Bellsbank kimberlite, south Africa, Part 1: Mineralogy, petrography, and whole rock chemistry. Journal of Geology, 97: 551-567.

Taylor, H.P. Jr., and Sheppard, S.M.F. 1986. Igneous rocks: I. Processes of isotopic fractionation and isotope systematics. *In* Stable isotopes in high temperature geological processes. Edited by J.W. Valley, H.P. Jr. Taylor, and J.R. O'Neil. Reviews in Mineralogy v. 16. p. 227-271.

Tompkins, L.A., and Haggerty, S.E. 1984. The Koidu kimberlite complex, Sierra Leone: Geological setting, petrology and mineral chemistry. Third International Kimberlite Conference, 1: 81-105.

Viljoen, K.S., Robinson, D.N., Swash, P.M., Griffin, W.L., Otter, M.L., Ryan, C.G. and Win, T.T. 1994. Diamond- and graphite-bearing peridotite xenoliths from the Roberts Victor kimberlite, South Africa. *In* Fifth International Kimberlite Conference, Brazil, 1991. CPRM, Special Publication 1/91, p. 285-303.

Wells, P.R.A. 1977. Pyroxene thermometry in simple and complex systems. Contributions to Mineralogy and Petrology, 62: 129-139.

Appendix A: List of standards used in electron microprobe analyses.

Appendix A. List of standards used in electron microprobe analyses.

Table 1. Olivine standards

Standard	Element
Kaersuitite	Na, Ti
Forsterite 90	Mg, Si, Ni
Forsterite 83	Fe
Augite	Al
Rhodonite	Ca
Chromite	Cr
Willemite	Mn

Table 2. Garnet standards

Standard	Element
Kaersuitite	Na, Ti
Pyrope	Ca, Al, Fe, Si, Mg
Willemite	Mn
Forsterite 90	Ni
Chromite	Cr

Table 3. Clinopyroxene standards

Standard	Element
Kaersuitite	Na, K, Ti
Augite	Mg, Al, Si, Ca, Fe
Chromite	Cr
Willemite	Mn
Forsterite 90	Ni

Table 4. Orthopyroxene standards

Standard	Element
Kaersuitite	Na, Ti
Forsterite 90	Mg, Ni
Augite	Si, Al
Chromite	Cr
Forsterite 83	Fe
Willemite	Mn
Rhodonite	Ca

Table 5. Phlogopite standards

Standard	Element
Calbiotite	F, Al, Si, K, Fe
Kaersuitite	Na, Mg, Ti
Tugtupite	Cl
Rhodonite	Ca
Sanidine	Ba
Chromite	Cr
Willemite	Mn
Forsterite 90	Ni

Table 6. Spinel standards

Standards	Element
NC chromite (60 % Cr_2O_3)	Mg, Cr
Chromite (40 % Cr_2O_3)	Cr, Al
Fayalite	Si
Ilmenite	Ti, Mn, Fe, Nb
Forsterite 90	Ni
Gahnite	Zn

Table 7. Ilmenite standards

Standards	Element
Chromite (40 % Cr_2O_3)	Cr, Al
Fayalite	Si
Ilmenite	Ti, Mn, Fe, Nb
Forsterite 90	Ni
Gahnite	Zn

Appendix B: Electron microprobe analyses

Table 1a: Microprobe analyses of Torrie olivines (cations on basis of 4 oxygen).

	M 1	M 2	M 3	M 4	M 5	M 6	M 7	M 8	M 9	M 10	M 11	M 12	M 13	M 14	M 15	M 16	M 17	M 18	Neo 19
SiO_2	39.82	40.28	40.08	40.52	40.10	40.36	40.19	40.28	40.82	40.41	40.63	40.16	40.14	40.55	40.51	40.72	40.58	40.68	40.45
TiO_2	0.05	0.04	0.03	0.03	0.05	0.04	0.00	0.06	0.04	0.02	0.05	0.00	0.01	0.00	0.01	0.01	0.02	0.02	0.03
Al_2O_3	0.00	0.00	0.01	0.00	0.02	0.02	0.01	0.01	0.00	0.00	0.01	0.00	0.01	0.02	0.01	0.00	0.01	0.02	0.00
Cr_2O_3	0.00	0.00	0.03	0.03	0.04	0.07	0.03	0.04	0.01	0.04	0.05	0.02	0.10	0.02	0.05	0.06	0.02	0.02	0.03
FeO_T	13.55	11.58	11.31	11.48	11.42	10.89	11.00	10.88	10.85	10.82	10.91	10.48	10.06	10.36	10.23	10.24	9.83	10.10	9.90
MnO	0.16	0.14	0.13	0.17	0.16	0.09	0.12	0.17	0.15	0.10	0.17	0.16	0.11	0.15	0.14	0.14	0.12	0.11	0.10
MgO	46.70	48.54	47.41	49.09	49.21	47.63	48.32	48.45	48.57	49.07	50.03	48.49	48.56	50.12	49.68	49.75	48.22	50.29	49.68
CaO	0.00	0.01	0.02	0.04	0.02	0.15	0.03	0.03	0.02	0.04	0.06	0.02	0.06	0.02	0.05	0.04	0.03	0.01	0.05
NiO	0.31	0.19	0.10	0.19	0.19	0.24	0.22	0.22	0.27	0.21	0.20	0.33	0.34	0.22	0.35	0.22	0.20	0.31	0.36
Na_2O	0.02	0.04	0.02	0.03	0.01	0.04	0.04	0.01	0.00	0.04	0.05	0.03	0.04	0.02	0.03	0.00	0.00	0.03	0.02
Total	100.60	100.81	99.14	101.57	101.21	99.52	99.94	100.13	100.73	100.74	102.13	99.69	99.44	101.47	101.07	101.17	99.04	101.59	100.62
Si	0.989	0.989	0.998	0.987	0.981	1.000	0.992	0.992	0.998	0.989	0.982	0.993	0.993	0.984	0.987	0.990	1.004	0.985	0.988
Ti	0.001	0.001	0.001	0.001	0.001	0.001	0.000	0.001	0.001	0.000	0.001	0.000	0.000	0.000	0.000	0.000	0.000	0.000	0.001
Al	0.000	0.000	0.000	0.000	0.000	0.001	0.000	0.000	0.000	0.000	0.000	0.000	0.000	0.000	0.000	0.000	0.000	0.000	0.000
Cr	0.000	0.000	0.001	0.000	0.001	0.001	0.001	0.001	0.000	0.001	0.001	0.000	0.002	0.000	0.001	0.001	0.000	0.000	0.001
Fe^{2+}_T	0.281	0.238	0.235	0.234	0.234	0.225	0.227	0.224	0.222	0.221	0.220	0.216	0.208	0.210	0.208	0.208	0.203	0.205	0.202
Mn	0.003	0.003	0.003	0.004	0.003	0.002	0.002	0.003	0.003	0.002	0.003	0.003	0.002	0.003	0.003	0.003	0.003	0.002	0.002
Mg	1.729	1.776	1.760	1.782	1.794	1.759	1.779	1.779	1.771	1.791	1.803	1.787	1.791	1.813	1.804	1.802	1.779	1.815	1.809
Ca	0.000	0.000	0.001	0.001	0.001	0.004	0.001	0.001	0.000	0.001	0.002	0.000	0.002	0.001	0.001	0.001	0.001	0.000	0.001
Ni	0.006	0.004	0.002	0.004	0.004	0.005	0.004	0.004	0.005	0.004	0.004	0.007	0.007	0.004	0.007	0.004	0.004	0.006	0.007
Na	0.001	0.002	0.001	0.001	0.000	0.002	0.002	0.000	0.000	0.002	0.002	0.002	0.002	0.001	0.001	0.000	0.000	0.001	0.001
Total	2.880	3.012	3.002	3.013	3.018	3.000	3.006	3.007	3.001	3.009	3.018	3.006	3.003	2.963	3.013	3.010	2.994	2.955	3.012
Fo	86.01	88.20	88.20	88.41	88.48	88.64	88.68	88.81	88.87	89.00	89.10	89.19	89.59	89.61	89.65	89.65	89.74	89.87	89.94
Fa	13.99	11.80	11.80	11.59	11.52	11.36	11.32	11.19	11.13	11.00	10.90	10.81	10.41	10.39	10.35	10.35	10.26	10.13	10.06

Fo (forsterite), Fa (fayalite)

E (euhedral), M (macrocryst), Mega (megacryst), Neo (neoblast)

Table 1a. (continued)

	M 20	Neo 21	Neo 22	M 23	Neo 24	Neo 25	E 26	M 27	M 28	Mega 29	Neo 30	M 31	M 32	Neo 33	Mega 34	Neo 35	M 36	M 37
SiO_2	40.55	40.22	40.74	40.87	40.52	40.59	40.71	40.97	40.56	40.91	40.71	40.91	40.40	40.38	40.71	40.52	40.90	40.27
TiO_2	0.03	0.05	0.05	0.03	0.01	0.04	0.01	0.06	0.04	0.00	0.03	0.00	0.04	0.02	0.05	0.01	0.05	0.04
Al_2O_3	0.02	0.00	0.00	0.01	0.00	0.00	0.01	0.00	0.00	0.00	0.00	0.03	0.01	0.00	0.01	0.00	0.03	0.02
Cr_2O_3	0.00	0.02	0.02	0.04	0.04	0.01	0.05	0.00	0.02	0.06	0.04	0.01	0.08	0.04	0.05	0.03	0.00	0.02
FeO_T	9.90	9.89	9.92	9.55	9.84	9.77	9.66	9.82	9.67	9.53	9.68	9.70	9.49	9.55	9.46	9.53	9.49	9.57
MnO	0.11	0.09	0.09	0.12	0.11	0.12	0.08	0.11	0.10	0.10	0.12	0.11	0.08	0.11	0.10	0.11	0.11	0.08
MgO	49.74	49.76	50.26	48.44	49.92	49.72	49.47	50.50	49.75	49.44	50.30	50.48	49.45	49.87	49.48	49.90	49.87	50.39
CaO	0.03	0.03	0.08	0.03	0.04	0.05	0.05	0.01	0.05	0.05	0.08	0.03	0.11	0.06	0.05	0.06	0.06	0.07
NiO	0.30	0.37	0.38	0.19	0.34	0.41	0.41	0.27	0.36	0.42	0.44	0.28	0.26	0.36	0.43	0.35	0.34	0.39
Na_2O	0.01	0.00	0.02	0.01	0.00	0.00	0.01	0.02	0.00	0.00	0.01	0.03	0.01	0.00	0.01	0.00	0.02	0.07
Total	100.69	100.43	101.56	99.31	100.81	100.71	100.45	101.76	100.55	100.51	101.41	101.57	99.92	100.39	100.36	100.49	100.86	100.91
Si	0.989	0.985	0.986	1.007	0.987	0.990	0.994	0.988	0.990	0.998	0.986	0.988	0.991	0.987	0.995	0.989	0.994	0.980
Ti	0.001	0.001	0.001	0.001	0.000	0.001	0.000	0.001	0.001	0.000	0.001	0.000	0.001	0.000	0.001	0.000	0.001	0.001
Al	0.000	0.000	0.000	0.000	0.000	0.000	0.000	0.000	0.000	0.000	0.000	0.001	0.000	0.000	0.000	0.000	0.001	0.001
Cr	0.000	0.000	0.000	0.001	0.001	0.000	0.001	0.000	0.000	0.001	0.001	0.000	0.002	0.001	0.001	0.001	0.000	0.000
Fe^{2+}_T	0.202	0.202	0.201	0.197	0.201	0.199	0.197	0.198	0.197	0.194	0.196	0.196	0.195	0.195	0.193	0.194	0.193	0.195
Mn	0.002	0.002	0.002	0.003	0.002	0.003	0.002	0.002	0.002	0.002	0.003	0.002	0.002	0.002	0.002	0.002	0.002	0.002
Mg	1.809	1.816	1.813	1.779	1.813	1.807	1.801	1.815	1.810	1.797	1.816	1.817	1.809	1.817	1.802	1.816	1.806	1.829
Ca	0.001	0.001	0.002	0.001	0.001	0.001	0.001	0.000	0.001	0.001	0.002	0.001	0.003	0.002	0.001	0.002	0.002	0.002
Ni	0.006	0.007	0.008	0.004	0.007	0.008	0.008	0.005	0.007	0.008	0.009	0.005	0.005	0.007	0.009	0.007	0.007	0.008
Na	0.000	0.000	0.001	0.001	0.000	0.000	0.001	0.001	0.000	0.000	0.000	0.001	0.001	0.000	0.000	0.000	0.001	0.003
Total	3.010	3.014	3.014	2.992	3.012	3.009	3.005	3.011	3.009	3.002	3.013	2.982	3.007	3.012	3.004	3.011	3.005	3.020
Fo	89.96	89.97	90.03	90.04	90.04	90.07	90.13	90.17	90.17	90.25	90.25	90.27	90.28	90.30	90.31	90.33	90.35	90.37
Fa	10.04	10.03	9.97	9.96	9.96	9.93	9.87	9.83	9.83	9.75	9.75	9.73	9.72	9.70	9.69	9.67	9.65	9.63

Table 1a. (continued)

	M 38	Neo 39	M 40	M 41	E 42	M 43	M 44	M 45	M 46	M 47	M 48	M 49	M 50	Neo 51	M 52	Neo 53	M 54	M 55
SiO_2	40.48	40.15	40.49	40.46	40.58	40.54	40.87	40.80	40.92	40.78	40.76	40.36	41.11	40.70	40.37	40.78	40.68	40.87
TiO_2	0.05	0.02	0.09	0.01	0.05	0.03	0.05	0.02	0.03	0.07	0.06	0.05	0.00	0.07	0.02	0.05	0.02	0.03
Al_2O_3	0.00	0.00	0.00	0.03	0.00	0.00	0.00	0.01	0.01	0.01	0.01	0.03	0.05	0.00	0.01	0.00	0.00	0.00
Cr_2O_3	0.03	0.07	0.04	0.08	0.04	0.04	0.03	0.03	0.01	0.03	0.02	0.02	0.07	0.07	0.03	0.05	0.02	0.07
FeO_T	9.42	9.47	9.39	9.42	9.27	9.47	9.20	9.17	9.26	9.22	9.21	9.04	9.16	9.09	9.00	9.04	8.84	8.99
MnO	0.12	0.10	0.13	0.13	0.09	0.14	0.13	0.11	0.10	0.13	0.11	0.11	0.12	0.09	0.10	0.12	0.11	0.12
MgO	49.70	50.13	49.74	50.03	49.45	50.75	49.75	49.78	50.47	50.28	50.43	49.93	50.66	50.39	49.91	50.39	49.70	50.53
CaO	0.04	0.09	0.04	0.06	0.01	0.03	0.03	0.01	0.04	0.07	0.06	0.02	0.05	0.06	0.05	0.07	0.04	0.05
NiO	0.30	0.35	0.31	0.38	0.31	0.25	0.23	0.34	0.41	0.17	0.35	0.39	0.41	0.39	0.35	0.38	0.45	0.35
Na_2O	0.05	0.00	0.00	0.04	0.00	0.04	0.01	0.04	0.03	0.03	0.01	0.05	0.02	0.00	0.02	0.00	0.00	0.01
Total	100.19	100.38	100.23	100.63	99.80	101.28	100.30	100.29	101.29	100.79	101.02	100.00	101.64	100.86	99.86	100.88	99.87	101.02
Si	0.991	0.982	0.990	0.987	0.995	0.982	0.997	0.995	0.990	0.990	0.988	0.988	0.990	0.988	0.989	0.989	0.996	0.990
Ti	0.001	0.000	0.002	0.000	0.001	0.001	0.001	0.000	0.001	0.001	0.001	0.001	0.000	0.001	0.000	0.001	0.000	0.001
Al	0.000	0.000	0.000	0.001	0.000	0.000	0.000	0.000	0.000	0.000	0.000	0.001	0.001	0.000	0.000	0.000	0.000	0.000
Cr	0.001	0.001	0.001	0.001	0.001	0.001	0.001	0.001	0.000	0.001	0.000	0.001	0.001	0.001	0.001	0.001	0.000	0.001
Fe^{2+}_T	0.193	0.194	0.192	0.192	0.190	0.192	0.187	0.187	0.187	0.187	0.187	0.185	0.184	0.185	0.184	0.183	0.181	0.182
Mn	0.002	0.002	0.003	0.003	0.002	0.003	0.003	0.002	0.002	0.003	0.002	0.002	0.002	0.002	0.002	0.003	0.002	0.002
Mg	1.813	1.828	1.813	1.819	1.808	1.833	1.809	1.810	1.820	1.820	1.823	1.823	1.819	1.824	1.824	1.823	1.814	1.824
Ca	0.001	0.002	0.001	0.002	0.000	0.001	0.001	0.000	0.001	0.002	0.002	0.001	0.001	0.002	0.001	0.002	0.001	0.001
Ni	0.006	0.007	0.006	0.007	0.006	0.005	0.005	0.007	0.008	0.003	0.007	0.008	0.008	0.008	0.007	0.007	0.009	0.007
Na	0.002	0.000	0.000	0.002	0.000	0.002	0.001	0.002	0.001	0.002	0.001	0.002	0.001	0.000	0.001	0.000	0.000	0.001
Total	3.009	3.017	3.008	3.013	3.003	3.018	3.003	3.003	2.984	3.009	3.011	3.011	3.004	3.010	3.009	3.009	3.004	3.009
Fo	90.39	90.42	90.42	90.45	90.48	90.52	90.61	90.63	90.67	90.67	90.71	90.78	90.79	90.81	90.81	90.86	90.92	90.93
Fa	9.61	9.58	9.58	9.55	9.52	9.48	9.39	9.37	9.33	9.33	9.29	9.22	9.21	9.19	9.19	9.14	9.08	9.07

Table 1a. (continued)

	M 56	Neo 57	M 58	Neo 59	E 60	M 61	M 62	E 63	M 64	Neo 65	Neo 66	E 67	M 68	M 69	M 70	M 71	M 72	M 73
SiO_2	40.95	40.45	40.77	40.63	40.84	41.02	40.69	40.97	40.99	40.96	40.75	40.57	40.85	40.84	40.56	40.94	40.49	40.90
TiO_2	0.00	0.03	0.03	0.01	0.01	0.01	0.01	0.01	0.06	0.03	0.03	0.00	0.00	0.03	0.00	0.01	0.00	0.01
Al_2O_3	0.02	0.00	0.03	0.00	0.02	0.00	0.01	0.00	0.00	0.00	0.00	0.00	0.00	0.00	0.01	0.01	0.02	0.01
Cr_2O_3	0.05	0.05	0.04	0.06	0.10	0.04	0.07	0.07	0.09	0.07	0.07	0.07	0.05	0.09	0.06	0.04	0.05	0.10
FeO_T	8.98	8.89	8.83	8.91	8.79	8.81	8.85	8.75	8.80	8.83	8.80	8.67	8.72	8.75	8.74	8.75	8.67	8.80
MnO	0.12	0.14	0.10	0.08	0.09	0.07	0.10	0.07	0.11	0.12	0.10	0.10	0.11	0.10	0.12	0.12	0.10	0.11
MgO	50.54	50.06	49.92	50.38	49.99	50.20	50.39	49.91	50.24	50.54	50.39	49.68	50.04	50.21	50.22	50.47	50.20	50.96
CaO	0.04	0.05	0.04	0.07	0.07	0.02	0.04	0.06	0.10	0.06	0.06	0.04	0.06	0.09	0.05	0.07	0.04	0.06
NiO	0.41	0.29	0.37	0.38	0.43	0.48	0.30	0.41	0.29	0.39	0.38	0.47	0.44	0.33	0.33	0.38	0.31	0.38
Na_2O	0.00	0.00	0.06	0.01	0.03	0.00	0.04	0.00	0.03	0.01	0.00	0.01	0.00	0.03	0.04	0.00	0.04	0.02
Total	101.11	99.97	100.18	100.53	100.35	100.65	100.49	100.25	100.72	101.01	100.59	99.61	100.27	100.45	100.14	100.79	99.91	101.36
Si	0.991	0.990	0.995	0.989	0.995	0.996	0.990	0.998	0.994	0.991	0.990	0.995	0.995	0.993	0.990	0.993	0.990	0.987
Ti	0.000	0.001	0.001	0.000	0.000	0.000	0.000	0.000	0.001	0.001	0.001	0.000	0.000	0.001	0.000	0.000	0.000	0.000
Al	0.001	0.000	0.001	0.000	0.001	0.000	0.000	0.000	0.000	0.000	0.000	0.000	0.000	0.000	0.000	0.000	0.001	0.000
Cr	0.001	0.001	0.001	0.001	0.002	0.001	0.001	0.001	0.002	0.001	0.001	0.001	0.001	0.002	0.001	0.001	0.001	0.002
Fe^{2+}_T	0.182	0.182	0.180	0.181	0.179	0.179	0.180	0.178	0.179	0.179	0.179	0.178	0.178	0.178	0.178	0.177	0.177	0.178
Mn	0.002	0.003	0.002	0.002	0.002	0.001	0.002	0.002	0.002	0.002	0.002	0.002	0.002	0.002	0.002	0.002	0.002	0.002
Mg	1.823	1.826	1.816	1.828	1.815	1.817	1.828	1.813	1.817	1.823	1.826	1.817	1.818	1.820	1.828	1.824	1.830	1.833
Ca	0.001	0.001	0.001	0.002	0.002	0.000	0.001	0.002	0.003	0.002	0.002	0.001	0.002	0.002	0.001	0.002	0.001	0.002
Ni	0.008	0.006	0.007	0.007	0.008	0.009	0.006	0.008	0.006	0.008	0.008	0.009	0.009	0.006	0.006	0.008	0.006	0.007
Na	0.000	0.000	0.003	0.001	0.001	0.000	0.002	0.000	0.001	0.001	0.000	0.000	0.000	0.001	0.002	0.000	0.002	0.001
Total	2.972	3.009	3.002	3.011	3.004	3.004	3.006	3.001	3.004	3.008	3.008	3.004	3.004	3.006	3.007	3.007	3.007	3.012
Fo	90.93	90.94	90.97	90.98	91.03	91.03	91.03	91.05	91.05	91.07	91.08	91.08	91.09	91.10	91.10	91.14	91.16	91.17
Fa	9.07	9.06	9.03	9.02	8.97	8.97	8.97	8.95	8.95	8.93	8.92	8.92	8.91	8.90	8.90	8.86	8.84	8.83

Table 1a. (continued)

	M 74	E 75	Neo 76	M 77	M 78	M 79	M 80	M 81	M 82	M 83	M 84	M 85	M 86	E 87	M 88	M 89	M 90	M 91	M 92
SiO$_2$	40.44	40.61	40.74	40.88	40.90	41.22	41.04	41.38	40.89	41.01	41.02	40.98	41.10	40.80	41.03	41.17	40.96	40.78	40.88
TiO$_2$	0.00	0.03	0.02	0.00	0.00	0.03	0.00	0.06	0.02	0.00	0.00	0.00	0.04	0.06	0.03	0.01	0.00	0.00	0.00
Al$_2$O$_3$	0.03	0.00	0.00	0.00	0.01	0.00	0.00	0.02	0.01	0.03	0.00	0.00	0.02	0.02	0.02	0.00	0.02	0.00	0.03
Cr$_2$O$_3$	0.05	0.05	0.07	0.02	0.06	0.03	0.04	0.11	0.05	0.06	0.04	0.03	0.03	0.00	0.04	0.04	0.06	0.05	0.06
FeO$_T$	8.84	8.58	8.74	8.46	8.46	8.43	8.39	8.67	8.42	8.65	8.33	8.45	8.41	8.38	8.39	8.44	8.24	8.28	8.38
MnO	0.10	0.10	0.09	0.11	0.10	0.09	0.11	0.11	0.13	0.08	0.12	0.14	0.12	0.12	0.08	0.11	0.11	0.11	0.10
MgO	51.32	49.86	50.91	49.35	49.40	49.54	49.29	51.07	49.68	51.02	49.30	50.77	50.51	50.35	50.56	50.87	49.97	50.35	51.06
CaO	0.05	0.05	0.08	0.01	0.04	0.00	0.01	0.06	0.08	0.05	0.02	0.03	0.03	0.07	0.08	0.02	0.02	0.02	0.04
NiO	0.35	0.43	0.38	0.25	0.29	0.22	0.24	0.33	0.33	0.34	0.25	0.32	0.39	0.25	0.35	0.39	0.34	0.35	0.42
Na$_2$O	0.02	0.01	0.00	0.03	0.02	0.02	0.02	0.04	0.00	0.04	0.01	0.00	0.01	0.01	0.06	0.03	0.05	0.04	0.02
Total	101.20	99.72	101.04	99.10	99.26	99.58	99.13	101.85	99.61	101.27	99.10	100.72	100.65	100.05	100.64	101.08	99.76	99.97	100.98
Si	0.978	0.995	0.986	1.005	1.004	1.007	1.008	0.992	1.001	0.989	1.007	0.992	0.996	0.994	0.994	0.994	1.000	0.994	0.988
Ti	0.000	0.001	0.000	0.000	0.000	0.001	0.000	0.001	0.000	0.000	0.000	0.000	0.001	0.001	0.001	0.000	0.000	0.000	0.000
Al	0.001	0.000	0.000	0.000	0.000	0.000	0.000	0.001	0.000	0.001	0.000	0.000	0.001	0.000	0.001	0.000	0.001	0.000	0.001
Cr	0.001	0.001	0.001	0.000	0.001	0.001	0.001	0.002	0.001	0.001	0.001	0.001	0.001	0.000	0.001	0.001	0.001	0.001	0.001
Fe$^{2+}_T$	0.179	0.176	0.177	0.174	0.174	0.172	0.172	0.174	0.172	0.174	0.171	0.171	0.170	0.171	0.170	0.170	0.168	0.169	0.169
Mn	0.002	0.002	0.002	0.002	0.002	0.002	0.002	0.002	0.003	0.002	0.003	0.003	0.003	0.003	0.002	0.002	0.002	0.002	0.002
Mg	1.851	1.820	1.837	1.808	1.807	1.805	1.804	1.825	1.813	1.834	1.805	1.833	1.824	1.829	1.827	1.830	1.819	1.831	1.840
Ca	0.001	0.001	0.002	0.000	0.001	0.000	0.000	0.002	0.002	0.001	0.001	0.001	0.001	0.002	0.002	0.001	0.000	0.001	0.001
Ni	0.007	0.008	0.007	0.005	0.006	0.004	0.005	0.006	0.006	0.007	0.005	0.006	0.008	0.005	0.007	0.008	0.007	0.007	0.008
Na	0.001	0.001	0.000	0.001	0.001	0.001	0.001	0.002	0.000	0.002	0.001	0.000	0.001	0.000	0.003	0.001	0.002	0.002	0.001
Total	2.990	3.005	3.013	2.996	2.996	2.992	2.993	3.006	2.997	3.006	2.993	3.007	3.003	3.005	2.974	3.007	2.997	3.003	3.052
Fo	91.19	91.20	91.21	91.23	91.23	91.28	91.29	91.31	91.32	91.32	91.34	91.46	91.46	91.47	91.49	91.49	91.54	91.56	91.58
Fa	8.81	8.80	8.79	8.77	8.77	8.72	8.71	8.69	8.68	8.68	8.66	8.54	8.54	8.53	8.51	8.51	8.46	8.44	8.42

Table 1a. (continued)

	M 93	M 94	M 95	M 96	M 97	M 98	M 99	M 100	M 101	MS 102	M 103	M 104	M 105	M 106	M 107	M 108	M 109	M 110	M 111
SiO_2	40.94	40.87	40.87	40.70	41.13	40.68	40.99	40.80	41.00	40.58	40.93	41.03	40.82	41.02	40.94	41.13	40.50	41.14	41.10
TiO_2	0.00	0.00	0.04	0.06	0.00	0.00	0.01	0.02	0.00	0.02	0.01	0.04	0.00	0.05	0.01	0.02	0.00	0.05	0.00
Al_2O_3	0.00	0.02	0.00	0.01	0.03	0.01	0.00	0.02	0.02	0.01	0.00	0.00	0.03	0.00	0.00	0.01	0.00	0.01	0.05
Cr_2O_3	0.10	0.07	0.01	0.04	0.03	0.05	0.03	0.02	0.05	0.05	0.02	0.02	0.04	0.01	0.04	0.06	0.01	0.01	0.04
FeO_T	8.16	8.09	8.18	8.17	8.28	8.27	8.19	8.08	8.17	7.86	7.72	7.96	7.99	7.85	7.80	7.70	7.81	7.82	7.89
MnO	0.10	0.08	0.10	0.11	0.08	0.12	0.10	0.09	0.11	0.10	0.10	0.13	0.09	0.13	0.11	0.09	0.09	0.10	0.09
MgO	50.37	50.14	50.76	50.81	51.74	51.95	51.87	51.23	51.87	49.97	49.56	51.24	51.69	50.83	50.61	50.39	51.18	51.41	51.97
CaO	0.05	0.05	0.01	0.03	0.04	0.05	0.03	0.05	0.06	0.02	0.00	0.04	0.01	0.04	0.02	0.03	0.00	0.04	0.00
NiO	0.36	0.37	0.32	0.34	0.35	0.41	0.39	0.42	0.37	0.32	0.27	0.32	0.36	0.38	0.35	0.38	0.37	0.37	0.36
Na_2O	0.01	0.05	0.01	0.00	0.00	0.03	0.02	0.02	0.00	0.05	0.02	0.00	0.04	0.00	0.02	0.02	0.00	0.03	0.00
Total	100.09	99.74	100.29	100.28	101.67	101.56	101.64	100.74	101.65	98.99	98.63	100.78	101.05	100.31	99.90	99.82	99.96	100.97	101.51
Si	0.996	0.998	0.993	0.989	0.986	0.978	0.984	0.987	0.984	0.997	1.007	0.991	0.984	0.995	0.996	1.001	0.986	0.991	0.986
Ti	0.000	0.000	0.001	0.001	0.000	0.000	0.000	0.000	0.000	0.000	0.000	0.001	0.000	0.001	0.000	0.000	0.000	0.001	0.000
Al	0.000	0.001	0.000	0.000	0.001	0.000	0.000	0.000	0.001	0.000	0.000	0.000	0.001	0.000	0.000	0.000	0.000	0.000	0.001
Cr	0.002	0.001	0.000	0.001	0.000	0.001	0.001	0.000	0.001	0.001	0.000	0.000	0.001	0.000	0.001	0.001	0.000	0.000	0.001
Fe^{2+}_T	0.166	0.165	0.166	0.166	0.166	0.166	0.164	0.163	0.164	0.162	0.159	0.161	0.161	0.159	0.159	0.157	0.159	0.157	0.158
Mn	0.002	0.002	0.002	0.002	0.002	0.003	0.002	0.002	0.002	0.002	0.002	0.003	0.002	0.003	0.002	0.002	0.002	0.002	0.002
Mg	1.828	1.825	1.838	1.842	1.850	1.863	1.856	1.848	1.855	1.831	1.818	1.845	1.858	1.838	1.837	1.828	1.859	1.847	1.858
Ca	0.001	0.001	0.000	0.001	0.001	0.001	0.001	0.001	0.001	0.001	0.000	0.001	0.000	0.001	0.001	0.001	0.000	0.001	0.000
Ni	0.007	0.007	0.006	0.007	0.007	0.008	0.008	0.008	0.007	0.006	0.005	0.006	0.007	0.007	0.007	0.007	0.007	0.007	0.007
Na	0.001	0.002	0.001	0.000	0.000	0.001	0.001	0.001	0.000	0.003	0.001	0.000	0.002	0.000	0.001	0.001	0.000	0.002	0.000
Total	3.000	2.998	2.980	3.009	3.005	3.022	3.016	3.012	3.015	3.000	2.993	3.014	3.050	3.004	3.002	2.996	3.013	3.021	3.008
Fo	91.67	91.70	91.71	91.73	91.76	91.80	91.86	91.87	91.88	91.89	91.96	91.99	92.02	92.03	92.04	92.10	92.11	92.14	92.15
Fa	8.33	8.30	8.29	8.27	8.24	8.20	8.14	8.13	8.12	8.11	8.04	8.01	7.98	7.97	7.96	7.90	7.89	7.86	7.85

Table 1a. (continued)

	M 112	M 113	M 114	M 115	M 116	M 117	M 118	M 119	M 120	M 121	M 122	M 123	M 124	M 125	M 126	M 127	M 128	M 129	M 130
SiO_2	40.64	40.88	41.05	41.12	41.20	40.78	41.13	41.02	40.99	41.06	40.99	41.00	41.22	41.12	41.26	41.11	40.81	40.99	41.18
TiO_2	0.00	0.00	0.00	0.00	0.02	0.00	0.00	0.00	0.06	0.02	0.00	0.02	0.00	0.02	0.00	0.00	0.02	0.05	0.00
Al_2O_3	0.00	0.01	0.00	0.02	0.01	0.00	0.00	0.04	0.01	0.00	0.01	0.00	0.00	0.04	0.00	0.01	0.02	0.00	0.03
Cr_2O_3	0.05	0.06	0.02	0.05	0.03	0.06	0.01	0.05	0.03	0.02	0.00	0.00	0.02	0.04	0.00	0.04	0.02	0.00	0.04
FeO_T	7.68	7.86	7.56	7.81	7.71	7.56	7.52	7.64	7.56	7.35	7.33	7.46	7.38	7.47	7.19	7.31	7.18	7.07	7.28
MnO	0.08	0.09	0.11	0.10	0.12	0.12	0.08	0.11	0.08	0.10	0.07	0.08	0.07	0.11	0.11	0.08	0.10	0.12	0.10
MgO	50.65	52.00	50.32	52.02	52.55	51.70	51.46	52.28	51.87	50.87	50.78	51.89	51.43	52.19	50.70	51.86	51.15	50.78	52.46
CaO	0.03	0.03	0.00	0.02	0.03	0.04	0.00	0.02	0.05	0.00	0.00	0.00	0.01	0.04	0.00	0.01	0.02	0.00	0.01
NiO	0.37	0.38	0.29	0.39	0.42	0.37	0.37	0.36	0.37	0.36	0.32	0.33	0.35	0.38	0.31	0.36	0.30	0.32	0.41
Na_2O	0.04	0.01	0.00	0.02	0.06	0.02	0.00	0.03	0.02	0.02	0.04	0.02	0.02	0.02	0.00	0.01	0.05	0.00	0.05
Total	99.55	101.32	99.35	101.54	102.15	100.66	100.57	101.54	101.04	99.79	99.54	100.80	100.52	101.44	99.56	100.78	99.67	99.34	101.57
Si	0.993	0.983	1.003	0.986	0.982	0.986	0.993	0.983	0.986	0.998	0.999	0.988	0.995	0.986	1.003	0.990	0.993	1.000	0.985
Ti	0.000	0.000	0.000	0.000	0.000	0.000	0.000	0.000	0.001	0.000	0.000	0.000	0.000	0.000	0.000	0.000	0.000	0.001	0.000
Al	0.000	0.000	0.000	0.001	0.000	0.000	0.000	0.001	0.000	0.000	0.000	0.000	0.000	0.001	0.000	0.000	0.000	0.000	0.001
Cr	0.001	0.001	0.000	0.001	0.001	0.001	0.000	0.001	0.001	0.000	0.000	0.000	0.000	0.001	0.000	0.001	0.000	0.000	0.001
Fe^{2+}_T	0.157	0.158	0.154	0.157	0.154	0.153	0.152	0.153	0.152	0.149	0.149	0.150	0.149	0.150	0.146	0.147	0.146	0.144	0.146
Mn	0.002	0.002	0.002	0.002	0.002	0.002	0.002	0.002	0.002	0.002	0.001	0.002	0.001	0.002	0.002	0.002	0.002	0.002	0.002
Mg	1.845	1.864	1.832	1.859	1.868	1.863	1.853	1.868	1.861	1.844	1.844	1.864	1.851	1.865	1.838	1.862	1.856	1.846	1.870
Ca	0.001	0.001	0.000	0.000	0.001	0.001	0.000	0.000	0.001	0.000	0.000	0.000	0.000	0.001	0.000	0.000	0.000	0.000	0.000
Ni	0.007	0.007	0.006	0.008	0.008	0.007	0.007	0.007	0.007	0.007	0.006	0.006	0.007	0.007	0.006	0.007	0.006	0.006	0.008
Na	0.002	0.000	0.000	0.001	0.003	0.001	0.000	0.001	0.001	0.001	0.002	0.001	0.001	0.001	0.000	0.000	0.002	0.000	0.003
Total	3.005	3.033	2.997	3.007	3.019	3.014	3.007	3.048	3.018	3.001	3.001	3.014	3.005	3.010	2.996	3.044	3.005	2.999	3.028
Fo	92.16	92.18	92.23	92.24	92.40	92.42	92.43	92.43	92.45	92.50	92.51	92.54	92.55	92.57	92.63	92.68	92.70	92.75	92.77
Fa	7.84	7.82	7.77	7.76	7.60	7.58	7.57	7.57	7.55	7.50	7.49	7.46	7.45	7.43	7.37	7.32	7.30	7.25	7.23

Table 1a. (continued)

	M 131	M 132	M 133	M 134	M 135	M 136	E 137	M 138	M 139	M 140	M 141	M 142	M 143
SiO_2	41.21	41.33	40.69	41.39	41.25	41.21	41.28	41.17	41.35	41.19	41.27	41.02	41.39
TiO_2	0.00	0.00	0.00	0.00	0.01	0.00	0.00	0.01	0.00	0.03	0.03	0.25	0.02
Al_2O_3	0.01	0.00	0.00	0.02	0.00	0.00	0.00	0.00	0.01	0.00	0.00	0.15	0.00
Cr_2O_3	0.02	0.00	0.02	0.00	0.02	0.00	0.04	0.00	0.03	-0.00	0.00	0.02	0.00
FeO_T	7.22	7.12	7.02	7.23	6.94	7.09	6.81	6.82	6.94	6.83	6.52	5.87	5.70
MnO	0.09	0.10	0.10	0.08	0.07	0.09	0.06	0.11	0.08	0.09	0.08	0.18	0.06
MgO	52.03	51.34	50.89	52.42	50.41	52.48	51.18	51.46	52.41	52.05	51.13	51.78	53.49
CaO	0.03	0.01	0.00	0.00	0.00	0.00	0.01	0.02	0.00	0.00	0.01	0.25	0.00
NiO	0.31	0.31	0.30	0.34	0.25	0.31	0.36	0.37	0.38	0.28	0.29	0.02	0.33
Na_2O	0.01	0.00	0.01	0.00	0.00	0.01	0.00	0.01	0.02	0.01	0.00	0.02	0.02
Total	100.93	100.21	99.02	101.47	98.94	101.20	99.73	99.97	101.21	100.48	99.32	99.56	101.01
Si	0.990	0.999	0.996	0.989	1.008	0.988	1.001	0.997	0.990	0.992	1.003	0.993	0.988
Ti	0.000	0.000	0.000	0.000	0.000	0.000	0.000	0.000	0.000	0.000	0.000	0.005	0.000
Al	0.000	0.000	0.000	0.000	0.000	0.000	0.000	0.000	0.000	0.000	0.000	0.004	0.000
Cr	0.000	0.000	0.000	0.000	0.000	0.000	0.001	0.000	0.001	0.000	0.000	0.001	0.000
Fe^{2+}_T	0.145	0.144	0.144	0.144	0.142	0.142	0.138	0.138	0.139	0.138	0.132	0.119	0.114
Mn	0.002	0.002	0.002	0.002	0.002	0.002	0.001	0.002	0.002	0.002	0.002	0.004	0.001
Mg	1.864	1.850	1.856	1.868	1.836	1.875	1.850	1.858	1.871	1.869	1.853	1.868	1.903
Ca	0.001	0.000	0.000	0.000	0.000	0.000	0.000	0.000	0.000	0.000	0.000	0.007	0.000
Ni	0.006	0.006	0.006	0.007	0.005	0.006	0.007	0.007	0.007	0.005	0.006	0.000	0.006
Na	0.001	0.000	0.000	0.000	0.000	0.000	0.000	0.000	0.001	0.000	0.000	0.001	0.001
Total	3.010	3.001	3.003	3.045	2.992	3.058	2.999	3.003	3.076	3.031	2.996	3.001	3.041
Fo	92.78	92.79	92.82	92.82	92.83	92.95	93.06	93.08	93.08	93.14	93.33	94.02	94.37
Fa	7.22	7.21	7.18	7.18	7.17	7.05	6.94	6.92	6.92	6.86	6.67	5.98	5.63

Table 1b: Microprobe analyses of Sputnik olivines (cations on basis of 4 oxygen).

	M 1	E 2	M 3	E 4	M 5	M 6	E 7	E 8	M 9	M 10	E 11	E 12	M 13	E 14	M 15	M 16	M 17
SiO_2	40.52	40.65	40.54	40.68	40.85	41.00	40.82	40.96	40.71	41.09	40.84	41.17	40.93	41.55	40.60	40.78	40.65
TiO_2	0.06	0.02	0.05	0.00	0.03	0.00	0.04	0.03	0.01	0.00	0.00	0.00	0.01	0.04	0.00	0.02	0.03
Al_2O_3	0.01	0.03	0.04	0.00	0.00	0.00	0.01	0.00	0.00	0.00	0.00	0.00	0.00	0.00	0.03	0.03	0.02
Cr_2O_3	0.01	0.08	0.05	0.04	0.04	0.03	0.06	0.06	0.04	0.02	0.05	0.03	0.05	0.04	0.03	0.05	0.04
FeO_T	10.65	10.12	9.95	9.23	9.19	9.20	9.12	9.17	9.07	9.08	9.08	9.06	8.98	8.97	8.62	8.64	8.65
MnO	0.17	0.14	0.12	0.09	0.10	0.09	0.10	0.11	0.12	0.11	0.13	0.09	0.11	0.12	0.10	0.10	0.11
MgO	49.14	49.77	49.08	50.10	49.93	50.50	50.09	50.78	50.26	50.36	50.46	50.35	50.32	50.50	49.43	49.56	50.17
CaO	0.04	0.04	0.04	0.04	0.03	0.02	0.02	0.03	0.05	0.02	0.07	0.05	0.04	0.05	0.05	0.05	0.06
NiO	0.15	0.37	0.27	0.34	0.36	0.39	0.35	0.38	0.36	0.37	0.25	0.36	0.38	0.36	0.31	0.26	0.26
Na_2O	0.02	0.01	0.00	0.00	0.03	0.01	0.00	0.01	0.00	0.00	0.01	0.00	0.02	0.00	0.02	0.03	0.03
Total	100.77	101.23	100.12	100.52	100.57	101.24	100.61	101.54	100.62	101.05	100.89	101.11	100.85	101.63	99.18	99.50	100.02
Si	0.990	0.988	0.994	0.991	0.994	0.991	0.993	0.988	0.990	0.995	0.990	0.995	0.993	0.999	0.999	1.000	0.993
Ti	0.001	0.000	0.001	0.000	0.001	0.000	0.001	0.001	0.000	0.000	0.000	0.000	0.000	0.001	0.000	0.000	0.001
Al	0.000	0.001	0.001	0.000	0.000	0.000	0.000	0.000	0.000	0.000	0.000	0.000	0.000	0.000	0.001	0.001	0.001
Cr	0.000	0.002	0.001	0.001	0.001	0.001	0.001	0.001	0.001	0.000	0.001	0.001	0.001	0.001	0.001	0.001	0.001
Fe^{2+}_T	0.218	0.206	0.204	0.188	0.187	0.186	0.185	0.185	0.184	0.184	0.184	0.183	0.182	0.180	0.177	0.177	0.176
Mn	0.003	0.003	0.002	0.002	0.002	0.002	0.002	0.002	0.003	0.002	0.003	0.002	0.002	0.003	0.002	0.002	0.002
Mg	1.790	1.803	1.794	1.819	1.812	1.820	1.816	1.826	1.823	1.817	1.824	1.815	1.819	1.809	1.813	1.811	1.826
Ca	0.001	0.001	0.001	0.001	0.001	0.001	0.001	0.001	0.001	0.001	0.002	0.001	0.001	0.001	0.001	0.001	0.002
Ni	0.003	0.007	0.005	0.007	0.007	0.008	0.007	0.007	0.007	0.007	0.005	0.007	0.007	0.007	0.006	0.005	0.005
Na	0.001	0.001	0.000	0.000	0.002	0.001	0.000	0.001	0.000	0.000	0.001	0.000	0.001	0.000	0.001	0.001	0.002
Total	3.009	3.011	3.004	3.009	3.006	3.009	3.006	3.011	3.009	3.005	3.009	3.004	3.007	3.000	3.001	3.000	3.007
Fo	89.16	89.76	89.79	90.64	90.64	90.72	90.74	90.80	90.81	90.82	90.83	90.83	90.90	90.94	91.09	91.09	91.19
Fa	10.84	10.24	10.21	9.36	9.36	9.28	9.26	9.20	9.19	9.18	9.17	9.17	9.10	9.06	8.91	8.91	8.81

Fo (forsterite), Fa (fayalite)
E (euhedral), M (macrocryst), Mega (megacryst)

Table 1b. (continued)

	M 18	M 19	M 20	M 21	M 22	M 23	M 24	E 25	M 26
SiO_2	40.60	40.94	41.05	41.05	41.48	41.07	40.83	41.25	41.48
TiO_2	0.00	0.00	0.00	0.02	0.05	0.00	0.01	0.00	0.00
Al_2O_3	0.03	0.03	0.04	0.02	0.00	0.01	0.02	0.00	0.00
Cr_2O_3	0.04	0.07	0.06	0.05	0.02	0.01	0.02	0.00	0.00
FeO_T	8.65	8.34	8.30	8.15	7.36	7.34	7.03	6.77	6.63
MnO	0.13	0.13	0.10	0.10	0.09	0.10	0.09	0.08	0.09
MgO	50.34	50.03	51.28	50.82	51.84	51.82	51.60	52.11	52.61
CaO	0.03	0.07	0.02	0.03	0.01	0.00	0.01	0.00	0.00
NiO	0.21	0.31	0.31	0.29	0.36	0.29	0.26	0.33	0.22
Na_2O	0.00	0.03	0.00	0.02	0.00	0.01	0.01	0.00	0.01
Total	100.02	99.95	101.15	100.54	101.21	100.64	99.88	100.53	101.05
Si	0.991	0.998	0.989	0.994	0.994	0.990	0.991	0.993	0.992
Ti	0.000	0.000	0.000	0.000	0.001	0.000	0.000	0.000	0.000
Al	0.001	0.001	0.001	0.001	0.000	0.000	0.001	0.000	0.000
Cr	0.001	0.001	0.001	0.001	0.000	0.000	0.000	0.000	0.000
Fe^{2+}_T	0.177	0.170	0.167	0.165	0.148	0.148	0.143	0.136	0.133
Mn	0.003	0.003	0.002	0.002	0.002	0.002	0.002	0.002	0.002
Mg	1.832	1.819	1.842	1.835	1.852	1.863	1.867	1.870	1.876
Ca	0.001	0.002	0.001	0.001	0.000	0.000	0.000	0.000	0.000
Ni	0.004	0.006	0.006	0.006	0.007	0.006	0.005	0.006	0.004
Na	0.000	0.001	0.000	0.001	0.000	0.000	0.000	0.000	0.000
Total	3.008	3.001	3.010	3.005	3.005	3.010	3.009	3.007	3.008
Fo	91.21	91.45	91.67	91.75	92.62	92.64	92.90	93.21	93.39
Fa	8.79	8.55	8.33	8.25	7.38	7.36	7.10	6.79	6.61

Table 2a: Microprobe analyses of Torrie garnets (cations on basis of 12 oxygen).

Group	1	1	1	1	1	1	1	1	1	1	1	3	3	3	3	5	5	5
SiO_2	41.15	41.11	40.46	40.44	40.92	41.77	41.54	41.71	41.89	41.52	41.06	41.65	39.95	40.49	40.22	39.49	37.60	37.60
Al_2O_3	20.33	19.52	19.90	20.08	19.45	20.48	21.07	20.95	22.42	21.78	20.46	21.91	22.48	22.69	22.61	22.68	21.96	22.21
Cr_2O_3	3.98	3.89	3.64	3.25	3.55	3.14	2.83	3.10	1.56	2.01	4.09	2.08	0.17	0.18	0.19	0.08	0.03	0.05
TiO_2	0.46	0.74	0.55	0.50	0.70	0.52	0.31	0.38	0.37	0.40	0.45	0.37	0.09	0.10	0.09	0.04	0.06	0.04
FeO_T	7.77	8.51	9.89	8.95	9.12	7.61	7.57	8.06	8.44	8.43	7.69	8.54	14.95	14.61	14.93	23.33	34.45	32.74
MnO	0.33	0.27	0.40	0.38	0.28	0.34	0.34	0.37	0.36	0.35	0.36	0.36	0.28	0.29	0.28	0.67	0.95	0.92
MgO	20.43	20.09	16.33	17.84	18.79	20.70	21.21	20.63	20.32	19.29	20.83	19.36	13.04	13.61	13.38	8.94	5.73	6.67
CaO	5.24	5.64	8.30	6.77	5.74	5.21	4.55	4.69	4.70	5.54	5.16	5.55	8.62	8.22	8.56	6.36	0.94	0.99
NiO	0.00	0.00	0.00	0.00	0.00	0.00	0.00	0.00	0.00	0.00	0.00	0.01	0.00	0.00	0.00	0.06	0.00	0.00
Na_2O	0.07	0.03	0.06	0.07	0.08	0.07	0.04	0.11	0.04	0.04	0.09	0.08	0.06	0.05	0.03	0.00	0.03	0.00
Total	99.78	99.78	99.52	98.27	98.62	99.82	99.46	99.99	100.09	99.36	100.19	99.90	99.64	100.24	100.29	101.66	101.75	101.22
Si	2.964	2.975	2.976	2.983	3.002	2.995	2.979	2.986	2.983	2.991	2.946	2.986	2.970	2.980	2.968	2.971	2.942	2.935
Al	1.726	1.665	1.725	1.745	1.681	1.730	1.781	1.767	1.881	1.849	1.730	1.851	1.969	1.968	1.966	2.011	2.026	2.043
Cr	0.227	0.222	0.211	0.190	0.206	0.178	0.160	0.175	0.088	0.114	0.232	0.118	0.010	0.011	0.011	0.005	0.002	0.003
Ti	0.025	0.040	0.030	0.027	0.038	0.028	0.017	0.020	0.020	0.022	0.024	0.020	0.005	0.005	0.005	0.002	0.003	0.002
Fe^{2+}	0.468	0.515	0.608	0.552	0.560	0.456	0.454	0.482	0.503	0.508	0.462	0.512	0.929	0.899	0.921	1.468	2.254	2.137
Mn	0.020	0.016	0.025	0.024	0.017	0.020	0.021	0.022	0.021	0.021	0.022	0.022	0.018	0.018	0.017	0.043	0.063	0.061
Mg	2.194	2.167	1.790	1.961	2.056	2.212	2.268	2.202	2.157	2.071	2.229	2.069	1.445	1.493	1.472	1.003	0.669	0.776
Ca	0.405	0.438	0.654	0.535	0.451	0.400	0.350	0.359	0.358	0.427	0.396	0.426	0.686	0.648	0.677	0.513	0.079	0.083
Ni	0.000	0.000	0.000	0.000	0.000	0.000	0.000	0.000	0.000	0.000	0.000	0.001	0.000	0.000	0.000	0.004	0.000	0.000
Na	0.010	0.004	0.009	0.010	0.011	0.009	0.006	0.015	0.005	0.006	0.012	0.011	0.008	0.007	0.004	0.000	0.005	0.000
Total	8.039	8.043	8.030	8.027	8.022	8.028	8.036	8.030	8.016	8.009	8.054	8.015	8.040	8.029	8.041	8.019	8.043	8.040
Mg#	82.41	80.80	74.65	78.05	78.60	82.91	83.32	82.03	81.10	80.31	82.84	80.15	60.85	62.43	61.51	40.59	22.88	26.64

Mg# = 100Mg/(Mg+Fe^{2+})
Groups according to Dawson and Stephens (1975).

Table 2a.(continued)

Group	5	5	5	5	5	9	9	9	9	9	9	9	9	9	9	9	9	9	9
SiO_2	37.89	39.81	37.80	38.24	38.26	40.68	40.67	41.25	41.30	40.95	41.20	41.04	40.59	40.61	40.45	40.81	40.94	40.82	40.82
Al_2O_3	21.95	22.46	21.46	21.71	20.83	19.25	20.68	21.20	20.15	20.40	21.06	20.62	20.18	20.97	18.67	19.92	18.14	20.58	18.61
Cr_2O_3	0.15	0.11	0.02	0.04	0.06	5.47	4.09	3.18	4.40	4.03	3.10	3.18	4.89	3.03	6.74	4.50	7.22	3.81	6.32
TiO_2	0.06	0.11	0.01	0.04	0.08	0.31	0.31	0.26	0.13	0.40	0.33	0.37	0.05	0.29	0.00	0.12	0.01	0.28	0.18
FeO_T	33.76	23.99	34.29	33.29	28.83	7.20	7.53	7.63	7.32	7.68	7.75	8.22	7.23	7.63	8.19	7.30	7.24	8.47	7.15
MnO	0.98	0.26	1.14	0.78	0.81	0.30	0.35	0.31	0.28	0.36	0.32	0.28	0.33	0.30	0.43	0.29	0.32	0.32	0.31
MgO	6.50	12.45	5.52	6.49	4.97	20.52	20.35	20.82	20.47	20.30	20.92	20.46	20.49	20.65	18.46	20.22	18.98	19.29	19.45
CaO	0.92	1.16	0.93	0.91	6.91	5.55	4.87	4.55	5.31	4.95	4.67	5.21	5.20	4.48	6.56	5.31	6.00	4.82	5.62
NiO	0.00	0.02	0.04	0.04	0.04	0.00	0.00	0.00	0.01	0.00	0.00	0.01	0.00	0.00	0.00	0.00	0.00	0.00	0.00
Na_2O	0.00	0.01	0.00	0.01	0.00	0.03	0.08	0.05	0.05	0.07	0.07	0.06	0.02	0.05	0.00	0.07	0.05	0.05	0.04
Total	102.21	100.38	101.20	101.53	100.80	99.30	98.93	99.25	99.42	99.14	99.43	99.43	98.98	98.01	99.49	98.53	98.90	98.44	98.50
Si	2.941	2.991	2.975	2.977	2.997	2.955	2.950	2.969	2.981	2.965	2.964	2.965	2.949	2.961	2.966	2.975	3.002	2.981	2.994
Al	2.008	1.988	1.991	1.992	1.923	1.648	1.767	1.798	1.714	1.741	1.785	1.756	1.728	1.802	1.613	1.711	1.568	1.772	1.609
Cr	0.009	0.006	0.001	0.002	0.004	0.314	0.235	0.181	0.251	0.231	0.176	0.182	0.281	0.175	0.391	0.259	0.418	0.220	0.366
Ti	0.004	0.006	0.000	0.002	0.005	0.017	0.017	0.014	0.007	0.022	0.018	0.020	0.003	0.016	0.000	0.007	0.001	0.015	0.010
Fe^{2+}	2.191	1.507	2.257	2.167	1.889	0.437	0.457	0.459	0.442	0.465	0.466	0.496	0.439	0.465	0.502	0.445	0.444	0.517	0.439
Mn	0.064	0.017	0.076	0.051	0.054	0.018	0.022	0.019	0.017	0.022	0.020	0.017	0.020	0.018	0.027	0.018	0.020	0.020	0.019
Mg	0.752	1.395	0.647	0.753	0.581	2.222	2.200	2.234	2.203	2.191	2.244	2.203	2.219	2.245	2.018	2.197	2.075	2.100	2.127
Ca	0.077	0.093	0.078	0.076	0.580	0.432	0.379	0.350	0.410	0.384	0.360	0.403	0.405	0.350	0.515	0.415	0.472	0.378	0.441
Ni	0.000	0.001	0.002	0.003	0.000	0.000	0.000	0.000	0.001	0.000	0.000	0.000	0.000	0.000	0.000	0.000	0.000	0.000	0.000
Na	0.000	0.002	0.000	0.001	0.000	0.005	0.011	0.007	0.008	0.010	0.010	0.008	0.003	0.007	0.000	0.010	0.008	0.007	0.005
Total	8.046	8.007	8.028	8.024	8.035	8.049	8.037	8.031	8.033	8.031	8.043	8.051	8.046	8.038	8.032	8.037	8.007	8.011	8.011
Mg#	25.55	48.06	22.29	25.79	23.51	83.55	82.81	82.96	83.30	82.49	82.80	81.61	83.48	82.83	80.09	83.15	82.38	80.24	82.90

Table 2a.(continued)

Group	9	9	9	9	9	9	9	9	9	9	9	9	9	9	9	9	9	9	9
SiO_2	41.40	41.42	41.14	40.59	40.49	41.42	40.50	41.74	41.43	41.47	41.14	41.46	41.36	41.31	41.02	41.73	40.67	41.07	41.92
Al_2O_3	21.18	21.62	20.54	18.43	18.44	21.10	18.63	20.80	19.43	18.04	18.58	23.23	22.14	20.09	19.21	21.22	18.97	19.19	21.29
Cr_2O_3	3.29	2.89	3.90	6.53	6.53	2.63	6.63	3.52	5.83	7.27	5.81	0.90	2.20	4.61	5.81	3.57	6.16	5.66	2.16
TiO_2	0.24	0.22	0.21	0.14	0.18	0.38	0.12	0.22	0.01	0.17	0.17	0.08	0.26	0.16	0.01	0.20	0.00	0.05	0.33
FeO_T	7.47	7.92	7.06	7.41	7.60	7.63	7.42	7.69	6.56	6.69	7.06	8.32	9.10	7.41	8.44	7.14	8.23	6.90	8.02
MnO	0.29	0.29	0.22	0.37	0.35	0.24	0.36	0.35	0.31	0.31	0.33	0.36	0.40	0.35	0.44	0.31	0.46	0.35	0.32
MgO	20.04	20.07	20.24	19.73	19.76	20.86	19.93	21.11	19.52	19.77	19.78	19.33	19.06	19.99	18.57	20.81	17.60	19.82	20.09
CaO	4.71	4.52	4.88	5.10	5.32	5.01	5.14	4.63	6.90	6.09	5.58	5.42	5.17	5.26	6.39	4.61	6.59	5.72	4.46
NiO	0.00	0.00	0.00	0.00	0.00	0.00	0.00	0.00	0.00	0.00	0.01	0.00	0.00	0.00	0.00	0.00	0.00	0.03	0.00
Na_2O	0.05	0.05	0.03	0.00	0.02	0.00	0.01	0.08	0.00	0.01	0.00	0.00	0.02	0.02	0.00	0.02	0.00	0.00	0.05
Total	98.65	99.00	98.21	98.29	98.70	99.27	98.74	100.14	99.99	99.82	98.46	99.09	99.70	99.20	99.90	99.61	98.67	98.79	98.64
Si	2.994	2.985	2.991	2.987	2.973	2.979	2.968	2.982	2.988	3.005	3.012	2.978	2.976	2.990	2.986	2.986	2.999	2.994	3.025
Al	1.805	1.836	1.760	1.598	1.596	1.788	1.609	1.751	1.652	1.541	1.603	1.967	1.877	1.714	1.648	1.789	1.648	1.648	1.811
Cr	0.188	0.165	0.224	0.380	0.379	0.150	0.384	0.199	0.332	0.417	0.336	0.051	0.125	0.264	0.334	0.202	0.359	0.326	0.123
Ti	0.013	0.012	0.012	0.008	0.010	0.020	0.007	0.012	0.000	0.009	0.009	0.004	0.014	0.008	0.000	0.011	0.000	0.003	0.018
Fe^{2+}	0.452	0.477	0.430	0.456	0.467	0.459	0.455	0.459	0.396	0.405	0.432	0.500	0.548	0.448	0.514	0.427	0.507	0.421	0.484
Mn	0.018	0.018	0.013	0.023	0.022	0.014	0.023	0.021	0.019	0.019	0.020	0.022	0.024	0.022	0.027	0.019	0.029	0.021	0.020
Mg	2.160	2.156	2.194	2.164	2.163	2.237	2.178	2.248	2.099	2.136	2.159	2.070	2.044	2.157	2.014	2.220	1.935	2.154	2.161
Ca	0.365	0.349	0.380	0.402	0.419	0.386	0.403	0.354	0.533	0.473	0.437	0.417	0.398	0.408	0.498	0.353	0.521	0.447	0.345
Ni	0.000	0.000	0.000	0.000	0.000	0.000	0.000	0.000	0.000	0.000	0.001	0.000	0.000	0.000	0.000	0.000	0.000	0.001	0.000
Na	0.006	0.006	0.004	0.001	0.003	0.000	0.001	0.011	0.000	0.001	0.000	0.003	0.003	0.002	0.000	0.003	0.000	0.001	0.007
Total	8.000	8.005	8.007	8.017	8.032	8.032	8.029	8.037	8.020	8.007	8.009	8.009	8.010	8.014	8.023	8.009	7.997	8.016	7.994
Mg#	82.71	81.87	83.63	82.61	82.25	82.98	82.72	83.03	84.14	84.05	83.32	80.55	78.87	82.79	79.68	83.86	79.23	83.65	81.71

Table 2a.(continued)

Group	9	9	9	9	9	9	9	9	9	9	9	9	9	9	9	9	9	9	9
SiO_2	42.04	41.12	41.26	41.03	41.20	41.31	42.80	40.97	40.68	40.64	40.52	40.39	40.61	40.66	40.24	40.30	41.41	41.66	40.76
Al_2O_3	20.11	18.00	18.83	17.56	18.98	19.07	22.89	19.21	18.02	18.84	18.13	18.50	17.76	18.78	17.89	18.71	19.53	18.73	17.36
Cr_2O_3	3.39	6.36	5.39	7.17	5.51	5.66	2.75	5.84	6.87	5.39	6.08	6.31	7.55	6.31	7.21	5.95	4.93	6.04	7.61
TiO_2	0.06	0.19	0.15	0.15	0.00	0.00	0.18	0.30	0.23	0.36	0.23	0.30	0.21	0.24	0.22	0.40	0.25	0.38	0.20
FeO_T	7.41	7.14	7.51	7.37	8.63	8.04	7.60	6.95	7.26	7.76	7.64	8.60	7.01	7.10	6.94	6.93	7.17	6.58	6.86
MnO	0.29	0.30	0.33	0.37	0.43	0.42	0.35	0.27	0.27	0.27	0.26	0.38	0.33	0.27	0.32	0.32	0.36	0.32	0.36
MgO	20.19	19.37	19.33	18.86	17.82	17.79	21.34	20.33	19.63	19.53	20.01	18.11	19.37	20.14	19.65	19.82	20.53	20.30	19.94
CaO	4.92	5.32	5.13	5.92	6.05	6.14	4.33	5.40	5.80	5.76	5.77	6.05	5.76	5.37	6.23	5.59	5.12	5.67	6.22
NiO	0.00	0.00	0.00	0.00	0.00	0.00	0.00	0.01	0.00	0.00	0.00	0.00	0.00	0.00	0.00	0.00	0.00	0.01	0.00
Na_2O	0.00	0.01	0.03	0.01	0.00	0.00	0.03	0.05	0.03	0.03	0.02	0.05	0.05	0.00	0.01	0.06	0.06	0.08	0.07
Total	98.42	97.81	97.96	98.44	98.61	98.44	102.28	99.32	98.79	98.58	98.66	98.69	98.66	98.89	98.70	98.07	99.35	99.77	99.37
Si	3.047	3.033	3.032	3.025	3.032	3.037	2.973	2.972	2.985	2.982	2.978	2.984	2.987	2.969	2.962	2.967	2.993	3.005	2.982
Al	1.718	1.565	1.631	1.526	1.645	1.652	1.874	1.642	1.559	1.629	1.570	1.610	1.540	1.617	1.552	1.624	1.664	1.592	1.497
Cr	0.194	0.371	0.313	0.418	0.320	0.329	0.151	0.335	0.399	0.313	0.353	0.368	0.439	0.364	0.420	0.346	0.282	0.344	0.440
Ti	0.003	0.010	0.008	0.008	0.000	0.000	0.009	0.016	0.013	0.020	0.012	0.017	0.012	0.013	0.012	0.022	0.013	0.020	0.011
Fe^{2+}	0.449	0.440	0.462	0.454	0.531	0.494	0.442	0.421	0.445	0.476	0.469	0.531	0.431	0.434	0.427	0.427	0.433	0.397	0.420
Mn	0.018	0.019	0.020	0.023	0.027	0.026	0.021	0.017	0.017	0.017	0.016	0.024	0.020	0.017	0.020	0.020	0.022	0.020	0.022
Mg	2.181	2.130	2.117	2.073	1.954	1.950	2.211	2.198	2.147	2.137	2.193	1.994	2.124	2.192	2.156	2.175	2.213	2.183	2.175
Ca	0.382	0.421	0.404	0.467	0.477	0.484	0.322	0.419	0.456	0.452	0.454	0.479	0.454	0.420	0.491	0.441	0.396	0.438	0.488
Ni	0.000	0.000	0.000	0.000	0.000	0.000	0.000	0.000	0.000	0.000	0.000	0.000	0.000	0.000	0.000	0.000	0.000	0.001	0.000
Na	0.000	0.001	0.004	0.002	0.000	0.000	0.004	0.006	0.005	0.005	0.002	0.007	0.007	0.000	0.002	0.009	0.008	0.011	0.010
Total	7.993	7.990	7.990	7.996	7.986	7.972	8.007	8.027	8.026	8.030	8.049	8.014	8.015	8.027	8.041	8.031	8.025	8.012	8.043
Mg#	82.92	82.87	82.10	82.03	78.65	79.78	83.35	83.92	82.83	81.78	82.37	78.97	83.13	83.48	83.46	83.59	83.62	84.61	83.83

Table 2a.(continued)

Group	9	9	9	9	9	9	9	9	10	11	11	11	11	11	11	11	11	11	11
SiO_2	40.46	40.54	40.54	42.64	41.09	41.55	40.99	41.09	41.87	40.35	40.51	40.31	40.38	40.28	40.68	40.05	39.29	40.16	41.23
Al_2O_3	18.18	17.51	17.98	19.92	18.33	19.26	18.31	19.05	20.78	15.56	17.12	17.58	17.33	16.78	19.39	17.09	18.23	17.30	17.33
Cr_2O_3	6.35	6.85	6.35	5.01	6.41	5.26	6.53	5.87	4.88	9.52	8.49	7.95	7.95	8.28	4.47	7.41	6.36	7.23	7.77
TiO_2	0.20	0.37	0.34	0.39	0.31	0.32	0.31	0.37	0.01	0.55	0.28	0.23	0.14	0.52	0.54	0.43	0.45	0.48	0.30
FeO_T	7.05	6.78	6.95	7.52	7.21	7.10	7.18	7.51	7.34	7.28	6.35	6.96	6.94	6.87	8.23	7.56	9.18	7.10	7.12
MnO	0.32	0.32	0.34	0.33	0.32	0.30	0.36	0.37	0.39	0.37	0.36	0.36	0.31	0.34	0.32	0.38	0.38	0.30	0.33
MgO	20.38	20.48	20.27	19.50	19.38	20.22	19.60	19.53	21.95	19.48	20.05	20.04	19.67	19.00	18.83	19.31	16.84	18.97	19.93
CaO	5.58	5.61	5.85	5.62	6.01	5.27	5.96	5.76	2.35	6.67	5.94	6.19	5.99	6.22	6.12	6.15	7.65	6.16	6.03
NiO	0.00	0.00	0.00	0.01	0.00	0.00	0.01	0.01	0.02	0.00	0.00	0.00	0.00	0.00	0.00	0.00	0.00	0.00	0.00
Na_2O	0.05	0.07	0.05	0.10	0.00	0.00	0.00	0.00	0.00	0.02	0.03	0.05	0.03	0.05	0.02	0.01	0.00	0.04	0.04
Total	98.56	98.51	98.67	101.04	99.06	99.27	99.24	99.56	99.58	99.80	99.14	99.67	98.74	98.32	98.59	98.37	98.37	97.74	100.08
Si	2.970	2.980	2.975	3.031	3.002	3.007	2.991	2.984	2.991	2.972	2.970	2.947	2.975	2.986	2.985	2.971	2.941	2.988	2.994
Al	1.573	1.517	1.555	1.669	1.578	1.642	1.575	1.630	1.749	1.350	1.479	1.514	1.505	1.466	1.676	1.494	1.608	1.517	1.484
Cr	0.368	0.398	0.369	0.282	0.370	0.301	0.376	0.337	0.276	0.554	0.492	0.459	0.463	0.485	0.259	0.434	0.376	0.425	0.446
Ti	0.011	0.020	0.019	0.021	0.017	0.017	0.017	0.020	0.001	0.030	0.015	0.013	0.008	0.029	0.030	0.024	0.025	0.027	0.017
Fe^{2+}	0.433	0.417	0.427	0.447	0.440	0.429	0.438	0.456	0.438	0.448	0.389	0.426	0.427	0.426	0.505	0.469	0.575	0.442	0.432
Mn	0.020	0.020	0.021	0.020	0.020	0.019	0.022	0.023	0.024	0.023	0.023	0.022	0.019	0.021	0.020	0.024	0.024	0.019	0.020
Mg	2.230	2.244	2.217	2.067	2.110	2.181	2.132	2.114	2.337	2.139	2.191	2.184	2.161	2.099	2.060	2.135	1.879	2.104	2.158
Ca	0.439	0.441	0.460	0.428	0.470	0.408	0.466	0.448	0.180	0.527	0.467	0.485	0.473	0.494	0.481	0.489	0.613	0.491	0.469
Ni	0.000	0.000	0.000	0.001	0.000	0.000	0.000	0.001	0.001	0.000	0.000	0.000	0.000	0.000	0.000	0.000	0.000	0.000	0.000
Na	0.007	0.009	0.007	0.013	0.000	0.000	0.000	0.000	0.000	0.003	0.004	0.007	0.004	0.006	0.003	0.001	0.000	0.006	0.006
Total	8.051	8.047	8.048	7.979	8.007	8.005	8.017	8.013	7.996	8.047	8.031	8.057	8.035	8.013	8.019	8.041	8.042	8.018	8.027
Mg#	83.75	84.34	83.87	82.22	82.74	83.55	82.97	82.25	84.21	82.67	84.91	83.69	83.49	83.14	80.32	81.99	76.58	82.65	83.30

Table 2a.(continued)

Group	11	11	11	11	11	11	11	11	11
SiO_2	41.37	40.80	41.24	39.98	40.85	41.33	41.24	41.12	41.38
Al_2O_3	18.66	18.46	18.73	17.73	18.52	19.61	17.89	19.93	19.28
Cr_2O_3	5.95	5.83	5.77	4.81	4.41	4.82	7.00	4.35	4.30
TiO_2	0.42	0.41	0.44	0.85	0.68	0.49	0.42	0.50	0.49
FeO_T	6.59	6.63	6.61	9.00	8.38	7.67	6.90	7.59	7.40
MnO	0.30	0.32	0.29	0.37	0.31	0.35	0.34	0.35	0.31
MgO	20.88	20.98	20.84	17.35	19.88	19.77	19.57	19.89	19.57
CaO	5.64	5.67	5.61	8.61	6.04	5.64	6.02	5.34	5.20
NiO	0.00	0.02	0.00	0.00	0.00	0.00	0.00	0.00	0.00
Na_2O	0.06	0.06	0.08	0.10	0.04	0.02	0.00	0.05	0.05
Total	99.87	99.19	99.62	98.81	99.09	99.69	99.37	99.11	97.98
Si	2.983	2.967	2.981	2.974	2.987	2.987	3.005	2.983	3.029
Al	1.586	1.582	1.595	1.554	1.596	1.671	1.536	1.704	1.664
Cr	0.339	0.335	0.330	0.283	0.255	0.276	0.403	0.250	0.249
Ti	0.023	0.023	0.024	0.048	0.037	0.026	0.023	0.027	0.027
Fe^{2+}	0.397	0.403	0.399	0.560	0.512	0.463	0.420	0.460	0.453
Mn	0.019	0.020	0.018	0.023	0.019	0.021	0.021	0.021	0.019
Mg	2.245	2.275	2.245	1.924	2.168	2.130	2.125	2.150	2.136
Ca	0.436	0.441	0.435	0.686	0.473	0.437	0.470	0.415	0.408
Ni	0.000	0.001	0.000	0.000	0.000	0.000	0.000	0.000	0.000
Na	0.008	0.009	0.012	0.015	0.005	0.003	0.001	0.007	0.006
Total	8.036	8.056	8.038	8.067	8.053	8.014	8.003	8.017	7.991
Mg#	84.96	84.95	84.90	77.47	80.89	82.14	83.50	82.38	82.50

Table 2b: Microprobe analyses of Sputnik garnets (cations on basis of 12 oxygen).

Group	1	5	5	5	9	9	9	9	9	9	11	11	11	11
SiO_2	41.41	37.63	38.38	37.98	40.71	41.40	41.10	41.51	41.08	40.71	40.55	39.78	40.40	40.42
Al_2O_3	20.82	22.08	22.35	22.23	20.93	20.27	17.83	20.18	17.44	17.58	19.35	14.48	18.30	15.39
Cr_2O_3	2.53	0.07	0.06	0.08	3.67	3.99	7.00	4.56	7.44	7.35	4.20	11.37	5.11	10.40
TiO_2	0.51	0.08	0.06	0.06	0.06	0.30	0.08	0.16	0.32	0.38	0.47	0.15	0.77	0.15
FeO_T	8.80	34.43	32.80	34.65	10.70	7.93	7.06	7.04	7.46	7.16	8.64	7.57	9.08	7.03
MnO	0.32	1.13	0.80	1.10	0.54	0.33	0.39	0.33	0.30	0.37	0.35	0.39	0.47	0.39
MgO	19.58	5.80	7.03	5.69	17.07	19.86	19.41	21.06	19.71	19.43	17.61	18.13	16.74	18.68
CaO	5.20	0.98	0.88	0.93	6.41	5.25	6.29	4.92	5.95	5.84	8.42	7.63	8.54	6.77
NiO	0.02	0.04	0.06	0.08	0.02	0.00	0.03	0.02	0.02	0.05	0.02	0.03	0.02	0.01
Na_2O	0.04	0.06	0.01	0.01	0.05	0.08	0.02	0.07	0.07	0.07	0.05	0.05	0.07	0.04
Total	99.22	102.31	102.42	102.81	100.18	99.39	99.20	99.83	99.79	98.93	99.68	99.58	99.49	99.26
Si	2.997	2.932	2.952	2.942	2.967	2.992	3.006	2.979	2.994	2.990	2.969	2.969	2.983	2.995
Al	1.776	2.027	2.026	2.030	1.797	1.726	1.536	1.706	1.498	1.521	1.670	1.273	1.592	1.344
Cr	0.145	0.004	0.003	0.005	0.212	0.228	0.405	0.259	0.429	0.427	0.243	0.671	0.298	0.609
Ti	0.027	0.005	0.003	0.003	0.004	0.016	0.004	0.008	0.017	0.021	0.026	0.008	0.043	0.008
Fe^{2+}	0.533	2.243	2.110	2.245	0.652	0.479	0.432	0.422	0.455	0.439	0.529	0.472	0.560	0.435
Mn	0.020	0.075	0.052	0.072	0.033	0.020	0.024	0.020	0.019	0.023	0.022	0.025	0.029	0.025
Mg	2.112	0.674	0.806	0.657	1.855	2.140	2.116	2.253	2.142	2.127	1.922	2.017	1.842	2.064
Ca	0.403	0.082	0.073	0.077	0.500	0.406	0.493	0.378	0.465	0.460	0.661	0.610	0.675	0.537
Ni	0.001	0.003	0.004	0.005	0.001	0.000	0.002	0.001	0.001	0.003	0.001	0.002	0.001	0.001
Na	0.006	0.009	0.002	0.002	0.007	0.011	0.002	0.010	0.010	0.010	0.007	0.007	0.009	0.005
Total	8.019	8.052	8.031	8.038	8.029	8.019	8.020	8.035	8.030	8.020	8.052	8.054	8.034	8.023
Mg#	79.86	23.09	27.63	22.65	73.99	81.70	83.05	84.21	82.49	82.88	78.41	81.03	76.68	82.58

Mg# = $100Mg/(Mg+Fe^{2+})$
Groups according to Dawson and Stephens (1975).

Table 3a: Microprobe analyses of Torrie clinopyroxene (cations on basis of 6 oxygen).

	1	2	3	4	5	6	7	8	9	10	11	12	13	14	15	16	17	18	19	20
SiO_2	54.80	55.19	54.75	55.08	55.15	54.56	54.66	54.47	54.49	54.64	54.43	54.28	53.98	54.42	54.50	55.07	54.61	54.43	54.61	54.62
TiO_2	0.18	0.19	0.18	0.19	0.15	0.24	0.22	0.25	0.22	0.23	0.26	0.24	0.14	0.27	0.18	0.19	0.25	0.24	0.21	0.24
Al_2O_3	1.62	1.57	1.46	1.69	1.64	1.65	1.62	1.74	1.80	1.71	1.60	1.65	1.63	1.79	1.44	1.56	1.67	1.82	1.70	1.73
Cr_2O_3	1.08	0.90	0.96	0.64	0.87	0.80	1.12	0.90	0.58	0.70	0.86	1.12	1.02	1.10	0.76	0.92	0.88	0.93	0.64	0.89
FeOt	2.91	2.98	2.71	2.85	2.95	3.06	2.93	3.00	2.89	3.22	2.92	2.92	2.86	3.01	2.78	2.90	2.98	2.95	2.92	3.13
MnO	0.07	0.06	0.10	0.09	0.07	0.07	0.08	0.11	0.07	0.07	0.05	0.11	0.11	0.09	0.09	0.08	0.05	0.07	0.07	0.09
MgO	17.27	17.86	17.10	17.48	17.97	16.96	16.86	16.95	16.66	17.01	16.73	16.76	17.03	17.05	16.96	17.31	17.40	16.83	16.77	17.05
CaO	20.36	20.82	21.30	21.47	20.30	21.06	20.62	20.76	21.59	21.01	21.30	20.52	20.99	20.29	21.95	20.82	20.45	20.58	21.63	20.36
NiO	0.04	0.00	0.05	0.00	0.00	0.01	0.01	0.03	0.03	0.00	0.04	0.02	0.02	0.00	0.00	0.00	0.00	0.01	0.01	0.02
Na_2O	1.30	1.18	1.26	1.19	1.21	1.17	1.34	1.40	1.16	1.24	1.18	1.16	1.17	1.46	1.12	1.09	1.31	1.18	1.23	1.44
K_2O	0.05	0.06	0.06	0.05	0.07	0.04	0.04	0.05	0.04	0.05	0.04	0.04	0.04	0.05	0.06	0.05	0.05	0.05	0.05	0.06
Total	99.67	100.79	99.93	100.73	100.38	99.61	99.50	99.65	99.53	99.86	99.40	98.82	98.99	99.54	99.85	99.99	99.66	99.09	99.82	99.62
Si	1.988	1.981	1.985	1.980	1.985	1.984	1.989	1.981	1.984	1.983	1.985	1.988	1.977	1.980	1.981	1.991	1.982	1.987	1.983	1.985
Ti	0.005	0.005	0.005	0.005	0.004	0.006	0.006	0.007	0.006	0.006	0.007	0.007	0.004	0.007	0.005	0.005	0.007	0.007	0.006	0.007
Al	0.069	0.066	0.062	0.072	0.069	0.071	0.069	0.075	0.077	0.073	0.069	0.071	0.070	0.077	0.062	0.066	0.072	0.078	0.073	0.074
Cr	0.031	0.026	0.028	0.018	0.025	0.023	0.032	0.026	0.017	0.020	0.025	0.033	0.030	0.032	0.022	0.026	0.025	0.027	0.018	0.026
Fe^{2+}	0.088	0.090	0.082	0.086	0.089	0.093	0.089	0.091	0.088	0.098	0.089	0.090	0.088	0.092	0.085	0.088	0.091	0.090	0.089	0.095
Mn	0.002	0.002	0.003	0.003	0.002	0.002	0.003	0.003	0.002	0.002	0.002	0.003	0.003	0.003	0.003	0.003	0.002	0.002	0.002	0.003
Mg	0.934	0.956	0.924	0.937	0.964	0.920	0.915	0.919	0.904	0.920	0.909	0.915	0.930	0.925	0.919	0.933	0.942	0.916	0.908	0.924
Ca	0.791	0.801	0.828	0.827	0.783	0.821	0.804	0.809	0.842	0.817	0.832	0.805	0.824	0.791	0.855	0.807	0.796	0.805	0.842	0.793
Ni	0.001	0.000	0.002	0.000	0.000	0.000	0.000	0.001	0.001	0.000	0.001	0.001	0.001	0.000	0.000	0.000	0.000	0.000	0.000	0.001
Na	0.091	0.082	0.089	0.083	0.084	0.082	0.095	0.099	0.082	0.087	0.084	0.082	0.083	0.103	0.079	0.076	0.092	0.084	0.087	0.101
K	0.002	0.003	0.003	0.002	0.003	0.002	0.002	0.002	0.002	0.002	0.002	0.002	0.002	0.002	0.003	0.002	0.002	0.002	0.003	0.003
Total	4.004	4.010	4.010	4.013	4.008	4.005	4.003	4.012	4.005	4.009	4.004	3.996	4.012	4.011	4.013	3.997	4.010	3.997	4.010	4.011
Mg#	91.35	91.43	91.83	91.64	91.57	90.81	91.11	90.95	91.12	90.39	91.09	91.09	91.38	90.98	91.58	91.41	91.22	91.05	91.09	90.68
Ca#	0.46	0.46	0.47	0.47	0.45	0.47	0.47	0.47	0.48	0.47	0.48	0.47	0.47	0.46	0.48	0.46	0.46	0.47	0.48	0.46
Ca%	43.64	43.38	45.13	44.72	42.63	44.77	44.47	44.46	45.91	44.53	45.46	44.49	44.74	43.76	46.00	44.15	43.53	44.45	45.79	43.76
Mg%	51.49	51.77	50.39	50.65	52.53	50.16	50.59	50.52	49.29	50.14	49.68	50.56	50.49	51.17	49.45	51.05	51.52	50.58	49.38	50.99
Fe%	4.87	4.85	4.48	4.62	4.84	5.08	4.93	5.02	4.80	5.33	4.86	4.95	4.76	5.07	4.55	4.80	4.96	4.97	4.83	5.24

$Mg\# = 100Mg/(Mg+Fe^{2+})$; $Ca\# = Ca/(Ca+Mg)$

Table 3a. (continued)

	21	22	23	24	25	26	27	28	29	30	31	32	33	34	35	36	37	38	39	40
SiO_2	54.60	54.51	54.71	54.43	54.36	54.84	54.67	54.50	54.78	54.62	54.70	55.19	54.64	54.55	54.54	54.73	53.91	54.67	54.34	54.65
TiO_2	0.23	0.19	0.19	0.21	0.21	0.21	0.22	0.22	0.30	0.22	0.30	0.25	0.27	0.27	0.28	0.22	0.22	0.26	0.26	0.20
Al_2O_3	1.78	1.67	1.60	1.63	1.75	1.61	1.70	1.84	1.91	1.63	1.69	1.62	1.84	1.74	1.72	1.67	1.92	1.82	1.91	1.63
Cr_2O_3	0.62	0.70	1.10	0.91	0.89	0.96	0.69	0.54	0.84	0.75	0.88	0.84	0.68	0.82	0.87	1.16	0.57	0.87	0.53	1.07
$FeOt$	2.73	2.86	2.81	2.91	3.03	2.85	2.79	2.89	3.03	2.95	2.79	3.01	2.95	3.01	2.84	2.90	3.12	3.06	3.00	2.94
MnO	0.06	0.07	0.09	0.08	0.09	0.08	0.07	0.07	0.09	0.08	0.05	0.10	0.06	0.07	0.10	0.09	0.08	0.08	0.06	0.06
MgO	16.73	16.63	17.01	16.75	16.88	16.93	17.04	16.47	16.51	17.14	16.79	17.21	16.50	16.65	16.79	17.21	16.72	16.55	16.95	17.30
CaO	21.54	21.63	20.60	20.57	20.81	20.80	21.70	21.49	20.54	21.38	21.18	20.73	21.21	20.90	21.16	20.29	20.77	20.44	21.25	20.37
NiO	0.00	0.00	0.01	0.04	0.00	0.00	0.02	0.03	0.01	0.03	0.04	0.03	0.03	0.00	0.02	0.03	0.02	0.06	0.04	0.02
Na_2O	1.07	1.25	1.27	1.25	1.31	1.20	1.15	1.31	1.42	1.09	1.15	1.10	1.18	1.34	1.25	1.27	1.19	1.35	1.27	1.22
K_2O	0.04	0.05	0.05	0.04	0.05	0.06	0.06	0.05	0.05	0.05	0.07	0.05	0.06	0.07	0.06	0.07	0.06	0.06	0.04	0.07
Total	99.42	99.56	99.42	98.81	99.39	99.54	100.10	99.39	99.49	99.94	99.63	100.11	99.39	99.41	99.62	99.62	98.56	99.21	99.65	99.52
Si	1.987	1.985	1.990	1.992	1.982	1.992	1.980	1.987	1.992	1.981	1.987	1.992	1.990	1.987	1.983	1.987	1.981	1.993	1.977	1.986
Ti	0.006	0.005	0.005	0.006	0.006	0.006	0.006	0.006	0.008	0.006	0.008	0.007	0.007	0.007	0.008	0.006	0.006	0.007	0.007	0.006
Al	0.077	0.072	0.068	0.070	0.075	0.069	0.073	0.079	0.082	0.070	0.072	0.069	0.079	0.075	0.074	0.071	0.083	0.078	0.082	0.070
Cr	0.018	0.020	0.032	0.026	0.026	0.028	0.020	0.016	0.024	0.021	0.025	0.024	0.020	0.024	0.025	0.033	0.017	0.025	0.015	0.031
Fe^{2+}	0.083	0.087	0.085	0.089	0.093	0.087	0.085	0.088	0.092	0.090	0.085	0.091	0.090	0.092	0.086	0.088	0.096	0.093	0.091	0.089
Mn	0.002	0.002	0.003	0.002	0.003	0.003	0.002	0.002	0.003	0.003	0.002	0.003	0.002	0.002	0.003	0.003	0.003	0.003	0.002	0.002
Mg	0.908	0.903	0.922	0.914	0.917	0.917	0.920	0.895	0.895	0.927	0.909	0.926	0.896	0.904	0.910	0.931	0.916	0.899	0.919	0.937
Ca	0.840	0.844	0.803	0.807	0.813	0.810	0.842	0.840	0.800	0.831	0.824	0.802	0.828	0.816	0.825	0.789	0.818	0.799	0.828	0.793
Ni	0.000	0.000	0.000	0.001	0.000	0.000	0.001	0.001	0.000	0.001	0.001	0.001	0.001	0.000	0.001	0.001	0.001	0.002	0.001	0.001
Na	0.076	0.088	0.089	0.088	0.093	0.084	0.081	0.092	0.100	0.077	0.081	0.077	0.083	0.095	0.088	0.089	0.085	0.095	0.090	0.086
K	0.002	0.002	0.003	0.002	0.002	0.003	0.003	0.002	0.003	0.002	0.003	0.002	0.003	0.003	0.003	0.003	0.003	0.003	0.002	0.003
Total	3.998	4.009	4.001	3.999	4.009	3.997	4.010	4.007	3.999	4.007	3.998	3.994	3.997	4.005	4.005	4.001	4.007	3.997	4.014	4.003
Mg#	91.61	91.19	91.53	91.13	90.84	91.36	91.59	91.05	90.66	91.18	91.47	91.08	90.88	90.80	91.34	91.38	90.53	90.60	90.98	91.29
Ca#	0.48	0.48	0.47	0.47	0.47	0.47	0.48	0.48	0.47	0.47	0.48	0.46	0.48	0.47	0.48	0.46	0.47	0.47	0.47	0.46
Ca%	45.89	46.03	44.35	44.58	44.60	44.64	45.60	46.07	44.78	44.98	45.34	44.08	45.65	45.03	45.28	43.64	44.70	44.58	45.05	43.59
Mg%	49.57	49.22	50.94	50.51	50.33	50.58	49.82	49.10	50.06	50.17	50.00	50.93	49.39	49.91	49.98	51.50	50.07	50.21	49.99	51.50
Fe%	4.54	4.75	4.71	4.92	5.07	4.78	4.58	4.83	5.16	4.85	4.66	4.99	4.96	5.06	4.74	4.86	5.24	5.21	4.96	4.91

Table 3a. (continued)

	41	42	43	44	45	46	47	48	49	50	51	52	53	54	55	56	57	58	59
SiO_2	54.25	54.36	54.34	54.89	54.58	54.13	54.44	54.20	54.71	55.05	55.24	54.63	54.77	54.61	54.67	54.42	54.71	54.69	54.72
TiO_2	0.22	0.22	0.17	0.18	0.22	0.04	0.16	0.21	0.16	0.24	0.07	0.19	0.19	0.20	0.12	0.20	0.17	0.18	0.19
Al_2O_3	1.51	1.78	1.13	1.47	1.63	2.53	1.32	2.24	1.65	1.85	1.26	1.70	1.72	1.79	1.28	1.71	1.81	1.26	1.61
Cr_2O_3	0.73	0.82	0.61	1.01	0.79	0.88	0.64	1.54	0.48	1.13	1.25	0.92	0.84	1.00	0.58	0.78	0.72	0.52	0.54
FeOt	2.70	2.92	2.81	2.83	2.79	1.77	2.97	3.10	3.17	3.05	3.19	2.99	3.06	3.08	3.01	2.82	3.17	2.82	2.81
MnO	0.06	0.06	0.06	0.12	0.04	0.07	0.10	0.09	0.10	0.09	0.11	0.09	0.07	0.06	0.08	0.07	0.09	0.09	0.08
MgO	16.96	17.06	17.07	17.33	16.96	17.82	16.68	16.56	16.91	17.01	19.41	16.93	16.71	16.55	16.81	16.89	17.07	16.68	16.91
CaO	21.44	20.92	21.95	21.03	21.57	22.38	21.97	19.92	21.66	19.64	18.14	21.10	20.93	20.47	22.29	21.68	20.51	22.17	22.09
NiO	0.00	0.05	0.00	0.02	0.06	0.05	0.03	0.02	0.05	0.01	0.07	0.00	0.03	0.05	0.03	0.00	0.00	0.01	0.00
Na_2O	1.13	1.20	0.93	1.18	1.22	0.41	0.99	1.68	1.17	1.43	1.08	1.23	1.26	1.54	1.01	1.22	1.30	1.02	1.03
K_2O	0.06	0.05	0.05	0.06	0.05	0.06	0.06	0.07	0.05	0.07	0.08	0.06	0.06	0.05	0.07	0.05	0.06	0.04	0.05
Total	99.05	99.45	99.11	100.10	99.91	100.12	99.36	99.61	100.11	99.57	99.89	99.84	99.63	99.41	99.96	99.83	99.60	99.45	100.02
Si	1.984	1.980	1.989	1.986	1.981	1.952	1.989	1.973	1.983	1.995	1.990	1.983	1.990	1.990	1.987	1.977	1.987	1.994	1.984
Ti	0.006	0.006	0.005	0.005	0.006	0.001	0.004	0.006	0.004	0.007	0.002	0.005	0.005	0.005	0.003	0.005	0.005	0.005	0.005
Al	0.065	0.076	0.049	0.063	0.070	0.107	0.057	0.096	0.071	0.079	0.054	0.073	0.074	0.077	0.055	0.073	0.078	0.054	0.069
Cr	0.021	0.024	0.018	0.029	0.023	0.025	0.019	0.044	0.014	0.032	0.036	0.026	0.024	0.029	0.017	0.022	0.021	0.015	0.016
Fe^{2+}	0.083	0.089	0.086	0.086	0.085	0.053	0.091	0.094	0.096	0.093	0.096	0.091	0.093	0.094	0.092	0.086	0.096	0.086	0.085
Mn	0.002	0.002	0.002	0.004	0.001	0.002	0.003	0.003	0.003	0.003	0.003	0.003	0.002	0.002	0.003	0.002	0.003	0.003	0.002
Mg	0.925	0.926	0.931	0.934	0.917	0.958	0.909	0.898	0.914	0.919	1.042	0.916	0.905	0.899	0.911	0.915	0.924	0.907	0.914
Ca	0.840	0.816	0.861	0.815	0.839	0.865	0.860	0.777	0.841	0.763	0.700	0.821	0.815	0.799	0.868	0.844	0.799	0.866	0.858
Ni	0.000	0.002	0.000	0.000	0.002	0.002	0.001	0.001	0.001	0.000	0.002	0.000	0.001	0.001	0.001	0.000	0.000	0.000	0.000
Na	0.080	0.085	0.066	0.083	0.086	0.029	0.070	0.118	0.082	0.100	0.075	0.086	0.089	0.109	0.072	0.086	0.091	0.072	0.073
K	0.003	0.003	0.002	0.003	0.003	0.003	0.003	0.003	0.003	0.003	0.004	0.003	0.003	0.003	0.003	0.002	0.003	0.002	0.002
Total	4.008	4.008	4.008	4.007	4.011	3.996	4.005	4.013	4.012	3.994	4.003	4.007	4.001	4.008	4.011	4.014	4.006	4.004	4.007
Mg#	91.81	91.25	91.55	91.61	91.54	94.73	90.91	90.50	90.49	90.86	91.57	90.99	90.68	90.54	90.86	91.44	90.56	91.34	91.49
Ca#	0.48	0.47	0.48	0.47	0.48	0.47	0.49	0.46	0.48	0.45	0.40	0.47	0.47	0.47	0.49	0.48	0.46	0.49	0.48
Ca%	45.48	44.57	45.84	44.42	45.56	46.09	46.26	43.89	45.44	42.99	38.08	44.91	44.93	44.60	46.41	45.76	43.90	46.61	46.21
Mg%	50.05	50.58	49.58	50.92	49.83	51.07	48.85	50.78	49.37	51.80	56.70	50.13	49.93	50.16	48.69	49.60	50.81	48.77	49.21
Fe%	4.47	4.85	4.58	4.66	4.61	2.84	4.88	5.33	5.19	5.21	5.22	4.96	5.13	5.24	4.90	4.65	5.29	4.62	4.58

Table 3a. (continued)

	60	61	62	63	64	65	66	67	68	69	70	71	72	73	74	75	76	77	78	79
SiO_2	54.85	54.84	54.62	54.74	54.97	54.47	54.22	54.53	54.44	54.67	54.36	54.83	54.62	55.28	54.93	54.73	54.47	54.68	55.01	54.46
TiO_2	0.10	0.14	0.18	0.19	0.18	0.16	0.15	0.18	0.18	0.13	0.17	0.11	0.18	0.08	0.15	0.17	0.23	0.18	0.18	0.20
Al_2O_3	1.57	1.89	1.87	1.63	1.83	1.54	1.26	1.75	1.34	1.28	1.30	1.65	1.26	1.56	1.27	1.66	1.93	1.31	1.59	1.85
Cr_2O_3	0.79	0.97	0.58	0.94	0.58	0.65	0.57	1.17	0.66	0.62	0.62	1.21	0.62	0.88	0.66	0.99	0.69	0.64	1.05	0.63
FeOt	3.15	3.07	3.11	3.01	2.92	2.94	2.88	2.93	2.93	2.87	2.89	2.91	2.92	3.04	2.86	2.82	3.13	2.98	2.92	3.11
MnO	0.12	0.10	0.07	0.08	0.08	0.09	0.09	0.09	0.09	0.07	0.09	0.10	0.08	0.13	0.11	0.09	0.08	0.10	0.10	0.10
MgO	18.28	17.10	16.57	17.02	16.98	16.68	16.67	16.72	16.06	16.11	16.14	17.64	16.27	18.04	16.55	16.91	16.18	16.70	16.72	16.19
CaO	19.59	20.30	20.99	20.77	21.35	21.41	22.21	20.22	22.08	22.03	21.96	19.24	21.88	19.49	21.61	20.57	21.01	22.17	20.45	21.26
NiO	0.02	0.00	0.00	0.04	0.00	0.00	0.00	0.01	0.00	0.00	0.00	0.06	0.00	0.05	0.00	0.00	0.00	0.00	0.01	0.00
Na_2O	1.20	1.50	1.30	1.18	1.15	1.16	1.09	1.46	0.96	1.03	1.13	1.29	1.02	1.06	1.02	1.23	1.24	1.00	1.25	1.23
K_2O	0.06	0.06	0.06	0.05	0.05	0.05	0.05	0.06	0.06	0.05	0.05	0.07	0.04	0.07	0.04	0.07	0.05	0.04	0.05	0.05
Total	99.74	99.97	99.35	99.65	100.09	99.15	99.20	99.13	98.79	98.86	98.72	99.10	98.88	99.69	99.21	99.23	99.00	99.78	99.32	99.10
Si	1.985	1.985	1.990	1.989	1.987	1.991	1.986	1.990	1.999	2.004	1.998	1.995	2.002	1.998	2.004	1.993	1.992	1.989	2.001	1.991
Ti	0.003	0.004	0.005	0.005	0.005	0.004	0.004	0.005	0.005	0.004	0.005	0.003	0.005	0.002	0.004	0.005	0.006	0.005	0.005	0.006
Al	0.067	0.081	0.080	0.070	0.078	0.066	0.055	0.075	0.058	0.055	0.056	0.071	0.054	0.067	0.055	0.071	0.083	0.056	0.068	0.080
Cr	0.023	0.028	0.017	0.027	0.017	0.019	0.017	0.034	0.019	0.018	0.018	0.035	0.018	0.025	0.019	0.029	0.020	0.018	0.030	0.018
Fe^{2+}	0.095	0.093	0.095	0.091	0.088	0.090	0.088	0.090	0.090	0.088	0.089	0.089	0.090	0.092	0.087	0.086	0.096	0.091	0.089	0.095
Mn	0.004	0.003	0.002	0.003	0.002	0.003	0.003	0.003	0.003	0.002	0.003	0.003	0.002	0.004	0.003	0.003	0.003	0.003	0.003	0.003
Mg	0.986	0.923	0.900	0.921	0.915	0.909	0.910	0.910	0.879	0.881	0.884	0.957	0.889	0.972	0.900	0.918	0.882	0.906	0.906	0.883
Ca	0.760	0.787	0.819	0.809	0.827	0.838	0.872	0.791	0.869	0.865	0.865	0.750	0.859	0.755	0.845	0.803	0.823	0.864	0.797	0.833
Ni	0.001	0.000	0.000	0.001	0.000	0.000	0.000	0.000	0.000	0.000	0.000	0.002	0.000	0.002	0.000	0.000	0.000	0.000	0.000	0.000
Na	0.084	0.105	0.092	0.083	0.081	0.082	0.077	0.103	0.068	0.073	0.081	0.091	0.073	0.075	0.072	0.087	0.088	0.070	0.088	0.088
K	0.003	0.003	0.003	0.002	0.002	0.002	0.002	0.003	0.003	0.002	0.002	0.003	0.002	0.003	0.002	0.003	0.003	0.002	0.003	0.003
Total	4.011	4.011	4.003	4.001	4.002	4.004	4.014	4.004	3.993	3.993	4.001	3.997	3.994	3.993	3.992	3.997	3.995	4.005	3.990	3.999
Mg#	91.20	90.85	90.48	90.98	91.22	91.00	91.18	91.03	90.71	90.91	90.86	91.51	90.84	91.37	91.16	91.45	90.21	90.91	91.09	90.26
Ca#	0.44	0.46	0.48	0.47	0.47	0.48	0.49	0.47	0.50	0.50	0.49	0.44	0.49	0.44	0.48	0.47	0.48	0.49	0.47	0.49
Ca%	41.26	43.66	45.16	44.39	45.19	45.63	46.61	44.17	47.26	47.19	47.05	41.78	46.76	41.50	46.10	44.44	45.72	46.44	44.47	46.00
Mg%	53.57	51.19	49.62	50.59	49.99	49.47	48.68	50.82	47.84	48.01	48.11	53.28	48.36	53.45	49.13	50.81	48.97	48.69	50.58	48.74
Fe%	5.17	5.15	5.22	5.02	4.81	4.89	4.71	5.01	4.90	4.80	4.84	4.94	4.88	5.05	4.76	4.75	5.31	4.87	4.95	5.26

Table 3a. (continued)

	80	81	82	83	84	85	86	87	88	89	90	91	92	93	94	95	96
SiO_2	54.64	51.66	51.16	54.77	54.85	55.67	55.70	55.95	55.97	55.80	55.77	55.73	56.11	55.51	56.31	55.84	55.65
TiO_2	0.17	0.24	0.29	0.30	0.29	0.28	0.20	0.22	0.24	0.22	0.18	0.26	0.26	0.28	0.15	0.23	0.24
Al_2O_3	1.24	2.03	1.94	1.98	1.39	1.81	1.50	1.58	1.66	1.52	1.57	1.56	1.86	1.92	1.46	1.61	1.67
Cr_2O_3	0.65	0.02	0.07	0.65	0.76	0.71	1.17	1.06	0.65	0.63	1.00	0.87	1.08	1.13	0.88	0.76	0.78
FeOt	2.90	11.42	13.81	2.55	2.68	2.78	2.92	2.90	2.82	2.77	2.65	2.83	3.08	3.14	2.88	2.85	2.79
MnO	0.11	0.34	0.38	0.15	0.12	0.08	0.11	0.09	0.08	0.09	0.09	0.06	0.08	0.08	0.10	0.10	0.08
MgO	16.34	11.64	10.80	16.95	17.19	17.27	17.91	17.71	17.10	17.14	17.07	17.04	17.37	16.72	18.43	17.49	17.11
CaO	22.15	21.52	20.91	20.61	21.67	20.85	19.49	20.15	21.14	21.39	20.98	20.96	19.54	20.28	19.55	20.89	21.11
NiO	0.00	0.02	0.09	0.08	0.10	0.00	0.01	0.02	0.01	0.00	0.00	0.00	0.01	0.00	0.00	0.00	0.00
Na_2O	1.04	0.44	0.48	1.46	1.13	1.14	1.20	1.13	1.01	1.08	1.14	0.99	1.44	1.33	0.97	1.14	1.06
K_2O	0.05	0.02	0.04	0.06	0.07	0.05	0.07	0.06	0.05	0.05	0.06	0.05	0.06	0.07	0.07	0.05	0.06
Total	99.28	99.35	99.98	99.56	100.23	100.62	100.29	100.85	100.73	100.69	100.51	100.34	100.87	100.45	100.81	100.96	100.53
Si	1.997	1.962	1.953	1.987	1.984	1.995	2.000	1.999	2.004	2.001	2.002	2.004	2.003	1.996	2.007	1.996	1.998
Ti	0.005	0.007	0.008	0.008	0.008	0.008	0.006	0.006	0.007	0.006	0.005	0.007	0.007	0.008	0.004	0.006	0.006
Al	0.054	0.091	0.087	0.085	0.059	0.076	0.063	0.067	0.070	0.064	0.067	0.066	0.078	0.081	0.061	0.068	0.071
Cr	0.019	0.001	0.002	0.019	0.022	0.020	0.033	0.030	0.018	0.018	0.029	0.025	0.031	0.032	0.025	0.021	0.022
Fe^{2+}	0.089	0.363	0.441	0.077	0.081	0.083	0.088	0.087	0.084	0.083	0.080	0.085	0.092	0.095	0.086	0.085	0.084
Mn	0.003	0.011	0.012	0.005	0.004	0.003	0.003	0.003	0.003	0.003	0.003	0.002	0.002	0.003	0.003	0.003	0.002
Mg	0.890	0.659	0.615	0.916	0.927	0.923	0.959	0.943	0.913	0.916	0.913	0.913	0.924	0.896	0.979	0.932	0.916
Ca	0.867	0.876	0.855	0.801	0.840	0.801	0.750	0.772	0.811	0.822	0.807	0.807	0.747	0.781	0.747	0.800	0.812
Ni	0.000	0.001	0.003	0.003	0.003	0.000	0.000	0.001	0.000	0.000	0.000	0.000	0.000	0.000	0.000	0.000	0.000
Na	0.074	0.033	0.035	0.103	0.079	0.079	0.084	0.078	0.070	0.075	0.079	0.069	0.100	0.093	0.067	0.079	0.074
K	0.002	0.491	0.003	0.046	0.037	0.002	0.003	0.003	0.002	0.002	0.003	0.002	0.003	0.003	0.003	0.002	0.003
Total	4.000	4.242	4.006	3.934	3.869	3.990	3.990	3.987	3.982	3.991	3.987	3.980	3.987	3.988	3.981	3.994	3.988
Mg#	90.94	64.50	58.22	92.22	91.96	91.72	91.63	91.58	91.54	91.69	91.98	91.50	90.96	90.46	91.93	91.62	91.62
Ca#	0.49	0.57	0.58	0.47	0.48	0.46	0.44	0.45	0.47	0.47	0.47	0.47	0.45	0.47	0.43	0.46	0.47
Ca%	46.98	46.16	44.75	44.64	45.46	44.32	41.74	42.82	44.86	45.12	44.83	44.71	42.39	44.09	41.21	44.03	44.83
Mg%	48.22	34.73	32.17	51.06	50.16	51.07	53.38	52.36	50.48	50.32	50.74	50.59	52.41	50.58	54.05	51.28	50.55
Fe%	4.80	19.12	23.08	4.31	4.38	4.61	4.88	4.81	4.66	4.56	4.42	4.70	5.21	5.33	4.74	4.69	4.62

Table 3a. (continued)

	97	98	99	100	101	102	103	104	105	106	107	108	109	110	111	112	113
SiO_2	55.67	55.52	55.70	55.61	55.60	55.59	55.80	55.71	55.59	55.69	55.80	56.01	55.81	55.91	55.73	55.90	54.73
TiO_2	0.22	0.21	0.26	0.29	0.29	0.24	0.19	0.26	0.23	0.19	0.18	0.13	0.19	0.20	0.24	0.24	0.19
Al_2O_3	1.66	1.66	1.64	1.60	1.65	1.60	1.53	1.65	1.54	1.48	1.56	1.33	1.51	1.45	1.52	1.60	1.63
Cr_2O_3	0.72	0.61	0.80	0.73	1.05	0.84	1.03	0.81	0.72	0.67	0.70	0.87	1.11	0.94	0.85	0.99	0.78
FeOt	2.81	2.79	3.04	2.86	3.00	3.06	2.72	2.97	2.93	2.64	2.72	2.98	2.86	3.04	2.91	2.92	2.72
MnO	0.07	0.09	0.10	0.07	0.09	0.07	0.09	0.06	0.07	0.08	0.08	0.09	0.08	0.07	0.05	0.09	0.10
MgO	17.25	17.05	16.86	16.98	17.39	17.46	17.58	17.20	17.26	17.21	17.19	18.87	17.61	17.69	17.40	17.39	17.18
CaO	20.78	21.24	20.73	21.11	19.80	19.76	20.50	20.13	20.85	21.21	21.46	19.47	20.19	20.34	20.82	19.95	21.06
NiO	0.00	0.00	0.00	0.00	0.00	0.00	0.01	0.02	0.05	0.05	0.07	0.09	0.06	0.06	0.04	0.09	0.00
Na_2O	1.12	1.07	1.08	1.05	1.20	1.10	1.05	1.10	1.09	1.03	1.05	0.98	1.18	1.13	1.09	1.27	1.12
K_2O	0.04	0.05	0.06	0.05	0.07	0.05	0.08	0.04	0.05	0.04	0.07	0.08	0.06	0.06	0.06	0.05	0.07
Total	100.34	100.28	100.26	100.35	100.13	99.77	100.58	99.96	100.36	100.31	100.86	100.89	100.65	100.89	100.70	100.47	99.57
Si	2.001	1.999	2.005	2.000	2.001	2.006	2.000	2.007	2.000	2.003	1.999	1.998	2.000	2.000	1.998	2.005	1.988
Ti	0.006	0.006	0.007	0.008	0.008	0.007	0.005	0.007	0.006	0.005	0.005	0.003	0.005	0.005	0.006	0.006	0.005
Al	0.070	0.071	0.070	0.068	0.070	0.068	0.065	0.070	0.065	0.063	0.066	0.056	0.064	0.061	0.064	0.067	0.070
Cr	0.021	0.017	0.023	0.021	0.030	0.024	0.029	0.023	0.021	0.019	0.020	0.025	0.031	0.027	0.024	0.028	0.022
Fe^{2+}	0.085	0.084	0.091	0.086	0.090	0.092	0.082	0.090	0.088	0.079	0.081	0.089	0.086	0.091	0.087	0.088	0.083
Mn	0.002	0.003	0.003	0.002	0.003	0.002	0.003	0.002	0.002	0.003	0.002	0.003	0.002	0.002	0.002	0.003	0.003
Mg	0.924	0.915	0.905	0.911	0.933	0.939	0.939	0.924	0.925	0.923	0.918	1.003	0.941	0.943	0.930	0.930	0.930
Ca	0.800	0.820	0.800	0.814	0.764	0.764	0.787	0.777	0.804	0.818	0.824	0.744	0.775	0.780	0.800	0.767	0.820
Ni	0.000	0.000	0.000	0.000	0.000	0.000	0.000	0.001	0.001	0.002	0.002	0.003	0.002	0.002	0.001	0.003	0.000
Na	0.078	0.075	0.075	0.073	0.084	0.077	0.073	0.077	0.076	0.072	0.073	0.068	0.082	0.079	0.075	0.089	0.079
K	0.002	0.002	0.003	0.002	0.003	0.003	0.003	0.002	0.002	0.002	0.003	0.004	0.003	0.003	0.003	0.002	0.003
Total	3.988	3.990	3.981	3.985	3.985	3.981	3.986	3.979	3.990	3.988	3.992	3.994	3.990	3.992	3.991	3.986	4.002
Mg#	91.62	91.59	90.82	91.37	91.18	91.05	92.01	91.16	91.32	92.08	91.85	91.87	91.66	91.20	91.43	91.38	91.85
Ca#	0.46	0.47	0.47	0.47	0.45	0.45	0.46	0.46	0.46	0.47	0.47	0.43	0.45	0.45	0.46	0.45	0.47
Ca%	44.24	45.07	44.53	44.95	42.74	42.54	43.55	43.41	44.24	44.93	45.18	40.53	43.03	42.98	44.02	42.97	44.73
Mg%	51.09	50.31	50.38	50.30	52.21	52.32	51.94	51.59	50.92	50.71	50.35	54.64	52.21	52.00	51.18	52.12	50.76
Fe%	4.67	4.62	5.09	4.75	5.05	5.14	4.51	5.00	4.84	4.36	4.47	4.84	4.75	5.02	4.80	4.92	4.50

Table 3a. (continued)

	114	115	116	117	118	119	120	121	122	123	124	125	126	127	128	129	130	131	132	133
SiO_2	52.06	54.85	55.07	55.03	55.36	55.16	54.85	55.23	54.70	55.07	55.09	55.26	55.09	55.01	55.07	54.91	54.96	51.24	54.98	54.46
TiO_2	0.16	0.18	0.22	0.24	0.08	0.21	0.24	0.23	0.25	0.27	0.22	0.27	0.20	0.14	0.19	0.24	0.24	0.31	0.22	0.22
Al_2O_3	1.55	1.93	1.49	1.60	1.43	1.63	1.66	1.69	1.68	1.81	1.65	1.70	1.67	1.12	1.64	1.70	1.56	3.27	1.66	1.80
Cr_2O_3	0.50	0.58	0.96	0.71	0.96	1.10	0.81	1.01	1.07	1.03	1.11	2.46	0.99	0.52	0.83	0.94	0.77	0.06	0.67	0.59
FeOt	2.45	2.92	2.82	2.89	2.97	2.78	2.82	2.74	2.94	3.00	2.85	2.14	2.98	2.70	3.03	2.83	2.93	12.44	2.88	2.79
MnO	0.04	0.10	0.12	0.11	0.11	0.06	0.08	0.08	0.09	0.11	0.09	0.10	0.09	0.10	0.11	0.08	0.09	0.26	0.10	0.06
MgO	17.06	17.00	17.73	17.29	18.47	17.35	17.12	16.77	16.96	17.05	16.92	16.81	16.85	16.83	17.23	16.81	17.12	10.21	16.10	15.84
CaO	19.12	21.38	20.52	20.50	18.64	19.74	20.28	20.45	20.32	19.14	19.71	18.54	20.19	21.77	19.92	20.42	20.36	21.11	20.99	21.21
NiO	0.00	0.00	0.01	0.03	0.09	0.00	0.03	0.02	0.03	0.02	0.03	0.03	0.03	0.02	0.01	0.01	0.00	0.00	0.02	0.00
Na_2O	1.17	1.15	1.16	1.05	1.05	1.24	1.08	1.12	1.15	1.39	1.15	1.68	1.26	0.91	1.07	1.08	1.11	0.97	1.28	1.23
K_2O	0.04	0.02	0.05	0.05	0.07	0.06	0.05	0.08	0.07	0.06	0.08	0.06	0.08	0.05	0.05	0.07	0.06	0.01	0.03	0.04
Total	94.17	100.12	100.15	99.49	99.23	99.33	99.03	99.42	99.24	98.95	98.89	99.06	99.43	99.16	99.14	99.08	99.20	99.89	98.93	98.23
Si	1.991	1.983	1.987	1.996	2.004	2.000	1.998	2.003	1.992	2.004	2.007	2.005	2.001	2.007	2.002	2.000	1.999	1.943	2.008	2.004
Ti	0.005	0.005	0.006	0.006	0.002	0.006	0.007	0.006	0.007	0.007	0.006	0.007	0.006	0.004	0.005	0.007	0.007	0.009	0.006	0.006
Al	0.070	0.082	0.064	0.068	0.061	0.070	0.071	0.072	0.072	0.078	0.071	0.073	0.071	0.048	0.070	0.073	0.067	0.146	0.071	0.078
Cr	0.015	0.017	0.027	0.020	0.028	0.032	0.023	0.029	0.031	0.030	0.032	0.071	0.028	0.015	0.024	0.027	0.022	0.002	0.019	0.017
Fe^{2+}	0.078	0.088	0.085	0.088	0.090	0.084	0.086	0.083	0.089	0.091	0.087	0.065	0.091	0.082	0.092	0.086	0.089	0.395	0.088	0.086
Mn	0.001	0.003	0.004	0.003	0.003	0.002	0.003	0.002	0.003	0.003	0.003	0.003	0.003	0.003	0.003	0.002	0.003	0.008	0.003	0.002
Mg	0.973	0.916	0.954	0.935	0.997	0.938	0.929	0.907	0.921	0.925	0.919	0.910	0.912	0.915	0.934	0.912	0.929	0.577	0.877	0.869
Ca	0.784	0.828	0.793	0.797	0.723	0.767	0.792	0.795	0.793	0.746	0.769	0.721	0.786	0.851	0.776	0.797	0.794	0.858	0.822	0.836
Ni	0.000	0.000	0.000	0.001	0.003	0.000	0.001	0.001	0.001	0.001	0.001	0.001	0.001	0.000	0.000	0.000	0.000	0.000	0.001	0.000
Na	0.087	0.081	0.081	0.074	0.074	0.087	0.076	0.079	0.081	0.098	0.081	0.119	0.089	0.064	0.076	0.076	0.078	0.071	0.091	0.088
K	0.002	0.001	0.002	0.002	0.003	0.003	0.002	0.004	0.003	0.003	0.004	0.003	0.004	0.002	0.002	0.003	0.003	0.001	0.001	0.002
Total	4.006	4.004	4.003	3.991	3.988	3.988	3.988	3.981	3.992	3.985	3.978	3.977	3.990	3.992	3.985	3.983	3.990	4.010	3.987	3.987
Mg#	92.54	91.22	91.82	91.41	91.73	91.75	91.53	91.60	91.15	91.02	91.38	93.33	90.97	91.76	91.03	91.37	91.23	59.40	90.88	91.02
Ca#	0.45	0.47	0.45	0.46	0.42	0.45	0.46	0.47	0.46	0.45	0.46	0.44	0.46	0.48	0.45	0.47	0.46	0.60	0.48	0.49
Ca%	42.71	45.20	43.30	43.80	39.96	42.87	43.81	44.52	43.97	42.34	43.34	42.51	43.93	46.05	43.06	44.39	43.81	46.89	46.00	46.70
Mg%	53.02	49.99	52.06	51.38	55.08	52.42	51.43	50.82	51.07	52.48	51.77	53.65	51.01	49.50	51.83	50.81	51.26	31.55	49.08	48.51
Fe%	4.27	4.81	4.64	4.83	4.97	4.71	4.76	4.66	4.96	5.18	4.89	3.83	5.06	4.45	5.11	4.80	4.93	21.56	4.93	4.79

Table 3a. (continued)

	134	135	136	137	138	139	140	141	142	143	144	145	146	147
SiO_2	55.63	55.61	55.86	55.59	55.95	56.01	55.68	55.45	55.80	55.68	55.95	55.50	55.70	55.09
TiO_2	0.22	0.22	0.24	0.22	0.07	0.26	0.18	0.24	0.12	0.23	0.09	0.22	0.16	0.21
Al_2O_3	1.37	0.99	1.46	1.51	1.43	1.44	1.40	1.68	1.19	1.62	1.43	1.50	0.92	1.62
Cr_2O_3	1.11	0.68	0.86	0.83	1.10	1.12	0.77	0.74	0.89	0.93	1.68	0.61	0.55	0.98
FeOt	2.57	2.69	2.90	2.95	2.69	2.79	2.77	2.93	2.67	2.94	2.39	2.65	2.76	2.89
MnO	0.08	0.06	0.07	0.09	0.09	0.10	0.08	0.07	0.07	0.10	0.06	0.07	0.08	0.10
MgO	17.41	17.10	17.52	17.33	18.14	17.58	17.25	17.11	17.32	17.55	18.00	17.24	16.24	16.44
CaO	20.24	21.60	20.60	20.46	19.54	20.01	21.14	20.97	21.18	20.23	19.22	21.40	21.83	20.48
NiO	0.04	0.02	0.05	0.03	0.08	0.04	0.04	0.03	0.03	0.06	0.12	0.05	0.01	0.04
Na_2O	1.19	0.92	1.07	1.05	1.16	1.16	1.03	1.19	1.06	1.31	1.52	0.94	0.83	1.08
K_2O	0.06	0.05	0.06	0.06	0.07	0.06	0.05	0.05	0.04	0.05	0.07	0.06	0.03	0.06
Total	99.91	99.93	100.68	100.11	100.31	100.56	100.38	100.47	100.38	100.70	100.52	100.23	99.12	98.99
Si	2.006	2.010	2.001	2.003	2.006	2.006	2.003	1.995	2.007	1.996	2.003	1.999	2.029	2.008
Ti	0.006	0.006	0.007	0.006	0.002	0.007	0.005	0.007	0.003	0.006	0.002	0.006	0.005	0.006
Al	0.058	0.042	0.062	0.064	0.061	0.061	0.059	0.071	0.051	0.069	0.060	0.064	0.039	0.070
Cr	0.032	0.019	0.024	0.024	0.031	0.032	0.022	0.021	0.025	0.027	0.048	0.017	0.016	0.028
Fe^{2+}	0.078	0.081	0.087	0.089	0.081	0.083	0.083	0.088	0.080	0.088	0.072	0.080	0.084	0.088
Mn	0.002	0.002	0.002	0.003	0.003	0.003	0.002	0.002	0.002	0.003	0.002	0.002	0.003	0.003
Mg	0.936	0.922	0.936	0.931	0.969	0.939	0.925	0.917	0.928	0.938	0.960	0.926	0.882	0.894
Ca	0.782	0.837	0.791	0.790	0.751	0.768	0.815	0.808	0.816	0.777	0.737	0.826	0.852	0.800
Ni	0.001	0.001	0.001	0.001	0.002	0.001	0.001	0.001	0.001	0.002	0.003	0.001	0.000	0.001
Na	0.083	0.064	0.074	0.073	0.080	0.080	0.072	0.083	0.074	0.091	0.106	0.066	0.059	0.077
K	0.003	0.002	0.003	0.003	0.003	0.003	0.003	0.002	0.002	0.002	0.003	0.003	0.002	0.003
Total	3.986	3.986	3.987	3.985	3.988	3.983	3.989	3.995	3.990	3.998	3.996	3.989	3.969	3.977
Mg#	92.34	91.89	91.50	91.28	92.31	91.84	91.75	91.25	92.03	91.40	93.06	92.06	91.28	91.03
Ca#	0.46	0.48	0.46	0.46	0.44	0.45	0.47	0.47	0.47	0.45	0.43	0.47	0.49	0.47
Ca%	43.56	45.47	43.61	43.65	41.69	42.90	44.69	44.56	44.73	43.09	41.67	45.09	46.87	44.91
Mg%	52.12	50.10	51.60	51.44	53.83	52.44	50.75	50.58	50.87	52.02	54.28	50.55	48.50	50.15
Fe%	4.32	4.42	4.79	4.91	4.48	4.66	4.56	4.85	4.41	4.89	4.05	4.36	4.63	4.94

Table 3b: Microprobe analyses of Sputnik clinopyroxene (cations on basis of 6 oxygen).

	1	2	3	4	5	6	7	8	9	10	11	12	13	14	15	16	17
SiO_2	55.01	54.89	54.97	54.97	54.82	54.95	55.05	55.19	54.93	54.81	54.65	54.77	54.95	54.83	54.81	54.77	54.73
TiO_2	0.22	0.06	0.20	0.23	0.22	0.24	0.04	0.18	0.25	0.23	0.20	0.23	0.11	0.23	0.19	0.27	0.26
Al_2O_3	1.66	1.57	1.67	1.58	1.63	1.69	2.20	1.36	1.66	1.58	1.65	1.55	0.53	1.65	1.59	1.77	1.70
Cr_2O_3	0.63	1.07	1.03	0.65	0.96	0.99	0.30	0.88	0.98	1.07	0.85	0.75	2.02	0.81	1.05	1.18	0.84
FeO_T	2.85	2.79	2.98	2.80	2.98	3.11	4.23	2.77	3.06	2.79	3.07	3.11	1.91	2.89	2.81	2.90	2.84
MnO	0.10	0.09	0.09	0.08	0.09	0.07	0.06	0.10	0.07	0.07	0.08	0.08	0.04	0.07	0.08	0.09	0.06
MgO	16.99	17.81	16.84	17.16	17.33	17.23	15.54	16.77	17.48	17.05	17.44	17.40	16.81	17.20	17.34	17.37	16.96
CaO	20.23	18.80	20.09	20.73	19.29	19.26	20.55	20.75	19.48	19.99	20.09	20.17	21.47	19.90	19.91	19.51	20.46
NiO	0.02	0.07	0.01	0.02	0.01	0.03	0.07	0.03	0.03	0.06	0.01	0.03	0.04	0.03	0.03	0.04	0.02
Na_2O	1.10	1.16	1.14	1.13	1.28	1.31	1.36	1.12	1.28	1.11	1.18	1.11	1.26	1.21	1.11	1.36	1.06
K_2O	0.05	0.06	0.07	0.06	0.07	0.06	0.02	0.06	0.05	0.07	0.06	0.05	0.04	0.07	0.06	0.05	0.08
Total	98.85	98.38	99.08	99.40	98.68	98.95	99.43	99.20	99.26	98.81	99.28	99.25	99.17	98.88	98.98	99.31	99.02
Si	2.005	2.005	2.002	1.997	2.001	2.001	2.007	2.008	1.995	2.000	1.989	1.993	2.006	1.999	1.997	1.990	1.995
Ti	0.006	0.002	0.006	0.006	0.006	0.007	0.001	0.005	0.007	0.006	0.005	0.006	0.003	0.006	0.005	0.008	0.007
Al	0.072	0.068	0.072	0.068	0.070	0.073	0.095	0.058	0.071	0.068	0.071	0.067	0.023	0.071	0.068	0.076	0.073
Cr	0.018	0.031	0.030	0.019	0.028	0.029	0.009	0.025	0.028	0.031	0.024	0.022	0.058	0.023	0.030	0.034	0.024
Fe^{2+}	0.087	0.085	0.091	0.085	0.091	0.095	0.129	0.084	0.093	0.085	0.093	0.095	0.058	0.088	0.086	0.088	0.087
Mn	0.003	0.003	0.003	0.002	0.003	0.002	0.002	0.003	0.002	0.002	0.003	0.002	0.001	0.002	0.003	0.003	0.002
Mg	0.923	0.970	0.914	0.929	0.943	0.936	0.845	0.910	0.947	0.927	0.946	0.944	0.915	0.935	0.942	0.941	0.922
Ca	0.790	0.736	0.784	0.807	0.754	0.752	0.803	0.809	0.758	0.782	0.783	0.787	0.840	0.777	0.777	0.759	0.799
Ni	0.001	0.002	0.000	0.001	0.000	0.001	0.002	0.001	0.001	0.002	0.000	0.001	0.001	0.001	0.001	0.001	0.001
Na	0.078	0.082	0.081	0.080	0.091	0.093	0.096	0.079	0.090	0.079	0.083	0.079	0.089	0.086	0.078	0.096	0.075
K	0.002	0.003	0.003	0.003	0.003	0.003	0.001	0.003	0.003	0.003	0.003	0.002	0.002	0.003	0.003	0.002	0.004
Total	3.984	3.986	3.984	3.995	3.990	3.989	3.989	3.986	3.994	3.985	4.001	3.997	3.996	3.992	3.990	3.997	3.988
Mg#	91.40	91.93	90.98	91.62	91.20	90.81	86.76	91.53	91.07	91.60	91.01	90.89	94.01	91.38	91.66	91.44	91.40
Ca/(Ca+Mg)	0.46	0.43	0.46	0.46	0.44	0.45	0.49	0.47	0.44	0.46	0.45	0.45	0.48	0.45	0.45	0.45	0.46
Ca%	43.90	41.08	43.82	44.30	42.19	42.18	45.20	44.87	42.17	43.57	42.97	43.10	46.32	43.18	43.06	42.47	44.21
Mg%	51.28	54.16	51.11	51.03	52.73	52.51	47.55	50.46	52.66	51.69	51.90	51.72	50.47	51.92	52.19	52.61	50.99
Fe%	4.82	4.76	5.07	4.67	5.09	5.31	7.26	4.67	5.16	4.74	5.12	5.18	3.22	4.90	4.75	4.93	4.80

Mg# = $100Mg/(Mg+Fe^{2+})$; Ca# = Ca/(Ca+Mg)

Table 3b. (continued)

	megacryst 18					megacryst 19			
	core	mid-1	mid-2	mid-3	rim	core	mid-1	mid-2	rim
SiO_2	53.57	54.02	53.74	53.62	54.09	54.04	53.54	53.60	54.11
TiO_2	0.19	0.20	0.24	0.25	0.26	0.25	0.21	0.20	0.19
Al_2O_3	1.58	1.52	1.57	1.62	1.57	1.54	1.56	1.58	1.56
Cr_2O_3	0.99	0.89	0.97	1.01	0.91	0.96	0.96	0.94	0.99
FeO_T	2.78	2.72	2.70	2.81	2.79	2.76	2.73	2.84	2.77
MnO	0.06	0.07	0.07	0.06	0.08	0.09	0.09	0.07	0.08
MgO	18.49	18.37	18.36	18.35	18.15	18.28	18.18	18.01	18.51
CaO	20.88	20.93	20.71	20.69	20.69	20.78	20.82	20.48	20.61
NiO	0.07	0.03	0.02	0.06	0.05	0.06	0.02	0.04	0.03
Na_2O	1.28	1.37	1.36	1.33	1.35	1.38	1.36	1.37	1.34
K_2O	0.07	0.07	0.04	0.05	0.05	0.06	0.06	0.07	0.07
Total	99.94	100.18	99.78	99.84	99.99	100.18	99.51	99.19	100.25
Si	1.948	1.957	1.954	1.950	1.962	1.958	1.954	1.961	1.958
Ti	0.005	0.005	0.006	0.007	0.007	0.007	0.006	0.006	0.005
Al	0.068	0.065	0.067	0.069	0.067	0.066	0.067	0.068	0.066
Cr	0.028	0.026	0.028	0.029	0.026	0.028	0.028	0.027	0.028
Fe^{2+}	0.085	0.083	0.082	0.086	0.085	0.084	0.083	0.087	0.084
Mn	0.002	0.002	0.002	0.002	0.003	0.003	0.003	0.002	0.003
Mg	1.002	0.992	0.995	0.995	0.981	0.987	0.989	0.982	0.998
Ca	0.813	0.812	0.807	0.806	0.804	0.807	0.814	0.803	0.799
Ni	0.002	0.001	0.001	0.002	0.002	0.002	0.001	0.001	0.001
Na	0.090	0.096	0.096	0.094	0.095	0.097	0.096	0.097	0.094
K	0.003	0.003	0.002	0.002	0.003	0.003	0.003	0.003	0.003
Total	4.046	4.042	4.041	4.042	4.033	4.039	4.042	4.036	4.038
Mg#	92.22	92.32	92.38	92.09	92.05	92.20	92.24	91.89	92.26
Ca/(Ca+Mg)	0.45	0.45	0.45	0.45	0.45	0.45	0.45	0.45	0.44
Ca%	42.80	43.06	42.83	42.73	43.01	42.97	43.16	42.89	42.48
Mg%	52.75	52.57	52.82	52.74	52.46	52.58	52.43	52.47	53.07
Fe%	4.45	4.37	4.36	4.53	4.53	4.45	4.41	4.63	4.45

Table 3c: Microprobe analyses of Eddie clinopyroxene (cations on basis of 6 oxygen).

	megacryst 1				
	core	mid-1	mid-2	mid-3	rim
SiO_2	54.74	54.26	54.40	54.42	54.46
TiO_2	0.18	0.22	0.18	0.24	0.24
Al_2O_3	1.56	1.62	1.55	1.57	1.57
Cr_2O_3	0.95	0.96	0.90	0.86	0.85
FeO_T	2.89	2.89	2.95	2.93	2.95
MnO	0.04	0.05	0.06	0.09	0.07
MgO	18.67	18.77	18.90	18.71	18.83
CaO	20.60	20.50	20.98	20.65	20.81
NiO	0.04	0.01	0.04	0.05	0.01
Na_2O	1.31	1.25	1.31	1.33	1.33
K_2O	0.06	0.06	0.05	0.05	0.05
Total	101.03	100.58	101.31	100.89	101.18
Si	1.963	1.955	1.950	1.957	1.953
Ti	0.005	0.006	0.005	0.006	0.006
Al	0.066	0.069	0.066	0.066	0.067
Cr	0.027	0.027	0.025	0.025	0.024
Fe^{2+}	0.087	0.087	0.089	0.088	0.088
Mn	0.001	0.001	0.002	0.003	0.002
Mg	0.998	1.008	1.010	1.003	1.007
Ca	0.792	0.792	0.806	0.795	0.800
Ni	0.001	0.000	0.001	0.001	0.000
Na	0.091	0.087	0.091	0.093	0.093
K	0.003	0.003	0.002	0.002	0.002
Total	4.033	4.036	4.046	4.039	4.043
Mg#	92.01	92.04	91.93	91.92	91.93
Ca/(Ca+Mg)	0.44	0.44	0.44	0.44	0.44
Ca%	42.19	41.96	42.32	42.17	42.20
Mg%	53.19	53.42	53.02	53.16	53.13
Fe%	4.62	4.62	4.65	4.67	4.67

$Mg\# = 100Mg/(Mg+Fe^{2+})$; $Ca\# = Ca/(Ca+Mg)$

Table 4a: Microprobe analyses of Torrie orthopyroxene (cations on basis of 6 oxygen).

	1	2	3	4	5	6	7	8	9	10	11	12	13
SiO_2	55.00	56.77	57.01	58.87	58.43	58.60	56.37	57.33	55.96	57.19	58.14	58.06	57.15
TiO_2	0.06	0.00	0.02	0.07	0.05	0.10	0.02	0.11	0.00	0.04	0.02	0.09	0.00
Al_2O_3	1.78	2.60	2.67	0.60	0.63	0.52	2.99	0.56	3.28	0.65	0.51	0.60	2.06
Cr_2O_3	0.00	0.57	0.60	0.25	0.21	0.34	0.54	0.33	0.63	0.33	0.22	0.30	0.37
FeOt	16.36	4.69	4.78	5.43	5.16	4.27	4.38	5.60	4.40	5.18	4.11	3.91	4.52
MnO	0.14	0.13	0.10	0.11	0.11	0.08	0.10	0.11	0.09	0.14	0.13	0.08	0.11
MgO	26.80	33.10	33.60	34.02	34.08	34.79	35.92	35.85	35.31	35.36	36.44	36.38	34.55
CaO	0.23	0.68	0.46	0.77	0.82	0.46	0.48	0.60	0.59	0.80	0.22	0.56	0.30
NiO	0.02	0.04	0.05	0.01	0.08	0.07	0.02	0.10	0.07	0.08	0.02	0.09	0.02
Na_2O	0.00	0.04	0.03	0.11	0.07	0.12	0.04	0.12	0.06	0.14	0.04	0.11	0.06
Total	100.42	98.63	99.30	100.25	99.66	99.36	100.84	100.71	100.40	99.91	99.84	100.17	99.14
Si	1.973	1.969	1.964	2.013	2.009	2.011	1.916	1.963	1.912	1.970	1.986	1.979	1.969
Ti	0.002	0.000	0.000	0.002	0.001	0.003	0.000	0.003	0.000	0.001	0.001	0.002	0.000
Al	0.075	0.106	0.109	0.024	0.026	0.021	0.120	0.022	0.132	0.026	0.021	0.024	0.083
Cr	0.000	0.016	0.016	0.007	0.006	0.009	0.015	0.009	0.017	0.009	0.006	0.008	0.010
Fe^{2+}	0.491	0.136	0.138	0.155	0.148	0.123	0.124	0.160	0.126	0.149	0.117	0.112	0.130
Mn	0.004	0.004	0.003	0.003	0.003	0.002	0.003	0.003	0.003	0.004	0.004	0.002	0.003
Mg	1.433	1.712	1.725	1.734	1.747	1.780	1.820	1.830	1.799	1.815	1.856	1.849	1.775
Ca	0.009	0.025	0.017	0.028	0.030	0.017	0.017	0.022	0.022	0.030	0.008	0.020	0.011
Ni	0.001	0.001	0.001	0.000	0.002	0.002	0.000	0.003	0.002	0.002	0.001	0.002	0.000
Na	0.000	0.003	0.002	0.008	0.005	0.008	0.003	0.008	0.004	0.009	0.003	0.007	0.004
Total	3.989	3.972	3.975	3.974	3.977	3.975	4.018	4.023	4.016	4.016	4.001	4.006	3.986
Mg#	74.49	92.63	92.61	91.78	92.17	93.56	93.62	91.96	93.45	92.41	94.07	94.29	93.18
Ca%	0.47	1.35	0.89	1.48	1.56	0.88	0.88	0.88	0.88	0.88	0.88	0.88	0.88
Mg%	74.14	91.39	91.78	90.43	90.74	92.73	92.73	92.73	92.73	92.73	92.73	92.73	92.73
Fe%	25.39	7.27	7.33	8.09	7.70	6.39	6.39	6.39	6.39	6.39	6.39	6.39	6.39

Table 4b: Microprobe analyses of Sputnik orthopyroxene (cations on basis of 6 oxygen).

	1	2	3	4	5	6	7	8	9	10	11	12	13
SiO_2	57.07	57.24	57.13	57.10	56.88	57.14	56.32	57.40	57.36	57.24	57.52	57.14	57.47
TiO_2	0.00	0.06	0.01	0.05	0.01	0.03	0.12	0.00	0.00	0.09	0.06	0.00	0.07
Al_2O_3	1.70	0.61	1.59	0.54	2.19	0.66	0.65	1.25	1.20	0.62	0.63	1.73	0.60
Cr_2O_3	0.37	0.48	0.49	0.27	0.40	0.25	0.25	0.35	0.49	0.30	0.37	0.54	0.41
FeOt	4.58	5.09	4.06	5.34	4.50	5.21	5.76	4.36	4.44	4.42	4.74	4.37	5.08
MnO	0.11	0.11	0.12	0.13	0.12	0.14	0.14	0.12	0.12	0.11	0.12	0.10	0.11
MgO	35.53	34.66	35.23	34.42	34.71	34.18	33.60	35.78	35.45	35.09	34.94	35.69	34.75
CaO	0.21	0.87	1.12	0.54	0.37	0.90	0.77	0.34	0.70	0.57	0.94	0.20	0.77
NiO	0.04	0.12	0.05	0.05	0.02	0.05	0.07	0.00	0.01	0.04	0.07	0.01	0.08
Na_2O	0.01	0.14	0.05	0.14	0.00	0.08	0.10	0.02	0.10	0.16	0.10	0.00	0.15
Total	99.60	99.37	99.85	98.58	99.18	98.63	97.77	99.62	99.87	98.63	99.48	99.78	99.48
Si	1.960	1.981	1.959	1.990	1.960	1.990	1.985	1.969	1.967	1.986	1.984	1.958	1.984
Ti	0.000	0.002	0.000	0.001	0.000	0.001	0.003	0.000	0.000	0.002	0.001	0.000	0.002
Al	0.069	0.025	0.064	0.022	0.089	0.027	0.027	0.051	0.048	0.025	0.026	0.070	0.025
Cr	0.010	0.013	0.013	0.007	0.011	0.007	0.007	0.010	0.013	0.008	0.010	0.015	0.011
Fe^{2+}	0.131	0.147	0.117	0.156	0.130	0.152	0.170	0.125	0.127	0.128	0.137	0.125	0.147
Mn	0.003	0.003	0.003	0.004	0.003	0.004	0.004	0.003	0.004	0.003	0.003	0.003	0.003
Mg	1.819	1.788	1.801	1.788	1.783	1.774	1.765	1.830	1.813	1.815	1.796	1.823	1.789
Ca	0.008	0.032	0.041	0.020	0.014	0.034	0.029	0.013	0.026	0.021	0.035	0.007	0.028
Ni	0.001	0.003	0.001	0.001	0.001	0.001	0.002	0.000	0.000	0.001	0.002	0.000	0.002
Na	0.001	0.010	0.003	0.009	0.000	0.006	0.007	0.001	0.006	0.011	0.006	0.000	0.010
Total	4.001	4.004	4.003	3.999	3.990	3.995	3.999	4.002	4.005	4.001	4.000	4.000	4.001
Mg#	93.28	92.40	93.90	91.98	93.20	92.11	91.21	93.61	93.45	93.41	92.91	93.58	92.41
Ca%	0.88	0.88	0.88	0.88	0.88	0.88	0.88	0.88	0.88	0.88	0.88	0.88	0.88
Mg%	92.73	92.73	92.73	92.73	92.73	92.73	92.73	92.73	92.73	92.73	92.73	92.73	92.73
Fe%	6.39	6.39	6.39	6.39	6.39	6.39	6.39	6.39	6.39	6.39	6.39	6.39	6.39

Table 5: Microprobe analyses of Eddie phlogopites (cations on basis of 22 oxygen).

	1	2	3	4	5	6	7	8	9	10	11	12	13	14	15	16	17	18
SiO_2	41.04	39.04	36.97	35.26	35.84	36.18	36.81	36.91	36.64	38.04	37.56	36.40	37.78	35.45	36.12	40.51	35.76	37.16
TiO_2	0.67	1.89	1.87	2.58	2.34	1.74	1.76	1.54	1.34	1.38	1.48	1.67	1.68	2.00	1.68	1.52	1.48	1.68
Al_2O_3	6.99	15.97	15.44	16.44	15.96	14.90	16.56	14.81	15.13	14.55	14.89	14.82	14.33	16.21	15.22	12.20	17.88	15.53
FeO_T	10.22	5.37	5.08	6.26	6.35	4.81	4.61	5.37	5.49	5.76	5.76	6.00	5.44	5.09	4.93	3.81	6.04	4.75
MnO	0.05	0.03	0.05	0.06	0.06	0.05	0.06	0.05	0.05	0.05	0.05	0.06	0.05	0.06	0.06	0.03	0.07	0.04
MgO	24.89	22.93	22.71	21.21	21.53	22.74	24.03	22.27	22.04	22.64	22.30	21.72	22.43	21.93	21.73	23.84	20.36	22.03
CaO	0.15	0.07	0.03	0.25	0.14	0.14	0.17	0.04	0.07	0.07	0.08	0.12	0.13	0.11	0.08	0.35	0.30	0.24
Na_2O	0.03	0.09	0.13	0.19	0.17	0.09	0.11	0.12	0.18	0.12	0.13	0.11	0.13	0.18	0.20	0.07	0.21	0.21
K_2O	9.10	9.76	10.28	9.09	9.63	10.29	9.56	10.36	10.41	10.45	10.31	10.23	10.15	10.03	10.34	10.30	9.62	10.13
BaO	0.07	1.13	1.03	1.68	1.47	1.59	2.81	0.78	0.84	0.68	0.67	0.84	0.73	1.56	1.10	0.32	0.96	0.99
Cr_2O_3	0.41	0.00	0.00	0.14	0.12	0.00	0.00	0.96	0.81	0.54	1.01	0.50	0.04	0.28	0.88	0.63	0.13	0.99
NiO	0.08	0.00	0.02	0.02	0.05	0.02	0.02	0.04	0.02	0.06	0.03	0.05	0.02	0.04	0.04	0.10	0.03	0.06
F	0.53	0.21	0.19	0.15	0.15	0.14	0.24	0.15	0.15	0.15	0.14	0.11	0.17	0.13	0.18	0.26	0.19	0.17
Cl	0.00	0.00	0.00	0.05	0.02	0.01	0.04	0.02	0.03	0.00	0.00	0.01	0.01	0.01	0.03	0.02	0.02	0.01
Total	93.99	96.39	93.71	93.30	93.77	92.63	96.68	93.37	93.12	94.42	94.36	92.58	93.00	93.03	92.49	93.83	92.98	93.91
Si	6.113	5.553	5.447	5.261	5.324	5.425	5.301	5.475	5.457	5.568	5.506	5.460	5.597	5.297	5.420	5.880	5.314	5.461
Ti	0.075	0.202	0.207	0.289	0.262	0.196	0.191	0.172	0.150	0.152	0.164	0.188	0.187	0.225	0.190	0.165	0.165	0.185
Al	1.228	2.677	2.681	2.891	2.795	2.633	2.811	2.590	2.656	2.510	2.574	2.619	2.501	2.854	2.692	2.087	3.133	2.691
Fe^{2+}	1.273	0.638	0.625	0.782	0.788	0.603	0.555	0.666	0.684	0.705	0.706	0.752	0.674	0.636	0.618	0.462	0.751	0.584
Mn	0.006	0.003	0.006	0.007	0.008	0.006	0.008	0.007	0.006	0.006	0.006	0.007	0.006	0.007	0.008	0.004	0.009	0.005
Mg	5.526	4.861	4.989	4.717	4.768	5.083	5.157	4.924	4.892	4.941	4.874	4.857	4.952	4.886	4.861	5.158	4.511	4.828
Ca	0.023	0.010	0.005	0.040	0.023	0.022	0.027	0.007	0.012	0.010	0.012	0.020	0.020	0.017	0.013	0.054	0.047	0.037
Na	0.007	0.026	0.037	0.054	0.048	0.027	0.032	0.035	0.051	0.033	0.038	0.032	0.036	0.053	0.057	0.021	0.059	0.059
K	1.729	1.770	1.932	1.730	1.824	1.969	1.756	1.961	1.977	1.952	1.928	1.958	1.918	1.912	1.979	1.907	1.824	1.900
Ba	0.004	0.063	0.059	0.098	0.086	0.094	0.158	0.045	0.049	0.039	0.039	0.049	0.042	0.091	0.065	0.018	0.056	0.057
Cr	0.049	0.000	0.000	0.017	0.015	0.000	0.000	0.113	0.096	0.063	0.117	0.059	0.005	0.033	0.104	0.072	0.016	0.115
Ni	0.010	0.000	0.002	0.002	0.005	0.002	0.002	0.005	0.002	0.007	0.004	0.006	0.002	0.005	0.004	0.011	0.003	0.007
F	0.249	0.095	0.090	0.068	0.072	0.065	0.110	0.071	0.072	0.067	0.064	0.052	0.079	0.062	0.086	0.117	0.091	0.080
Cl	0.001	0.000	0.000	0.013	0.005	0.002	0.009	0.005	0.007	0.000	0.001	0.003	0.002	0.002	0.007	0.004	0.006	0.003
Total	16.292	15.899	16.081	15.970	16.023	16.127	16.116	16.076	16.111	16.053	16.033	16.063	16.022	16.082	16.103	15.961	15.986	16.014
Mg#	81.28	88.39	88.86	85.79	85.81	89.39	90.29	88.09	87.73	87.51	87.35	86.59	88.01	88.48	88.72	91.78	85.72	89.21

Mg# = 100Mg/ (Mg+Fe^{2+})

Table 5. (continued)

	19	20	21	22	23	24	25	26	27	28	29	30	31	32	kinked 33	kinked 34
SiO_2	38.02	37.58	37.95	35.91	36.71	36.02	37.21	36.42	36.34	36.94	41.77	41.99	40.64	40.32	40.08	39.76
TiO_2	1.49	1.37	1.30	1.50	1.53	2.27	1.53	1.90	1.92	1.88	2.79	2.91	0.87	0.87	1.79	1.59
Al_2O_3	14.44	14.78	13.99	15.44	15.56	17.00	14.73	16.37	16.79	16.11	12.22	12.39	11.82	11.93	14.95	14.49
FeO_T	5.97	5.83	6.37	5.32	5.42	5.41	5.10	4.81	4.99	4.92	4.18	4.08	4.69	4.83	7.72	7.70
MnO	0.06	0.08	0.05	0.07	0.06	0.04	0.06	0.07	0.04	0.05	0.03	0.02	0.03	0.04	0.02	0.01
MgO	21.99	22.06	22.23	21.38	21.98	21.87	21.92	21.98	21.47	22.32	20.95	20.88	24.15	24.09	20.68	20.35
CaO	0.16	0.09	0.14	0.10	0.12	0.08	0.19	0.11	0.21	0.11	0.41	0.39	0.10	0.06	0.20	0.10
Na_2O	0.21	0.16	0.18	0.22	0.11	0.14	0.16	0.16	0.11	0.19	0.26	0.21	0.06	0.04	0.23	0.24
K_2O	10.41	10.43	10.72	10.39	10.21	10.35	10.75	10.55	10.18	10.18	10.13	9.99	10.10	10.56	10.49	10.52
BaO	0.48	0.74	0.72	1.15	1.43	1.90	0.76	1.35	1.50	1.42	0.16	0.16	0.06	0.09	0.12	0.12
Cr_2O_3	0.43	0.81	0.27	0.67	0.55	0.13	1.08	0.42	0.31	0.30	2.18	2.16	0.31	0.29	0.52	0.57
NiO	0.05	0.09	0.08	0.06	0.03	0.05	0.05	0.03	0.06	0.04	0.14	0.15	0.15	0.14	0.10	0.15
F	0.17	0.13	0.18	0.11	0.17	0.14	0.14	0.13	0.13	0.14	0.16	0.19	0.26	0.23	1.33	1.30
Cl	0.02	0.00	0.04	0.36	0.03	0.00	0.00	0.05	0.14	0.02	0.07	0.04	0.07	0.07	0.10	0.10
Total	93.83	94.10	94.13	92.55	93.83	95.32	93.61	94.27	94.08	94.55	95.38	95.47	93.19	93.45	97.73	96.42
Si	5.599	5.534	5.606	5.411	5.436	5.268	5.509	5.359	5.356	5.404	5.967	5.977	5.939	5.899	5.709	5.746
Ti	0.165	0.152	0.145	0.170	0.171	0.250	0.170	0.210	0.213	0.207	0.300	0.312	0.096	0.096	0.191	0.173
Al	2.507	2.565	2.436	2.743	2.716	2.930	2.571	2.838	2.916	2.779	2.057	2.079	2.035	2.058	2.510	2.469
Fe^{2+}	0.735	0.718	0.787	0.670	0.671	0.661	0.631	0.591	0.615	0.601	0.499	0.485	0.573	0.591	0.919	0.931
Mn	0.008	0.010	0.007	0.009	0.007	0.005	0.008	0.008	0.005	0.006	0.004	0.003	0.004	0.005	0.002	0.001
Mg	4.827	4.841	4.895	4.802	4.853	4.769	4.839	4.821	4.717	4.869	4.461	4.431	5.261	5.253	4.391	4.385
Ca	0.025	0.013	0.022	0.016	0.018	0.012	0.029	0.017	0.032	0.018	0.063	0.060	0.016	0.010	0.030	0.015
Na	0.059	0.046	0.051	0.063	0.032	0.039	0.046	0.045	0.031	0.053	0.071	0.058	0.018	0.013	0.064	0.067
K	1.955	1.960	2.020	1.997	1.929	1.932	2.031	1.981	1.915	1.900	1.846	1.814	1.883	1.971	1.907	1.939
Ba	0.028	0.043	0.042	0.068	0.083	0.109	0.044	0.078	0.086	0.081	0.009	0.009	0.003	0.005	0.007	0.007
Cr	0.050	0.094	0.032	0.080	0.064	0.015	0.126	0.049	0.036	0.034	0.246	0.243	0.036	0.034	0.059	0.065
Ni	0.006	0.011	0.010	0.008	0.004	0.005	0.006	0.004	0.007	0.005	0.016	0.017	0.018	0.017	0.011	0.017
F	0.077	0.060	0.084	0.054	0.079	0.064	0.066	0.059	0.061	0.067	0.072	0.085	0.122	0.106	0.601	0.595
Cl	0.006	0.000	0.010	0.091	0.007	0.000	0.000	0.012	0.036	0.004	0.017	0.011	0.018	0.016	0.024	0.024
Total	16.047	16.047	16.145	16.183	16.069	16.059	16.077	16.073	16.026	16.029	15.629	15.582	16.019	16.073	16.426	16.435
Mg#	86.78	87.09	86.15	87.75	87.85	87.82	88.46	89.07	88.46	89.01	89.94	90.13	90.18	89.89	82.69	82.49

Table 6a: Microprobe analyses of Torrie spinels (cations on basis of 4 oxygen).

name	1 AMC	2 AMC	3 TIMAC	4 TIMAC	5 TIMAC	6 TIMAC	7 TIMAC	8 TIMAC	9 TIMAC	10 TIMAC	11 TIMAC*	12 TIMAC*	13 TIMAC*	14 TIMAC*	15 TIMAC*	16 TIMAC*
SiO_2	0.031	0.033	0.092	0.075	0.271	0.256	0.123	0.103	0.090	0.128	0.189	0.107	0.139	0.092	0.081	8.805
TiO_2	0.160	0.212	2.597	2.641	2.849	2.531	2.609	4.188	2.503	2.404	2.503	2.383	4.092	4.107	3.813	3.408
Al_2O_3	4.061	4.536	8.264	8.224	8.870	9.508	11.345	8.425	11.495	12.262	8.948	9.096	8.984	7.809	8.421	6.020
Cr_2O_3	66.632	59.561	51.321	51.008	49.687	49.252	48.041	47.228	47.126	46.451	50.163	49.970	46.535	46.321	45.289	38.952
FeO_T	21.112	20.670	20.714	20.831	20.477	21.231	20.432	23.320	20.411	20.383	20.689	20.362	23.325	22.794	22.666	20.688
FeO	18.190	14.561	14.010	14.030	13.991	14.110	13.801	16.207	13.194	13.132	14.066	13.829	15.563	15.228	14.792	15.585
Fe_2O_3	3.247	6.788	7.450	7.558	7.208	7.914	7.369	7.905	8.020	8.058	7.361	7.260	8.626	8.408	8.750	5.671
MnO	0.415	0.392	0.353	0.367	0.306	0.290	0.308	0.336	0.340	0.306	0.342	0.352	0.322	0.261	0.309	0.275
MgO	9.828	10.964	13.372	13.305	13.599	13.497	13.887	12.892	13.981	14.069	13.302	13.117	13.236	12.953	12.866	20.199
NiO	0.000	0.142	0.114	0.110	0.217	0.184	0.142	0.157	0.161	0.211	0.164	0.173	0.206	0.203	0.213	0.231
ZnO	0.058	0.263	0.012	0.012	0.000	0.132	0.000	0.000	0.096	0.144	0.000	0.117	0.276	0.012	0.096	0.340
Nb_2O_5	0.000	0.004	0.000	0.000	0.000	0.027	0.000	0.044	0.000	0.000	0.000	0.000	0.013	0.000	0.000	0.000
Total	102.62	97.46	97.59	97.33	97.00	97.70	97.63	97.48	97.01	97.16	97.04	96.40	97.99	95.39	94.63	99.49
Si	0.001	0.001	0.003	0.003	0.009	0.008	0.004	0.003	0.003	0.004	0.006	0.004	0.005	0.003	0.003	0.271
Ti	0.004	0.006	0.065	0.066	0.071	0.063	0.064	0.105	0.062	0.059	0.063	0.060	0.102	0.106	0.099	0.079
Al	0.159	0.185	0.325	0.324	0.349	0.371	0.438	0.332	0.446	0.473	0.352	0.360	0.351	0.315	0.341	0.219
Cr	1.750	1.626	1.352	1.348	1.310	1.288	1.244	1.249	1.226	1.202	1.324	1.328	1.220	1.252	1.230	0.949
Fe^{2+}	0.505	0.420	0.390	0.392	0.390	0.390	0.378	0.453	0.363	0.359	0.393	0.389	0.431	0.435	0.425	0.402
Fe^{3+}	0.081	0.176	0.187	0.190	0.181	0.197	0.182	0.199	0.199	0.198	0.185	0.184	0.215	0.216	0.226	0.132
Mn	0.012	0.011	0.010	0.010	0.009	0.008	0.009	0.010	0.009	0.008	0.010	0.010	0.009	0.008	0.009	0.007
Mg	0.487	0.564	0.664	0.663	0.676	0.666	0.678	0.643	0.686	0.686	0.662	0.657	0.654	0.660	0.659	0.928
Ni	0.000	0.004	0.003	0.003	0.006	0.005	0.004	0.004	0.004	0.006	0.004	0.005	0.005	0.006	0.006	0.006
Zn	0.001	0.007	0.000	0.000	0.000	0.003	0.000	0.000	0.002	0.003	0.000	0.003	0.007	0.000	0.002	0.008
Nb	0.000	0.000	0.000	0.000	0.000	0.000	0.000	0.001	0.000	0.000	0.000	0.000	0.000	0.000	0.000	0.000
Total	3.000	3.000	3.000	3.000	3.000	3.000	3.000	3.000	3.000	3.000	3.000	3.000	3.000	3.000	3.000	3.000
Fe^{2+}_T	0.5924	0.6102	0.5911	0.5965	0.5841	0.6022	0.5726	0.6690	0.5759	0.5720	0.5914	0.5859	0.504	0.504	0.504	0.369
Cr/(Cr+Al)	0.917	0.898	0.806	0.806	0.790	0.777	0.740	0.790	0.733	0.718	0.790	0.787	0.777	0.799	0.783	0.813
Ti/(Ti+Cr+Al)	0.002	0.003	0.037	0.038	0.041	0.037	0.037	0.062	0.036	0.034	0.036	0.034	0.061	0.063	0.059	0.063
Al/(Al+Cr)	0.083	0.102	0.194	0.194	0.210	0.223	0.260	0.210	0.267	0.282	0.210	0.213	0.223	0.201	0.217	0.187

* inclusion in olivine macrocryst   ** inclusion in garnet xenocryst (G9)

$Fe\# = Fe_T^{2+}/(Mg + Fe_T^{2+})$

Appendix 6a. (continued)

name	17 TIMAC core	Cr-hercynitic spinel rim	18 TIMAC core	Cr-hercynitic spinel rim	19 Ti-Fe pleonastes (19-56)	20	21	22	23	24	25	26	27	28	29	30
SiO_2	0.083	0.263	0.126	0.086	0.094	0.042	0.039	0.047	0.125	0.043	0.036	0.080	0.079	0.242	0.037	0.047
TiO_2	2.405	3.229	2.830	3.540	16.982	20.936	19.530	18.623	20.692	19.699	20.833	21.779	19.735	19.404	20.008	21.195
Al_2O_3	9.000	36.191	9.391	36.906	7.574	11.406	12.332	12.931	11.753	12.302	12.037	10.546	12.033	11.368	12.862	11.720
Cr_2O_3	51.249	14.993	49.301	11.184	5.101	3.424	2.993	2.929	2.558	2.495	2.472	2.380	2.311	2.276	2.170	2.139
FeO_T	20.683	21.183	20.897	23.074	46.931	33.831	34.865	34.715	36.445	35.206	36.876	38.894	35.003	36.606	39.968	37.521
FeO	13.903	8.573	13.980	8.623	19.794	13.712	12.023	12.617	16.702	12.280	15.963	17.697	13.016	12.596	18.204	18.152
Fe_2O_3	7.535	14.014	7.687	16.059	30.157	22.358	25.385	24.558	21.941	25.478	23.241	23.557	24.434	26.683	24.187	21.525
MnO	0.358	0.208	0.352	0.186	0.569	0.500	0.469	0.439	0.554	0.537	0.504	0.563	0.599	0.563	0.495	0.469
MgO	13.457	20.453	13.615	20.310	17.560	24.248	24.640	23.543	22.092	24.614	23.059	22.530	23.834	24.225	21.446	21.644
NiO	0.125	0.089	0.171	0.075	0.170	0.174	0.215	0.202	0.203	0.213	0.153	0.183	0.182	0.179	0.145	0.131
ZnO	0.120	0.000	0.000	0.000	0.468	0.000	0.134	0.000	0.230	0.000	0.000	0.000	0.000	0.182	0.000	0.000
Nb_2O_5	0.000	0.000	0.000	0.000	0.086	0.073	0.000	0.037	0.086	0.032	0.032	0.045	0.018	0.059	0.014	0.077
Total	98.23	98.01	97.45	96.97	98.56	96.87	97.76	95.93	96.94	97.69	98.33	99.36	96.24	97.78	99.57	97.10
Si	0.003	0.007	0.004	0.002	0.003	0.001	0.001	0.001	0.004	0.001	0.001	0.002	0.002	0.007	0.001	0.001
Ti	0.060	0.069	0.071	0.076	0.415	0.487	0.449	0.436	0.487	0.453	0.482	0.504	0.462	0.449	0.461	0.500
Al	0.350	1.211	0.367	1.244	0.290	0.416	0.444	0.475	0.434	0.443	0.436	0.382	0.441	0.412	0.465	0.433
Cr	1.338	0.337	1.292	0.253	0.131	0.084	0.072	0.072	0.063	0.060	0.060	0.058	0.057	0.055	0.053	0.053
Fe^{2+}	0.384	0.204	0.387	0.206	0.538	0.355	0.307	0.329	0.437	0.314	0.410	0.455	0.339	0.324	0.466	0.476
Fe^{3+}	0.187	0.299	0.192	0.346	0.738	0.520	0.584	0.576	0.517	0.586	0.537	0.545	0.572	0.618	0.558	0.508
Mn	0.010	0.005	0.010	0.005	0.016	0.013	0.012	0.012	0.015	0.014	0.013	0.015	0.016	0.015	0.013	0.012
Mg	0.662	0.866	0.673	0.866	0.851	1.118	1.122	1.094	1.031	1.122	1.056	1.033	1.106	1.111	0.980	1.012
Ni	0.003	0.002	0.005	0.002	0.004	0.004	0.005	0.005	0.005	0.005	0.004	0.005	0.005	0.004	0.004	0.003
Zn	0.003	0.000	0.000	0.000	0.011	0.000	0.003	0.000	0.005	0.000	0.000	0.000	0.000	0.004	0.000	0.000
Nb	0.000	0.000	0.000	0.000	0.001	0.001	0.000	0.001	0.001	0.000	0.000	0.001	0.000	0.001	0.000	0.001
Total	3.000	3.000	3.000	3.000	3.000	3.000	3.000	3.000	3.000	3.000	3.000	3.000	3.000	3.000	3.000	3.000
Fe^{2+}_T	0.469	0.376	0.469	0.400	0.600	0.439	0.442	0.453	0.481	0.445	0.473	0.492	0.452	0.459	0.511	0.493
Cr/(Cr+Al)	0.793	0.217	0.779	0.169	0.311	0.168	0.140	0.132	0.127	0.120	0.121	0.131	0.114	0.118	0.102	0.109
Ti/(Ti+Cr+Al)	0.034	0.043	0.041	0.048	0.496	0.494	0.465	0.444	0.495	0.474	0.493	0.534	0.481	0.490	0.471	0.507
Al/(Al+Cr)	0.207	0.783	0.221	0.831	0.689	0.832	0.860	0.868	0.873	0.880	0.879	0.869	0.886	0.882	0.898	0.891

Table 6a. (continued)

name	31	32	33	34	35	36	37	38	39	40	41	42	43	44	45	46	47
	Ti-Fe pleonastes (19-56)																
SiO_2	0.133	0.116	0.073	0.059	0.104	0.082	0.114	0.029	0.061	0.106	0.031	0.119	0.088	0.061	0.180	0.131	0.104
TiO_2	21.188	19.623	19.149	18.938	21.898	21.153	20.640	18.505	19.538	20.122	19.995	22.464	20.791	20.836	21.941	19.670	20.132
Al_2O_3	11.826	12.422	12.779	11.915	11.286	11.976	10.740	14.085	12.606	11.368	13.023	11.499	11.781	12.514	10.728	10.602	12.038
Cr_2O_3	2.139	2.125	2.101	2.033	2.026	2.004	2.003	1.947	1.934	1.920	1.908	1.869	1.788	1.780	1.779	1.748	1.668
FeO_T	36.295	37.028	38.600	38.234	36.800	36.347	37.518	39.952	39.991	39.398	40.831	36.522	37.898	35.222	37.549	43.174	35.730
FeO	14.622	14.040	16.139	13.427	16.590	15.942	14.267	16.345	17.376	15.215	18.332	18.003	15.662	14.619	19.175	20.393	14.005
Fe_2O_3	24.086	25.547	24.961	27.568	22.460	22.676	25.839	26.234	25.132	26.875	25.003	20.580	24.711	22.896	20.419	25.317	24.143
MnO	0.651	0.528	0.455	0.459	0.500	0.539	0.619	0.483	0.529	0.505	0.489	0.672	0.468	0.527	0.670	0.661	0.625
MgO	24.121	23.626	21.911	23.494	23.090	23.080	23.718	21.893	21.561	23.221	21.533	22.490	23.340	23.713	21.078	19.011	23.375
NiO	0.206	0.220	0.208	0.227	0.177	0.210	0.170	0.147	0.146	0.193	0.161	0.196	0.207	0.167	0.192	0.204	0.158
ZnO	0.207	0.000	0.133	0.000	0.255	0.000	0.315	0.000	0.000	0.170	0.000	0.000	0.000	0.049	0.000	0.314	0.171
Nb_2O_5	0.027	0.041	0.069	0.014	0.000	0.000	0.041	0.000	0.050	0.000	0.000	0.014	0.037	0.023	0.068	0.023	0.009
Total	99.21	98.29	97.98	98.13	98.39	97.66	98.47	99.67	98.93	99.69	100.48	97.91	98.87	97.19	96.23	98.07	96.43
Si	0.004	0.004	0.002	0.002	0.003	0.003	0.004	0.001	0.002	0.003	0.001	0.004	0.003	0.002	0.006	0.004	0.003
Ti	0.483	0.452	0.446	0.438	0.507	0.491	0.478	0.423	0.453	0.461	0.457	0.523	0.478	0.483	0.525	0.471	0.472
Al	0.423	0.448	0.467	0.432	0.410	0.436	0.389	0.505	0.458	0.408	0.466	0.420	0.425	0.455	0.402	0.398	0.442
Cr	0.051	0.051	0.051	0.049	0.049	0.049	0.049	0.047	0.047	0.046	0.046	0.046	0.043	0.043	0.045	0.044	0.041
Fe^{2+}	0.371	0.359	0.418	0.345	0.427	0.412	0.367	0.416	0.448	0.388	0.466	0.466	0.401	0.377	0.510	0.543	0.365
Fe^{3+}	0.550	0.588	0.582	0.638	0.520	0.527	0.598	0.600	0.583	0.616	0.572	0.480	0.569	0.531	0.489	0.607	0.566
Mn	0.017	0.014	0.012	0.012	0.013	0.014	0.016	0.012	0.014	0.013	0.013	0.018	0.012	0.014	0.018	0.018	0.016
Mg	1.091	1.078	1.012	1.077	1.060	1.063	1.088	0.992	0.991	1.055	0.976	1.039	1.064	1.090	1.000	0.903	1.086
Ni	0.005	0.005	0.005	0.006	0.004	0.005	0.004	0.004	0.004	0.005	0.004	0.005	0.005	0.004	0.005	0.005	0.004
Zn	0.005	0.000	0.003	0.000	0.006	0.000	0.007	0.000	0.000	0.004	0.000	0.000	0.000	0.001	0.000	0.007	0.004
Nb	0.000	0.001	0.001	0.000	0.000	0.000	0.001	0.000	0.001	0.000	0.000	0.000	0.001	0.000	0.001	0.000	0.000
Total	3.000	3.000	3.000	3.000	3.000	3.000	3.000	3.000	3.000	3.000	3.000	3.000	3.000	3.000	3.000	3.000	3.000
Fe^{2+}_T	0.458	0.468	0.497	0.477	0.472	0.469	0.470	0.506	0.510	0.488	0.515	0.477	0.477	0.454	0.500	0.560	0.462
Cr/(Cr+Al)	0.108	0.103	0.099	0.103	0.107	0.101	0.111	0.085	0.093	0.102	0.089	0.098	0.092	0.087	0.100	0.100	0.085
Ti/(Ti+Cr+Al)	0.505	0.475	0.463	0.476	0.525	0.503	0.522	0.434	0.473	0.504	0.472	0.529	0.505	0.492	0.540	0.516	0.494
Al/(Al+Cr)	0.892	0.897	0.901	0.897	0.893	0.899	0.889	0.915	0.907	0.898	0.911	0.902	0.908	0.913	0.900	0.900	0.915

Table 6a. (continued)

name	48	49	50	51	52	53	54	55	56
	Ti-Fe pleonastes (19-56)								
SiO_2	0.077	0.021	0.050	0.009	0.113	0.041	0.192	3.685	6.132
TiO_2	21.220	20.057	21.626	19.597	19.590	18.719	19.908	18.141	12.328
Al_2O_3	12.118	12.876	11.167	13.148	11.507	10.881	10.553	10.815	10.801
Cr_2O_3	1.624	1.514	1.498	1.471	1.396	1.342	1.281	1.969	1.382
FeO_T	39.599	40.703	39.347	40.365	41.373	39.163	41.470	34.405	39.854
FeO	17.809	18.628	17.382	16.658	17.539	13.381	18.482	15.443	16.173
Fe_2O_3	24.215	24.532	24.410	26.345	26.486	28.651	25.546	21.072	26.317
MnO	0.552	0.525	0.496	0.423	0.499	0.503	0.656	0.567	0.890
MgO	22.473	21.137	22.723	22.361	21.343	22.936	20.398	24.300	22.222
NiO	0.158	0.164	0.248	0.159	0.279	0.231	0.139	0.124	0.048
ZnO	0.000	0.000	0.000	0.000	0.024	0.073	0.193	0.122	0.317
Nb_2O_5	0.014	0.023	0.027	0.009	0.100	0.055	0.005	0.046	0.037
Total	100.26	99.48	99.63	100.18	98.88	96.81	97.35	96.28	96.65
Si	0.002	0.001	0.002	0.000	0.004	0.001	0.006	0.114	0.190
Ti	0.485	0.464	0.498	0.447	0.457	0.442	0.475	0.421	0.288
Al	0.434	0.466	0.403	0.470	0.421	0.402	0.395	0.393	0.395
Cr	0.039	0.037	0.036	0.035	0.034	0.033	0.032	0.048	0.034
Fe^{2+}	0.452	0.479	0.445	0.422	0.455	0.351	0.491	0.398	0.419
Fe^{3+}	0.553	0.567	0.562	0.601	0.619	0.676	0.610	0.489	0.614
Mn	0.014	0.014	0.013	0.011	0.013	0.013	0.018	0.015	0.023
Mg	1.017	0.968	1.036	1.010	0.988	1.073	0.965	1.117	1.028
Ni	0.004	0.004	0.006	0.004	0.007	0.006	0.004	0.003	0.001
Zn	0.000	0.000	0.000	0.000	0.001	0.002	0.005	0.003	0.007
Nb	0.000	0.000	0.000	0.000	0.001	0.001	0.000	0.001	0.001
Total	3.000	3.000	3.000	3.000	3.000	3.000	3.000	3.000	3.000
Fe^{2+}_T	0.497	0.519	0.493	0.503	0.521	0.489	0.533	0.443	0.501
Cr/(Cr+Al)	0.082	0.073	0.083	0.070	0.075	0.076	0.075	0.109	0.079
Ti/(Ti+Cr+Al)	0.506	0.480	0.531	0.469	0.501	0.503	0.527	0.488	0.402
Al/(Al+Cr)	0.918	0.927	0.917	0.930	0.925	0.924	0.925	0.891	0.921

Table 6b: Microprobe analyses of Sputnik spinels (cations on basis of 4 oxygen)

name	1 TIMAC*	2 TIMAC*	3 SPINEL**	4 SPINEL**	5 SPINEL**	6 MUM	7 MUM	8 MUM	9 MUM
SiO_2	0.136	0.122	0.000	0.508	0.250	0.016	0.076	0.055	0.055
TiO_2	2.823	1.631	0.144	0.228	0.152	14.112	14.555	15.205	14.938
Al_2O_3	8.853	9.499	46.629	46.179	46.708	10.300	9.903	9.917	13.003
Cr_2O_3	48.805	51.718	12.588	10.982	10.255	0.032	0.157	0.000	0.009
FeO_T	20.844	19.686	14.711	16.136	17.950	55.676	55.400	55.595	50.563
FeO	13.423	13.072	8.294	8.962	10.684	22.767	23.462	24.049	22.361
Fe_2O_3	8.246	7.350	7.131	7.973	8.074	36.572	35.492	35.057	31.341
MnO	0.275	0.302	0.137	0.240	0.303	0.519	0.477	0.478	0.457
MgO	13.737	13.574	18.983	18.925	17.542	14.465	14.224	14.307	15.426
NiO	0.223	0.134	0.000	0.000	0.000	0.033	0.086	0.124	0.102
ZnO	0.059	0.088	0.000	0.000	0.000	0.117	0.010	0.097	0.029
Nb_2O_5	0.019	0.058	0.000	0.000	0.000	0.034	0.005	0.000	0.094
Total	96.60	97.55	93.91	94.00	93.97	98.97	98.45	99.29	97.81
Si	0.005	0.004	0.000	0.014	0.007	0.001	0.003	0.002	0.002
Ti	0.071	0.041	0.003	0.005	0.003	0.348	0.362	0.375	0.365
Al	0.349	0.371	1.559	1.545	1.574	0.398	0.385	0.383	0.497
Cr	1.291	1.354	0.282	0.246	0.232	0.001	0.004	0.000	0.000
Fe^{2+}	0.376	0.362	0.197	0.213	0.255	0.624	0.648	0.659	0.607
Fe^{3+}	0.208	0.183	0.152	0.170	0.174	0.902	0.882	0.864	0.765
Mn	0.008	0.008	0.003	0.006	0.007	0.014	0.013	0.013	0.013
Mg	0.685	0.670	0.803	0.801	0.748	0.707	0.700	0.699	0.746
Ni	0.006	0.004	0.000	0.000	0.000	0.001	0.002	0.003	0.003
Zn	0.001	0.002	0.000	0.000	0.000	0.003	0.000	0.002	0.001
Nb	0.000	0.001	0.000	0.000	0.000	0.001	0.000	0.000	0.001
Total	3.000	3.000	3.000	3.000	3.000	3.000	3.000	3.000	3.000
Fe^{2+}_T	0.466	0.454	0.307	0.328	0.370	0.709	0.711	0.710	0.670
Cr/(Cr+Al)	0.787	0.785	0.153	0.138	0.128	0.002	0.011	0.000	0.000
Ti/(Ti+Cr+Al)	0.042	0.023	0.002	0.003	0.002	0.466	0.481	0.495	0.423
Al/(Al+Cr)	0.213	0.215	0.847	0.862	0.872	0.998	0.989	1.000	1.000

Table 6c: Microprobe analyses of Eddie spinels (cations on basis of 4 oxygen)

name	1 AMC	2 AMC	3 TMC core	4 herc. spinel middle	5 herc. spinel rim	6 TIMAC	7 TIMAC	8 TIMAC core	9 Cr-herc.spinel rim	10 UM	11 UM	12 UM	13 UM	14 UM	15 UM	16 MUM
SiO_2	0.178	0.000	0.037	0.000	0.005	0.223	0.078	0.121	0.177	0.020	0.045	0.017	0.070	0.035	0.023	0.086
TiO_2	1.612	0.059	1.532	1.377	2.873	1.776	2.258	2.097	2.494	16.906	13.573	15.919	14.657	13.169	13.093	10.259
Al_2O_3	7.102	12.919	1.928	46.027	39.799	7.216	7.092	7.278	32.842	0.868	1.335	2.068	3.382	5.397	5.554	14.368
Cr_2O_3	57.221	56.036	61.948	0.392	0.000	56.100	55.060	56.983	13.451	0.570	9.082	1.834	1.011	0.175	0.274	0.000
FeO_T	17.715	18.029	22.159	22.206	30.104	18.791	19.772	18.413	26.059	67.190	58.864	64.649	62.807	63.935	63.713	53.634
FeO	11.950	15.212	16.522	5.645	8.704	13.664	13.167	13.118	8.508	31.770	26.192	28.722	26.146	25.682	24.981	18.901
Fe_2O_3	6.406	3.131	6.264	18.404	23.782	5.698	7.340	5.885	19.504	39.362	36.309	39.925	40.741	42.511	43.042	38.599
MnO	0.373	0.353	0.401	0.118	0.169	0.357	0.378	0.363	0.182	0.646	0.832	0.697	0.600	0.563	0.507	0.477
MgO	14.455	12.109	10.835	21.097	19.682	13.335	13.984	14.144	19.370	9.275	10.675	10.792	11.632	11.466	12.070	15.069
NiO	0.143	0.033	0.105	0.000	0.000	0.101	0.204	0.133	0.000	0.216	0.145	0.200	0.186	0.140	0.129	0.000
ZnO	0.029	0.000	0.087	0.000	0.000	0.000	0.000	0.000	0.000	0.000	0.000	0.184	0.174	0.000	0.000	0.000
Nb_2O_5	0.000	0.043	0.062	0.000	0.021	0.000	0.053	0.029	0.021	0.063	0.058	0.029	0.054	0.024	0.064	0.050
Total	99.47	99.89	99.72	93.06	95.03	98.47	99.61	100.15	96.55	99.70	98.25	100.39	98.65	99.16	99.74	97.81
Si	0.006	0.000	0.001	0.000	0.000	0.007	0.003	0.004	0.005	0.001	0.002	0.001	0.002	0.001	0.001	0.003
Ti	0.040	0.001	0.039	0.029	0.062	0.044	0.056	0.051	0.055	0.449	0.360	0.413	0.382	0.339	0.334	0.250
Al	0.273	0.491	0.078	1.539	1.356	0.282	0.274	0.279	1.136	0.036	0.056	0.084	0.138	0.218	0.222	0.549
Cr	1.478	1.428	1.677	0.009	0.000	1.472	1.426	1.465	0.312	0.016	0.253	0.050	0.028	0.005	0.007	0.000
Fe^{2+}	0.327	0.410	0.473	0.134	0.210	0.379	0.361	0.357	0.209	0.938	0.773	0.829	0.758	0.735	0.708	0.513
Fe^{3+}	0.158	0.076	0.161	0.393	0.517	0.142	0.181	0.144	0.431	1.046	0.964	1.037	1.063	1.096	1.098	0.942
Mn	0.010	0.010	0.012	0.003	0.004	0.010	0.010	0.010	0.005	0.019	0.025	0.020	0.018	0.016	0.015	0.013
Mg	0.704	0.582	0.553	0.893	0.849	0.660	0.683	0.686	0.847	0.488	0.562	0.555	0.601	0.585	0.610	0.729
Ni	0.004	0.001	0.003	0.000	0.000	0.003	0.005	0.003	0.000	0.006	0.004	0.006	0.005	0.004	0.004	0.000
Zn	0.001	0.000	0.002	0.000	0.000	0.000	0.000	0.000	0.000	0.000	0.000	0.005	0.004	0.000	0.000	0.000
Nb	0.000	0.001	0.001	0.000	0.000	0.000	0.001	0.000	0.000	0.001	0.001	0.000	0.001	0.000	0.001	0.001
Total	3.000	3.000	3.000	3.000	3.000	3.000	3.000	3.000	3.000	3.000	3.000	3.000	3.000	3.000	3.000	3.000
Fe^{2+}_T	0.412	0.457	0.539	0.383	0.478	0.446	0.448	0.426	0.444	0.824	0.779	0.794	0.777	0.784	0.774	0.694
Cr/(Cr+Al)	0.844	0.744	0.956	0.006	0.000	0.839	0.839	0.840	0.216	0.306	0.820	0.373	0.167	0.021	0.032	0.000
Ti/(Ti+Cr+Al)	0.022	0.001	0.022	0.019	0.044	0.025	0.032	0.029	0.037	0.896	0.538	0.755	0.697	0.604	0.593	0.313
Al/(Al+Cr)	0.156	0.256	0.044	0.994	1.000	0.161	0.161	0.160	0.784	0.694	0.180	0.627	0.833	0.979	0.968	1.000

Table 6c. (continued)

name	17 MUM	18 MUM	19 MUM	20 MUM	21 MUM	22 MUM	23 MUM	24 MUM	25 MUM	26 MUM	27 MUM	28 MUM	29 MUM	30 MUM	31 MUM core	32 MUM rim
SiO_2	0.041	0.024	0.057	0.045	0.048	0.062	0.035	0.038	0.021	0.044	0.022	0.031	0.015	0.054	0.012	0.129
TiO_2	11.871	11.817	11.614	9.301	8.764	10.131	9.853	10.486	10.230	10.235	9.657	10.712	9.216	10.694	10.548	9.063
Al_2O_3	11.716	12.285	11.764	16.789	12.179	12.863	14.832	13.993	13.884	14.038	14.168	10.588	14.098	13.736	13.375	13.987
Cr_2O_3	0.219	0.033	0.070	0.000	0.000	0.057	0.030	0.000	0.018	0.000	0.000	0.469	0.000	0.000	0.400	0.003
FeO_T	56.183	57.508	57.209	53.453	60.565	55.584	56.341	55.866	54.842	56.524	55.283	58.034	54.317	54.776	55.741	56.425
FeO	20.567	22.529	21.785	17.181	20.189	18.710	19.796	20.340	19.598	20.591	18.839	20.495	18.068	20.432	19.850	18.543
Fe_2O_3	39.580	38.872	39.366	40.309	44.870	40.979	40.612	39.480	39.166	39.932	40.500	41.717	40.284	38.166	39.886	42.099
MnO	0.473	0.390	0.487	0.529	0.491	0.480	0.440	0.421	0.437	0.416	0.499	0.500	0.471	0.428	0.471	0.646
MgO	14.865	13.789	13.855	16.296	13.404	14.944	14.764	14.465	14.492	14.251	14.744	13.875	14.685	14.223	14.654	14.689
NiO	0.052	0.050	0.070	0.000	0.003	0.064	0.028	0.045	0.038	0.092	0.000	0.068	0.034	0.001	0.052	0.000
ZnO	0.020	0.029	0.108	0.039	0.068	0.000	0.000	0.000	0.000	0.000	0.000	0.000	0.000	0.079	0.069	0.029
Nb_2O_5	0.000	0.055	0.045	0.000	0.000	0.000	0.025	0.010	0.025	0.070	0.000	0.005	0.045	0.040	0.000	0.000
Total	99.40	99.87	99.22	100.49	100.02	98.29	100.42	99.28	97.91	99.67	98.43	98.46	96.92	97.85	99.32	99.19
Si	0.001	0.001	0.002	0.001	0.002	0.002	0.001	0.001	0.001	0.001	0.001	0.001	0.000	0.002	0.000	0.004
Ti	0.289	0.288	0.286	0.218	0.215	0.248	0.235	0.254	0.251	0.248	0.235	0.267	0.228	0.263	0.256	0.220
Al	0.448	0.470	0.453	0.616	0.468	0.494	0.555	0.531	0.534	0.532	0.541	0.413	0.546	0.529	0.509	0.531
Cr	0.006	0.001	0.002	0.000	0.000	0.001	0.001	0.000	0.000	0.000	0.000	0.012	0.000	0.000	0.010	0.000
Fe^{2+}	0.557	0.611	0.595	0.448	0.550	0.510	0.526	0.548	0.535	0.554	0.510	0.567	0.496	0.559	0.536	0.500
Fe^{3+}	0.965	0.949	0.968	0.945	1.100	1.004	0.970	0.957	0.961	0.967	0.987	1.039	0.996	0.939	0.968	1.021
Mn	0.013	0.011	0.013	0.014	0.014	0.013	0.012	0.011	0.012	0.011	0.014	0.014	0.013	0.012	0.013	0.018
Mg	0.718	0.667	0.675	0.757	0.651	0.726	0.699	0.695	0.705	0.683	0.712	0.685	0.719	0.693	0.705	0.706
Ni	0.001	0.001	0.002	0.000	0.000	0.002	0.001	0.001	0.001	0.002	0.000	0.002	0.001	0.000	0.001	0.000
Zn	0.000	0.001	0.003	0.001	0.002	0.000	0.000	0.000	0.000	0.000	0.000	0.000	0.000	0.002	0.002	0.001
Nb	0.000	0.001	0.001	0.000	0.000	0.000	0.000	0.000	0.000	0.001	0.000	0.000	0.001	0.001	0.000	0.000
Total	3.000	3.000	3.000	3.000	3.000	3.000	3.000	3.000	3.000	3.000	3.000	3.000	3.000	3.000	3.000	3.000
Fe^{2+}_T	0.707	0.726	0.725	0.676	0.746	0.705	0.709	0.711	0.768	0.776	0.767	0.729	0.703	0.710	0.769	0.772
Cr/(Cr+Al)	0.012	0.002	0.004	0.000	0.000	0.003	0.001	0.000	0.001	0.000	0.000	0.029	0.000	0.000	0.020	0.000
Ti/(Ti+Cr+Al)	0.390	0.380	0.386	0.261	0.315	0.334	0.297	0.324	0.320	0.318	0.303	0.385	0.294	0.332	0.330	0.293
Al/(Al+Cr)	0.988	0.998	0.996	1.000	1.000	0.997	0.999	1.000	0.999	1.000	1.000	0.971	1.000	1.000	0.980	1.000

Table 6c. (continued)

name	33 MUM core	34 herc. Spinel rim
SiO_2	0.019	0.000
TiO_2	9.098	2.824
Al_2O_3	13.274	41.281
Cr_2O_3	0.000	0.000
FeO_T	56.240	29.748
FeO	18.029	8.689
Fe_2O_3	42.464	23.403
MnO	0.563	0.222
MgO	14.736	20.072
NiO	0.000	0.000
ZnO	0.000	0.000
Nb_2O_5	0.000	0.000
Total	98.18	96.49
Si	0.001	0.000
Ti	0.223	0.060
Al	0.510	1.380
Cr	0.000	0.000
Fe^{2+}	0.492	0.206
Fe^{3+}	1.042	0.500
Mn	0.016	0.005
Mg	0.717	0.849
Ni	0.000	0.000
Zn	0.000	0.000
Nb	0.000	0.000
Total	3.000	3.000
Fe^{2+}_T	0.771	0.470
Cr/(Cr+Al)	0.000	0.000
Ti/(Ti+Cr+Al)	0.304	0.042
Al/(Al+Cr)	1.000	1.000

Table 7a: Microprobe analyses of Torrie ilmenite (cations on basis of 3 oxygen).

	core 1	rim 2	3	4	5	6	7	core 8	rim 9	10	11	12	13	14	core 15	rim 16	core 17	rim 18
SiO_2	0.04	0.01	0.00	0.00	0.01	0.00	0.05	0.05	0.04	0.03	0.01	0.06	0.05	0.02	0.03	0.00	0.03	0.00
TiO_2	48.84	49.06	44.64	45.10	47.72	48.35	48.21	47.99	47.46	49.89	49.07	48.29	49.62	48.70	48.84	49.51	48.17	47.78
Al_2O_3	0.07	0.07	0.22	0.24	0.25	0.23	0.25	0.26	0.27	0.31	0.27	0.24	0.32	0.27	0.32	0.35	0.33	0.33
Cr_2O_3	0.19	0.15	2.06	2.38	2.91	1.94	2.08	2.17	2.10	1.89	1.90	1.90	1.85	1.78	2.07	2.06	1.87	1.85
FeO_T	48.64	48.51	31.92	36.41	35.12	36.28	36.23	36.51	35.32	35.05	35.12	36.25	35.46	34.52	34.52	33.61	34.51	35.57
FeO	42.05	42.45	22.50	22.28	24.41	24.81	24.51	23.88	23.66	25.39	24.37	24.04	24.79	24.09	23.69	23.72	23.34	22.52
Fe_2O_3	7.33	6.73	10.46	15.71	11.90	12.74	13.03	14.03	12.96	10.73	11.95	13.57	11.86	11.60	12.04	10.98	12.41	14.50
MnO	0.52	0.54	0.28	0.29	0.29	0.28	0.34	0.29	0.33	0.30	0.34	0.33	0.34	0.33	0.37	0.36	0.31	0.28
MgO	0.78	0.69	10.20	10.68	10.69	10.75	10.98	11.15	11.01	11.18	11.24	11.24	11.34	11.37	11.38	11.79	11.45	11.84
NiO	0.06	0.06	0.00	0.11	0.10	0.11	0.10	0.08	0.08	0.07	0.10	0.08	0.05	0.06	0.13	0.15	0.06	0.09
ZnO	0.21	0.16	0.00	0.09	0.00	0.00	0.04	0.19	0.03	0.01	0.16	0.00	0.13	0.05	0.34	0.06	0.11	0.05
Nb_2O_5	0.06	0.13	0.43	0.46	0.48	0.38	0.59	0.48	0.46	0.44	0.39	0.42	0.39	0.54	0.36	0.40	0.39	0.42
Total	99.46	99.45	90.20	96.27	98.16	98.73	99.35	99.63	97.56	99.60	99.01	99.21	99.97	98.07	98.81	98.74	97.65	98.63
Si	0.001	0.000	0.000	0.000	0.000	0.000	0.001	0.001	0.001	0.001	0.000	0.001	0.001	0.000	0.001	0.000	0.001	0.000
Ti	0.946	0.950	0.895	0.860	0.884	0.890	0.882	0.877	0.883	0.903	0.896	0.884	0.896	0.896	0.893	0.900	0.890	0.878
Al	0.002	0.002	0.007	0.007	0.007	0.007	0.007	0.007	0.008	0.009	0.008	0.007	0.009	0.008	0.009	0.010	0.010	0.009
Cr	0.004	0.003	0.043	0.048	0.057	0.038	0.040	0.042	0.041	0.036	0.036	0.036	0.035	0.034	0.040	0.039	0.036	0.036
Fe^{2+}_T	1.048	1.045	0.711	0.772	0.723	0.743	0.737	0.742	0.731	0.705	0.713	0.737	0.712	0.706	0.701	0.679	0.709	0.726
Mn	0.011	0.012	0.006	0.006	0.006	0.006	0.007	0.006	0.007	0.006	0.007	0.007	0.007	0.007	0.008	0.007	0.006	0.006
Mg	0.030	0.026	0.405	0.404	0.392	0.392	0.398	0.404	0.406	0.401	0.407	0.408	0.406	0.415	0.412	0.425	0.420	0.431
Ni	0.001	0.001	0.000	0.002	0.002	0.002	0.002	0.002	0.002	0.001	0.002	0.002	0.001	0.001	0.002	0.003	0.001	0.002
Zn	0.004	0.003	0.000	0.002	0.000	0.000	0.001	0.003	0.001	0.000	0.003	0.000	0.002	0.001	0.006	0.001	0.002	0.001
Nb	0.001	0.002	0.005	0.005	0.005	0.004	0.007	0.005	0.005	0.005	0.004	0.005	0.004	0.006	0.004	0.004	0.004	0.005
Total	2.049	2.044	2.072	2.105	2.076	2.081	2.083	2.089	2.084	2.067	2.075	2.086	2.074	2.074	2.076	2.069	2.080	2.093
Mg#	2.77	2.46	36.29	34.34	35.18	34.57	35.07	35.25	35.72	36.26	36.32	35.60	36.30	37.00	37.02	38.48	37.18	37.24
Fe^{2+}	0.91	0.91	0.501	0.472	0.503	0.508	0.499	0.485	0.489	0.511	0.495	0.489	0.498	0.493	0.481	0.479	0.48	0.46
Fe^{3+}	0.14	0.13	0.21	0.3	0.22	0.235	0.239	0.257	0.241	0.194	0.218	0.248	0.214	0.213	0.22	0.2	0.229	0.266
Hem%	7.06	6.49	10.37	14.61	10.96	11.53	11.74	12.61	11.87	9.62	10.80	12.16	10.60	10.52	10.97	9.95	11.31	13.01

Hematite% = $0.5Fe^{3+}/(0.5Fe^{3+}+Fe^{2+}+Mg)100$

Mg# = $100Mg/(Mg+Fe^{2+})$

Table 7a. (continued)

	19	20	21	22	core 23	rim 24	25	26	27	28	29	core 30	rim 31	32	33	34	35	36
SiO_2	0.00	0.00	0.02	0.01	0.06	0.02	0.04	0.00	0.04	0.02	0.00	0.04	0.00	0.00	0.03	0.00	0.00	0.03
TiO_2	48.09	50.24	49.86	47.37	48.31	49.64	49.56	49.59	50.55	45.36	49.56	48.42	49.16	49.23	49.15	46.65	49.39	49.76
Al_2O_3	0.35	0.33	0.31	0.35	0.34	0.36	0.32	0.31	0.35	0.38	0.40	0.32	0.36	0.34	0.46	0.39	0.42	0.58
Cr_2O_3	2.12	1.86	2.01	1.92	1.94	2.02	2.19	1.97	1.96	2.26	2.09	2.18	2.04	2.15	2.63	2.33	2.31	2.42
FeO_T	35.48	34.89	34.44	34.70	34.68	35.34	34.76	34.67	34.43	30.80	34.17	34.35	34.94	35.24	33.08	33.34	33.67	33.60
FeO	22.89	25.01	24.59	22.61	23.32	24.90	23.85	24.06	24.83	20.24	23.88	23.04	23.47	23.65	23.27	21.40	23.56	23.51
Fe_2O_3	13.99	10.98	10.95	13.44	12.63	11.59	12.12	11.79	10.67	11.74	11.43	12.58	12.74	12.87	10.91	13.26	11.23	11.22
MnO	0.34	0.30	0.37	0.29	0.30	0.29	0.35	0.34	0.34	0.30	0.28	0.26	0.30	0.26	0.30	0.28	0.29	0.29
MgO	11.46	11.48	11.52	11.55	11.59	11.24	11.66	11.67	11.68	11.73	11.73	11.75	11.82	11.77	11.79	11.81	11.84	11.96
NiO	0.16	0.13	0.09	0.10	0.12	0.13	0.12	0.14	0.10	0.12	0.14	0.09	0.15	0.11	0.20	0.10	0.14	0.16
ZnO	0.34	0.00	0.01	0.06	0.03	0.05	0.29	0.14	0.15	0.00	0.06	0.08	0.11	0.07	0.19	0.13	0.00	0.16
Nb_2O_5	0.29	0.35	0.35	0.44	0.41	0.31	0.31	0.44	0.37	0.31	0.30	0.32	0.38	0.30	0.34	0.42	0.29	0.25
Total	99.09	100.00	99.43	97.23	98.22	99.84	100.07	99.72	100.40	91.77	99.18	98.27	99.72	99.95	98.75	95.95	98.84	99.76
Si	0.000	0.000	0.001	0.000	0.001	0.001	0.001	0.000	0.001	0.000	0.000	0.001	0.000	0.000	0.001	0.000	0.000	0.001
Ti	0.881	0.904	0.902	0.881	0.888	0.898	0.893	0.896	0.904	0.886	0.898	0.888	0.889	0.889	0.894	0.877	0.897	0.895
Al	0.010	0.009	0.009	0.010	0.010	0.010	0.009	0.009	0.010	0.012	0.011	0.009	0.010	0.010	0.013	0.011	0.012	0.016
Cr	0.041	0.035	0.038	0.037	0.038	0.038	0.042	0.037	0.037	0.046	0.040	0.042	0.039	0.041	0.050	0.046	0.044	0.046
Fe^{2+}_T	0.722	0.698	0.693	0.718	0.709	0.710	0.696	0.697	0.685	0.669	0.688	0.701	0.703	0.708	0.669	0.697	0.680	0.672
Mn	0.007	0.006	0.007	0.006	0.006	0.006	0.007	0.007	0.007	0.007	0.006	0.005	0.006	0.005	0.006	0.006	0.006	0.006
Mg	0.416	0.409	0.413	0.426	0.422	0.403	0.417	0.418	0.414	0.454	0.421	0.427	0.424	0.421	0.425	0.440	0.426	0.426
Ni	0.003	0.002	0.002	0.002	0.002	0.003	0.002	0.003	0.002	0.003	0.003	0.002	0.003	0.002	0.004	0.002	0.003	0.003
Zn	0.006	0.000	0.000	0.001	0.001	0.001	0.005	0.002	0.003	0.000	0.001	0.001	0.002	0.001	0.003	0.002	0.000	0.003
Nb	0.003	0.004	0.004	0.005	0.005	0.003	0.003	0.005	0.004	0.004	0.003	0.003	0.004	0.003	0.004	0.005	0.003	0.003
Total	2.089	2.068	2.068	2.087	2.081	2.072	2.076	2.074	2.066	2.079	2.072	2.080	2.080	2.081	2.068	2.087	2.070	2.070
Mg#	36.54	36.98	37.36	37.24	37.33	36.18	37.43	37.50	37.68	40.45	37.97	37.88	37.62	37.32	38.85	38.71	38.53	38.81
Fe^{2+}	0.466	0.5	0.494	0.468	0.476	0.501	0.478	0.483	0.494	0.439	0.481	0.47	0.472	0.475	0.47	0.447	0.476	0.47
Fe^{3+}	0.256	0.198	0.198	0.25	0.232	0.21	0.218	0.213	0.191	0.229	0.207	0.231	0.231	0.233	0.198	0.25	0.204	0.202
Hem%	12.69	9.80	9.84	12.28	11.44	10.40	10.88	10.57	9.52	11.37	10.29	11.40	11.40	11.49	9.98	12.33	10.16	10.12

Table 7a. (continued)

	37	core 38	rim 39	40	41	42	43	44	45	core 46	rim 47	core 48	rim 49	50	51	52	53	54
SiO_2	0.04	0.01	0.03	0.02	0.00	0.04	0.01	0.05	0.03	0.01	0.03	0.02	0.04	0.05	0.03	0.03	0.00	0.01
TiO_2	49.31	48.95	49.96	51.13	46.89	50.21	48.21	50.16	49.76	48.74	49.51	48.29	50.03	48.17	50.18	48.79	48.03	46.23
Al_2O_3	0.53	0.44	0.45	0.40	0.48	0.43	0.45	0.51	0.53	0.44	0.45	0.48	0.51	0.54	0.54	0.51	0.61	0.54
Cr_2O_3	2.78	2.41	2.44	2.24	2.56	2.39	2.44	2.20	2.41	2.72	2.69	2.66	2.65	3.37	2.34	2.72	3.81	4.07
FeO_T	33.25	33.28	30.03	32.82	32.95	33.25	33.04	33.80	33.36	33.23	32.38	31.65	31.89	32.55	33.67	33.11	32.25	28.64
FeO	23.26	22.81	19.58	24.62	21.18	23.89	22.24	23.98	23.42	22.39	22.91	21.67	23.42	21.88	23.68	22.20	21.40	19.77
Fe_2O_3	11.10	11.63	11.62	9.11	13.08	10.40	12.00	10.91	11.04	12.04	10.53	11.09	9.41	11.86	11.10	12.12	12.05	9.86
MnO	0.31	0.27	0.26	0.30	0.26	0.32	0.27	0.28	0.26	0.34	0.33	0.32	0.30	0.27	0.29	0.28	0.30	0.25
MgO	11.98	11.99	14.46	12.01	12.02	12.05	12.07	12.10	12.12	12.12	12.15	12.29	12.12	12.19	12.22	12.24	12.26	12.31
NiO	0.12	0.11	0.10	0.13	0.13	0.11	0.10	0.09	0.13	0.17	0.18	0.15	0.17	0.12	0.13	0.18	0.18	0.11
ZnO	0.00	0.10	0.04	0.00	0.07	0.13	0.00	0.03	0.00	0.06	0.09	0.10	0.10	0.00	0.00	0.12	0.23	0.01
Nb_2O_5	0.28	0.21	0.37	0.20	0.36	0.38	0.32	0.40	0.26	0.27	0.25	0.30	0.27	0.21	0.35	0.24	0.30	0.19
Total	99.19	98.29	98.68	99.71	96.31	99.84	97.46	100.14	99.39	98.64	98.64	96.82	98.66	98.16	100.29	98.80	98.75	93.16
Si	0.001	0.000	0.001	0.001	0.000	0.001	0.000	0.001	0.001	0.000	0.001	0.000	0.001	0.001	0.001	0.001	0.000	0.000
Ti	0.891	0.893	0.892	0.914	0.877	0.900	0.888	0.897	0.896	0.887	0.897	0.891	0.904	0.880	0.896	0.886	0.874	0.883
Al	0.015	0.013	0.013	0.011	0.014	0.012	0.013	0.014	0.015	0.012	0.013	0.014	0.014	0.015	0.015	0.015	0.017	0.016
Cr	0.053	0.046	0.046	0.042	0.050	0.045	0.047	0.041	0.046	0.052	0.051	0.052	0.050	0.065	0.044	0.052	0.073	0.082
Fe^{2+}_T	0.668	0.675	0.596	0.652	0.685	0.663	0.676	0.672	0.668	0.672	0.653	0.649	0.641	0.661	0.668	0.668	0.652	0.608
Mn	0.006	0.006	0.005	0.006	0.006	0.007	0.006	0.006	0.005	0.007	0.007	0.007	0.006	0.005	0.006	0.006	0.006	0.005
Mg	0.429	0.434	0.512	0.425	0.446	0.428	0.441	0.429	0.433	0.437	0.436	0.450	0.434	0.442	0.433	0.441	0.442	0.466
Ni	0.002	0.002	0.002	0.003	0.003	0.002	0.002	0.002	0.002	0.003	0.004	0.003	0.003	0.002	0.003	0.003	0.003	0.002
Zn	0.000	0.002	0.001	0.000	0.001	0.002	0.000	0.001	0.000	0.001	0.002	0.002	0.002	0.000	0.000	0.002	0.004	0.000
Nb	0.003	0.002	0.004	0.002	0.004	0.004	0.004	0.004	0.003	0.003	0.003	0.003	0.003	0.002	0.004	0.003	0.003	0.002
Total	2.069	2.073	2.072	2.056	2.085	2.064	2.077	2.067	2.069	2.076	2.066	2.071	2.058	2.075	2.068	2.076	2.076	2.065
Mg#	39.10	39.10	46.19	39.47	39.41	39.26	39.45	38.95	39.30	39.41	40.07	40.91	40.39	40.04	39.29	39.73	40.41	43.39
Fe^{2+}	0.468	0.463	0.389	0.489	0.44	0.476	0.455	0.477	0.469	0.453	0.462	0.445	0.47	0.445	0.47	0.448	0.433	0.42
Fe^{3+}	0.201	0.212	0.208	0.163	0.245	0.187	0.221	0.195	0.199	0.219	0.191	0.205	0.17	0.217	0.198	0.22	0.219	0.188
Hem%	10.07	10.59	10.33	8.18	12.14	9.35	10.98	9.73	9.94	10.97	9.61	10.28	8.60	10.90	9.89	11.02	11.14	9.61

Table 7a. (continued)

	55	56	57	58	59	60	61	62	63	core 64	rim 65	66	core 67	rim 68	69	70	71	72
SiO_2	0.03	0.02	0.01	0.00	0.01	0.01	0.03	0.03	0.05	0.04	0.02	0.00	0.01	0.01	0.01	0.00	0.02	0.02
TiO_2	48.27	50.35	48.66	49.22	46.44	48.44	50.59	49.35	49.91	47.64	49.33	47.52	49.02	48.43	45.85	49.35	49.42	49.76
Al_2O_3	0.52	0.50	0.52	0.49	0.53	0.47	0.43	0.54	0.44	0.61	0.61	0.38	0.59	0.58	0.59	0.43	0.53	0.47
Cr_2O_3	3.09	3.14	2.75	2.95	3.18	2.58	2.61	2.86	2.45	2.95	3.17	2.61	3.84	3.72	4.35	2.33	3.90	3.03
FeO_T	32.55	31.25	32.22	32.77	33.22	33.04	32.17	32.44	33.64	33.28	30.92	32.77	32.68	32.80	32.04	32.47	32.77	32.04
FeO	21.54	23.45	22.04	22.49	20.27	21.86	23.67	22.62	23.10	21.15	20.87	21.06	22.25	21.70	19.58	22.37	22.35	22.58
Fe_2O_3	12.24	8.66	11.32	11.43	14.39	12.43	9.44	10.92	11.72	13.48	11.16	13.01	11.59	12.34	13.85	11.23	11.58	10.51
MnO	0.31	0.25	0.29	0.27	0.23	0.29	0.31	0.21	0.32	0.22	0.24	0.28	0.22	0.23	0.20	0.36	0.25	0.28
MgO	12.32	12.33	12.33	12.35	12.36	12.37	12.38	12.38	12.39	12.40	13.28	12.40	12.41	12.39	12.43	12.44	12.47	12.53
NiO	0.24	0.14	0.15	0.13	0.10	0.15	0.10	0.18	0.13	0.12	0.12	0.10	0.14	0.15	0.14	0.12	0.19	0.15
ZnO	0.16	0.00	0.00	0.00	0.09	0.06	0.00	0.02	0.18	0.18	0.12	0.04	0.04	0.11	0.00	0.05	0.00	0.00
Nb_2O_5	0.29	0.26	0.28	0.25	0.30	0.35	0.33	0.32	0.43	0.30	0.26	0.34	0.26	0.24	0.25	0.31	0.17	0.23
Total	98.44	98.88	97.81	99.06	97.12	98.34	99.50	98.96	100.51	98.38	98.75	96.99	99.98	99.40	96.73	98.36	100.49	99.14
Si	0.001	0.001	0.000	0.000	0.000	0.000	0.001	0.001	0.001	0.001	0.001	0.000	0.000	0.000	0.000	0.000	0.000	0.001
Ti	0.880	0.905	0.890	0.890	0.863	0.884	0.905	0.891	0.891	0.871	0.888	0.880	0.879	0.875	0.854	0.896	0.882	0.895
Al	0.015	0.014	0.015	0.014	0.015	0.013	0.012	0.015	0.012	0.017	0.017	0.011	0.016	0.016	0.017	0.012	0.015	0.013
Cr	0.059	0.059	0.053	0.056	0.062	0.049	0.049	0.054	0.046	0.057	0.060	0.051	0.072	0.071	0.085	0.044	0.073	0.057
Fe^{2+}_T	0.660	0.625	0.655	0.658	0.686	0.670	0.640	0.651	0.667	0.677	0.618	0.675	0.652	0.659	0.664	0.656	0.650	0.641
Mn	0.006	0.005	0.006	0.006	0.005	0.006	0.006	0.004	0.006	0.004	0.005	0.006	0.004	0.005	0.004	0.007	0.005	0.006
Mg	0.445	0.439	0.447	0.443	0.455	0.447	0.439	0.443	0.438	0.449	0.474	0.455	0.441	0.444	0.459	0.448	0.441	0.447
Ni	0.005	0.003	0.003	0.003	0.002	0.003	0.002	0.003	0.002	0.002	0.002	0.002	0.003	0.003	0.003	0.002	0.004	0.003
Zn	0.003	0.000	0.000	0.000	0.002	0.001	0.000	0.000	0.003	0.003	0.002	0.001	0.001	0.002	0.000	0.001	0.000	0.000
Nb	0.003	0.003	0.003	0.003	0.003	0.004	0.004	0.003	0.005	0.003	0.003	0.004	0.003	0.003	0.003	0.003	0.002	0.003
Total	2.077	2.053	2.072	2.071	2.093	2.079	2.058	2.068	2.072	2.086	2.069	2.084	2.072	2.077	2.090	2.070	2.071	2.065
Mg#	40.28	41.29	40.55	40.19	39.88	40.03	40.69	40.49	39.64	39.91	43.37	40.28	40.38	40.23	40.88	40.58	40.43	41.07
Fe^{2+}	0.437	0.469	0.448	0.452	0.419	0.443	0.471	0.454	0.458	0.43	0.418	0.434	0.444	0.436	0.406	0.452	0.443	0.452
Fe^{3+}	0.223	0.156	0.207	0.207	0.267	0.227	0.169	0.197	0.209	0.247	0.201	0.241	0.208	0.223	0.258	0.204	0.207	0.189
Hem%	11.24	7.90	10.37	10.36	13.27	11.30	8.50	9.90	10.45	12.30	10.13	11.94	10.52	11.25	12.99	10.18	10.46	9.53

Table 7a. (continued)

	73	core 74	rim 75	76	77	78	79	80	81	core 82	rim 83	84	85
SiO_2	0.01	0.01	0.00	0.01	0.01	0.00	0.01	0.07	0.00	0.02	0.04	0.00	0.01
TiO_2	45.07	49.21	49.40	47.34	49.20	47.28	49.08	49.33	49.62	47.01	45.55	49.32	51.68
Al_2O_3	0.62	0.50	0.60	0.54	0.53	0.59	0.49	0.54	0.53	0.52	0.54	0.52	0.55
Cr_2O_3	4.35	3.13	3.17	2.30	3.89	3.96	3.12	3.35	3.27	2.91	2.84	3.29	3.09
FeO_T	32.92	32.68	32.20	32.35	31.23	31.78	31.20	32.18	30.98	32.95	32.88	30.66	29.93
FeO	18.87	21.92	21.97	20.45	21.88	20.27	21.73	21.99	21.94	19.84	19.50	20.98	22.89
Fe_2O_3	15.61	11.95	11.37	13.23	10.39	12.79	10.52	11.32	10.05	14.56	14.86	10.76	7.82
MnO	0.24	0.36	0.35	0.24	0.22	0.22	0.22	0.29	0.22	0.24	0.26	0.25	0.21
MgO	12.53	12.56	12.60	12.62	12.63	12.66	12.71	12.73	12.82	12.82	12.35	13.20	13.29
NiO	0.13	0.22	0.17	0.18	0.19	0.14	0.14	0.18	0.13	0.13	0.09	0.17	0.16
ZnO	0.00	0.09	0.17	0.00	0.00	0.07	0.00	0.00	0.00	0.10	0.00	0.00	0.00
Nb_2O_5	0.30	0.28	0.28	0.25	0.23	0.25	0.26	0.31	0.21	0.22	0.18	0.22	0.26
Total	97.05	99.69	99.62	96.35	98.89	97.76	97.88	99.68	98.45	97.54	95.33	98.31	99.84
Si	0.000	0.000	0.000	0.000	0.000	0.000	0.000	0.002	0.000	0.001	0.001	0.000	0.000
Ti	0.841	0.884	0.887	0.880	0.887	0.868	0.893	0.884	0.896	0.866	0.861	0.891	0.912
Al	0.018	0.014	0.017	0.016	0.015	0.017	0.014	0.015	0.015	0.015	0.016	0.015	0.015
Cr	0.085	0.059	0.060	0.045	0.074	0.076	0.060	0.063	0.062	0.056	0.056	0.063	0.057
Fe^{2+}_T	0.683	0.653	0.642	0.668	0.626	0.648	0.631	0.641	0.622	0.675	0.691	0.616	0.587
Mn	0.005	0.007	0.007	0.005	0.004	0.005	0.005	0.006	0.005	0.005	0.006	0.005	0.004
Mg	0.464	0.448	0.448	0.465	0.452	0.461	0.458	0.452	0.459	0.468	0.463	0.473	0.465
Ni	0.003	0.004	0.003	0.004	0.004	0.003	0.003	0.003	0.003	0.003	0.002	0.003	0.003
Zn	0.000	0.002	0.003	0.000	0.000	0.001	0.000	0.000	0.000	0.002	0.000	0.000	0.000
Nb	0.003	0.003	0.003	0.003	0.002	0.003	0.003	0.003	0.002	0.002	0.002	0.002	0.003
Total	2.102	2.074	2.070	2.085	2.064	2.081	2.066	2.070	2.062	2.094	2.098	2.067	2.047
Mg#	40.43	40.67	41.11	41.02	41.90	41.53	42.08	41.36	42.44	40.96	40.11	43.42	44.18
Fe^{2+}	0.392	0.438	0.438	0.423	0.439	0.414	0.439	0.438	0.44	0.407	0.41	0.421	0.449
Fe^{3+}	0.291	0.215	0.204	0.246	0.187	0.235	0.191	0.203	0.181	0.268	0.281	0.194	0.138
Hem%	14.56	10.82	10.32	12.17	9.52	11.84	9.64	10.23	9.17	13.30	13.87	9.81	7.02

Table 7b: Microprobe analyses of Sputnik ilmenite (cations on basis of 3 oxygen).

	1	2	3	4	5	6	7	8	9	10	11	12	13	14	15	16	17	18
SiO_2	0.03	0.00	0.01	0.00	0.02	0.04	0.03	0.02	0.02	0.01	0.04	0.03	0.03	0.03	0.05	0.03	0.01	0.01
TiO_2	46.75	48.33	48.01	48.68	48.75	47.49	48.37	48.65	47.23	47.78	48.76	49.35	47.99	47.42	49.70	47.85	48.51	49.24
Al_2O_3	0.31	0.28	0.29	0.36	0.63	0.61	0.44	0.56	0.59	0.62	0.40	0.47	0.59	0.61	0.56	0.63	0.54	0.53
Cr_2O_3	1.89	1.86	1.93	1.89	4.39	4.14	2.42	2.38	4.34	4.25	2.27	2.42	3.60	3.55	2.86	3.17	4.11	3.45
FeO_T	35.61	35.46	35.23	34.70	30.72	32.27	33.34	32.73	32.34	31.75	33.03	33.00	32.45	30.93	32.47	33.09	31.84	30.55
FeO	23.18	24.2	23.72	24.01	23	21.59	22.52	22.57	21.36	21.61	22.6	23.06	21.76	21	22.81	21.33	21.43	20.52
Fe_2O_3	13.82	12.5	12.79	11.88	8.586	11.87	12.02	11.29	12.2	11.27	11.6	11.04	11.88	11.03	10.73	13.07	11.58	11.16
MnO	0.33	0.34	0.37	0.32	0.25	0.23	0.34	0.27	0.25	0.29	0.33	0.33	0.32	0.24	0.27	0.29	0.25	0.31
MgO	10.87	11.14	11.17	11.34	11.80	11.92	12.03	12.04	12.04	12.06	12.07	12.08	12.14	12.24	12.27	12.30	12.51	13.45
NiO	0.06	0.07	0.08	0.08	0.11	0.16	0.08	0.12	0.11	0.16	0.09	0.10	0.13	0.13	0.09	0.11	0.13	0.12
ZnO	0.01	0.00	0.00	0.00	0.04	0.15	0.00	0.00	0.00	0.08	0.12	0.11	0.10	0.02	0.37	0.07	0.18	0.00
Nb_2O_5	0.29	0.49	0.38	0.40	0.31	0.17	0.40	0.25	0.23	0.25	0.32	0.32	0.31	0.16	0.26	0.14	0.22	0.26
Total	96.55	98.41	97.88	98.21	97.90	98.00	98.01	97.53	98.02	98.10	97.91	98.72	98.41	96.05	99.52	98.34	99.13	98.64
Si	0.001	0.000	0.000	0.000	0.001	0.001	0.001	0.000	0.001	0.000	0.001	0.001	0.001	0.001	0.001	0.001	0.000	0.000
Ti	0.880	0.890	0.888	0.894	0.890	0.872	0.887	0.893	0.868	0.875	0.893	0.895	0.876	0.882	0.893	0.875	0.877	0.886
Al	0.009	0.008	0.008	0.010	0.018	0.018	0.013	0.016	0.017	0.018	0.011	0.013	0.017	0.018	0.016	0.018	0.015	0.015
Cr	0.037	0.036	0.037	0.037	0.084	0.080	0.047	0.046	0.084	0.082	0.044	0.046	0.069	0.069	0.054	0.061	0.078	0.065
$Fe^{2+}{}_T$	0.746	0.726	0.725	0.709	0.623	0.659	0.679	0.668	0.660	0.646	0.673	0.666	0.659	0.640	0.649	0.672	0.640	0.611
Mn	0.007	0.007	0.008	0.007	0.005	0.005	0.007	0.005	0.005	0.006	0.007	0.007	0.007	0.005	0.005	0.006	0.005	0.006
Mg	0.406	0.406	0.410	0.413	0.427	0.434	0.437	0.438	0.438	0.438	0.438	0.434	0.439	0.451	0.437	0.446	0.448	0.480
Ni	0.001	0.001	0.002	0.002	0.002	0.003	0.002	0.002	0.002	0.003	0.002	0.002	0.003	0.003	0.002	0.002	0.002	0.002
Zn	0.000	0.000	0.000	0.000	0.001	0.003	0.000	0.000	0.000	0.001	0.002	0.002	0.002	0.000	0.006	0.001	0.003	0.000
Nb	0.003	0.005	0.004	0.004	0.003	0.002	0.004	0.003	0.003	0.003	0.003	0.003	0.003	0.002	0.003	0.002	0.002	0.003
Total	2.091	2.080	2.082	2.076	2.054	2.075	2.076	2.072	2.078	2.071	2.073	2.069	2.075	2.071	2.066	2.083	2.072	2.069
Mg#	35.23	35.90	36.11	36.81	40.64	39.70	39.16	39.60	39.89	40.37	39.44	39.48	40.02	41.37	40.26	39.86	41.19	43.98
Fe^{2+}	0.485	0.5	0.488	0.49	0.467	0.441	0.459	0.461	0.436	0.44	0.46	0.465	0.442	0.434	0.456	0.433	0.431	0.41
Fe^{3+}	0.26	0.23	0.237	0.218	0.157	0.218	0.22	0.207	0.224	0.206	0.212	0.2	0.217	0.205	0.193	0.239	0.209	0.201
Hem%	12.75	11.3	11.65	10.78	8.066	11.08	10.95	10.35	11.36	10.52	10.58	10.02	10.96	10.39	9.749	11.97	10.64	10.13

Hematite% = $0.5Fe^{3+}/(0.5Fe^{3+} +Fe^{2+} +Mg)100$

Mg# = $100Mg/(Mg+Fe^{2+})$

Table 8: Microprobe analyses of garnet websterite xenolith.

	Clinopyroxene												
	1	2	3	4	5	6	7	8	9	10	11	12	13
SiO_2	54.94	55.10	54.99	55.13	54.94	55.11	55.30	54.88	55.15	54.97	55.57	55.19	55.29
TiO_2	0.19	0.22	0.16	0.22	0.21	0.22	0.20	0.20	0.19	0.23	0.21	0.17	0.19
Al_2O_3	1.53	1.47	1.55	1.41	1.48	1.57	1.52	1.51	1.45	1.59	1.55	1.54	1.53
Cr_2O_3	1.58	1.63	1.68	1.63	1.68	1.63	1.71	1.70	1.66	1.69	1.56	1.70	1.59
FeOt	2.77	2.79	2.74	2.76	2.78	2.83	2.82	2.84	2.89	2.83	2.91	2.74	2.76
MnO	0.09	0.08	0.10	0.09	0.11	0.09	0.06	0.07	0.09	0.05	0.07	0.07	0.10
MgO	17.88	18.06	17.91	17.78	17.96	18.22	18.18	18.09	17.92	17.92	17.96	17.92	17.74
CaO	19.44	19.22	19.44	19.38	19.32	19.34	19.37	19.17	19.27	19.11	19.38	19.23	19.37
NiO	0.04	0.04	0.02	0.07	0.02	0.06	0.05	0.06	0.06	0.04	0.05	0.02	0.05
Na_2O	1.62	1.69	1.64	1.55	1.68	1.74	1.69	1.63	1.63	1.72	1.68	1.61	1.65
K_2O	0.11	0.09	0.08	0.08	0.10	0.08	0.09	0.09	0.10	0.11	0.10	0.10	0.09
Total	100.19	100.38	100.31	100.09	100.27	100.88	101.00	100.25	100.40	100.26	101.01	100.27	100.34
Si	1.982	1.983	1.982	1.990	1.981	1.976	1.979	1.979	1.985	1.981	1.987	1.987	1.990
Ti	0.005	0.006	0.004	0.006	0.006	0.006	0.005	0.005	0.005	0.006	0.006	0.005	0.005
Al	0.065	0.062	0.066	0.060	0.063	0.066	0.064	0.064	0.062	0.068	0.065	0.065	0.065
Cr	0.045	0.047	0.048	0.046	0.048	0.046	0.048	0.049	0.047	0.048	0.044	0.048	0.045
$Fe^{2+}{}_T$	0.084	0.084	0.083	0.083	0.084	0.085	0.085	0.086	0.087	0.085	0.087	0.083	0.083
Mn	0.003	0.002	0.003	0.003	0.003	0.003	0.002	0.002	0.003	0.002	0.002	0.002	0.003
Mg	0.962	0.969	0.962	0.956	0.966	0.974	0.970	0.973	0.962	0.963	0.958	0.962	0.952
Ca	0.752	0.741	0.751	0.749	0.747	0.743	0.743	0.741	0.743	0.738	0.742	0.742	0.747
Ni	0.001	0.001	0.001	0.002	0.001	0.002	0.002	0.002	0.002	0.001	0.001	0.001	0.001
Na	0.113	0.118	0.114	0.109	0.118	0.121	0.118	0.114	0.114	0.120	0.116	0.112	0.115
K	0.005	0.004	0.004	0.004	0.004	0.004	0.004	0.004	0.004	0.005	0.005	0.004	0.004
Total	4.016	4.017	4.017	4.008	4.019	4.024	4.020	4.018	4.014	4.017	4.013	4.010	4.010
Mg#	92.00	92.03	92.10	91.99	92.01	91.99	91.99	91.91	91.70	91.87	91.67	92.09	91.99
Ca%	41.82	41.32	41.81	41.89	41.56	41.24	41.34	41.18	41.48	41.33	41.55	41.53	41.94
Mg%	53.52	54.00	53.60	53.45	53.76	54.05	53.96	54.07	53.66	53.90	53.58	53.85	53.41
Fe%	4.65	4.68	4.60	4.66	4.67	4.71	4.70	4.76	4.85	4.77	4.87	4.63	4.65

Table 8. (continued)

	Garnet												
	1	2	3	4	5	6	7	8	9	10	11	12	13
SiO_2	40.76	40.78	40.93	40.93	40.75	40.70	41.03	40.68	40.61	40.87	40.84	40.75	40.80
TiO_2	0.59	0.67	0.65	0.63	0.64	0.65	0.60	0.68	0.68	0.65	0.65	0.71	0.73
Al_2O_3	17.60	17.65	18.06	18.27	17.56	17.66	17.86	17.32	17.28	17.79	17.75	17.66	17.91
Cr_2O_3	6.95	6.59	6.43	6.10	6.46	6.58	6.59	6.53	6.84	6.64	6.30	6.51	6.63
FeOt	8.74	8.76	8.77	8.77	8.87	8.95	8.93	8.71	8.69	8.86	8.70	8.81	8.72
MnO	0.38	0.37	0.43	0.40	0.38	0.37	0.39	0.36	0.37	0.38	0.35	0.36	0.39
MgO	18.26	18.27	18.48	18.57	18.20	18.48	18.60	18.19	18.01	18.43	18.46	18.28	18.56
CaO	6.36	6.14	6.03	5.81	6.08	6.01	6.04	6.15	6.11	6.09	5.91	6.14	6.01
NiO	0.01	0.00	0.02	0.00	0.00	0.00	0.04	0.01	0.01	0.00	0.02	0.00	0.04
Na_2O	0.12	0.10	0.10	0.09	0.06	0.08	0.09	0.06	0.11	0.05	0.04	0.07	0.07
K_2O	n.a.	n.a.	n.a.	n.a.	n.a.	n.a.	n.a.	n.a.	n.a.	n.a.	n.a.	n.a.	n.a.
Total	99.78	99.33	99.89	99.57	98.99	99.47	100.17	98.68	98.69	99.75	99.00	99.29	99.86
Si	2.991	3.000	2.991	2.994	3.007	2.992	2.994	3.012	3.008	2.994	3.007	2.998	2.985
Ti	0.033	0.037	0.036	0.035	0.036	0.036	0.033	0.038	0.038	0.036	0.036	0.039	0.040
Al	1.522	1.530	1.555	1.576	1.527	1.530	1.536	1.511	1.509	1.536	1.540	1.532	1.544
Cr	0.403	0.383	0.371	0.353	0.377	0.383	0.380	0.382	0.400	0.385	0.366	0.379	0.383
Fe^{2+}_T	0.536	0.539	0.536	0.537	0.547	0.550	0.545	0.539	0.539	0.543	0.536	0.542	0.534
Mn	0.023	0.023	0.027	0.025	0.024	0.023	0.024	0.023	0.023	0.023	0.022	0.023	0.024
Mg	1.997	2.004	2.014	2.026	2.002	2.025	2.024	2.008	1.989	2.013	2.027	2.005	2.024
Ca	0.500	0.484	0.472	0.456	0.481	0.473	0.472	0.488	0.485	0.478	0.466	0.484	0.471
Ni	0.001	0.000	0.001	0.000	0.000	0.000	0.002	0.000	0.000	0.000	0.001	0.000	0.002
Na	0.017	0.015	0.014	0.012	0.008	0.011	0.013	0.009	0.015	0.007	0.006	0.010	0.010
K													
Total	8.023	8.014	8.016	8.013	8.009	8.022	8.022	8.009	8.007	8.013	8.007	8.012	8.017
Mg#	78.84	78.81	78.99	79.05	78.54	78.64	78.80	78.84	78.70	78.76	79.09	78.72	79.14

Table 8. (continued)

	Orthopyroxene																
	1-core	rim	2-core	middle	rim	3-core	middle	rim	4-core	middle	rim	5-core	rim	6	7	8	9
SiO_2	57.62	57.38	57.41	56.67	57.38	57.53	57.50	57.77	57.38	57.66	57.72	57.52	58.17	57.54	57.58	57.61	57.28
TiO_2	0.12	0.14	0.08	0.12	0.11	0.08	0.07	0.07	0.09	0.08	0.09	0.07	0.09	0.09	0.12	0.13	0.09
Al_2O_3	0.50	0.49	0.46	0.45	0.47	0.41	0.43	0.46	0.46	0.45	0.46	0.46	0.45	0.44	0.47	0.47	0.44
Cr_2O_3	0.23	0.27	0.31	0.34	0.36	0.19	0.21	0.18	0.26	0.18	0.22	0.22	0.19	0.21	0.19	0.23	0.20
$FeOt$	5.74	5.79	5.80	5.71	5.71	5.69	5.66	5.69	5.77	5.54	5.80	5.71	5.71	5.78	5.77	5.68	5.60
MnO	0.08	0.09	0.08	0.10	0.09	0.11	0.09	0.07	0.09	0.08	0.12	0.11	0.09	0.12	0.09	0.09	0.09
MgO	32.96	33.20	33.05	32.79	33.16	33.35	33.48	33.07	33.13	33.49	33.55	33.15	33.41	33.15	33.07	33.12	32.63
CaO	0.47	0.53	0.52	0.57	0.53	0.52	0.56	0.54	0.59	0.53	0.52	0.57	0.54	0.53	0.52	0.53	0.52
NiO	0.09	0.06	0.05	0.05	0.09	0.10	0.09	0.10	0.11	0.10	0.08	0.10	0.07	0.08	0.09	0.10	0.11
Na_2O	0.10	0.13	0.17	0.14	0.15	0.10	0.12	0.16	0.13	0.14	0.12	0.12	0.13	0.12	0.15	0.11	0.14
K_2O	n.a.	n.a.	n.a.	n.a.	n.a.	n.a.	n.a.	n.a.	n.a.	n.a.	n.a.	n.a.	n.a.	n.a.	n.a.	n.a.	n.a.
Total	97.89	98.08	97.91	96.92	98.07	98.09	98.21	98.11	98.00	98.23	98.68	98.03	98.84	98.05	98.05	98.06	97.10
Si	2.019	2.010	2.014	2.009	2.010	2.014	2.010	2.020	2.012	2.013	2.009	2.015	2.019	2.015	2.016	2.016	2.023
Ti	0.003	0.004	0.002	0.003	0.003	0.002	0.002	0.002	0.002	0.002	0.002	0.002	0.002	0.002	0.003	0.004	0.002
Al	0.020	0.020	0.019	0.019	0.020	0.017	0.018	0.019	0.019	0.018	0.019	0.019	0.018	0.018	0.020	0.019	0.019
Cr	0.006	0.008	0.009	0.010	0.010	0.005	0.006	0.005	0.007	0.005	0.006	0.006	0.005	0.006	0.005	0.006	0.006
$Fe^{2+}T$	0.168	0.170	0.170	0.169	0.167	0.167	0.166	0.166	0.169	0.162	0.169	0.167	0.166	0.169	0.169	0.166	0.166
Mn	0.003	0.003	0.002	0.003	0.003	0.003	0.003	0.002	0.003	0.002	0.003	0.003	0.003	0.003	0.003	0.003	0.003
Mg	1.722	1.733	1.728	1.733	1.732	1.740	1.745	1.723	1.732	1.743	1.741	1.731	1.728	1.730	1.726	1.728	1.718
Ca	0.018	0.020	0.020	0.022	0.020	0.020	0.021	0.020	0.022	0.020	0.019	0.022	0.020	0.020	0.020	0.020	0.020
Ni	0.003	0.002	0.001	0.001	0.003	0.003	0.003	0.003	0.003	0.003	0.002	0.003	0.002	0.002	0.003	0.003	0.003
Na	0.007	0.009	0.012	0.010	0.011	0.007	0.008	0.011	0.009	0.009	0.008	0.008	0.009	0.008	0.010	0.007	0.009
K																	
Total	3.968	3.977	3.976	3.979	3.977	3.977	3.980	3.972	3.978	3.978	3.980	3.975	3.972	3.975	3.974	3.971	3.967
Mg#	91.11	91.09	91.04	91.10	91.19	91.26	91.34	91.19	91.09	91.51	91.16	91.19	91.25	91.09	91.09	91.23	91.21

Table 8. (continued)

	Orthopyroxene																	
	10	11	12	13	14	15-core	middle	rim	16	17	18	19	20	21	22	23	24	25
SiO_2	57.33	57.75	57.31	57.57	57.45	57.35	57.69	57.76	57.37	55.13	57.64	57.56	57.49	57.30	57.39	57.54	57.37	57.49
TiO_2	0.06	0.13	0.09	0.15	0.13	0.13	0.10	0.12	0.16	0.09	0.13	0.15	0.17	0.13	0.16	0.13	0.15	0.19
Al_2O_3	0.45	0.48	0.44	0.43	0.46	0.44	0.42	0.44	0.43	0.42	0.44	0.41	0.45	0.43	0.42	0.46	0.43	0.44
Cr_2O_3	0.18	0.27	0.19	0.25	0.24	0.23	0.27	0.24	0.32	0.31	0.24	0.30	0.23	0.25	0.18	0.29	0.23	0.27
$FeOt$	5.74	5.76	5.77	5.69	5.76	5.75	5.70	5.77	5.66	5.70	5.73	5.75	5.80	5.70	5.70	5.78	5.51	5.59
MnO	0.09	0.09	0.09	0.11	0.13	0.10	0.14	0.11	0.12	0.13	0.09	0.14	0.11	0.11	0.13	0.13	0.11	0.13
MgO	33.37	33.21	32.78	34.26	34.37	34.30	34.03	34.70	34.42	34.50	34.53	34.15	34.32	34.62	34.27	34.03	34.25	33.86
CaO	0.48	0.58	0.52	0.53	0.54	0.56	0.54	0.49	0.51	0.51	0.54	0.53	0.54	0.53	0.54	0.55	0.54	0.49
NiO	0.07	0.08	0.08	0.11	0.12	0.07	0.09	0.10	0.11	0.12	0.14	0.12	0.11	0.10	0.11	0.13	0.09	0.08
Na_2O	0.12	0.16	0.14	0.12	0.11	0.09	0.10	0.10	0.10	0.15	0.11	0.09	0.13	0.11	0.12	0.10	0.12	0.13
K_2O	n.a.	n.a.	n.a.	n.a.	n.a.	n.a.	n.a.	n.a.	n.a.	n.a.	n.a.	n.a.	n.a.	n.a.	n.a.	n.a.	n.a.	n.a.
Total	97.90	98.51	97.40	99.20	99.31	99.01	99.07	99.83	99.19	97.05	99.57	99.21	99.34	99.26	99.03	99.14	98.79	98.67
Si	2.011	2.013	2.019	1.996	1.991	1.993	2.002	1.991	1.990	1.962	1.992	1.996	1.992	1.987	1.994	1.997	1.995	2.002
Ti	0.002	0.003	0.003	0.004	0.003	0.003	0.003	0.003	0.004	0.003	0.003	0.004	0.004	0.003	0.004	0.003	0.004	0.005
Al	0.019	0.020	0.018	0.018	0.019	0.018	0.017	0.018	0.018	0.018	0.018	0.017	0.019	0.017	0.017	0.019	0.018	0.018
Cr	0.005	0.007	0.005	0.007	0.006	0.006	0.007	0.007	0.009	0.009	0.006	0.008	0.006	0.007	0.005	0.008	0.006	0.007
Fe^{2+}_T	0.168	0.168	0.170	0.165	0.167	0.167	0.166	0.166	0.164	0.170	0.165	0.167	0.168	0.165	0.165	0.168	0.160	0.163
Mn	0.003	0.003	0.003	0.003	0.004	0.003	0.004	0.003	0.004	0.004	0.003	0.004	0.003	0.003	0.004	0.004	0.003	0.004
Mg	1.744	1.726	1.722	1.770	1.776	1.777	1.760	1.782	1.780	1.830	1.778	1.765	1.772	1.789	1.774	1.761	1.776	1.758
Ca	0.018	0.022	0.019	0.020	0.020	0.021	0.020	0.018	0.019	0.019	0.020	0.020	0.020	0.020	0.020	0.020	0.020	0.018
Ni	0.002	0.002	0.002	0.003	0.003	0.002	0.002	0.003	0.003	0.004	0.004	0.003	0.003	0.003	0.003	0.004	0.003	0.002
Na	0.008	0.011	0.009	0.008	0.008	0.006	0.007	0.007	0.007	0.010	0.007	0.006	0.009	0.008	0.008	0.007	0.008	0.009
K																		
Total	3.980	3.975	3.971	3.993	3.997	3.995	3.987	3.998	3.996	4.027	3.997	3.991	3.996	4.002	3.995	3.990	3.993	3.985
Mg#	91.20	91.13	91.02	91.48	91.41	91.41	91.41	91.47	91.56	91.51	91.49	91.36	91.35	91.54	91.47	91.30	91.72	91.52

Table 8. (continued)

	Orthopyroxene						Olivine			
	26	27	28	29	30	31	1	2	3	4
SiO_2	57.46	57.48	57.48	56.92	57.53	57.19	40.72	41.20	40.93	40.95
TiO_2	0.16	0.20	0.20	0.14	0.17	0.16	0.03	0.02	0.00	0.00
Al_2O_3	0.46	0.43	0.44	0.42	0.46	0.45	0.00	0.00	0.00	0.01
Cr_2O_3	0.29	0.22	0.22	0.23	0.25	0.33	0.04	0.04	0.02	0.03
FeOt	5.45	5.56	5.50	5.42	5.58	5.47	9.38	9.47	9.59	9.45
MnO	0.13	0.10	0.12	0.11	0.12	0.11	0.10	0.10	0.10	0.11
MgO	34.18	34.16	33.96	34.05	34.39	34.08	49.28	49.56	49.35	49.62
CaO	0.52	0.50	0.49	0.52	0.53	0.52	0.05	0.02	0.05	0.03
NiO	0.10	0.13	0.07	0.11	0.11	0.13	0.28	0.28	0.28	0.31
Na_2O	0.17	0.11	0.10	0.11	0.13	0.12	0.01	0.02	0.01	0.00
K_2O	n.a.	n.a.	n.a.	n.a.	n.a.	n.a.	n.a.	n.a.	n.a.	n.a.
Total	98.91	98.87	98.58	98.04	99.28	98.56	99.93	100.70	100.33	100.49
Si	1.996	1.998	2.002	1.995	1.992	1.994	0.999	1.011	0.999	0.998
Ti	0.004	0.005	0.005	0.004	0.005	0.004	0.000	0.000	0.000	0.000
Al	0.019	0.017	0.018	0.017	0.019	0.018	0.000	0.000	0.000	0.000
Cr	0.008	0.006	0.006	0.006	0.007	0.009	0.001	0.000	0.000	0.000
Fe^{2+}_T	0.158	0.162	0.160	0.159	0.162	0.159	0.192	0.192	0.196	0.193
Mn	0.004	0.003	0.004	0.003	0.004	0.003	0.002	0.000	0.000	0.000
Mg	1.770	1.769	1.763	1.779	1.776	1.772	1.799	1.795	1.796	1.802
Ca	0.019	0.018	0.018	0.020	0.020	0.020	0.001	0.000	0.000	0.000
Ni	0.003	0.004	0.002	0.003	0.003	0.004	0.005	0.006	0.006	0.006
Na	0.012	0.008	0.007	0.008	0.009	0.008	0.000	0.000	0.000	0.000
K										
Total	3.992	3.990	3.985	3.994	3.995	3.992	3.000	2.999	3.001	3.002
Mg#	91.78	91.64	91.67	91.81	91.65	91.75	90.35	90.32	90.17	90.35

Table 9: Microprobe analyses of eclogite xenolith.

Clinopyroxene

	1-core	middle	rim	2-core	rim	3-core	middle	rim	4-core	rim	5-core	rim	6-core	rim	7-core	rim	8-core	rim
SiO_2	55.71	55.90	55.66	56.05	55.83	55.63	55.37	55.64	55.80	55.54	55.84	55.79	55.43	55.79	55.92	55.77	55.69	55.70
TiO_2	0.10	0.09	0.06	0.10	0.09	0.12	0.13	0.10	0.11	0.08	0.08	0.07	0.11	0.08	0.08	0.08	0.09	0.03
Al_2O_3	7.59	7.31	6.85	7.13	7.08	7.13	7.53	7.54	7.78	7.85	7.56	7.58	7.39	7.60	6.98	7.14	7.66	7.96
Cr_2O_3	0.18	0.21	0.18	0.16	0.19	0.17	0.22	0.17	0.19	0.19	0.20	0.16	0.21	0.20	0.19	0.20	0.19	0.15
FeOt	1.98	2.12	2.08	2.06	2.09	2.10	2.07	2.01	2.03	2.08	2.03	1.99	2.05	1.96	2.12	2.07	2.02	2.06
MnO	0.00	0.02	0.03	0.02	0.03	0.05	0.04	0.01	0.03	0.01	0.02	0.02	0.01	0.02	0.03	0.00	0.00	0.00
MgO	12.48	12.97	13.27	13.23	13.30	13.02	13.05	12.84	12.56	12.46	12.94	12.70	12.81	12.69	13.28	12.94	12.90	12.63
CaO	17.81	18.28	18.64	18.57	18.38	18.23	17.92	18.21	17.87	17.78	17.97	17.93	18.10	18.00	18.29	18.40	17.90	17.69
NiO	0.10	0.08	0.09	0.10	0.09	0.09	0.09	0.10	0.07	0.07	0.06	0.07	0.08	0.06	0.07	0.08	0.06	0.09
Na_2O	3.80	3.77	3.55	3.66	3.69	3.64	3.95	3.93	3.82	3.91	3.87	3.99	3.78	3.83	3.61	3.54	3.94	3.91
K_2O	0.01	0.03	0.03	0.02	0.00	0.02	0.02	0.03	0.02	0.02	0.01	0.02	0.02	0.02	0.02	0.03	0.02	0.03
Total	99.77	100.76	100.42	101.10	100.75	100.20	100.37	100.59	100.26	99.99	100.58	100.33	99.97	100.26	100.59	100.25	100.46	100.24
Si	1.99	1.98	1.98	1.98	1.98	1.98	1.97	1.97	1.98	1.98	1.98	1.98	1.98	1.98	1.98	1.98	1.97	1.98
Ti	0.00	0.00	0.00	0.00	0.00	0.00	0.00	0.00	0.00	0.00	0.00	0.00	0.00	0.00	0.00	0.00	0.00	0.00
Al	0.32	0.30	0.29	0.30	0.30	0.30	0.32	0.32	0.33	0.33	0.32	0.32	0.31	0.32	0.29	0.30	0.32	0.33
Cr	0.01	0.01	0.01	0.00	0.01	0.00	0.01	0.00	0.01	0.01	0.01	0.00	0.01	0.01	0.01	0.01	0.01	0.00
Fe^{2+}_T	0.06	0.06	0.06	0.06	0.06	0.06	0.06	0.06	0.06	0.06	0.06	0.06	0.06	0.06	0.06	0.06	0.06	0.06
Mn	0.00	0.00	0.00	0.00	0.00	0.00	0.00	0.00	0.00	0.00	0.00	0.00	0.00	0.00	0.00	0.00	0.00	0.00
Mg	0.66	0.68	0.70	0.70	0.70	0.69	0.69	0.68	0.66	0.66	0.68	0.67	0.68	0.67	0.70	0.69	0.68	0.67
Ca	0.68	0.69	0.71	0.70	0.70	0.70	0.68	0.69	0.68	0.68	0.68	0.68	0.69	0.68	0.69	0.70	0.68	0.67
Ni	0.00	0.00	0.00	0.00	0.00	0.00	0.00	0.00	0.00	0.00	0.00	0.00	0.00	0.00	0.00	0.00	0.00	0.00
Na	0.26	0.26	0.24	0.25	0.25	0.25	0.27	0.27	0.26	0.27	0.27	0.27	0.26	0.26	0.25	0.24	0.27	0.27
K	0.00	0.00	0.00	0.00	0.00	0.00	0.00	0.00	0.00	0.00	0.00	0.00	0.00	0.00	0.00	0.00	0.00	0.00
Total	3.98	3.99	4.00	3.99	4.00	3.99	4.00	4.00	3.98	3.99	3.99	3.99	3.99	3.99	3.99	3.99	4.00	3.99
Mg#	0.92	0.92	0.92	0.92	0.92	0.92	0.92	0.92	0.92	0.91	0.92	0.92	0.92	0.92	0.92	0.92	0.92	0.92
Fe^{2+}	0.06	0.06	0.06	0.06	0.06	0.06	0.06	0.06	0.06	0.06	0.06	0.06	0.06	0.06	0.06	0.06	0.06	0.06
Fe^{3+}	0.00	0.00	0.00	0.00	0.00	0.00	0.00	0.00	0.00	0.00	0.00	0.00	0.00	0.00	0.00	0.00	0.00	0.00
Ca%	48.51	48.14	48.14	48.13	47.73	48.00	47.55	48.38	48.38	48.42	47.85	48.27	48.23	48.40	47.61	48.41	47.83	47.99
Mg%	47.27	47.51	47.68	47.70	48.04	47.67	48.17	47.45	47.33	47.17	47.94	47.55	47.51	47.48	48.09	47.35	47.95	47.64
Fe%	4.21	4.35	4.18	4.17	4.22	4.32	4.28	4.17	4.29	4.41	4.22	4.18	4.26	4.11	4.30	4.24	4.22	4.37

$Mg\# = Mg/(Fe^{2+}_T + Mg)$

Table 9. (continued)

Clinopyroxene

	9-core	middle	rim	10	11-core	rim	12	13	14-core	middle	middle	rim
SiO_2	55.60	56.16	55.92	55.79	55.38	55.82	56.08	55.75	53.00	53.30	52.61	53.54
TiO_2	0.10	0.14	0.11	0.09	0.14	0.12	0.12	0.12	0.26	0.12	0.28	0.24
Al_2O_3	7.83	7.31	7.18	7.05	7.69	7.40	7.54	7.44	5.87	4.81	4.98	5.52
Cr_2O_3	0.18	0.17	0.23	0.17	0.17	0.19	0.17	0.17	0.19	0.20	0.21	0.21
FeOt	1.99	2.13	2.25	2.24	2.20	2.19	2.22	2.18	3.39	2.85	3.53	3.31
MnO	0.01	0.01	0.01	0.00	0.06	0.01	0.01	0.03	0.04	0.02	0.05	0.02
MgO	12.49	12.80	12.82	12.95	12.50	12.85	13.00	12.87	14.79	15.16	15.42	14.93
CaO	18.05	18.28	18.04	18.35	17.93	17.96	17.87	18.11	20.78	21.60	21.33	20.43
NiO	0.10	0.08	0.11	0.07	0.12	0.09	0.07	0.07	0.06	0.14	0.09	0.09
Na_2O	3.92	3.75	3.84	3.89	4.06	3.99	3.87	3.88	1.68	1.73	1.56	1.94
K_2O	0.01	0.02	0.02	0.02	0.02	0.01	0.02	0.01	0.02	0.04	0.01	0.02
Total	100.27	100.83	100.51	100.61	100.25	100.63	100.97	100.62	100.08	99.96	100.08	100.26
Si	1.97	1.98	1.98	1.98	1.97	1.98	1.98	1.98	1.92	1.93	1.91	1.93
Ti	0.00	0.00	0.00	0.00	0.00	0.00	0.00	0.00	0.01	0.00	0.01	0.01
Al	0.33	0.30	0.30	0.30	0.32	0.31	0.31	0.31	0.25	0.21	0.21	0.23
Cr	0.01	0.00	0.01	0.00	0.00	0.01	0.00	0.00	0.01	0.01	0.01	0.01
Fe^{2+}_T	0.06	0.06	0.07	0.07	0.07	0.06	0.07	0.06	0.10	0.09	0.11	0.10
Mn	0.00	0.00	0.00	0.00	0.00	0.00	0.00	0.00	0.00	0.00	0.00	0.00
Mg	0.66	0.67	0.68	0.69	0.66	0.68	0.68	0.68	0.80	0.82	0.84	0.80
Ca	0.69	0.69	0.69	0.70	0.68	0.68	0.68	0.69	0.81	0.84	0.83	0.79
Ni	0.00	0.00	0.00	0.00	0.00	0.00	0.00	0.00	0.00	0.00	0.00	0.00
Na	0.27	0.26	0.26	0.27	0.28	0.27	0.26	0.27	0.12	0.12	0.11	0.14
K	0.00	0.00	0.00	0.00	0.00	0.00	0.00	0.00	0.00	0.00	0.00	0.00
Total	3.99	3.99	3.99	4.00	4.00	4.00	3.99	4.00	4.01	4.02	4.03	4.01
Mg#	0.92	0.91	0.91	0.91	0.91	0.91	0.91	0.91	0.89	0.90	0.89	0.89
Fe^{2+}	0.06	0.06	0.07	0.07	0.07	0.06	0.07	0.06	0.10	0.09	0.11	0.10
Fe^{3+}	0.00	0.00	0.00	0.00	0.00	0.00	0.00	0.00	0.00	0.00	0.00	0.00
Ca%	48.81	48.42	47.94	48.15	48.41	47.84	47.42	48.01	47.23	48.08	46.83	46.67
Mg%	46.99	47.18	47.40	47.27	46.96	47.61	47.99	47.47	46.75	46.97	47.11	47.42
Fe%	4.19	4.40	4.66	4.58	4.63	4.55	4.59	4.52	6.02	4.95	6.06	5.91

Mg#=Mg/(Fe^{2+}_T+Mg)

Table 9. (continued)

Garnet

	1-core	rim	2-core	middle	rim	3-core	rim	4-core	rim	5-core	rim	6-core	rim	7	8	9	10	11-core	rim	12-core
SiO_2	39.80	40.10	40.32	40.23	40.40	40.09	38.88	40.29	40.23	40.07	40.01	40.27	39.56	40.32	40.17	40.13	40.23	40.49	40.65	40.10
Al_2O_3	22.51	22.18	22.66	22.58	22.65	22.90	22.17	22.75	22.51	22.47	22.43	22.68	22.35	22.36	22.67	22.60	22.76	22.61	22.76	22.56
Cr_2O_3	0.15	0.09	0.12	0.14	0.17	0.13	0.06	0.15	0.11	0.13	0.18	0.18	0.11	0.12	0.10	0.13	0.13	0.14	0.17	0.14
TiO_2	0.04	0.00	0.09	0.04	0.05	0.04	0.01	0.02	0.00	0.01	0.00	0.04	0.00	0.07	0.01	0.09	0.03	0.02	0.01	0.09
$FeOt$	15.07	15.03	14.89	14.80	14.97	15.25	14.98	15.06	15.05	15.20	14.91	15.03	15.06	15.20	15.39	15.05	15.17	15.40	15.28	14.85
MnO	0.29	0.30	0.26	0.27	0.27	0.27	0.28	0.26	0.31	0.29	0.28	0.26	0.30	0.28	0.30	0.31	0.31	0.26	0.30	0.25
MgO	12.55	12.51	13.00	12.70	12.64	12.49	11.87	12.44	12.55	12.43	12.85	12.54	12.33	12.14	12.73	12.59	12.61	12.84	11.93	12.76
CaO	8.20	8.40	8.16	8.08	7.86	7.91	8.28	8.11	8.10	8.07	8.01	8.04	7.99	8.13	7.73	8.20	8.35	8.00	8.09	8.26
NiO	0.00	0.00	0.00	0.01	0.00	0.00	0.00	0.00	0.01	0.00	0.00	0.02	0.00	0.01	0.00	0.00	0.01	0.00	0.00	0.01
Na_2O	0.05	0.03	0.05	0.02	0.04	0.08	0.04	0.02	0.04	0.03	0.02	0.03	0.05	0.04	0.04	0.04	0.05	0.03	0.02	0.03
K_2O	n.a.	n.a.	n.a.	n.a.	n.a.	n.a.	n.a.	n.a.	n.a.	n.a.	n.a.	n.a.	n.a.	n.a.	n.a.	n.a.	n.a.	n.a.	n.a.	n.a.
Total	98.66	98.64	99.55	98.87	99.04	99.14	96.57	99.12	98.89	98.70	98.68	99.10	97.74	98.66	99.13	99.14	99.64	99.78	99.21	99.02
Si	2.98	3.01	2.99	3.00	3.01	2.99	2.98	3.00	3.01	3.00	2.99	3.00	2.99	3.02	2.99	2.99	2.99	3.00	3.02	2.99
Al	1.99	1.96	1.98	1.99	1.99	2.01	2.00	2.00	1.98	1.98	1.98	1.99	1.99	1.97	1.99	1.99	1.99	1.97	2.00	1.98
Cr	0.01	0.01	0.01	0.01	0.01	0.01	0.00	0.01	0.01	0.01	0.01	0.01	0.01	0.01	0.01	0.01	0.01	0.01	0.01	0.01
Ti	0.00	0.00	0.00	0.00	0.00	0.00	0.00	0.00	0.00	0.00	0.00	0.00	0.00	0.00	0.00	0.00	0.00	0.00	0.00	0.00
Fe^{2+}_T	0.95	0.94	0.92	0.92	0.93	0.95	0.96	0.94	0.94	0.95	0.93	0.94	0.95	0.95	0.96	0.94	0.94	0.95	0.95	0.93
Mn	0.02	0.02	0.02	0.02	0.02	0.02	0.02	0.02	0.02	0.02	0.02	0.02	0.02	0.02	0.02	0.02	0.02	0.02	0.02	0.02
Mg	1.40	1.40	1.44	1.41	1.40	1.39	1.36	1.38	1.40	1.39	1.43	1.39	1.39	1.36	1.41	1.40	1.40	1.42	1.32	1.42
Ca	0.66	0.67	0.65	0.65	0.63	0.63	0.68	0.65	0.65	0.65	0.64	0.64	0.65	0.65	0.62	0.66	0.66	0.63	0.65	0.66
Ni	0.00	0.00	0.00	0.00	0.00	0.00	0.00	0.00	0.00	0.00	0.00	0.00	0.00	0.00	0.00	0.00	0.00	0.00	0.00	0.00
Na	0.01	0.00	0.01	0.00	0.01	0.01	0.01	0.00	0.01	0.00	0.00	0.00	0.01	0.01	0.01	0.01	0.01	0.00	0.00	0.00
K	n.a.	n.a.	n.a.	n.a.	n.a.	n.a.	n.a.	n.a.	n.a.	n.a.	n.a.	n.a.	n.a.	n.a.	n.a.	n.a.	n.a.	n.a.	n.a.	n.a.
Total	8.02	8.01	8.01	8.00	7.99	8.01	8.01	8.00	8.00	8.00	8.01	8.00	8.01	7.99	8.01	8.01	8.02	8.01	7.97	8.01
Mg#	0.60	0.60	0.61	0.60	0.60	0.59	0.59	0.60	0.60	0.59	0.61	0.60	0.59	0.59	0.60	0.60	0.60	0.60	0.58	0.61
Fe^{2+}	0.89	0.90	0.88	0.92	0.93	0.93	0.91	0.94	0.93	0.94	0.89	0.94	0.92	0.95	0.93	0.91	0.89	0.92	0.95	0.89
Fe^{3+}	0.05	0.04	0.04	0.00	0.00	0.02	0.04	0.00	0.01	0.01	0.04	0.00	0.03	0.00	0.03	0.03	0.05	0.03	0.00	0.03

Table 9. (continued)

Garnet

	middle	rim	13	14-core	middle	rim	15
SiO_2	40.23	40.11	40.00	40.50	40.55	40.25	40.11
Al_2O_3	23.47	23.47	23.26	23.11	23.02	23.25	23.52
Cr_2O_3	0.15	0.13	0.13	0.15	0.14	0.12	0.14
TiO_2	0.06	0.05	0.05	0.11	0.12	0.06	0.05
FeOt	14.99	14.89	15.07	14.98	14.69	15.17	15.10
MnO	0.28	0.29	0.32	0.30	0.30	0.30	0.29
MgO	12.64	12.58	12.38	12.71	12.71	12.72	12.33
CaO	8.46	8.59	8.25	8.14	8.33	8.23	8.83
NiO	0.01	0.02	0.02	0.02	0.01	0.00	0.01
Na_2O	0.01	0.04	0.00	0.03	0.02	0.02	0.06
K_2O	n.a.	n.a.	n.a.	n.a.	n.a.	n.a.	n.a.
Total	100.29	100.17	99.47	100.04	99.88	100.11	100.43
Si	2.96	2.96	2.97	2.99	2.99	2.97	2.96
Al	2.04	2.04	2.04	2.01	2.00	2.02	2.04
Cr	0.01	0.01	0.01	0.01	0.01	0.01	0.01
Ti	0.00	0.00	0.00	0.01	0.01	0.00	0.00
Fe^{2+}_T	0.92	0.92	0.94	0.92	0.91	0.94	0.93
Mn	0.02	0.02	0.02	0.02	0.02	0.02	0.02
Mg	1.39	1.38	1.37	1.40	1.40	1.40	1.36
Ca	0.67	0.68	0.66	0.64	0.66	0.65	0.70
Ni	0.00	0.00	0.00	0.00	0.00	0.00	0.00
Na	0.00	0.01	0.00	0.00	0.00	0.00	0.01
K	n.a.	n.a.	n.a.	n.a.	n.a.	n.a.	n.a.
Total	8.01	8.02	8.00	8.00	8.00	8.01	8.02
Mg#	0.60	0.60	0.59	0.60	0.61	0.60	0.59
Fe^{2+}	0.89	0.87	0.93	0.92	0.91	0.90	0.87
Fe^{3+}	0.03	0.05	0.01	0.00	0.00	0.04	0.06